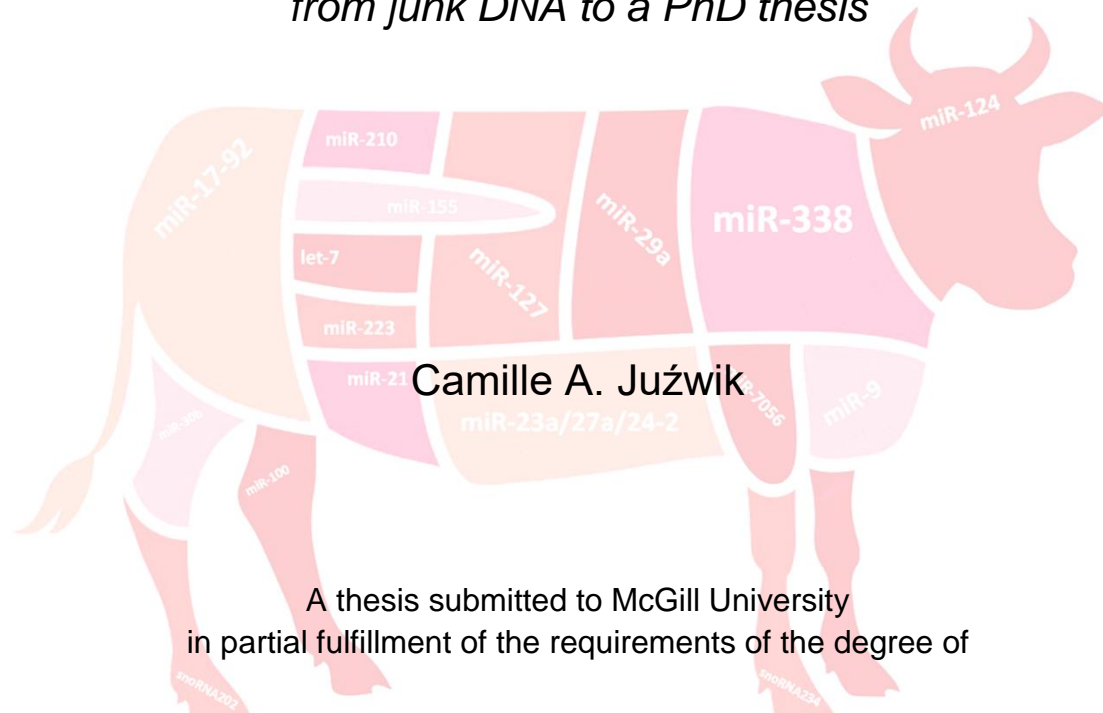


microRNA regulation during neuroinflammation: *from junk DNA to a PhD thesis*



Camille A. Juźwik

A thesis submitted to McGill University
in partial fulfillment of the requirements of the degree of
Doctor of Philosophy in Neurological Sciences

Integrated Program in Neuroscience
Department of Neurology and Neurosurgery - McGill University
3801 University Street - Montreal, QC, H3A 2B4, Canada

March 2019

© Camille A. Juźwik, 2019
All rights reserved

Table of Contents

1	Forward	5
1.1	Abstract.....	5
1.2	Résumé.....	6
1.3	Acknowledgments.....	8
1.4	Preface and Author Contributions.....	10
1.5	List of Figures and Tables.....	12
1.6	List of Abbreviations.....	15
1.7	List of Publications.....	17
2	Chapter 1. Introduction	19
2.1	General Introduction	19
2.2	Multiple Sclerosis	22
2.2.1	White matter lesions: axonal pathology.....	24
2.2.2	Gray matter lesions: soma pathology.....	25
2.2.3	Experimental autoimmune encephalomyelitis.....	27
2.2.4	Not all inflammation is bad.....	27
2.3	Regulators of axon regeneration	29
2.3.1	Inflammatory mediators of neuronal repair and regeneration.....	30
2.3.2	Intrinsic neuronal mediators regeneration.....	31
2.4	microRNA	32
2.4.1	microRNA biogenesis and function.....	33
2.4.2	microRNA in central nervous system disease and injury.....	36
2.4.3	Note on microRNA nomenclature.....	37
2.5	Rationale	38
	Results	39
	Preface	40
3	Chapter 2. Neuronal microRNA regulation in Experimental Autoimmune Encephalomyelitis	41
3.1	Abstract	42
3.2	Introduction	43
3.3	Results	45
3.3.1	Differential miRNA expression over the course of EAE in lumbar motor neurons.....	48
3.3.2	Differential miRNA expression over the course of EAE in the RGC layer.....	52
3.3.3	miR-Seq identified and validated miRNAs in EAE neurons are found regulated in other EAE/MS tissue....	54
3.3.4	<i>In silico</i> assessment of putative targets identifies novel pathways predicted to be affected in the neurons of EAE mice.....	54
3.4	Discussion	61
3.5	Acknowledgments	66
3.6	Competing Financial Interests	66
3.7	Materials and Methods	67
3.7.1	Active EAE Disease Induction and Scoring.....	67
3.7.2	CNS tissue isolation.....	67
3.7.3	Laser capture microdissection.....	67
3.7.4	RNA extraction from LCM tissue.....	68
3.7.5	Cell cultures.....	68
3.7.6	Next-Generation Sequencing (NGS).....	69
3.7.7	Quantitative RT-PCR (qRT-PCR).....	70
3.7.8	<i>In silico</i> assessment of predicted targets.....	71
3.8	Supplementary Tables	72
	Preface	81
4	Chapter 3. MicroRNA-223 protects neurons from degeneration in Experimental Autoimmune Encephalomyelitis	82
4.1	Abstract	83
4.2	Introduction	84
4.3	Results	86
4.3.1	miR-23a-3p, miR-27a-3p, miR-146a-5p and miR-223-3p are upregulated in EAE and MS.....	86
4.3.2	miR-27a-3p and miR-223-3p are neuroprotective.....	88
4.3.3	miR-223 overexpression rescues axonal degeneration in EAE optic nerve.....	90

4.3.4	miR-27a-3p and miR-223-3p mediate neuroprotection through glutamate receptor (GluR) signaling.....	95
4.4	Discussion.....	101
4.5	Acknowledgments and Funding.....	105
4.6	Competing Financial Interests.....	105
4.7	Materials and Methods.....	106
4.7.1	Experimental animals.....	106
4.7.2	Preparation of peripheral blood mononuclear cell conditioned media (PBMC-CM).....	106
4.7.3	Degeneration assays.....	106
4.7.4	Neuronal survival assay.....	107
4.7.5	Cell viability.....	107
4.7.6	Quantitative RT-PCR (qRT-PCR).....	107
4.7.7	Active EAE Induction.....	107
4.7.8	Laser-capture microdissection.....	108
4.7.9	Human brain samples	108
4.7.10	Histology.....	109
4.7.11	Whole mount optic nerve staining and clearing	109
4.7.12	Immunohistochemistry (IHC) in retinal sections.....	109
4.7.13	Intravitreal injection and AAV2-virus delivery.....	110
4.7.14	Quantification of RGC survival.....	110
4.7.15	<i>In silico</i> assessment of predicated targets.....	110
4.7.16	Luciferase assays.....	111
4.7.17	Statistical analyses.....	111
4.8	Supplementary Figures and Tables.....	112
	Preface.....	118
5	Chapter 4. Inhibition of miR-383 promotes axon regeneration following injury by a distributed relief of targets.....	119
5.1	Abstract.....	120
5.2	Introduction.....	121
5.3	Results.....	124
5.3.1	miR-383-5p is downregulated in growth-permissive conditions and upregulated in growth-inhibitory conditions.....	124
5.3.2	miR-383-5p downregulation is sufficient to promote axon growth	127
5.3.3	Inhibition of miR-383-5p promotes RGC axon regeneration following ONC	129
5.3.4	miR-383-5p is regulated by CNTF.....	131
5.3.5	miR-383-5p targets multiple genes contributing to axon regeneration.....	132
5.3.6	Crmp2 and Prdx3 regulates neurite outgrowth <i>in vitro</i>	133
5.3.7	Crmp2 and Prdx3 are upregulated in retinal neurons following zymosan-primed ONC.....	135
5.4	Discussion.....	136
5.5	Acknowledgments.....	140
5.6	Competing Financial Interests.....	140
5.7	Materials and Methods.....	141
5.7.1	Preparation of conditioned media.....	141
5.7.2	Neuronal cultures.....	141
5.7.3	Semi-quantitative RT-PCR.....	142
5.7.4	Quantitative RT-PCR (qRT-PCR).....	144
5.7.5	Luciferase assays.....	144
5.7.6	miR-383-5p sponge generation.....	145
5.7.7	<i>In vivo</i> axonal injury	145
5.7.8	Whole mount optic nerve clearing and axonal quantification.....	146
5.7.9	<i>In silico</i> assessment of predicated targets.....	147
5.7.10	Immunohistochemistry.....	147
5.7.11	Western blot.....	147
5.7.12	Statistical analyses.....	148
5.8	Supplementary Figures and Tables.....	149
	Discussion.....	155
6	Chapter 5. Discussion and conclusion.....	156
6.1	Summary of results.....	156
6.2	How to share your miRNAs with others.....	158
6.3	miR-27a-3p and miR-223-3p.....	160
6.3.1	GluR signaling in EAE/MS.....	160
6.3.2	miR-27a-3p and miR-223-3p as general mediators of neuroprotection.....	161
6.4	miR-383-5p.....	165
6.4.1	miR-383-5 in neurodegenerative disease.....	166

6.4.2	Determining additional roles of miR-383-5p in neurons.....	167
6.5	Making miR-iffic strides.....	167
6.5.1	miRNAs as druggable targets.....	167
6.5.2	miRNAs are on the menu.....	169
6.4	Conclusion.....	170
7	References.....	171

1 Forward

1.1 Abstract

Damages to the central nervous system (CNS) during neurodegenerative disease or by acute injury is marked by neuroinflammation. Neuroinflammation is dichotomous in that it can both positively and negatively impact repair and regeneration. In this thesis we are interested in understanding how neurons respond to pathological and positive inflammation and in using this information to develop neuroprotective and pro-regenerative therapies. To determine the molecular response to neuroinflammation, we investigated neuronal microRNA (miRNA) expression in models of neuroinflammation. miRNA are potent post-transcriptional regulators that coordinate hubs of gene expression. We first employed an animal model of pathological CNS inflammation, experimental autoimmune encephalomyelitis (EAE), to identify differentially expressed neuronal miRNAs and determine their mechanism of action. We identified miR-27a-3p and miR-223-3p as upregulated in the neurons of EAE animals. Yet, miR-27a-3p and miR-223-3p overexpression *in vitro* blocked inflammation-mediated neurodegeneration, and miR-223-3p overexpression *in vivo* limited EAE-axonopathy. Neuroprotection by miR-27a-3p and miR-223-3p was mediated by limiting pathogenic glutamate receptor signaling, demonstrating their upregulation in EAE as a neuroprotective response. Next, we examined the response of neurons to an inflammatory stimulus that promotes neuroprotection and axon regeneration. We identified miR-383-5p as a miRNA that is downregulated in retinal ganglion cells in response to intraocular inflammation. miR-383-5p inhibition following optic nerve crush was sufficient to promote axon regeneration. Regeneration by miR-383-5p loss-of-function was mediated by multiple signaling cascades including JAK/STAT3 signaling, cytoskeleton regulation, and oxidative stress management. Thus, using these models of neuroinflammation, we were able to describe the regulation of neuronal miRNA in pathological and neuroprotective models of inflammation and to harness this information to identify molecular strategies that promote neuroprotection and repair. Ultimately, this suggests new approaches for the development of disease-modifying therapies that promote repair and regeneration following CNS damage.

1.2 Résumé

Les dommages au système nerveux central (SNC) observés lors des maladies dégénératives ou suite à une lésion aiguë sont marqués par la neuroinflammation. La neuroinflammation est dichotomique, car elle peut avoir un impact tant positif que négatif sur la réparation et la régénération des neurones. Dans cette thèse, nous élucidons comment les neurones réagissent à l'inflammation pathologique et positive, dans le but de développer des stratégies qui favorisent la réparation et la régénération du SNC. Ici, nous utilisons des modèles de neuroinflammation pour investiguer l'expression des microARNs et pour élucider la réponse moléculaire des neurones. Les microARNs sont de puissants régulateurs post-transcriptionnels qui coordonnent les centres d'expression génique. Nous avons d'abord utilisé un modèle animal d'inflammation pathologique du SNC, encéphalomyélite auto-immune expérimentale (EAE), pour identifier les variations de l'expression des microARNs dans les neurones et déterminer leur mécanisme d'action. Nous avons observé que les microARNs miR-27a-3p et miR-223-3p sont régulés à la hausse dans les neurones des animaux EAE. Toutefois, la surexpression de miR-27a-3p et miR-223-3p *in vitro* bloquait la neurodégénérescence induite par l'inflammation. De plus, la surexpression de miR-223-3p *in vivo* limitait l'axonopathie observée lors de l'EAE. L'augmentation de l'expression de miR-27a-3p et miR-223-3p limitait la signalisation pathologique des récepteurs de glutamate, ce qui suggère que ces microARNs sont impliqués dans la neuroprotection. Ensuite, nous avons examiné la réponse des neurones suite à un stimulus inflammatoire qui favorise la neuroprotection et la régénération des axones. Nous identifions que l'expression de miR-383-5p diminuait dans les cellules ganglionnaires de la rétine en réponse à l'inflammation intraoculaire. L'inhibition de miR-383-5p suivant l'écrasement du nerf optique était suffisante pour permettre la régénération du nerf optique. La régénération était médiée par plusieurs mécanismes d'action qui incluent JAK/STAT3, la régulation du cytosquelette, et la gestion du stress oxydatif. Ainsi, avec ces modèles de neuroinflammation, nous avons décrit la régulation des microARNs dans les neurones suite à des scénarios pathologiques et protecteurs, et nous avons utilisé ces informations pour générer des stratégies qui permettent la réparation et régénération. Nos découvertes suggèrent de nouvelles

approches pour le développement de thérapies qui favorisent la réparation et la régénération des neurones suite à des maladies et/ou blessures du SNC.

1.3 Acknowledgments

Saying thank you to everyone who have helped me throughout the course of my PhD is incredibly challenging as I have been very fortunate throughout the whole process. As they do during the Oscars, I want to thank my parents first: Bo and Waldi. Both encouraging me throughout all of my struggles; though maybe too much, as they often suggested never leaving school. They also promised to read my thesis but were put off when I told them it is nearing 200 pages. To quote Waldi, “Why it so long, you writing a romance novel or something?”. I told them it’s because I have a lot of very impressive results.

Working at the Montreal Neurological Institute (MNI) has been the greatest fortune during my studies. There is always free food to be found, the kindest of staff, many shared student and staff appreciation events (i.e. Reitmans’ lunch, Spring Fling), beer hours, personal catering (thanks Anthony!), and collaborative research efforts- I even struggled finding an internal examiner because our laboratory has collaborated with so many other investigators within the MNI! Thank you to Dr Alyson E. Fournier for letting me become part of this community, and for including Dr Amit Bar-Or as my unofficial co-supervisor for the initiation of my doctorate. Drs Fournier and Bar-Or suggested key events and courses for me to take that shaped my understanding of neuroinflammation and passion for multiple sclerosis research. Drs Samuel David and Timothy Kennedy have also been instrumental to my scientific progression as my thesis advisors. Thank you to Tim for also letting me come into his office unannounced to talk about both results and non-results, including times I would come into his office crying about positive results that were a long-time coming.

The MNI community has been instrumental to my studies and I cannot imagine completing my doctorate at any other facility (though maybe the Google offices, I heard they have puppies). I am also on the best floor at the MNI, with the Stefano, Cloutier, Ruthazer, Kennedy, Levine, Sossin, and the former Coleman laboratory groups whom I often volun-forced to participate in themed events such as Halloween costume contests and Secret Santas (I expect Mardja Bueno and Sienna Drake to carry my torch when I leave). Of the Coleman group I have Drs Ajit Dhaunchak and Omar de Faria Junior to thank for sparking my interest in microRNA and training me during my first year. I am

leaving the MNI having made amazing friends including my work-wife Stephanie Nicole Harris; the other Kennedy lab members who graciously allow me to enter their lab trips; super woman Angie Giannakopoulos; Reesha Raja (thank you for re-teaching me how to do microscopy each time I come into your lab); Marie-Pier Girouard (for knowing literally everything); every single Fournier lab member past and present; the poor girls who were forced to attend conferences with me and therefore do all of the local activities (Zahraa Chorghay and Maran Ma); and so many more!! Most of all, thank you to Isabel Rambaldi who is the beating heart of the Fournier group. Not only does she run the laboratory, but she also ensures that each lab member is running well themselves. When I had my knee surgery midst-PhD, Isabel drove me to-and-back EVERYDAY for 3 months. She also started meal-prepping for me during the times I was overwhelmed with grant writing (but then kept doing it, because she realized I barely know how to cook rice).

I would also like to acknowledge my funding sources, specifically Dr Josephine Nalbantoglu for believing in me and driving my Vanier CIHR application; the MNI for regularly providing internal funding for either my stipend or travel; and the MS Society of Canada along with the endMS Network who provided me with the opportunity to network with fantastic researchers across the globe and to learn about MS on a bigger picture scale.

Finally, I cannot express how fortunate I am to have such a great support network outside of academia. Without this network I would also have never met my partner Paul Clavère. Thank you Paul for being the man you are: you have stood by me during the toughest times and pushed me to keep striving for the best. I cannot wait to continue 'Henrying' with you in our next chapter of life. And my cat, I cannot forget my cat, Bogdan Chmielnicki (aka Chmiel): thank you for being the world's most affectionate cat. I wish you meowed less in the mornings though.

1.4 Preface and Author Contributions

This thesis describes microRNA (miRNA) regulation in the context of neuroinflammation. It begins with a non-biased assessment of neuronal miRNA expression in a model of central nervous system (CNS) inflammation, experimental autoimmune encephalomyelitis (EAE) (chapter 2). This is followed by a characterization of two highly upregulated miRNAs in EAE, miR-27a-3p and miR-223-3p, which we identified as neuroprotective against inflammation-induced neurodegeneration. We go on to demonstrate that miR-223-3p overexpression blocked EAE-axonopathy *in vivo* (chapter 3). Finally, we move from neurodegeneration to regeneration. Using a model of axotomy, we identify that miR-383-5p loss-of-function promotes neurite outgrowth *in vitro* and regeneration *in vivo* through multiple signaling pathways (chapter 4). All the data described from chapters 2-4 are considered original scholarship.

Chapters 1 and 5 contain some text modified from a manuscript under peer-review at *Progress in Neurobiology* (submitted Nov 2018, reviewer comments received March 2019):

Jużwik C, Drake S, Zhang Y, Paradis-Isler N, Sylvester A, Amar-Zifkin A, Douglas C, Morquette B, Moore C, Fournier AE. microRNA dysregulation in neurodegenerative diseases: a systematic review. *Submitted to Progress in Neurobiology*.

Chapter 2 originally appeared as:

Jużwik C, Drake S, Lécuyer MA, Johnson RM, Morquette B, Zhang Y, Charabati M, Sagan S, Bar-Or A, Prat A, Fournier AE. (2018) Neuronal microRNA regulation in Experimental Autoimmune Encephalomyelitis. *Scientific Reports*. 8 (1): 13437.

C.A.J., B.M., A.P., S.M.S., A.B.O. and A.F. conceived and designed the experiments. C.A.J., S.D., M.A.L., B.M., Y.Z. and M.A. performed the experiments. C.A.J. and R.J. analyzed the data. C.A.J. and A.F. wrote the manuscript. C.A.J. and S.D. made the final figures. All authors read and approved the final manuscript.

Chapter 3 was submitted to *Brain* Nov 2018, revisions submitted March 2019:

Morquette B*, Jużwik C*, Drake S, Charabati M, Zhang Y, Lécuyer MA, Galloway DA, Dumas A, de Faria Junior O, Bueno M, Rambaldi I, Moore C, Bar-Or A, Vallieres L, Prat

A, Fournier AE. MicroRNA-223 protects neurons from degeneration in experimental autoimmune encephalomyelitis. [*co-authors contributed equally](#)

C.A.J., B.M., A.P., A.B.O. and A.F. conceived and designed the experiments. M.A.L. and M.C. performed EAE. B.M. developed the iDISCO method, characterized EAE-axonopathy in the optic nerve by iDISCO, performed *in vivo* experiments with AAV-miR-223, and made the associated figure. A.D., L.V., and S.Z. characterized and provided human MS tissue. Y.Z. aided in portions of the degeneration assays, retina sectioning, and development of ImageJ program to quantify degeneration in EAE optic nerve; and completed, analyzed and made the associated figure for the Luciferase assays. SD aided in portions of the degeneration assays and *in silico* analysis; and conducted the retinal IHC and made the associated IHC figure. D.A.G. and C.M. provided the miR-223 KO mice. N.P.-I. completed and analyzed the glutamate assays. I.R., O.F.J. and M.B. provided technical assistance. C.A.J. performed and analyzed all *in vitro* and *in silico* data; and B.M. the *in vivo* data. C.A.J., S.D. and A.F. wrote the manuscript. C.A.J. made all the final figures. All authors read and approved the final manuscript.

Chapter 4 is a manuscript in preparation:

Juźwik C*, Morquette B*, Zhang Y, Rambaldi I., Gowing E., Boudreau-Pinsonneault C, Liu Z, Vangoor V, Pasterkamp J, Moore C, Fournier AE. Inhibition of miR-383 promotes axon regeneration following injury by a distributed relief of targets.

[*co-authors contributed equally](#)

C.A.J., B.M., and A.F. conceived and designed the experiments. A.B.O. and A.F. supervised. B.M. performed ONC experiments. V.V. and P.J. aided in design of LNA *in vivo* experiments. B.M. and C.A.J. performed tissue whole mount, imaging, and analyses of all optic nerves together. Y.Z. performed retina sectioning, Luciferase assays, designed the miR-383 sponge, and made the mechanism schematic figure. I.R. provided technical assistance. E.G. and C.B.P. aided in initial candidate miRNA screens. Z.L. aided in Luciferase assays. C.M. provided ACM. C.A.J. performed and analyzed all other *in vitro* and *in silico* data. C.A.J. and Y.Z. wrote the manuscript. C.A.J. made all the final data figures.

1.5 List of Figures and Tables

Chapter 1. Introduction

Figure 1. Neuroinflammation is dichotomous: it can both promote neuronal damage or mediate repair and regeneration.....	21
Figure 2. microRNA processing.....	35
Table 1. Currently-approved DMTs used for the treatment of MS in North America.....	23

Chapter 2. Neuronal microRNA regulation in Experimental Autoimmune Encephalomyelitis

Figure 1. Laser captured lumbar motor neurons from EAE and control naive mice.....	46
Figure 2. Heat Map summary of significantly regulated miRNA as identified by miR-Seq in EAE....	47
Figure 3. Differentially regulated miRNAs in the lumbar motor neurons of EAE mice over the course of the disease.....	49
Figure 4. Profiling miRNA expression in the RGC layer of EAE mice.....	53
Figure 5. Flow-through of the <i>in silico</i> assessment for putative mRNA targets of the differentially regulated miRNAs in the lumbar motor neurons and RGC layer of EAE mice.....	55
Figure 6. The upregulated miRNAs of neurons during EAE potentially block neuroprotective responses to inflammation.....	57
Figure 7. Expression of predicted miRNA gene targets as identified by <i>in silico</i> analysis in the RGC layer.....	59
Table 1. miR-Seq validated miRNA expression in the EAE neuronal subtypes and as previously described in EAE and/or MS.....	50
Table 2. Overrepresented pathways and cellular components by the upregulated miRNAs in EAE neurons.....	56
Table 3. Overrepresented pathways and cellular components by the downregulated miRNAs in EAE lumbar motor neurons.....	60
Table 1 Supplemental. miRNA sequence information for custom design Taqman MicroRNA Assays.....	73
Table 2 Supplemental. Predicted gene targets in affected PANTHER Pathways of upregulated neuronal miRNAs.....	73
Table 3 Supplemental. Predicted gene targets in affected Reactome Pathways of upregulated neuronal miRNAs.....	74
Table 4 Supplemental. Predicted gene targets in affected GO cellular components of upregulated neuronal miRNAs.....	76
Table 5 Supplemental. Predicted gene targets in affected PANTHER Pathways of downregulated miRNAs in lumbar motor neurons.....	77

Table 6 Supplemental. Predicted gene targets in affected Reactome Pathways of downregulated miRNAs in lumbar motor neurons.....	79
Table 7 Supplemental. Predicted gene targets in affected GO cellular components of downregulated miRNAs in lumbar motor neurons.....	80

Chapter 3. MicroRNA-223 protects neurons from degeneration in Experimental Autoimmune Encephalomyelitis

Figure 1. Candidate miRNA expression in EAE and MS.....	87
Figure 2. miR-27a-3p and miR-223-3p overexpression prevents PBMC-CM-dependent neurodegeneration.....	89
Figure 3. miR-27a-3p and miR-223 loss-of-function reduces basal neurite growth without further sensitization to PBMC-CM.....	91
Figure 4. Axonal degeneration is rescued by neuronal overexpression of miR-223 <i>in vivo</i> in the EAE model.....	94
Figure 5. Inhibition of ionotropic GluR signaling protects against neurodegeneration <i>in vitro</i>	96
Figure 6. miR-27a-3p and miR-223-3p loss-of-function growth deficits can be restored through ionotropic GluR inhibition.....	98
Figure 7. miR-27a-3p and miR-223-3p target ionotropic glutamate receptor subunits.....	100
Supplementary Figure 1. Characterization of human MS lesion material.....	113
Supplementary Figure 2. Transfection validation of miRNA mimics and inhibitors.....	114
Supplementary Figure 3. PBMC-CM induces significant neurite degeneration independent of cell loss or death.....	115
Table 1 Supplemental. Putative filtered mRNA targets of miR-27a-3p and miR-223-3p.....	116
Table 2 Supplemental. Putative mRNA targets of miR-27a and miR-223 in investigated pathways as identified by PANTHER.....	117

Chapter 4. Inhibition of miR-383 promotes axon regeneration following injury by a distributed relief of targets

Figure 1. miR-383-5p is inversely regulated to neurite outgrowth.....	125
Figure 2. miR-383-5p is downregulated in retinal neurons in a model of CNS regeneration.....	126
Figure 3. miR-383-5p negatively regulates neurite outgrowth.....	128
Figure 4. Inhibition of miR-383-5p promotes optic nerve regeneration following optic nerve crush..	130
Figure 5. miR-383-5p is regulated by CNTF and regulates multiples cues promoting axon regeneration.....	131
Figure 6. miR-383-5p overexpression downregulates targets Crmp2 and Prdx3 in mouse cortical neurons.....	133

Figure 7. Crmp2 or Prdx3 knockdown prevents LNA-383 induced neurite outgrowth promotion...	134
Figure 8. Crmp2 and Prdx3 are upregulated in retinal neurons of zymosan-injected eyes post-ONC.....	135
Figure 9. Inhibition of miR-383-5p promotes axon regeneration following injury through a distributed relief of regenerative and growth associated mRNA targets.	137
Supplementary Figure 1. Candidate miRNA expression in cortical neurons stimulated with CNS injury-relevant conditioned media.....	149
Supplementary Figure 2. Validation of miR-383-5p expression for gain-of-function and loss-of-function experiments.....	149
Supplementary Figure 3. miR-383-sponge and control sponge design.....	150
Table 1 Supplemental. Primers of candidate miRNA used for semi-quantitative RT-PCR analysis.	151
Table 2 Supplemental. Expression of candidate miRNA in cortical neurons as assessed by semi-quantitative RT-PCR.....	152
Table 3 Supplemental. 3'UTR Sequences of Putative miR-383-5p mRNA targets used for Luciferase Assays (miR-383-5p seed regions in red).....	153

Chapter 5. Discussion and conclusion

Figure 1. We can harness the positive aspects of neuroinflammation to promote repair and regeneration.....	157
Table 1. Differential expression of miR-27a-3p and miR-223-3p across CNS disease and injury....	163

1.6 List of Abbreviations

3'UTR: 3' untranslated region

AAV2: adeno-associated virus 2

ACM: Astrocyte conditioned media

ALS: amyotrophic lateral sclerosis

AMD: aged-macular degeneration

AMPA: AMPA receptor

APP: amyloid precursor protein

AD: Alzheimer's disease

BMP: bone morphogenic protein

cAMP: cyclic adenosine monophosphate

CCAC: Canadian Council on Animal Care

CCKR: cholecystokinin receptor

CFA: complete Freund's adjuvant

CIS: clinically isolated syndrome

CNS: central nervous system

CNTF: ciliary neurotrophic factor

CSF: cerebrospinal fluid

CSPG: chondroitin sulfate proteoglycan

CTG: CellTitre-Glo

DBE: benzyl ether

DGCR8: DiGeorge Syndrome Critical Region 8

DIV: days in vitro

DM: myotonic dystrophy

DMT: disease-modifying therapy

dpi: days post injury

DRG: dorsal root ganglion cell

E: embryonic day

EAE: experimental autoimmune encephalomyelitis

EGF: epidermal growth factor

FBS: fetal bovine serum

FGF: fibroblast growth factor

GluR: glutamate receptor

GnRH: gonadotropin-releasing hormone

GO: gene ontology

HC: healthy control

HD: Huntington's disease

HIF: hypoxia inducible factor

iDISCO: immunolabeling-enabled three-dimensional imaging of solvent cleared

IGF: insulin-growth factor

IL: interleukin

JAK: Janus kinase

KLF4: krüppel-like factor 4

KO: knockout

LCM: laser capture microdissection

LI: lens injury

MBP: myelin basic protein

MeOH: methanol

MHC: major histocompatibility complex

miRISC: microRNA-induced silencing complex

miRNA: microRNA

MOG: myelin oligodendrocyte glycoprotein

mRNA: messenger RNA

MRI: magnetic resonance imaging

MS: multiple sclerosis

mTOR: mammalian target of rapamycin

MWCS: Multiwavelength Cell Scoring

NAWM: normal-appearing white matter

NGS: next-generation sequencing

NMDAR: NMDA receptor

NO: nitric oxide

OCT: optimal cutting temperature

ON: optic nerve

ONC: optic nerve crush

PANTHER: Protein ANalysis THrough Evolutionary Relationships

PFA: paraformaldehyde

PBMC: peripheral blood mononuclear cell

PBMC-CM: PBMC conditioned media

PCR: polymerase chain reaction

PD: Parkinson's disease

PDGF: platelet-derived growth factor

PI3K: phosphatidylinositol 3-kinase

PIP: phosphatidylinositol phosphate

PKMT: protein lysine methyltransferase

PLL: poly-L-lysine

PLP: phospholipid protein

PNS: peripheral nervous system

PP2A: protein phosphatase type 2A

PPMS: primary progressive multiple sclerosis

PTX: pertussis toxin

PTEN: phosphatase and tensin homolog

qPCR: quantitative polymerase chain reaction

RAG: regeneration-associated gene

RGC: retinal ganglion cell

RNA Pol: RNA Polymerase

ROS: reactive oxygen species

RRMS: relapsing-remitting multiple sclerosis

RT: reverse transcription

RT-PCR: reverse transcription polymerase chain reaction

SCI: spinal cord injury

SDS-PAGE: sodium dodecyl sulphate- polyacrylamide gel electrophoresis

SG: stress granule

snRNA: small nuclear RNA

SOCS3: suppressor of cytokine 3

SPMS: secondary progressive multiple sclerosis

STAT: signal transducers and activators of transcription

TBI: traumatic brain injury

T_H: T helper

TLR2: toll-like receptor 2

TNF: tumor necrosis factor

TRAIL: TNF-related apoptosis inducing ligand

T_{reg}: T regulatory cells

WM: white matter

WT: wild-type

1.7 List of Publications

* **co-authors contributed equally**

[1] **Jużwik C**, Drake S, Zhang Y, Paradis-Isler N, Sylvester A, Amar-Zifkin A, Douglas C, Morquette B, Moore C, Fournier AE. microRNA dysregulation in neurodegenerative diseases: a systematic review. *Submitted to Progress in Neurobiology, reviewer comments received March 21, 2019.*

[2] Morquette B*, **Jużwik C***, Drake S, Charabati M, Zhang Y, Lécuyer MA, Galloway DA, Dumas A, de Faria Junior O, Bueno M, Rambaldi I, Moore C, Bar-Or A, Vallieres L, Prat A, Fournier AE. MicroRNA-223 protects neurons from degeneration in experimental autoimmune encephalomyelitis. *Submitted to Brain, Nov 2018, revisions received Feb 2019, revisions submitted March 25 2019; earlier version available on BioRxiv.*

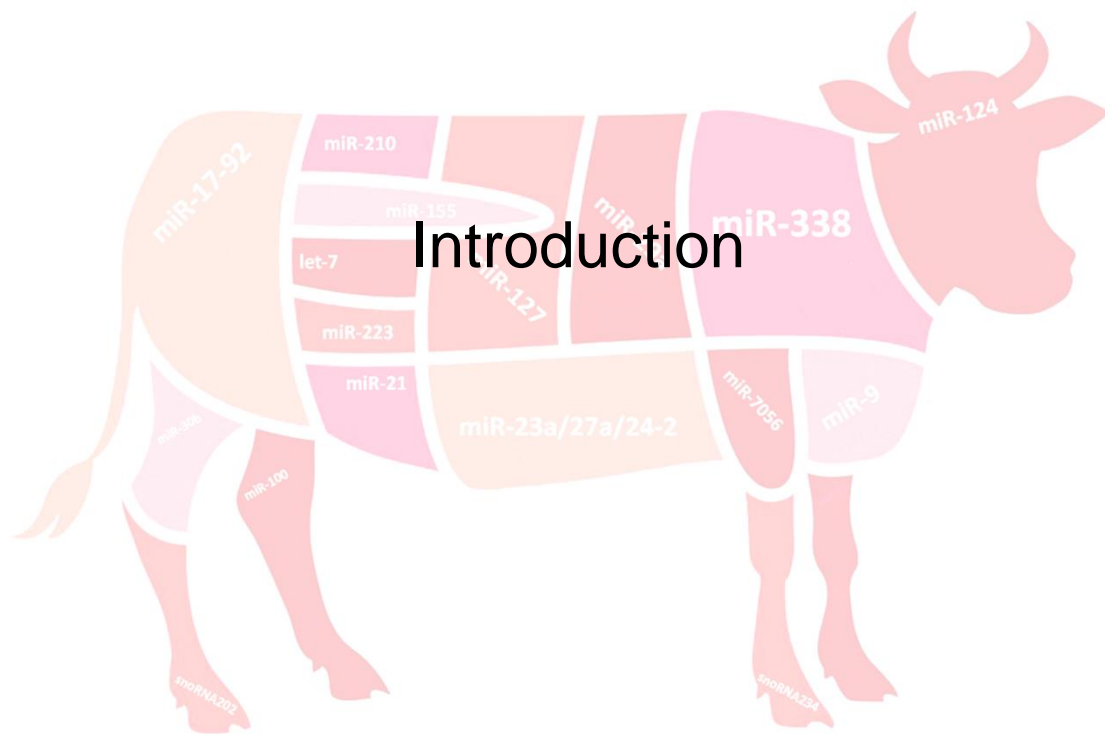
[3] **Jużwik C**, Drake S, Lécuyer MA, Johnson RM, Morquette B, Zhang Y, Charabati M, Sagan S, Bar-Or A, Prat A, Fournier AE. (2018) Neuronal microRNA regulation in Experimental Autoimmune Encephalomyelitis. *Scientific Reports*. 8 (1): 13437.

[4] Paré A, Mailhot B, Lévesque SA, **Jużwik C**, Doss PMIA, Lécuyer MA, Prat A, Rangachari M, Fournier A, Lacroix S. (2018) IL-1 β enables CNS access to CCR2^{hi} monocytes and the generation of pathogenic cells through GM-CSF released by CNS endothelial cells. *PNAS*. 115 (6).

[5] Plemel JR*, **Jużwik C***, Benson CA*, Monks M, Harris C, Ploughman M. (2015) Over-the-counter anti-oxidant therapies for use in multiple sclerosis: a systematic review. *Multiple Sclerosis Journal*. 21(12): 1485-1495.

[6] Belkaid W, Thostrup P, Yam PT, **Jużwik C**, Ruthazer ES, Dhaunchak A, Colman DR. (2013) Cellular response to micropatterned growth promoting and inhibitory substrates. *BMC Biotechnology*. 13:86.

[7] Shen S, Callaghan D, **Jużwik C**, Xiong H, Huang P, Zhang W (2010). ABCG2 reduces ROS-mediated toxicity and inflammation: a potential role in Alzheimer's disease. *J Neurochem*. 114(6):1590-604.



2 Chapter 1. Introduction

2.1 General Introduction

Neurons are the fundamental signaling units of the nervous system. A neuron consists of a soma (the cell body) and neurite processes that are the axon and dendrites. An axon is the longest neurite of a neuron, and extends onto other neuronal cell bodies, muscle, or glands to transmit information. Dendrites are shorter neurites extending from the cell body, onto which upstream axons transmit their information. This connection between axonal ends and tissue or dendrites is termed a synapse, and its structural maintenance is essential for proper neuronal function. Neurons can be damaged during neurodegenerative disease or by acute cell damage such as spinal cord injury (SCI). Neurons that are part of the central nervous system (CNS), consisting of the brain, spinal cord, and optic nerve, fail to spontaneously repair. Without spontaneous repair, neurons experience progressive structural and functional loss that leads to cell death. It is thus important to design therapeutics which promote neuroprotection and repair following injury. In response to CNS damage, microglia are activated and elicit a series of inflammatory events. Microglia are the innate immune cells of the CNS, constantly patrolling the CNS for infectious agents and damaged neurons, which they engulf by phagocytosis (DiSabato, Quan et al. 2016). At the same time there is a physical barrier surrounding the CNS, termed the blood brain barrier (BBB) (Abbott, Patabendige et al. 2010, Michell-Robinson, Touil et al. 2015). The BBB is maintained by tight junctions between brain endothelial cells, the basal lamina of these cells, and astrocytic endfeet processes (Abbott, Patabendige et al. 2010). Any breaches to the BBB allow for the aberrant infiltration of peripherally-circulating immune cells or pathogens into the otherwise immune privileged CNS to further enhance inflammation (Popovich and Jones 2003, Donnelly and Popovich 2008, Yong, Chartier et al. 2018). Neuroinflammation is this series of inflammatory events in the CNS.

Neuroinflammation is dichotomous in that it promotes both positive and negative effects (Fig. 1). In the context of neuronal degeneration, inflammation can be positive by promoting microglia and infiltrating-macrophages to phagocytose growth-inhibitory debris around injury sites, by promoting repair mechanisms such as remyelination, and in some contexts by promoting neuroprotection and regeneration (Leon, Yin et al. 2000, Michell-

Robinson, Touil et al. 2015). Simultaneously, inflammation can be negative by promoting demyelination, reactive astrocytes, and the secretion of neurotoxic cytokines and excitotoxic mediators (Schroeter and Jander 2005). These negative effects are emphasized during chronic inflammatory situations as in neurodegenerative disease and acute injury. We are interested in understanding how neurons respond to different types of neuroinflammation and in using this information to protect neurons from negative neuroinflammatory elements while harnessing positive inflammatory responses to promote repair and regeneration.

In this thesis we would like to define a molecular approach that could regulate programs of gene expression in neurons in response to injury to mediate neuroprotection or repair. For this reason, we have focused on microRNAs (miRNAs). miRNAs are small, non-coding sequences of RNA that act as potent post-transcriptional regulators to coordinate hubs of gene expression (Lewis, Shih et al. 2003, Cui, Yu et al. 2006, Shalgi, Lieber et al. 2007). A single miRNA can target multiple mRNA transcripts from either a shared pathway, or from functionally unrelated pathways (Friedman, Farh et al. 2009). Dysregulation of a single miRNA can in turn disrupt the expression of multiple genes and their signaling networks. Determining differential neuronal miRNA expression during inflammation is thus a worthwhile approach to determine the comprehensive neuronal response to inflammation during CNS damage. In the studies discussed herein, we investigate the regulation of miRNA expression in models of neuroinflammation to determine their functional role during neurodegeneration and regeneration; with emphasis on multiple sclerosis (MS), as it is a chronic inflammatory, neurodegenerative disease with extensive neuronal and axonal damage. We employ an animal model of CNS inflammation, experimental autoimmune encephalomyelitis (EAE). EAE is a widely used model to study components of MS. As well, we use a model intraocular inflammation to investigate positive neuroinflammatory stimuli. Using these models of neuroinflammation, we aim to determine the global neuronal response to inflammation and harness that information to determine molecular strategies that promote neuroprotection and repair. Ultimately our findings can improve our approach in the development of disease-modifying therapies (DMTs) that promote repair and regeneration following CNS damage.

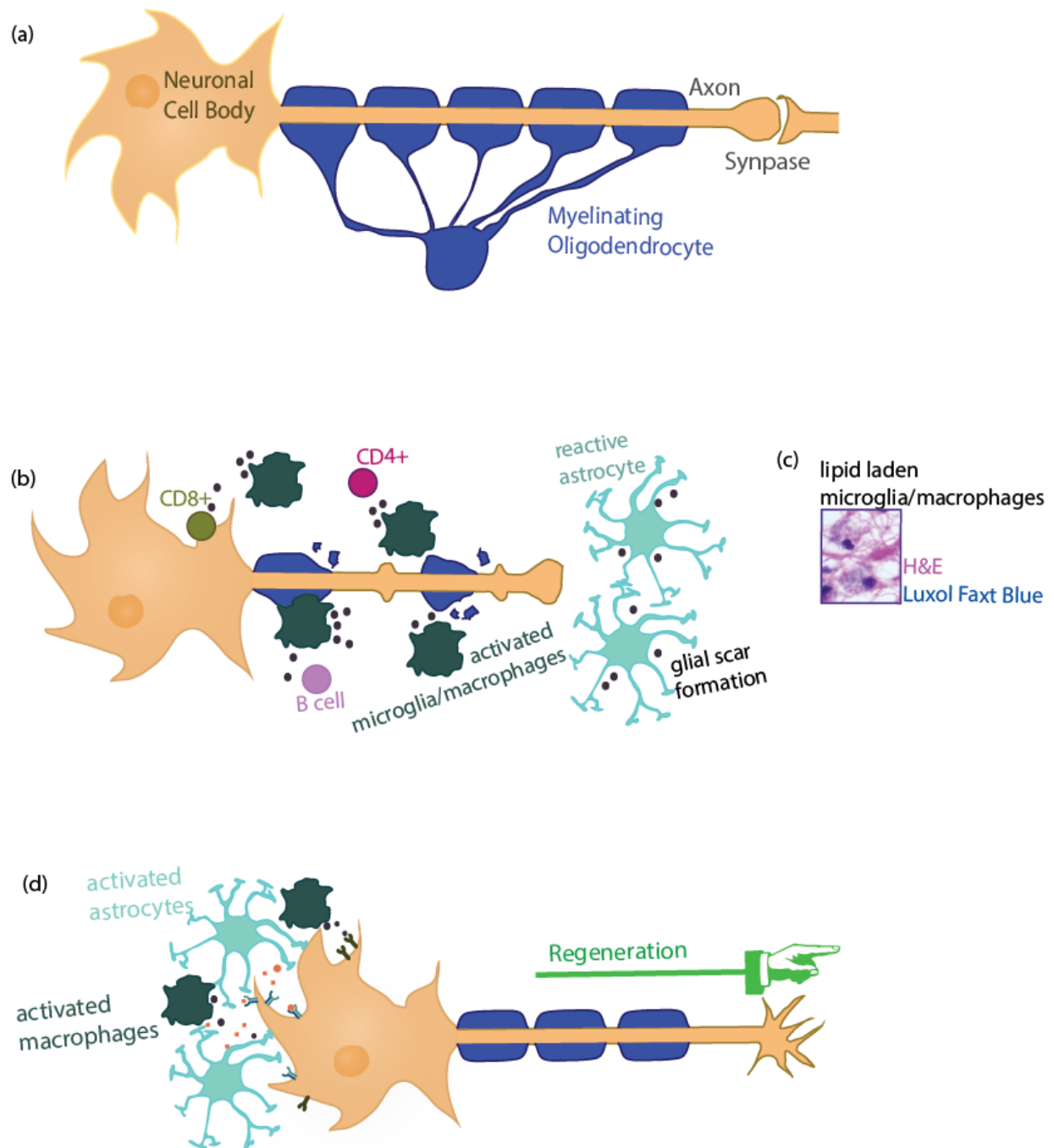


Figure 1. Neuroinflammation is dichotomous: it can both promote neuronal damage or mediate repair and regeneration. (a) A healthy neuron is myelinated and functionally connected via a synapse to another neuron. (b) During neuroinflammatory diseases such as MS, the infiltration of peripheral immune cells and the activation of innate microglia and astrocytes contributes to demyelination and axonal transection. (c) Lipid laden microglia/macrophages depicted in an active lesion of an SPMS patient, visualized with hematoxylin and eosin (H&E) and Luxol Fast Blue, a myelin stain. Clearance of this debris is also essential for any possible remyelination. (d) Artificial inflammation following an optic nerve crush promotes activation of astrocytes and the infiltration of peripheral macrophages into the vitreous. These cells secrete neurotrophic factors that drive axonal regeneration.

2.2 Multiple Sclerosis

MS is the most common neurological disability in young adults, with diagnoses between 20-40 years of age; and with an incidence of 290 per 100 000 in Canada, one of the highest incidences worldwide (Gilmour, Ramage-Morin et al. 2018). MS is an inflammatory demyelinating, neurodegenerative disease primarily affecting the CNS (Peterson and Fujinami 2007, Toosy, Ciccarelli et al. 2014). In 1868, French neurologist Jean-Martin Charcot gave the first description of MS, coining it *la sclérose en plaques* (Charcot 1868). He formulated a diagnostic criterion formed by the Charcot triad that is nystagmus, intention tremor, and scanning speech; along with illustrations of pathological lesions, where he detailed how axons are stripped of their myelin. Since then the diagnostic criteria has evolved to form the 2017 McDonald Criteria, which requires two of three criteria for MS diagnosis that are ≥ 1 clinical attack(s); clinical CNS lesions disseminated in space, as detected by magnetic resonance imaging (MRI); and a measure of cerebrospinal fluid (CSF) oligoclonal bands (Thompson, Banwell et al. 2018).

MS is a heterogenous disease that is broken down into multiple subtypes. Approximately 85% of MS patients are diagnosed with relapsing-remitting MS (RRMS), where patients experience a neurological attack, or 'relapse', followed by a period of 'remission' where their neurological deficit(s) resolves (Filippi, Bar-Or et al. 2018). In RRMS aberrantly activated peripheral immune cells cross a compromised BBB to promote an inflammatory course of disease. An estimated 50% of individuals diagnosed with RRMS convert to a secondary progressive MS (SPMS) phase 10-20 years following their initial diagnosis, where patients suffer from increasing clinical disability that matches an increasing neurodegenerative pathology (Miller 2012). The remaining 15% of MS patients are primary progressive (PPMS) follow an uninterrupted progressive clinical deterioration from onset of diagnosis that is due to increasing neurodegeneration, independent of inflammatory infiltrates (Filippi, Bar-Or et al. 2018). Almost all current DMTs manage RRMS by targeting immune cell infiltrates, without addressing the underlying neurodegenerative pathology (Table 1). Yet the neurodegeneration seen in MS is directly associated with clinical disability (Dutta and Trapp 2007). The DMTs suggested for SPMS are Interferon- β , which limits relapses but not disease progression, and mitoxantrane, which comes with a high risk of systolic dysfunction and leukemia,

meaning there is still no clear-cut DMT for SPMS (Marriott, Miyasaki et al. 2010, La Mantia, Vacchi et al. 2013). Only recently in 2017, has ocrelizumab been identified to reduce progression in early PPMS (Wolinsky, Montalban et al. 2018). This emphasizes the current gap in knowledge between the inflammatory and neurodegenerative disease components of MS. Here we will discuss the heterogeneity of MS lesions, the neuronal response at the lesion, and how we can employ EAE to investigate components of the neuroinflammatory MS environment.

Table 1.

*Currently-approved DMTs used for the treatment of MS in North America**

DMT		Intended usage** (method of administration)
Scientific name	Drug name, Company (year released)	
Interferon-β1b	<ul style="list-style-type: none"> Betaseron, Bayer (1993 US, 1995 Canada) Extavia, Novartis (2009 US, Canada) 	RRMS first-line treatment, SPMS*** (injectable)
Interferon-β1a	<ul style="list-style-type: none"> Avonex, Biogen (1996 US, 1998 Canada) Rebif, Serono (1998 US, 2002 Canada) 	RRMS first-line treatment, SPMS*** (injectable)
Glatiramer acetate	<ul style="list-style-type: none"> Copaxone, Teva (1996 US, 1997 Canada) Glatopa, Novartis (2015 US) Glatiramer acetate, Mylan (2017 US) Glatect, PendoPharm (2017 Canada) 	RRMS first-line treatment (injectable)
Mitoxantrone	<ul style="list-style-type: none"> Novantrone, generic medication (2000 US, only as “off-label” use in Canada) 	RRMS second-line treatment, SPMS (intravenous)
Natalizumab	<ul style="list-style-type: none"> Tysabri, Biogen (2006 US, Canada) 	RRMS second-line treatment (intravenous)
Fingolimod	<ul style="list-style-type: none"> Gilenya, Novartis (2010 US, 2011 Canada) 	RRMS second-line treatment (oral)
Teriflunomide	<ul style="list-style-type: none"> Aubagio, Sanofi (2012 US, 2013 Canada) 	RRMS first-line treatment (oral)
Dimethyl fumarate	<ul style="list-style-type: none"> Tecfidera, Biogen (2013 US, Canada) 	RRMS first-line treatment (oral)
Ocrelizumab	<ul style="list-style-type: none"> Ocrevus, Roche (2013 Canada, 2017 US) 	RRMS second-line treatment, early PPMS (intravenous)
Pegylated Interferon-β1a	<ul style="list-style-type: none"> Plegridy, Biogen (2014 US, 2015 Canada) 	RRMS first-line treatment (injectable)
Alemtuzumab	<ul style="list-style-type: none"> Lemtrada, Sanofi (2014 US, Canada) 	RRMS second-line treatment (intravenous)
Cladribine	<ul style="list-style-type: none"> Mavenclad, Serono (2017 Canada) 	RRMS second-line treatment (oral)

*Information adapted from the American and Canadian MS Society webpages (Canada 2018, Society 2018).

**RRMS second-line treatment are for those who experienced rapidly evolving lesions, diagnosed as ≥ 3 MRI lesions within a year while on RRMS first-line treatment.

***SPMS patients with relapses. None of the Interferon- 1β products are approved for SPMS treatment in the United States.

2.2.1 White matter lesions: axonal pathology

The pathological hallmark of all MS subtypes is lesions, also known as plaques, which are areas of demyelination and axonal degeneration (Filippi, Bar-Or et al. 2018). They occur at random throughout the CNS, including the white and gray matter of the brain, spinal cord and optic nerve. Generally, the anatomical location corresponds to specific clinical deficits, such that a lesion on the optic nerve corresponds to optic neuritis (Charil, Zijdenbos et al. 2003, Rocca, Amato et al. 2015, Gass and Costello 2018). Lesions can increase or decrease in number and size. This heterogeneity is attributed to the variety of inflammatory cells and their secreted products which oligodendrocytes and neurons are exposed to. The inflammatory cells that can be found in MS lesions include reactive microglia, reactive astrocytes, and immune cell infiltrates such as T cells, B cells, and macrophages (Dendrou, Fugger et al. 2015). To note, when macrophages have phagocytosed cellular material, they cannot be distinguished from microglia based on their morphology or antigenic profile and in turn are referred to as macrophage/microglia (David, Zarruk et al. 2012). To investigate the molecular signaling in neurons and their axons in response to inflammation, it is important to understand the biology of these white and gray matter lesions in MS.

The white matter consists of axons, their myelin sheath and oligodendrocytes, all of which are affected in MS lesions. Specifically, early active white matter lesions are hypercellular, filled with reactive macrophages/microglia, reactive astrocytes, and lymphocyte infiltrates that mediate the axon and myelin damage (Kuhlmann, Ludwin et al. 2017). As early as active lesions, axonal ovoids characteristic of transected axons are detectable, along with amyloid precursor protein (APP) accumulation (Ferguson, Matyszak et al. 1997). As APP is required for fast axonal transport, it is detectable only when axons are injured due to accumulation from disturbed axonal transport (Gentleman,

Nash et al. 1993, Sherriff, Bridges et al. 1994). APP accumulation occurs as soon as 2 hours after injury and remains detectable in axons and bulbs for 10 to 14 days post injury, acting as an early marker of axonal injury (Gentleman, Nash et al. 1993, Geddes, Vowles et al. 1997). Deficits in axonal transport results in a reduction of the net organelle delivery from the soma to synapses, such that axonal function and integrity become compromised due to the loss of essential organelles like mitochondria (Sorbara, Wagner et al. 2014). Reactive macrophages/microglia secrete excitotoxic mediators such as glutamate, reactive oxygen species (ROS) and nitrogen specie (RNS). Neutralizing ROS and RNS can resolve early axonal swellings and transport deficits, as demonstrated in EAE (Nikic, Merkler et al. 2011, Sorbara, Wagner et al. 2014). Infiltrating T cells are suggested to also contribute to axonal injury, though the exact mechanism is still unknown (Dendrou, Fugger et al. 2015). T cells exist as major histocompatibility complex (MHC) class-I restricted CD8⁺ T cells and MHC class-II restricted CD4⁺ T cells (Murphy, Travers et al. 2012). Neurons express neither MHC class-I or class-II, though aged motor neurons as well as hippocampal neurons stimulated with IFN- γ do express MHC class-I, making them vulnerable targets for CD8⁺ T cell cytotoxic targeting (Neumann, Cavalie et al. 1995, Edstrom, Kullberg et al. 2004). IFN- γ can be secreted by both CD4⁺ and CD8⁺ T cells (Rostami and Ciric 2013, Salou, Nicol et al. 2015, van Langelaar, van der Vuurst de Vries et al. 2018). Simultaneously, immune cell infiltrates mediate axonal demyelination, though the exact mechanism is also not completely understood, that results in production of growth-inhibitory myelin debris; decreased myelin-derived trophic support; and a forced redistribution of sodium channels at the Nodes of Ranvier, altering axonal conduction (Waxman 2006, Yiu and He 2006, Dutta and Trapp 2011, Dendrou, Fugger et al. 2015). Lesions are inactive when they become hypocellular and an astrocytic scar forms, impeding potential tissue repair (Holley, Gveric et al. 2003, Kuhlmann, Ludwin et al. 2017). Thus, inflammatory cells compromise axonal integrity via multiple methods, leading to neurodegeneration at the lesions.

2.2.2. Gray matter lesions: soma pathology

The gray matter contains neuronal cell bodies and their dendrites, with relatively less myelin. Demyelination can be detected in MS gray matter, along with neuronal loss

as identified in MS spinal cord, neocortex, and retina (Vogt, Paul et al. 2009, Green, McQuaid et al. 2010, Magliozzi, Howell et al. 2010, Balk, Cruz-Herranz et al. 2016, Carassiti, Altmann et al. 2018). The extent of inflammatory infiltrates is however lower in gray matter lesions than in white matter lesions, though not completely absent (Filippi, Preziosa et al. 2013, Rocca, Sormani et al. 2017). In the spinal cord, dying motor neurons of the gray column are regularly surrounded by CD4⁺ and CD8⁺ T cells expressing tumor necrosis factor (TNF)-related apoptosis inducing ligand (TRAIL), an inducer of apoptosis (Vogt, Paul et al. 2009). In cortical lesions, activated macrophages/microglia closely appose and envelope neuritic elements and neuronal cell bodies (Peterson, Bo et al. 2001). Cortical lesions are broken down into three subtypes that are type I leukocortical, demyelinating both the white and grey matter; type II intracortical, where only the inner cortical layers are involved; and type III subpial, extending from the pial surface to the cortex (Peterson, Bo et al. 2001). From these three subtypes of cortical lesions, intracortical are the most difficult to study in terms of the neuronal response to inflammation. Assuming intracortical lesions arise due to downstream damaged axons by retrograde injury to the cortex, it is difficult to trace axons back to their respective soma (Calabrese, Magliozzi et al. 2015). Leukocortical lesions are ideal candidates for investigation of the direct inflammatory impact on neurons, as the inflammation impacting the white matter is immediately adjacent the inflamed gray matter. In turn, leukocortical lesions display significant neuronal, glial, and synaptic loss (Wegner, Esiri et al. 2006). As well, subpial lesions, unique to MS pathology, are believed to arise from the B cells, T cells, and macrophages that induce meningeal inflammation, secreting their factors into the CSF and in turn bathing the cerebral cortex (Calabrese, Magliozzi et al. 2015, Machado-Santos, Saji et al. 2018). In line with this, SMPS cases with exaggerated meningeal inflammation coincide with extensive subpial demyelination; higher neuronal, astrocyte, and oligodendrocyte loss; and increased microglial activation (Magliozzi, Howell et al. 2010, Howell, Reeves et al. 2011). Thus, both in white and gray matter lesions it is evident that neurons undergo extensive inflammation-mediated damage during MS, however the molecular responses of neurons to this inflammation are still unclear.

2.2.3 Experimental autoimmune encephalomyelitis

Much of what we know about MS comes from a mouse model of CNS inflammation, EAE (Miller 2012). EAE is induced by immunization with a myelin peptide as antigen and complete Freund's adjuvant (CFA), along with an injection of pertussis toxin (PTX) on the day of immunization and two days later (Miller, Karpus et al. 2010, Bittner, Afzali et al. 2014). In turn, T cells are activated in the periphery, which then migrate into the CNS across a leaky BBB, made leaky by the PTX. This results in a monophasic disease course that follows an ascending paralysis tracked with a simple scoring system from 0 to 5, where 0 refers to no clinical deficits and 5 refers to moribund (Miller, Karpus et al. 2010). EAE induction in C57Bl/6 mice with myelin oligodendrocyte glycoprotein (MOG) peptide is the most commonly used model of EAE. It mimics the T-cell and macrophage-mediated demyelination of MS, along with the axonal injury found within demyelinated plaques (Gold, Linington et al. 2006). The EAE mouse model is a useful tool for studying CNS inflammation and it phenocopies central components of MS, including the neuroaxonal pathology. As in MS spinal cord, there is lumbar motor neuron loss that begins at onset of disease and is significant at peak disease (Vogt, Paul et al. 2009). This coincides with APP accumulation and axonal transection in the lumbosacral region of the spinal cord (Bannerman, Hahn et al. 2005, Hassen, Feliberti et al. 2008, Vogt, Paul et al. 2009, Hoflich, Beyer et al. 2016). Optic nerve pathology has also been identified in EAE like in MS, including immune cell infiltration, demyelination, glial activation, retinal ganglion cell (RGC) loss, and axonal swellings (Shindler, Ventura et al. 2008, Quinn, Dutt et al. 2011, Horstmann, Schmid et al. 2013, Horstmann, Kuehn et al. 2016). Thus, using the chronologically anticipated clinical deficits in EAE, we can track the molecular responses to neuroinflammation.

2.2.4 Not all inflammation is bad

There is extensive inflammation-mediated damage in the CNS during neurodegenerative disease, particularly in MS. However, not all of these inflammatory responses are negative, some of these responses are an attempt to mediate repair and regeneration. The inflammatory mediators in MS are reactive macrophages/microglia, reactive astrocytes, and infiltrating lymphocytes (Filippi, Bar-Or et al. 2018). Each of these

components can be broken down to demonstrate their ability to mediate repair and regeneration. Reactive macrophages/microglia perform both pro-inflammatory and anti-inflammatory roles. Pro-inflammatory roles are affiliated with the production of deleterious factors such as excess glutamate, ROS, and RNS that contribute to the functional blockade and/or structural damage in axons discussed above (Dutta and Trapp 2007, Chu, Shi et al. 2018). Anti-inflammatory macrophages/microglia instead produce immunosuppressive cytokines and neurotrophic factors; promote remyelination; and show greater phagocytosing ability, all of which can contribute to neuronal repair and regeneration (Miron, Boyd et al. 2013, Nakagawa and Chiba 2015, Chu, Shi et al. 2018). To note, the designation of pro- and anti-inflammatory macrophages/microglia helps us conceptualize myeloid-cell involvement in disease, however it is a spectrum of myeloid-cell function (formerly “M1” and “M2”, respectively), as macrophages/microglia have high plasticity and can adopt a range of polarizations depending on the microenvironment (Stout, Jiang et al. 2005, Xue, Schmidt et al. 2014, Ransohoff 2016). Both pro- and anti-inflammatory macrophages/microglia have been described in MS and EAE, as reviewed (Chu, Shi et al. 2018).

Similarly, the dichotomous reactivity of astrocytes has been coined as A1/A2; and like macrophages/microglia, astrocytes are believed to assume a range of profiles with mixed A1 and A2 features (Liddelw and Barres 2017, Ponath, Park et al. 2018). CNS injury prompts astrocytic hypertrophy (astrogliosis) and proliferation (astrocytosis), with subsequent glial scar formation at the injury site (Montgomery 1994). In neurodegenerative disease including MS, A1 is induced by activated microglia, gaining a neurotoxic function, rapidly killing neurons and mature differentiated oligodendrocytes (Liddelw and Barres 2017). Yet, not all A1 functions are negative. In demyelinating MS lesions, hypertrophic A1 astrocytes express chemokines that prompt immune cell recruitment (Van Der Voorn, Tekstra et al. 1999). Genetic ablation of astrocytes in a cuprizone model of demyelination prevented the recruitment of microglia to the injury site, delaying removal of myelin debris and thus axonal remyelination (Skripuletz, Hackstette et al. 2013). As well, the A1-formed glial scar, present in inactive MS lesions, has been demonstrated to prevent axonal dieback (Holley, Gveric et al. 2003, Anderson, Burda et al. 2016).

Lastly, the infiltrating immune cells, particularly T cells, also demonstrate an ability to promote neuronal repair and regeneration. In our laboratory we demonstrated that activated CD4⁺ T cells promote cerebellar neurite outgrowth *in vitro* (Pool, Rambaldi et al. 2012). Another group demonstrated that IFN- γ expressing CD4⁺ T cells (T_h1) promote cortical neurite outgrowth *in vitro* (Ishii, Kubo et al. 2010). T_h1 and T_h17, interleukin (IL)-17 expressing CD4⁺ T cells, are the most widely implicated pro-inflammatory effector T cells in MS and EAE pathology (Filippi, Bar-Or et al. 2018). Current DMTs or experimental approaches attempt to drive the T_h1/T_h17 profile of MS patients and EAE, respectively, to an anti-inflammatory, regulatory T cell profile. In summation, the environment in MS is highly heterogeneous; however, the final outcome is pathological, and neurons and oligodendrocytes undergo degeneration and death. What is missing in the field of neurodegenerative disease research is an investigation of the molecular response of neurons to inflammation. This information can help develop molecular strategies that promote neuroprotection and repair.

2.3 Regulators of axon regeneration

Models of acute axonal damage have revealed positive aspects of inflammation. Intraocular inflammation by lens injury (LI) or intravitreal injection of toll-like receptor 2 (TLR2) agonists, such as zymosan, can promote axonal survival and axon regeneration following acute nerve cell damage (Leon, Yin et al. 2000, Yin, Cui et al. 2003, Muller, Hauk et al. 2007, Leibinger, Muller et al. 2009, Hauk, Leibinger et al. 2010, Kurimoto, Yin et al. 2013). In the adult mammalian CNS, neurons have a decreased intrinsic capacity for repair and regeneration that is further hampered by external factors such as myelin debris and glial scar formation (Cai, Qiu et al. 2001, Yiu and He 2006, Fitch and Silver 2008). Intraocular inflammation thus promotes the intrinsic mechanisms of repair in neurons and their axons to overcome the inhibitory factors that block CNS regeneration. In neurodegenerative diseases such as MS, axons undergo swelling and eventual transection, as discussed above. When we are thinking about chronic stages of disease we may also have to think about repairing this damage through axon regrowth strategies. Here we will discuss how inflammation can promote regeneration, and what we currently know about the molecular response of neurons to injury.

2.3.1 Inflammatory mediators of neuronal repair and regeneration

The optic nerve crush (ONC) model is ideal for investigating the neuronal response to injury as it is a more accessible CNS structure, and a more homogenous neuronal response to injury as the transection corresponds to retinal ganglion cell (RGC) axons exclusively (London, Benhar et al. 2013). RGCs being the soma which form the optic nerve. Two weeks post-injury RGC death is as high 80%, mediated by reactive macrophages/microglia, reactive astrocytes and infiltrating immune cells (Berkelaar, Clarke et al. 1994, Tezel, Yang et al. 2004, Qu and Jakobs 2013, Ha, Liu et al. 2017, Liddelow, Guttenplan et al. 2017). Intravitreal injection of zymosan, a microbial polysaccharide, or LI concurrently with ONC can overcome the intrinsic and extrinsic barriers to regeneration in the CNS (Leon, Yin et al. 2000). Zymosan and LI promote intraocular inflammation that activates macrophages, neutrophils, retinal astrocytes, and Müller cells (Leon, Yin et al. 2000, Yin, Cui et al. 2003, Muller, Hauk et al. 2007, Leibinger, Muller et al. 2009, Kurimoto, Yin et al. 2013). Infiltrating macrophages and neutrophils express oncomodulin which promotes optic nerve regeneration, oncomodulin mRNA levels rising dramatically within a day of zymosan injection or LI (Yin, Cui et al. 2003, Yin, Cui et al. 2009). The receptor through which oncomodulin may signal through has yet to be identified, it is believed to be a high-affinity RGC surface receptor that is cyclic adenosine monophosphate (cAMP)-dependent (Yin, Cui et al. 2009). Astrocyte activation by zymosan or LI promotes the secretion of neurotrophic factors and cytokines that include ciliary neurotrophic factor (CNTF), leukemia inhibitory factor (LIF), and IL-6, eliciting pro-survival and pro-regenerative signaling through their respective receptor complexes expressed on RGCs (Muller, Hauk et al. 2007, Leibinger, Muller et al. 2009, Leibinger, Andreadaki et al. 2016). Zymosan is a TLR2 agonist, Pam3Cys is another TLR2 agonist identified to promote optic nerve regeneration (Hauk, Leibinger et al. 2010). While TLR2 agonists appear promising for CNS injury, manipulating inflammation post-injury can be a double-edged sword as uncontrolled processes can lead to increased degeneration. Mouse spinal cord treated with zymosan-activated macrophages (ZAMs) show significant dorsal root ganglion (DRG) outgrowth, but with a concurrent neurotoxic effect leading to 33% cell loss by 72h (Gensel, Nakamura et al. 2009). DRGs treated *in vitro* with ZAM conditioned media display 60% cell loss as early as 48h. The degenerative

processes promoted by ZAMs is related to the production of proinflammatory cytokines TNF- α and IL-1 β , directing a T_H1 response, following TLR2 activation (Young, Ye et al. 2001, Murphy, Travers et al. 2012, Liu, Jia et al. 2018). This demonstrates a narrow window for advantageous stimulation of inflammatory processes, thus rendering potential therapeutic options unsafe. Understanding how neurons respond to pathological and positive inflammation can aid us in determining how to develop neuroprotective and neuro-regenerative therapies, bypassing the narrow window provided by inflammatory stimuli such as zymosan.

2.3.2 Intrinsic neuronal mediators of regeneration

Following axotomy, there is an increase in extrinsic factors blocking regeneration, as well as an age-associated loss in the intrinsic neuronal capacity for repair and regeneration (Cai, Qiu et al. 2001, Fournier, GrandPre et al. 2001, Bradbury, Moon et al. 2002, Park, Liu et al. 2008, Qin, Zou et al. 2013). A decline in the ability of RGCs to extend axons occurs as soon as birth, attributed to intrinsic changes and a loss of trophic support (Chen, Jhaveri et al. 1995, Goldberg, Espinosa et al. 2002). Indeed, if neurons are given the appropriate trophic support, they can overcome the growth-inhibitory environment of CNS lesions. David and Aguayo gave the first evidence that injured CNS axons can elongate for unprecedented distance when the CNS glial environment is replaced by that of peripheral nerves (David and Aguayo 1981). Unlike the CNS, the peripheral nervous system (PNS) maintains its intrinsic ability to regenerate. Injury to the PNS prompts a robust cell body response of regeneration-associated genes (RAGs) that promote regeneration of the severed DRG peripheral processes (Mar, Bonni et al. 2014). As DRG neurons are pseudo unipolar, they lead one branch into the periphery and the other into the spinal cord. Their CNS branch can be primed to regenerate if the peripheral branch is severed initially, coined a conditioning lesion as you are conditioning the central branch to regenerate by priming the DRG cell body with RAG expression (Neumann and Woolf 1999, Mar, Bonni et al. 2014). Filbin and colleagues identified an age-associated decline of cAMP, a promoter of RAG expression as emphasized by the regeneration of injured DRG central branches primed with cAMP analogs (Cai, Qiu et al. 2001, Neumann, Bradke et al. 2002, Qiu, Cai et al. 2002). Similarly, developmental decline of mammalian target

of rapamycin (mTOR) limits regeneration (Park, Liu et al. 2008, Belin, Nawabi et al. 2015). Genetic deletion of phosphatase and tensin homolog (PTEN), a negative regulator of mTOR, promotes axon regeneration following ONC (Park, Liu et al. 2008). Genetic deletion of PTEN is now often used as the benchmark for effective axon regeneration. Other critical regulators of axon regeneration include c-myc, suppressor of cytokine 3 (SOCS3), and krüppel-like factor 4 (KLF4) (Smith, Sun et al. 2009, Qin, Zou et al. 2013, Belin, Nawabi et al. 2015). Both mTOR and c-myc are implicated as master regulators of cell metabolism (Dang 2013, Xie and Proud 2013). While SOCS3 and transcription factor KLF4 are negative regulators of the Janus kinase/signal transducers and activators of transcription (JAK/STAT) pathway (Smith, Sun et al. 2009, Qin, Zou et al. 2013). These positive outcomes have resulted in a greater focus on manipulating the neuro-intrinsic capacity for repair and regenerate. However, these approaches are still limited to single program of gene expression and do not incorporate the inflammatory milieu, a critical factor for the development of effective DMTs for the treatment of neurodegenerative disease.

2.4 microRNA

We would like to define a molecular approach that could regulate programs of gene expression in neurons in response to injury to mediate neuroprotection or repair. For this reason, we have focused on microRNAs (miRNAs). miRNAs regulate hubs of gene expression, making them lucrative candidates to investigate in CNS damage, where multiple pathways require engagement for proper CNS repair and regeneration (Lewis, Shih et al. 2003, Cui, Yu et al. 2006, Shalgi, Lieber et al. 2007, Thomas, Gross et al. 2018). miRNAs are small, non-coding RNA sequences approximately 22 nucleotides in length that target messenger RNA (mRNA) (Lewis, Shih et al. 2003). Each mammalian miRNA contains a short seed region from nucleotides 2-7 that binds complementary regions within the 3' untranslated region (3'UTR) of target mRNA, leading to the target mRNA degradation or translationally repression (Lewis, Burge et al. 2005, Guo, Ingolia et al. 2010, Agarwal, Bell et al. 2015). miRNA are found either within intron sequences, where they are transcribed with their host gene; or as intergenic sequences, where they

are found between genes and are transcribed as independent transcription units (Lee, Jeon et al. 2002, Lee, Kim et al. 2004, Kim and Kim 2007). As miRNAs are found within non-protein-coding DNA, they were initially viewed as junk DNA, a term coined by Ohno in 1972 (Ohno 1972). The first miRNA described was lin-4 in *C.elegans*, initially thought to be a gene, as identified by the group of Horvitz in 1980 (Horvitz and Sulston 1980). After leaving the laboratory of Horvitz, Ambros and Ruvkun continued to study lin-4 in their separate laboratories, simultaneously publishing their findings in 1993 (Lee, Feinbaum et al. 1993, Wightman, Ha et al. 1993). Small non-protein-coding transcript lin-4 was described to regulate lin-14 through its 3'UTR region. Today over 83 000 miRNA-related peer-reviewed publications can be found on Pubmed. What was originally identified as junk DNA, is now crucial genomic information we know to regulate gene networks. Here we will discuss in more detail miRNA biogenesis and function, and the relevance of miRNAs in CNS damage.

2.4.1 microRNA biogenesis and function

miRNAs are transcribed by RNA Polymerase II (RNA Pol II) to produce a primary miRNA (pri-miRNA) hairpin, typically several hundred-nucleotides long, that has a 5' cap and a 3' poly-adenylated tail, typical of class II gene transcripts (Lee, Kim et al. 2004, Ha and Kim 2014). The pri-miRNA contains a stem-loop structure in which the mature miRNA sequences are embedded (Ha and Kim 2014). Next, a two-step cleavage process occurs such that the hairpin structure is made progressively shorter. Ribonuclease Drosha associates with essential cofactor DiGeorge Syndrome Critical Region 8 (DGCR8) to form the Microprocessor complex, where DGCR8 recognizes the double-stranded RNA sequence of the hairpin structure. Within the complex, DGCR8 orients the catalytic RNase III domain of Drosha such that it liberates the hairpin loop of the pri-miRNA, forming a shorter hairpin of about 70 nucleotides length, termed the precursor miRNA (pre-miRNA) (Lee, Ahn et al. 2003). The resulting pre-miRNA has a two-nucleotide overhang at its 3' end (Ha and Kim 2014). Exportin-5, GTP-binding nuclear protein RAN, and the pre-miRNA form a complex that is translocated through a nuclear pore complex, hydrolysing the GTP and thus disassembling the complex, releasing the pre-miRNA into the cytosol (Yi, Qin et al. 2003). Next, RNase III enzyme Dicer cleaves the pre-miRNA loop,

producing a mature miRNA duplex about 22 nucleotides in length (Ha and Kim 2014). The duplex is loaded onto an Argonaute protein to form the core of the miRNA-induced silencing complex (miRISC), where a passenger strand of the duplex is ejected and the remaining miRNA strand acts as the guide strand. Using the seed region of the guide strand at nucleotides 2-7, the miRISC binds to complementary region(s) on the 3'UTR of target mRNA strands (Bartel 2009). At sites with extensive complementarity, the miRNA directs Argonaute-catalyzed cleavage of the mRNA. More frequently the mammalian miRNAs direct translational repression or destabilization of target mRNA transcripts (Filipowicz, Bhattacharyya et al. 2008, Agarwal, Bell et al. 2015). A single mRNA can also be targeted by multiple miRNAs, demonstrating a miRNA-network mediated mRNA repression (Flamand, Gan et al. 2017).

It is estimated that mammalian miRNAs regulate approximately 30% of all protein-coding genes, emphasizing their influence on gene networks (Filipowicz, Bhattacharyya et al. 2008). Most miRNAs are believed to regulate hubs of gene expression, targeting major transcription factors, regulating feedback loops, and dictating developmental switches (Lim, Lau et al. 2005, Shalgi, Lieber et al. 2007, Tsang, Zhu et al. 2007, Ivey and Srivastava 2015). As miRNAs regulate hubs of gene networks, as well as target multiple mRNAs, we can uncover multiple affected pathways during disease and injury when uncovering a single dysregulated miRNA.

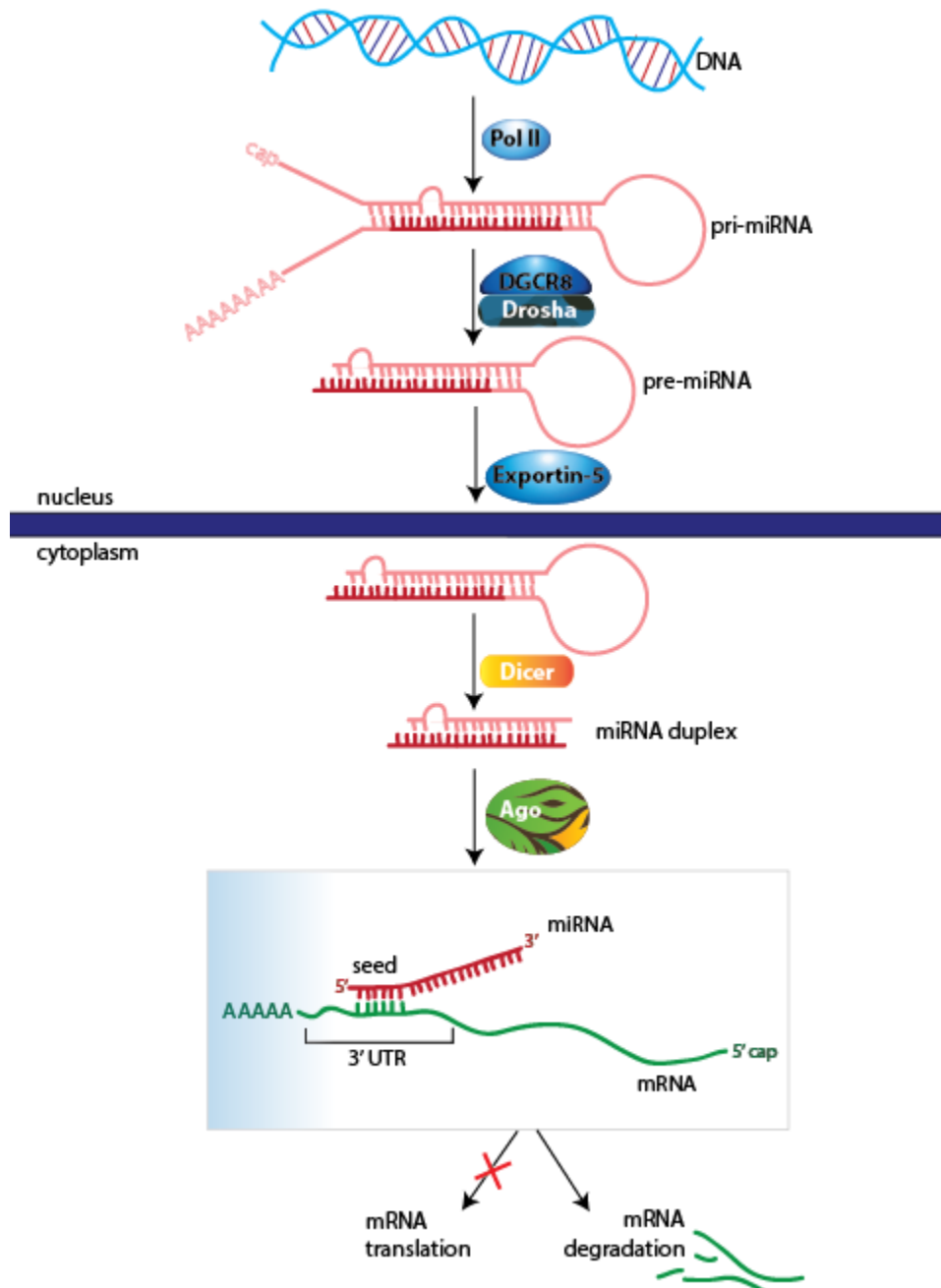


Figure 2. microRNA processing. miRNAs are transcribed in the nuclear from intro or intergenic regions by RNA Polymerase II (Pol II) to form the primary miRNA transcript (pri-miRNA). This is processed by DGCR8 and Drosha to form the precursor miRNA transcript (pre-miRNA) that is exported from the nucleus into the cytoplasm by Exportin-5. In the cytoplasm Dicer further cleaves the pre-miRNA to form a miRNA duplex that is loaded onto Ago, ejecting the passenger miRNA strand of the duplex to form the miRNA-induced silencing complex. The complex guides the miRNA to its target mRNA, which recognizes a region within the 3' untranslated region (UTR) of the mRNA. In the blue gradient-coloured square we see the miRNA binding its target mRNA via its seed region. This interaction promotes either the disruption of the target mRNA translation or Ago-mediated cleavage of the mRNA transcript.

2.4.2 microRNA in central nervous system disease and injury

miRNAs play a prominent role in CNS development, as was first demonstrated with transfection of HeLa cells with miR-124, shifting the expression profile towards that of brain (Lim, Lau et al. 2005). Disruption of the miRNA biogenesis machinery has been used to demonstrate the critical role of miRNAs in CNS development and disease. Specifically, deletion of Dicer in different brain regions leads to brain atrophy, neurodegeneration, gliosis, locomotor deficits, and shortened lifespans (Cuellar, Davis et al. 2008, Shin, Shin et al. 2009, Hebert, Papadopoulou et al. 2010, Tao, Wu et al. 2011, Cheng, Zhang et al. 2014, Fiorenza, Lopez-Atalaya et al. 2016, Chmielarz, Konovalova et al. 2017). Similarly, retinal deletion of Dicer or Dgcr8 leads to retinal degeneration and loss of visual function (Damiani, Alexander et al. 2008, Iida, Shinoe et al. 2011, Kaneko, Dridi et al. 2011, Sundermeier, Zhang et al. 2014, Akhtar, Patnaik et al. 2015, Sundermeier, Sakami et al. 2017). Decreased Dicer expression has also been observed in patients with advanced aged-macular degeneration (AMD), epilepsy, and MS (Kaneko, Dridi et al. 2011, McKiernan, Jimenez-Mateos et al. 2012, Aung and Balashov 2015, Magner, Weinstock-Guttman et al. 2016). Animal models of aging, epilepsy, and MS also exhibit decreased Dicer expression (McKiernan, Jimenez-Mateos et al. 2012, Lewkowicz, Cwiklinska et al. 2015, Chmielarz, Konovalova et al. 2017). Disruption of the miRNA-processing machinery provides proof-of-principle evidence that miRNAs are essential to nervous system function and integrity, and that disruption of miRNA expression can contribute to deficits identified in neurodegenerative disease and injury.

As miRNAs regulate gene networks, it is unsurprising that miRNA dysregulation is a prominent feature of CNS disease and injury (Lim, Lau et al. 2005, Liang and Li 2007, Shalgi, Lieber et al. 2007, Williams, Piaton et al. 2007, Nelson, Wang et al. 2008, Bhalala, Srikanth et al. 2013, Thomas, Gross et al. 2018). Dysregulation of a single miRNA can promote the disruption of multiple genes and their signaling networks, thus it is likely that the dysregulated miRNAs of CNS disease and injury are contributing to multiple disrupted pathways. By determining the neuronal miRNA profile during CNS damage, we can determine the global neuronal response to the multifactorial, inflammatory environment.

2.4.3 Note on microRNA nomenclature

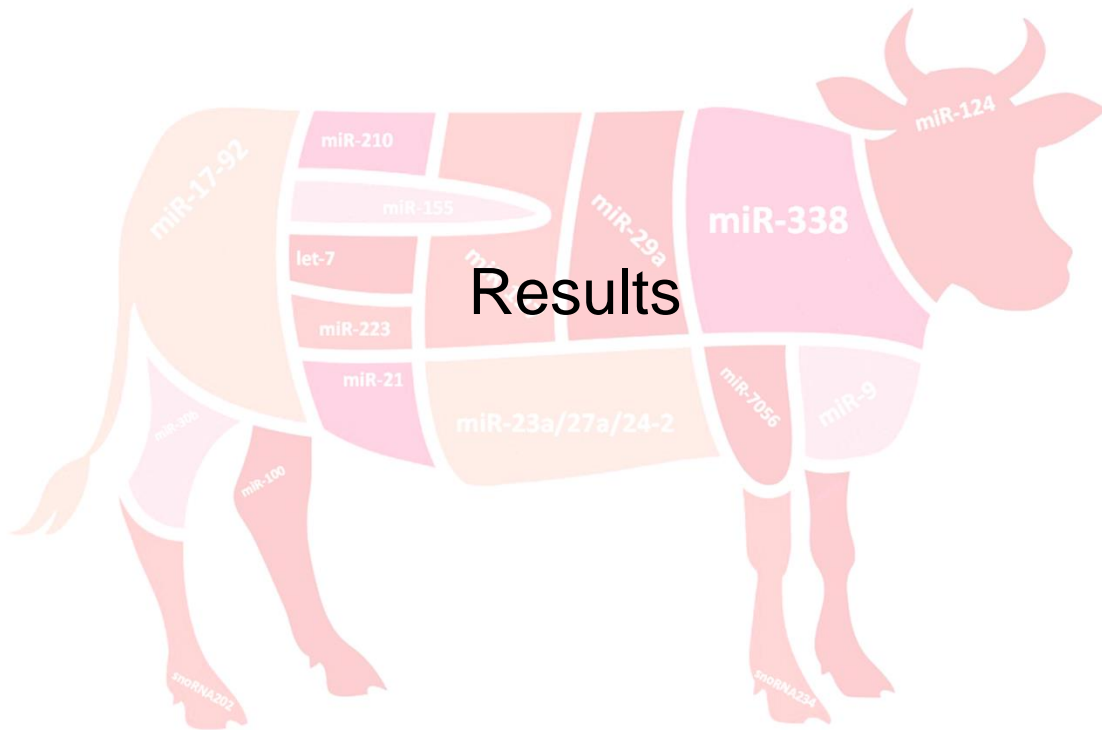
miRNA nomenclature is inconsistent in the literature and has nuances that are confusing. To understand miRNA nomenclature, it is important to understand the breakdown of the miRNA name. miRNAs are generally numbered progressively, such that miR-223 was identified prior to miR-7056. The miRNAs let-7 and lin-4 have a different numbering scheme for historical reasons, as they are the first two identified miRNAs (Lee, Feinbaum et al. 1993, Wightman, Ha et al. 1993, Reinhart, Slack et al. 2000). Every species has their species name written before the miRNA name as well, such that miR-223 from mice is mmu-miR-223. When new miRNAs are submitted, it is first determined if it has homology to an already identified miRNA, such that rather than naming a new miRNA as miR-39101039921 (this is an exaggeration), it can become hsa-miR-“*number belonging to homologous miRNA*” (Ambros, Bartel et al. 2003).

Of most importance is understanding the ending to a miRNA name, i.e. miR-223-5p versus miR-223-3p. In the miRNA duplex there are two strands of approximately 22 nucleotides in length (Ha and Kim 2014). In the past it was believed that there is a dominant strand in the duplex, and that the other passenger strand does not have biological relevance. Using miR-223 as an example, miR-223 would be the dominant strand, and miR-223* the passenger strand. It is clear now that both strands from the duplex may have biological relevance, and so the nomenclature has adjusted for this biological finding. Based on directionality, the 5'end of the duplex is now coined the 5p miRNA, or miR-223-5p, and the 3'end is the 3p miRNA, or miR-223-3p.

An additional detail for those interested in knowing more: closely related mature sequences share suffixes (Ambros, Bartel et al. 2003). For example, mmu-miR-27a-3p and mmu-miR-27b-3p share similar sequences but have distinct precursor sequences and genomic loci. Another example is miR-24-1 and miR-24-2. If a miRNA ends with a number rather than a letter, they share identical mature sequences but have distinct precursor sequences and genomic loci. miRbase.org is an excellent resource that catalogues all known miRNAs.

2.5 Rationale

Neuroinflammation is a double-edged sword that both enhances tissue damage while simultaneously promoting repair and regeneration. Understanding how we can harness the positive aspects of neuroinflammation can help us develop more effective therapies against neurodegenerative disease and CNS injury. Current research in disease and injury often focuses on investigating a single pathway rather than determining the global neuronal response. We focus on miRNA expression and their mechanisms of action as they are potent regulators of post-transcription. miRNAs regulate hubs of gene expression, targeting major transcription factors, regulating feedback loops, and dictating developmental switches. By investigating miRNA expression in models of neuroinflammation, we hope to elucidate their mechanisms of action in these specific models to promote CNS repair and regeneration.



Preface

In this chapter we employ an animal model of CNS inflammation, EAE, to investigate the neuronal miRNA response to inflammation and identify affected gene networks. By laser capture microdissection we isolated two types of CNS neurons that are pathologically affected in EAE, and profiled their miRNA expression throughout the course of disease. We identified shared miRNA profiles between neuronal types. Through *in silico* analysis and qPCR validation we identified signaling pathways targeted by regulated miRNA that are detrimental to neuronal survival. Our results describe neuronal miRNA expression in EAE and pave the road for future work determining the functional role of these miRNAs in neuroinflammation.

3 Chapter 2. Neuronal microRNA regulation in Experimental Autoimmune Encephalomyelitis

Camille A. Juźwik¹, Sienna Drake¹, Marc-André Lécuyer², Radia Marie Johnson³, Barbara Morquette¹, Yang Zhang¹, Marc Charabati², Selena M. Sagan⁴, Amit Bar-Or^{1,5}, Alexandre Prat², Alyson E. Fournier¹

¹ McGill University, Montréal Neurological Institute, Montréal, QC H3A 2B4, Canada

² Centre de Recherche du Centre Hospitalier de l'Université de Montréal, Université de Montréal, Montréal, QC H2X 0A9, Canada

³ McGill University, Goodman Cancer Research Centre, Montréal H3A 1A3 Canada

⁴ McGill University, Departments of Microbiology & Immunology and Biochemistry, Montréal, QC H3G 0B1 Canada

⁵ Perelman School of Medicine, University of Pennsylvania, Philadelphia, PA 19104 USA

Published in *Scientific Reports*, 2018, 8 (1): 13437.

3.1 Abstract

Multiple sclerosis (MS) is an autoimmune, neurodegenerative disease but the molecular mechanisms underlying neurodegenerative aspects of the disease are poorly understood. microRNAs (miRNAs) are powerful regulators of gene expression that regulate numerous mRNAs simultaneously and can thus regulate programs of gene expression. Here, we describe miRNA expression in neurons captured from mice subjected to experimental autoimmune encephalomyelitis (EAE), a model of central nervous system (CNS) inflammation. Lumbar motor neurons and retinal neurons were laser captured from EAE mice and miRNA expression was assessed by next-generation sequencing and validated by qPCR. We describe 14 miRNAs that are differentially regulated in both neuronal subtypes and determine putative mRNA targets through *in silico* analysis. Several upregulated neuronal miRNAs are predicted to target pathways that could mediate repair and regeneration during EAE. This work identifies miRNAs that are affected by inflammation and suggests novel candidates that may be targeted to improve neuroprotection in the context of pathological inflammation.

3.2 Introduction

Multiple sclerosis (MS) is an autoimmune neurodegenerative disease characterized by the infiltration of peripherally activated immune cells into the central nervous system (CNS) (Frohman, Racke et al. 2006). Inflammation results in multiple foci of oligodendrocyte damage and demyelination throughout the CNS including the cerebral cortex, spinal cord, and optic nerve (Fisher, Jacobs et al. 2006, Dutta and Trapp 2007). Active lesions also contain axonal ovoids, indicative of newly damaged axons, and extensive accumulation of amyloid precursor protein (APP) resulting from impaired axonal transport (Ferguson, Matyszak et al. 1997). Axonal transection is apparent early in the disease and is thought to be a major cause of persistent neurological disability (Ferguson, Matyszak et al. 1997, Dutta and Trapp 2007). Gray matter atrophy and cortical thinning, as a result of neuronal death, also increase with MS-related disability, and are characteristic of the progressive forms of MS (Peterson, Bo et al. 2001, Sailer, Fischl et al. 2003, Jonkman, Rosenthal et al. 2015).

In experimental autoimmune encephalomyelitis (EAE), an animal model of CNS inflammation induced by active sensitization with myelin antigens, foci of demyelination and axon damage are also apparent (Miller, Karpus et al. 2010). Infiltration begins at the lumbar region of the spinal cord and progresses anteriorly resulting in ascending paralysis. Evidence of sub-lethal neuronal damage includes dendrite shortening, thinning and fragmentation while axons display accumulations of APP and transections (Bannerman, Hahn et al. 2005, Vogt, Paul et al. 2009, Hoflich, Beyer et al. 2016). Significant loss of α - and γ -motor neurons in lumbar spinal cord has also been reported over the course of the disease, beginning as early as 14 days post immunization (dpi) (Vogt, Paul et al. 2009). Similarly, the visual system is affected in EAE with loss of retinal ganglion cells (RGCs) and optic nerve pathology including immune cell infiltration, demyelination and glial activation (Shindler, Ventura et al. 2008, Quinn, Dutt et al. 2011, Horstmann, Schmid et al. 2013). The pathology is delayed in the optic nerve relative to the spinal cord, with loss of RGCs occurring after the peak stage, around 35 dpi (Quinn, Dutt et al. 2011).

The molecular changes occurring within neurons in EAE and MS that mediate pathological responses to inflammation have not been fully characterized. Understanding the molecular response to damage will be critical to devising neuroprotective strategies to mitigate sub-lethal axonal damage and neuronal cell death. We sought to identify conserved molecular networks that regulate the response to injury in all neuronal subtypes by profiling neuronal microRNAs (miRNAs) in affected neuronal subtypes. miRNAs are short RNA molecules approximately 22 nucleotides in length that bind to target messenger RNAs (mRNAs) to regulate hubs of gene expression (Lewis, Shih et al. 2003). A single miRNA can target several different mRNAs, and several miRNAs often work cooperatively to target a single mRNA (Lewis, Shih et al. 2003, Flamand, Gan et al. 2017). Altered miRNA expression has been identified in the blood cells of MS patients, in active and inactive MS lesions, and in immune cell subsets and oligodendrocytes in EAE, but neuronal miRNAs have not been profiled (Junker, Krumbholz et al. 2009, Cox, Cairns et al. 2010, De Santis, Ferracin et al. 2010, Lindberg, Hoffmann et al. 2010, Noorbakhsh, Ellestad et al. 2011, Jr Ode, Moore et al. 2012, Lewkowicz, Cwiklinska et al. 2015). Here, we describe miRNA regulation in lumbar motor neurons and retinal neurons collected from mice afflicted with EAE. mRNA targets of regulated miRNAs were assessed by *in silico* approaches. We describe considerable overlap in miRNA regulation between lumbar motor neurons and retinal neurons derived from EAE mice suggesting conserved responses to inflammation. We also identify several molecular pathways that are predicted targets of regulated miRNAs, with confirmed regulation of representative genes of these pathways, suggesting novel avenues of investigation to mediate neuroprotection in the context of inflammation.

3.3 Results

3.3.1 Differential miRNA expression over the course of EAE in lumbar motor neurons - To assess neuronal miRNA expression in response to neuroinflammation we isolated lumbar motor neurons of EAE mice over the course of their disease and profiled miRNA expression by miR-Seq NGS. EAE was induced in C57Bl/6 mice by immunization with MOG₃₅₋₅₅ in CFA. EAE mice were sacrificed at three time points: naïve (score 0), onset (score 0.5-1) and peak (score 3-3.5) (Fig. 1a). Demyelination and immune cell infiltration were visible within the lumbar spinal cord by HistoGene stain at peak disease (Fig. 1b). Lumbar motor neurons were isolated from sections of fresh frozen spinal cord tissue by laser capture microdissection (LCM) (Fig. 1c-f). Neuronal purity of total RNA from the LCM tissue was confirmed by assessing the levels of glial cell and immune cell RNA markers relative to neuron specific Tubb3 levels (Fig. 1g). The efficacy of individual probes was validated on purified immune cells and astrocytes (Supplementary Table S1). We focused on the lumbar motor neurons of the spinal cord because the disease pathology of EAE begins in the lumbar region with a limp tail (score 1) and ascends the spinal cord with loss of hindlimb function (score 2-3), until mice are moribund (score 5) (Bittner, Afzali et al. 2014). By collecting lumbar motor neurons at onset, we captured miRNA changes at a time when APP-positive ovoids were present but prior to significant motor neuron loss (Vogt, Paul et al. 2009). Total extracted RNA was used to prepare miRNA sequencing libraries and sequenced on Illumina HiSeq. The rlog transformed counts for miRNAs identified as significantly regulated by DeSeq2 are depicted in Fig. 2, where we can see that the animals for each EAE disease stage cluster most closely together (n= 3-4 per animal group). From the miR-Seq data, 997 miRNAs were identified, 43 of which were differentially regulated. Six of the miRNAs were novel miRNAs.

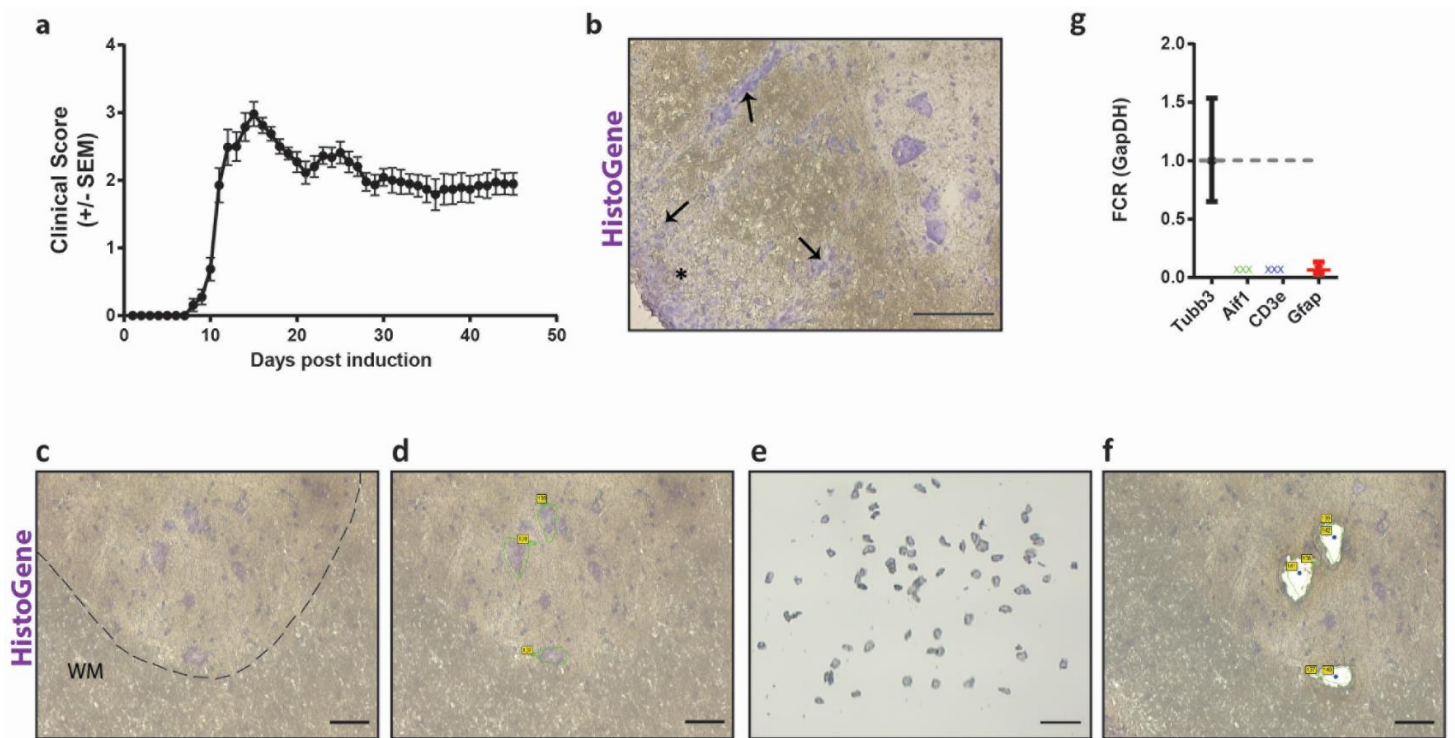


Figure 1. Laser captured lumbar motor neurons from EAE and control naive mice. (a) Clinical scores of mice immunized with MOG₃₅₋₅₀ peptide. Animals of interest were taken at onset (score 0.5 to 1) and peak (score 3-3.5) of disease. Curve represents a cohort of 38 immunized animals, with representative animals taken at onset and peak. (b) Representative EAE spinal cord section from an animal at peak disease (score 3-3.5) stained with HistoGene and displaying immune cell infiltrates (arrows) and areas of demyelination (*) (scale bar at 100 μ m). (c-f) Micrographs of the laser capture microdissection flow-through. Sections of frozen mouse spinal cord on PEN membrane slides stained with HistoGene. Area above the dotted line is the dorsal horn and the area below is the white matter, WM (c). The tissue surrounding the lumbar motor neurons was traced and ablated loosening the neuron of interest (d). The neuron was then catapulted into an adhesive cap (e) leaving a void on the slide (f). Scale bar; 50 μ m (c, d, f), 250 μ m (e)). (g) qPCR of LCM motor neuron tissue for microglia/macrophages (Aif1), immune cells (Cd3e), and astrocytes (Gfap) relative to neuronal RNA expression (Tubb3). FCR, Fold Change Range.

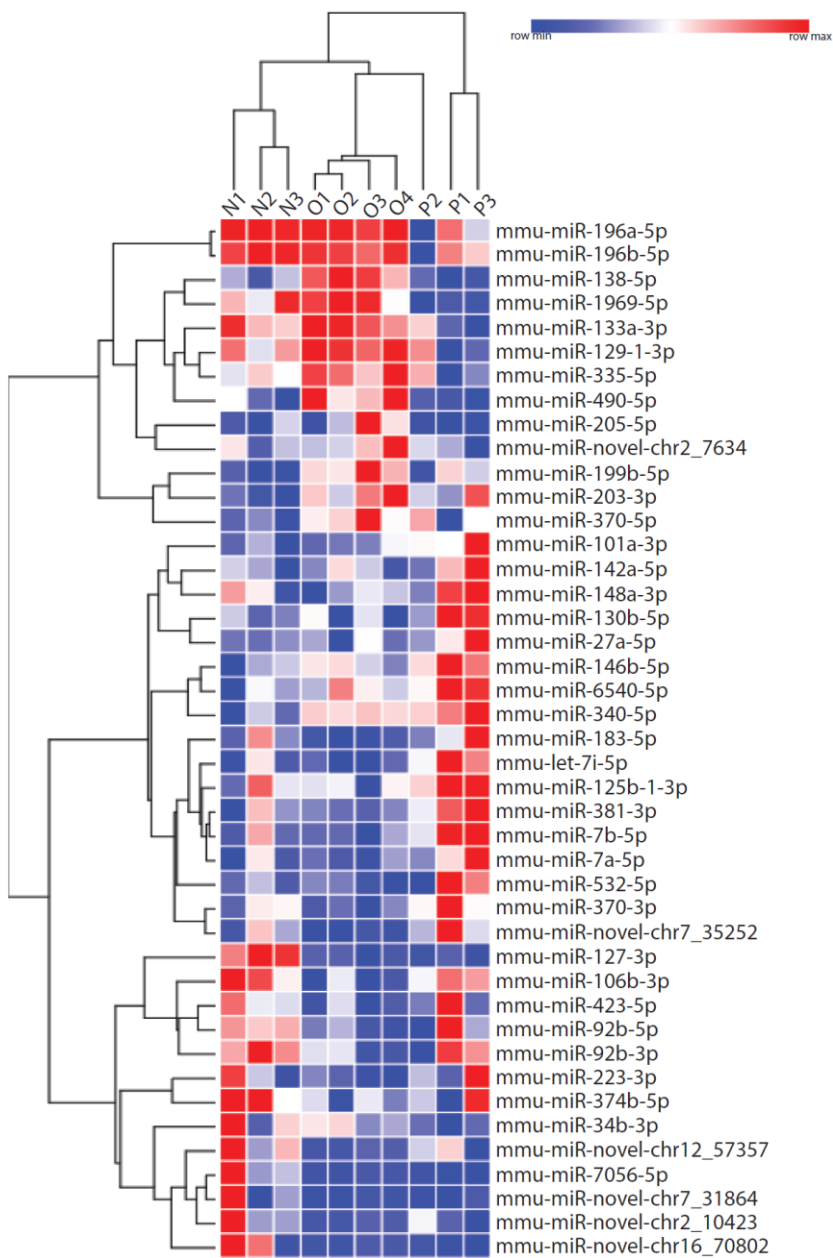


Figure 2. Heat Map summary of significantly regulated miRNA as identified by miR-Seq in EAE. miRNA and animals (N= naive, O= onset, P= peak) are hierarchically clustered by Euclidean distance using rlog transformed counts. Blue data represents low expression of that microRNA within its own row, and red indicates high expression. 997 miRNAs were identified by miR-Seq, 43 of these were identified as significantly regulated ($p < 0.05$); 6 of which are novel miRNAs.

To validate the miR-Seq data, miRNA expression was analyzed using Taqman MicroRNA Assays. For the novel miRNAs and mmu-miR-92b-3p, custom Taqman MicroRNA Assays were designed (Supplementary Table S2). Probes for miR-92b-3p and miR-novel-chr2_10423 failed quality control testing thus qPCR validation was performed for 41 of the 43 regulated miRNAs. The fold change miRNA expression was relative to naïve levels, after normalization to endogenous control snoRNA202, using the $2^{-\Delta\Delta Ct}$ method (Livak and Schmittgen 2001). Of the 41 miRNAs significantly regulated by miR-Seq, 24 were significantly regulated similarly between the miR-Seq and qPCR analyses

(Fig. 3, Table 1). Three miRNAs, miR-1969, miR-7056-5p, and miR-novel-chr7_31864, were regulated in the opposite direction compared to the miR-Seq analysis. These miRNAs carry GC rich areas which create an alignment issue during NGS, making quality reads in those regions more difficult to produce (Chen, Liu et al. 2013). Low quality reads for a miRNA are discarded during the NGS process; this alignment issue is reduced with increased amounts of total RNA. As our total RNA was collected from LCM material, we were able to submit approximately 300 ng per biological replicate, this runs a risk of lower sequencing read counts, lower detectable rates and higher false discovery rates. Some miRNAs (specifically miR-335-5p, miR-183-5p, miR-125b-1-3p, miR-129-1-3p, miR-490-5p, miR-6540-5p, miR-205-5p, and miR-223-3p) showed significance at either onset or peak by miR-Seq and are regulated in the same direction but at a different time point during EAE by qPCR validation. For these miRNAs, the tag counts of some biological replicates were below 100 counts per million. For qPCR validation, biological replicates are expected to have strong correlation with sequence rates ranging from 10 to 100 000< counts per million (Eminaga, Christodoulou et al. 2013). To control for this inherent limitation in NGS, we increased the amount of biological replicates for our qPCR validation. Thus, our qPCR data was considered to be more reliable. From the 27 miRNAs statistically regulated, as identified by qPCR, 10 were downregulated during onset or peak disease; 16 miRNAs were upregulated at onset or peak; and one miRNA, miR-6540-5p, was significantly downregulated at onset and significantly upregulated at peak.

All upregulated miRNAs showed an initial increase at onset, with significant upregulation at peak disease. These miRNAs, in order of increasing expression, included miR-340-5p, miR-142a-5p, miR-203-3p, miR-490-5p, miR-423-5p, miR-370-5p, miR-205-5p, miR-101a-3p, miR-1969, miR-7a-5p, miR-381-3p, miR-374b-5p, miR-199b-5p, miR-223-3p, and miR-7056-5p. Only the two most highly upregulated miRNAs, miR-223-3p and miR-7056-5p, were significantly upregulated at onset and peak. The miRNAs that were downregulated show a more unique biology. miR-novel-chr7_35252, miR-novel-chr12_57357, miR-129-1-3p, and miR-148a-3p were uniquely downregulated at onset whereas miR-novel-chr16_70802, miR-125b-1-3p, and miR-92b-5p were downregulated at peak. miR-335-5p, miR-183-5p, and miR-127-3p were downregulated at both onset and peak EAE.

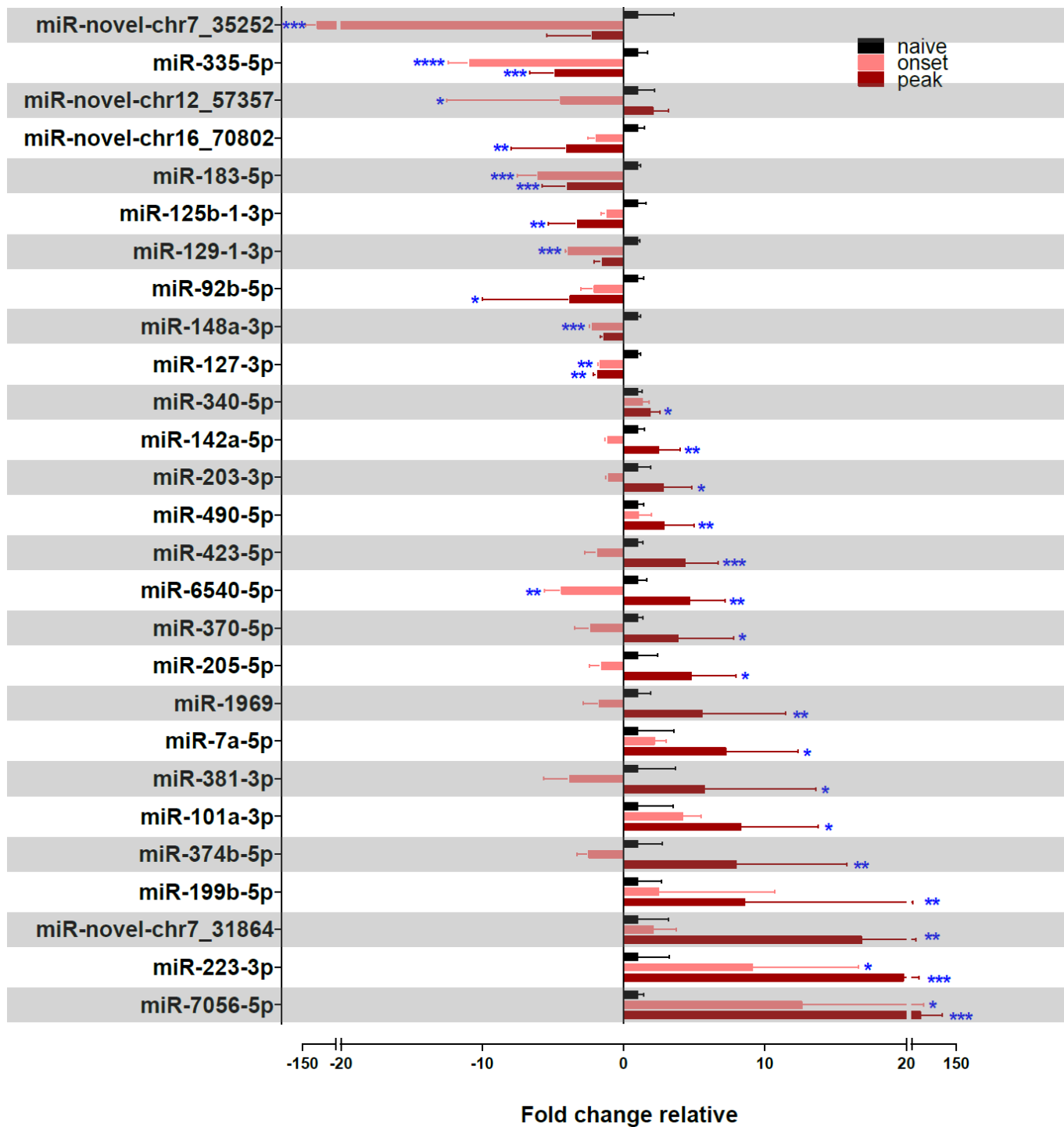


Figure 3. Differentially regulated miRNAs in the lumbar motor neurons of EAE mice over the course of the disease. Taqman MicroRNA Assay (qPCR) validation of miR-Seq identified differentially regulated miRNAs in the lumbar motor neurons of EAE mice over the course of the disease, normalized to endogenous control snoRNA202 for each individual miRNA and depicted as fold change relative to normalized naive levels. ****p<0.0001, ***p<0.001, **p<0.01, *p<0.05 (n=3-6, one-way ANOVA, p<0.05, Dunnett's multiple comparisons test).

Table 1

miR-Seq validated miRNA expression in the EAE neuronal subtypes and as previously described in EAE and/or MS

miRNA	lumbar motor neurons (2 ^{ΔΔCt})				RGC layer (2 ^{ΔΔCt})				EAE/MS expression
	onset		peak		peak		chronic		
	FC	p-adj	FC	p-adj	FC	p-adj	FC	p-adj	
miR-novel- chr7_35252	-91.0	0.0001	-2.2	0.3856	-1.9	0.1803	1.3	0.5714	N/A
miR-335-5p	-10.9	<0.0001	-4.8	0.0002	-1.0	0.9619	1.2	0.6167	downregulated in MS NAWM versus HC (Noorbakhsh, Ellestad et al. 2011)
miR-novel- chr12_57357	-4.4	0.0285	-2.1	0.2195	2.5	0.0708	2.1	0.0970	N/A
miR-novel- chr16_70802	-1.9	0.2347	-4.0	0.0062	-1.7	0.1007	1.0	0.9847	N/A
miR-183-5p	-6.0	<0.0001	-4.0	<0.0001	-1.4	0.6590	1.5	0.3293	<i>Rag1</i> ^{-/-} mice immunized with MOG ₃₅₋₅₅ and transferred with <i>miR-183</i> ^{-/-} CD4 ⁺ T cells show reduced clinical score compared to WT CD4 ⁺ T cells (Ichiyama, Gonzalez-Martin et al. 2016); serum expression showed pathogenic correlation with MS clinical/MRI data (Regev, Healy et al. 2017)
miR-125b-1- 3p	-1.2	0.8225	-3.3	0.0038	-1.0	0.9966	1.0	0.9896	upregulated in MS NAWM versus HC (Noorbakhsh, Ellestad et al. 2011)
miR-129-1-3p	-3.9	0.0003	-1.5	0.1016	-1.8	0.0448	-2.2	0.0019	downregulated in MS NAWM versus HC (Noorbakhsh, Ellestad et al. 2011)
miR-92b-5p	-2.0	0.2592	-3.8	0.0231	-2.1	0.2233	1.2	0.8287	N/A
miR-127-3p	-1.7	0.0060	-1.8	0.0025	1.1	0.9071	-2.0	0.0259	upregulated in serum exosomes of S/PPMS versus HC (Ebrahimkhani, Vafaei et al. 2017); downregulated in female RRMS leukocytes during remission versus HC (Munoz-Culla, Irizar et al. 2016)
miR-148a-3p	-2.2	0.0003	-1.3	0.051	1.5	0.0409	1.0	0.9002	upregulated in MS inactive lesions versus NAWM (Junker, Krumbholz et al. 2009); upregulated in T _{regs} from MS patients versus HC (De Santis, Ferracin et al. 2010); upregulated in PBMCs of RRMS remission versus HC (Baulina, Kulakova et al. 2018)
miR-6540-5p	-4.4	0.0076	4.7	0.0062	1.7	0.2983	1.1	0.8995	N/A
miR-340-5p	1.3	0.3650	1.9	0.0346	2.8	0.0041	1.1	0.9369	downregulated in both MS active and inactive lesions versus normal brain WM (Junker, Krumbholz et al. 2009); upregulated in MS CD4 ⁺ T cells versus HC (Guerau-de-Arellano, Smith et al. 2011); upregulated in plasma of EAE mice vs control (Singh, Deshpande et al. 2016)
miR-142a-5p	-1.1	0.8945	2.5	0.0084	1.3	0.6656	2.4	0.0249	upregulated in MS NAWM versus HC (Noorbakhsh, Ellestad et al. 2011); upregulated in MS NAWM versus HC, and EAE lumbar spinal cord at peak and chronic phases of disease versus control (Talebi, Ghorbani et al. 2017); serum expression showed protective correlation with MS clinical/MRI data (Regev, Healy et al. 2017)
miR-203-3p	-1.0	0.9881	2.8	0.0241	41.6	<0.0001	1.2	0.6928	upregulated in lymph nodes of EAE-susceptible rats versus non-susceptible controls (Bergman, James et al. 2013); downregulated in B cells of RRMS vs HC (Sievers, Meira et al. 2012); upregulated in PBMCs of RRMS remission versus HC, and RRMS remission vs RRMS relapse (Baulina, Kulakova et al. 2018)
miR-490-5p	1.1	0.9755	2.9	0.0086	1.3	0.5863	1.1	0.9291	N/A

miR-423-5p	-1.8	0.0959	4.4	0.0005	-1.3	0.2228	1.0	0.9863	downregulated in MS CD3+T cells versus HC (Jernas, Malmstrom et al. 2013)
miR-370-5p	-2.3	0.1139	3.9	0.0122	1.3	0.6134	1.9	0.0438	N/A
miR-205-5p	-1.6	0.6079	4.8	0.0127	-1.1	0.9749	3.7	0.0257	N/A
miR-1969	-1.7	0.4603	5.5	0.0044	5.5	0.0712	5.9	0.0199	N/A
miR-7a-5p	2.2	0.4451	7.2	0.0436	3.2	0.0009	2.1	0.0037	downregulated in MS NAWM versus HC (Noorbakhsh, Ellestad et al. 2011); upregulated in lymph nodes of EAE-susceptible rats versus non-susceptible controls (Bergman, James et al. 2013); downregulated in CIS/RRMS whole blood versus HC (Keller, Leidingner et al. 2014); serum expression showed pathogenic correlation with MS clinical/MRI data (Regev, Healy et al. 2017)
miR-381-3p	-3.8	0.1636	5.7	0.0324	2.9	0.0069	2.1	0.0130	N/A
miR-101a-3p	3.1	0.0971	8.3	0.0118	3.3	0.0006	1.3	0.2863	downregulated in RRMS leukocytes versus HC (Magner, Weinstock-Guttman et al. 2016); serum expression showed protective correlation with MS clinical/MRI data (Regev, Healy et al. 2017)
miR-374b-5p	-2.4	0.2454	8.0	0.0034	1.1	0.8913	1.6	0.0069	N/A
miR-199b-5p	2.5	0.4402	8.6	0.0247	1.7	0.0575	1.9	0.0052	N/A
miR-novel-chr7_31864	2.1	0.4659	16.8	0.0032	1.1	0.9767	1.2	0.8166	N/A
miR-223-3p	9.1	0.0129	19.8	0.0006	1.3	0.0755	-1.0	0.9778	upregulated in RRMS whole blood versus HC (Keller, Leidingner et al. 2009); upregulated in MS active lesions versus NAWM (Junker, Krumbholz et al. 2009); upregulated in T _{regs} from MS patients versus HC (De Santis, Ferracin et al. 2010); downregulated in serum of RRMS and PPMS versus HC (Fenoglio, Ridolfi et al. 2013); upregulated in lymph nodes of EAE-susceptible rats versus non-susceptible controls (Bergman, James et al. 2013); upregulated in PBMCs from RRMS vs HC (Ridolfi, Fenoglio et al. 2013); downregulated in serum from RRMS vs HC (Ridolfi, Fenoglio et al. 2013); upregulated in MS NAWM vs HC (Guerau-de-Arellano, Liu et al. 2015); upregulated in CD4+T cells during relapse phase of RRMS versus remission and HC (Hosseini, Ghaedi et al. 2016); <i>miR-223</i> ^{-/-} mice immunized with MOG ₃₅₋₅₅ show reduced clinical severity versus control (Ifergan, Chen et al. 2016, Satoorian, Li et al. 2016, Cantoni, Cignarella et al. 2017); upregulated in serum exosomes of RRMS vs S/PPMS, and S/PPMS versus HC (Ebrahimkhani, Vafaei et al. 2017); serum expression showed protective correlation with MS clinical/MRI data (Regev, Healy et al. 2017); upregulated in PBMCs of RRMS remission versus HC (Baulina, Kulakova et al. 2018)
miR-7056-5p	12.6	0.0111	45.6	0.0004	-1.1	0.9528	2.1	0.0373	N/A

miRNAs are organized from most significantly downregulated to most significantly upregulated. Bold FC (fold change) and p-adj (adjusted p-value) values are statistically significant (n=3-8 RGC layer and n=3-6 motor neurons, one-way ANOVA, p<0.05, Dunnett's multiple comparisons test), N/A= not applicable.

3.3.2 Differential miRNA expression over the course of EAE in the RGC layer- We next asked if miRNA regulation in lumbar motor neurons was conserved in RGCs, another neuronal population that is affected in EAE and MS. To investigate the miRNA changes in the RGCs, we isolated the RGC layer from EAE mice, which is comprised of approximately 50% RGCs (Schlamp, Montgomery et al. 2013). RGCs were isolated at the presymptomatic stage (before onset of symptoms), peak and chronic stages using LCM (Fig. 4a), and neuronal purity of total RNA was similarly confirmed as in motor neurons (Fig. 4b). Again we saw little or no microglia/macrophages or immune cells, and some astrocyte RNA expression as expected from retinal astrocytes in the RGC layer (Schlamp, Montgomery et al. 2013). We investigated the expression of the 27 miRNAs that were validated in the motor neurons of EAE mice. From these 27 miRNAs, 15 miRNAs were identified as significantly regulated in the RGC layer of EAE mice (Fig. 4c, Table 1); where 14 miRNAs were expressed in the same direction as those in the motor neurons. Specifically, miR-340-5p, miR-101-3p, and miR-203-3p were upregulated at peak; and miR-374b-5p, miR-199b-5p, miR-370-5p, miR-7056-5p, miR-142a-5p, miR-205-5p and miR-1969 were upregulated at chronic EAE. At both peak and chronic stage, miR-381-3p and miR-7a-5p were upregulated. Interestingly, miR-148a-3p was upregulated in the RGC layer, while it was downregulated in the motor neurons. From the downregulated miRNAs in motor neurons, only miR-129-1-3p and miR-127-3p were also downregulated in the RGC layer. None of the novel miRNAs identified in the motor neurons remained significantly regulated in the RGC layer. This gave approximately 50% overlap in miRNA expression profiles between the two neuronal subtypes. These results are summarized in Fig. 4 and Table 1 for the lumbar motor neurons and the RGC layer of EAE mice.

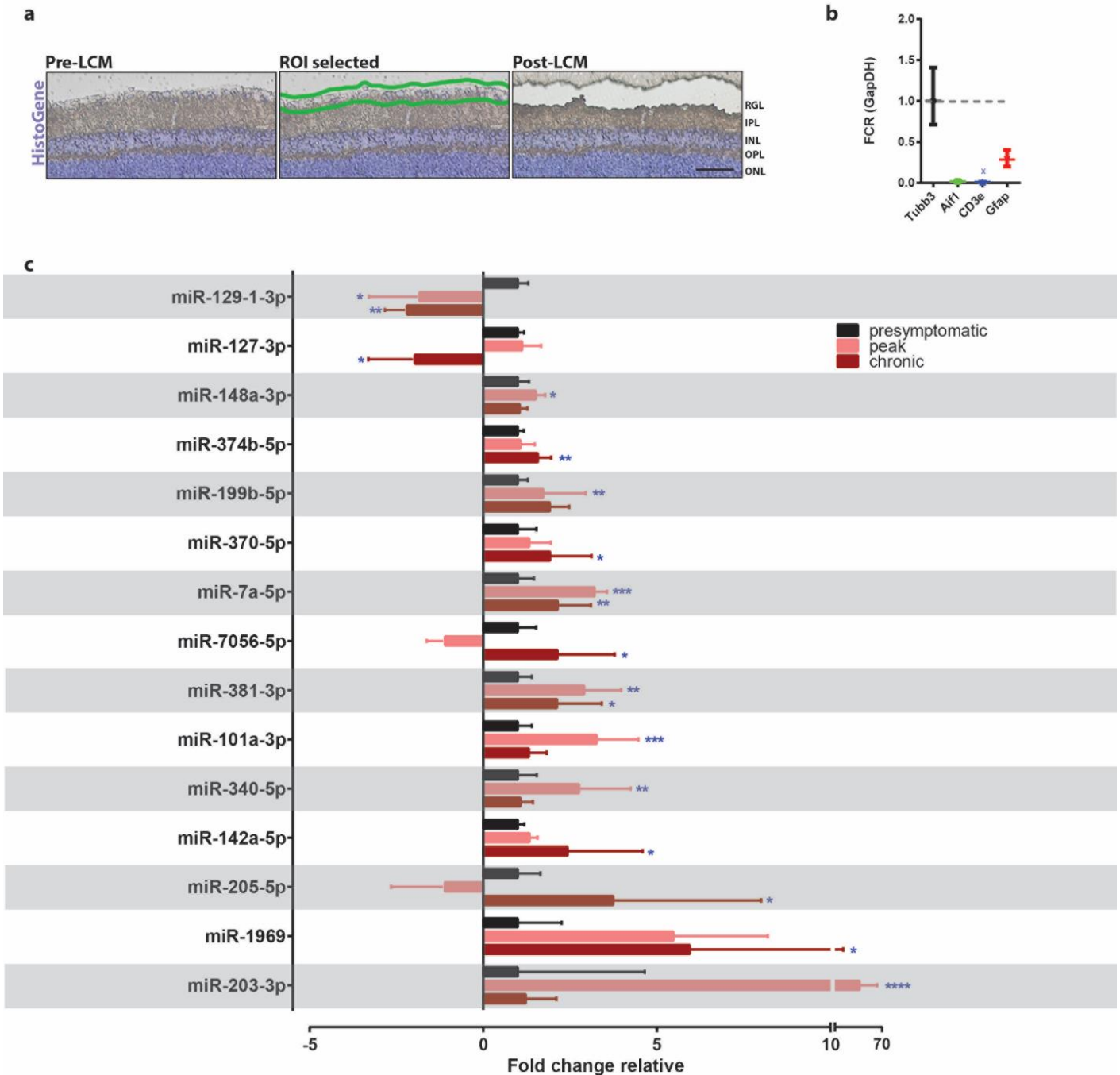


Figure 4. Profiling miRNA expression in the RGC layer of EAE mice. (a) Representative retinal sections stained with HistoGene following LCM (ROI= region of interest, RGC= retinal ganglion cell layer, IPL= inner plexiform layer, INL= inner nuclear layer, OPL= outer plexiform layer, ONL= outer nuclear layer), 50 um scale bar. (b) qPCR of LCM RGC layer tissue for microglia/macrophages (Aif1), immune cells (Cd3e), and astrocytes (Gfap) relative to neuronal RNA expression (Tubb3). FCR, Fold Change Range. (c) Taqman MicroRNA Assay (qPCR) of miRNAs in the RGC layer of EAE mice over the course of the disease, normalized to endogenous control snoRNA202 for each individual miRNA and depicted as fold change relative to normalized presymptomatic levels. ****p<0.0001, ***p<0.001, **p<0.01, *p<0.05 (n=3-8, one-way ANOVA, p<0.05, Dunnett's multiple comparisons test).

3.3.3 miR-Seq identified and validated miRNAs in EAE neurons are found regulated

in other EAE/MS tissue- Next, we asked if the miRNAs identified by miR-Seq and validated in the neurons of EAE mice were previously described as differentially regulated in other tissues and cells in EAE and/or MS. Of the 27 regulated miRNAs in motor neurons, 13 have been previously implicated in EAE and/or MS (Table 1). Regulation of individual miRNAs was previously identified in immune populations including lymph nodes (Bergman, James et al. 2013), whole blood (Keller, Leidinger et al. 2009, Keller, Leidinger et al. 2014), serum (Fenoglio, Ridolfi et al. 2013, Ridolfi, Fenoglio et al. 2013, Ebrahimkhani, Vafaei et al. 2017, Regev, Healy et al. 2017), plasma (Singh, Deshpande et al. 2016), peripheral blood mononuclear cells (PBMCs) (Ridolfi, Fenoglio et al. 2013, Baulina, Kulakova et al. 2018), leukocytes (Magner, Weinstock-Guttman et al. 2016, Munoz-Culla, Irizar et al. 2016), CD3+T cells (Jernas, Malmstrom et al. 2013), CD4+ T cells (Guerau-de-Arellano, Smith et al. 2011, Hosseini, Ghaedi et al. 2016), T regulatory cells (T_{regs}) (De Santis, Ferracin et al. 2010), or B cells (Sievers, Meira et al. 2012); or in the brain within MS lesions (Junker, Krumbholz et al. 2009, Dutta, Chomyk et al. 2013) or normal appearing white matter (NAWM) (Noorbakhsh, Ellestad et al. 2011, Guerau-de-Arellano, Liu et al. 2015, Talebi, Ghorbani et al. 2017). In a small number of cases the miRNA of interest was genetically manipulated for investigation in EAE (Ichiyama, Gonzalez-Martin et al. 2016, Ifergan, Chen et al. 2016, Satoorian, Li et al. 2016, Cantoni, Cignarella et al. 2017). The miRNAs overlapping with those previously implicated in EAE and/or MS include miR-101-3p, miR-125b-1-3p, miR-127-3p, miR-129-1-3p, miR-142a-5p, miR-148a-3p, miR-183-5p, miR-203-3p, miR-223-3p, miR-335-5p, miR-340-5p, miR-423-5p, and miR-7a-5p. Intriguingly the only miRNAs that were regulated in the same direction in neurons as in previously described tissue were miR-129-1-3p, miR-142a-5p and miR-335-5p, all regulated in MS NAWM (Noorbakhsh, Ellestad et al. 2011).

3.3.4 *in silico* assessment of putative targets identifies novel pathways predicted

to be affected in the neurons of EAE mice- To predict programs of gene expression that may be regulated by miRNAs that were commonly regulated in motor neurons and RGCs, we performed a non-biased *in silico* analysis to identify putative mRNA targets of regulated miRNAs (Fig. 5).

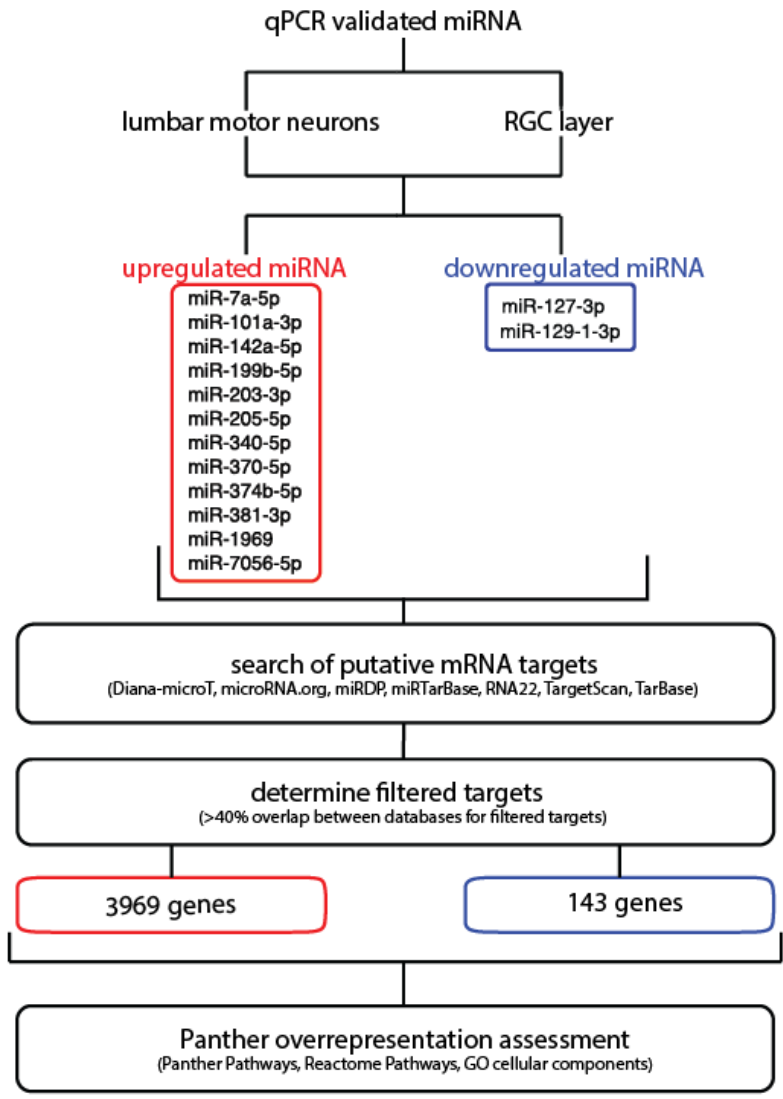


Figure 5. Flow-through of the *in silico* assessment for putative mRNA targets of the differentially regulated miRNAs in the lumbar motor neurons and RGC layer of EAE mice.

We mined predicted targets of miRNAs using Diana-microT (Reczko, Maragkakis et al. 2012, Paraskevopoulou, Georgakilas et al. 2013), microRNA.org (Betel, Wilson et al. 2008), miRDP (Wong and Wang 2015), miRTarBase (Chou, Chang et al. 2016), RNA22 (Miranda, Huynh et al. 2006), TargetScan (Agarwal, Bell et al. 2015), and TarBase (Vlachos, Paraskevopoulou et al. 2015). mRNAs that were predicted targets in at least 3 of 7 databases were coined ‘filtered targets’. To determine conserved pathways between the neuronal subtypes in EAE, we overlapped the filtered targets of regulated miRNAs in lumbar motor neurons and the RGC layer and performed an overrepresentation test using Protein ANalysis THrough Evolutionary Relationships (PANTHER) tools (Mi, Muruganujan et al. 2013, Mi, Huang et al. 2017). We identified

several enriched PANTHER Pathways, Reactome Pathways and gene ontology (GO) cellular components that are targeted by upregulated miRNAs (Table 2). Specific gene targets identified in the PANTHER, Reactome and GO cellular component pathways are recorded in Supplementary Tables S3-5, respectively. The upregulated miRNAs in neurons harvested from EAE mice are predicted to target and downregulate genes in PANTHER Pathways including hypoxia response via hypoxia-inducible factors (HIF) activation, and axon guidance mediated by Slit/Robo. Predicted Reactome Pathways include: KIT signaling; signaling by bone morphogenic protein (BMP); netrin-1 signaling; CD28 co-stimulation; protein lysine methyltransferases (PKMTs) methylate histone lysines; and synthesis of phosphatidylinositol phosphates (PIPs) at the plasma membrane. PANTHER and Reactome analyses differ in how they classify terms (Mi, Huang et al. 2017). The GO cellular components targeted by the upregulated miRNAs are the CCR4-NOT complex, and cytoplasmic stress granules (SG). The predicted targets suggest that upregulated miRNAs target pathways converging on cell survival and growth, cytoskeleton rearrangement, and the stress response. These pathways and how they may act in concert are summarized in Fig. 6.

Table 2

Overrepresented pathways and cellular components by the upregulated miRNAs in EAE neurons

	Fold enrichment	p-value
PANTHER Pathways		
Hypoxia response via HIF activation	3.32	0.00416
Axon guidance mediated by Slit/Robo	3.30	0.02160
Reactome Pathways		
Regulation of KIT signaling	4.53	0.03230
Signaling by BMP	3.69	0.03460
Netrin-1 signaling	3.69	0.03460
CD28 co-stimulation	3.51	0.01080
PKMTs methylate histone lysines	3.24	0.01150
Synthesis of PIPs at the plasma membrane	3.16	0.02580
GO Cellular Component		
CCR4-NOT complex	4.16	0.01130
cytoplasmic stress granule	3.10	0.00442

miRNA expression of the respective targeting miRNAs (Fig. 7). Genes *Bmpr1a*, *Cdc42*, *Hif1a*, *Pik3r1*, *Eif4e*, and *Mbnl1* showed a significant downregulation at peak disease, corresponding with increased expression of their targeting miRNAs at peak disease. Genes *Rictor* and *Smad4* showed the same trend, but were not significant. *Larp1* was uniquely downregulated at chronic disease stage, and accordingly its targeting miRNAs were upregulated at the chronic stage. Genes *Pik3c2a* and *Pum1* were downregulated throughout EAE relative to presymptomatic levels. *Pum1* is targeted by the most miRNAs, and showed the strongest downregulation throughout EAE, emphasizing the validity of our *in silico* approach for determining the (1) filtered targets of our differentially regulated miRNAs; and (2) PANTHER pathways and cellular components assessment of the filtered targets. The overrepresentation test for filtered targets of miRNAs that were downregulated in both neuronal subtypes generated a small list of 143 genes, and this was insufficient to identify overrepresented pathways or cellular components. Therefore, we performed an overrepresentation analysis for pathways that were predicted to be downregulated in lumbar motor neurons alone. We identified several enriched PANTHER Pathways, Reactome Pathways, and GO cellular components that were targeted by downregulated miRNAs (Table 3). The PANTHER Pathways included signaling mediated by the following: histamine H₁ receptor; oxytocin receptor; phosphoinositide 3-kinase (PI3K); thyrotropin-releasing hormone receptor; Alzheimer's disease (AD)-amyloid secretase; epidermal growth factor receptor (EGFR); 5-HT₂ type receptor; and fibroblast growth factor (FGF). The Reactome Pathways included: post-transcriptional silencing by small RNAs; signaling by TGF- β Receptor Complex; and several events activating PI3K/Akt via GAB1 signalsome, EGFR, and FGF receptor (FGFR). Finally, the cellular components enriched in targeted genes of downregulated motor neuron miRNAs included protein phosphatase type 2A (PP2A) complex, and endocytic vesicles. Specific gene targets identified in the PANTHER Pathways, Reactome Pathways, and GO cellular components are recorded in Supplementary Tables S6-8, respectively. As these pathways and cellular components were targeted by the downregulated miRNAs, it is suggested that they are now activated or relieved of inhibition.

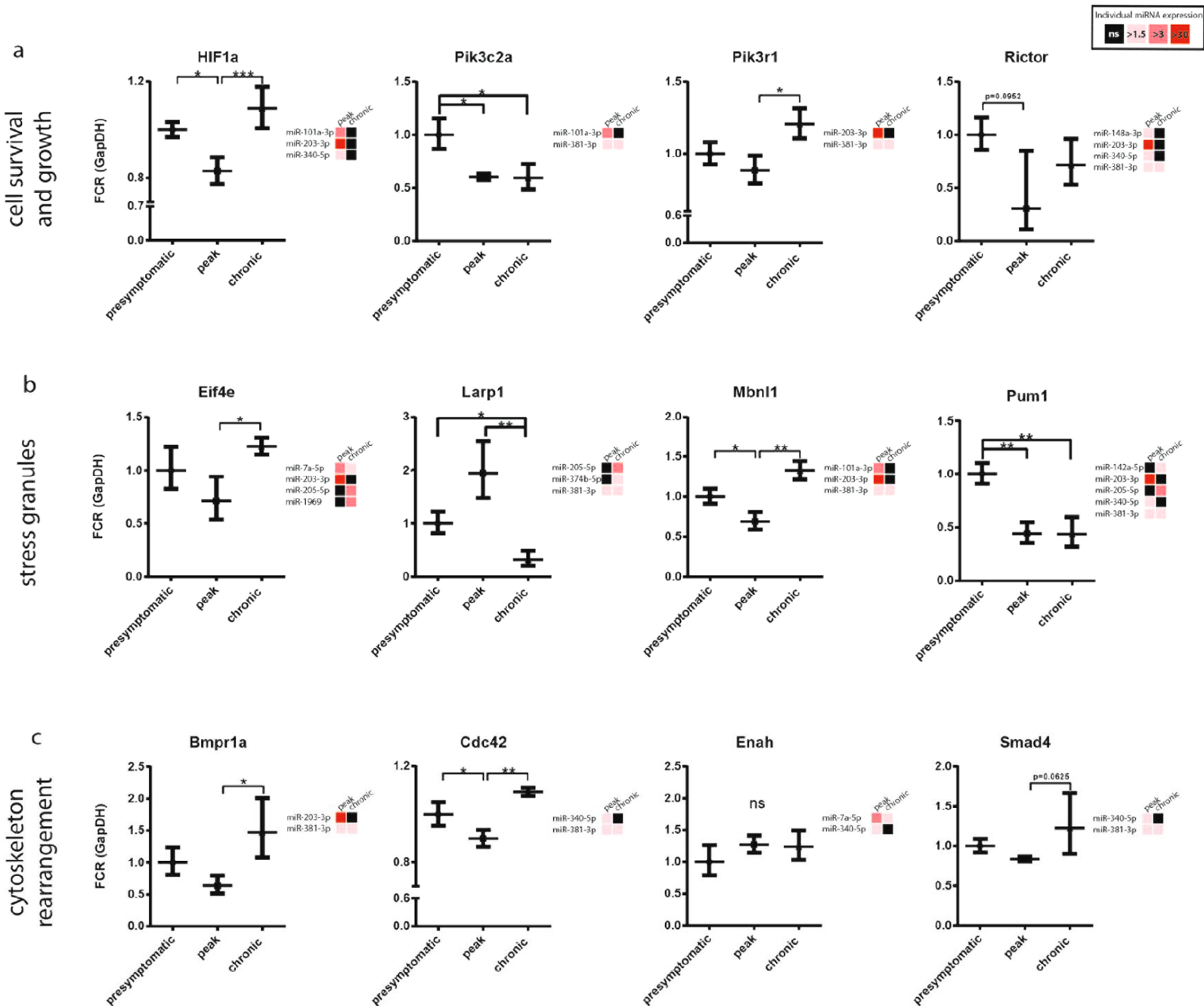


Figure 7. Expression of predicted miRNA gene targets as identified by *in silico* analysis in the RGC layer. Right-hand side of every qPCR profile for target genes is their respective targeting miRNA expression profiles with fold upregulation relative to presymptomatic levels. Black, not significant (ns). Genes are organized by their physiological roles, specifically (a) cell survival and growth (b), stress granule formation, and (c) cytoskeleton rearrangement. Gene expression was normalized to endogenous GapDH, FCR=Fold Change Range. *** $p < 0.001$, ** $p < 0.01$, * $p < 0.05$ ($n = 3-6$, one-way ANOVA, $p < 0.05$, Tukey's multiple comparisons test)

Table 3

Overrepresented pathways and cellular components by the downregulated miRNAs in EAE lumbar motor neurons

	Fold enrichment	p-value
PANTHER Pathways		
Histamine H ₁ receptor mediated signaling pathway	3.77	0.03600
Oxytocin receptor mediated signaling pathway	3.68	0.00696
PI3 kinase pathway	3.57	0.03120
Thyrotropin-releasing hormone receptor signaling pathway	3.50	0.01160
AD-amyloid secretase pathway	3.34	0.01870
EGF receptor signaling pathway	3.34	0.00001
5-HT ₂ type receptor mediated signaling pathway	3.20	0.02930
FGF signaling pathway	3.15	0.00024
Reactome Pathways		
Post-transcriptional silencing by small RNAs	13.51	0.01070
Signaling by TGF-beta Receptor Complex	3.94	0.00829
GAB1 Signalsome	3.15	0.00970
PI3K events (ERBB4, FGFR4, FGFR3, FGFR2, FGFR1)	3.09	0.02100
PIP3 activates Akt signaling	3.09	0.02100
PI3K/Akt activation	3.00	0.03150
GO Cellular Component		
PP2A complex	6.64	0.04940
endocytic vesicle	3.60	0.00001

3.4 Discussion

In this study, we took an unbiased approach to determine the changes in neuronal miRNA expression in a model of CNS inflammation. We compared the miR-Seq validated profile of lumbar motor neurons to RGCs in EAE, and identified potentially regulated pathways and cellular components during neuroinflammation, using an *in silico* bioinformatics approach. This provides the first analysis of miRNA expression in neurons over the course of EAE. Currently only immune-related material (Keller, Leidinger et al. 2009, De Santis, Ferracin et al. 2010, Siegel, Mackenzie et al. 2012, Bergman, James et al. 2013, Fenoglio, Ridolfi et al. 2013, Ridolfi, Fenoglio et al. 2013, Keller, Leidinger et al. 2014, Ebrahimkhani, Vafaei et al. 2017); or CNS tissue with mixed cell types such as lesions (Junker, Krumbholz et al. 2009) or NAWM (Noorbakhsh, Ellestad et al. 2011, Guerau-de-Arellano, Liu et al. 2015) have been isolated to profile differential miRNA expression in MS.

The time course assessment of miRNA expression revealed massive upregulation at peak disease. The loss of motor neurons and axons in the ventrolateral and dorsal columns begins early at onset of EAE disease; thus, we hypothesized that lumbar motor neurons would exhibit miRNA regulation at disease onset (Vogt, Paul et al. 2009, Recks, Stormanns et al. 2013). Rather, almost all miRNAs were uniquely upregulated at peak disease alone, in some cases trending towards upregulation at onset (Fig 3). Animals may have slightly different kinetics of disease and have more variability at onset.

There are several potential explanations for exaggerated miRNA upregulation at peak disease. Specifically, miRNAs may be trapped in the cell body compartment as result of axonal transection and compromised axonal transport early in EAE, leading to their accumulation over the course of disease (Bannerman, Hahn et al. 2005, Recks, Stormanns et al. 2013). Alternatively, it is predicted that genes involved in post-transcriptional silencing by small RNAs would be dramatically enriched 13.5 fold as a consequence of downregulation of select miRNAs in motor neurons (Table 3). The predicted increase in neuronal RISC pathway components contrasts with a report of decreased miR-mediated transcriptional silencing in the T cells and oligodendrocytes of EAE mice (Lewkowicz, Cwiklinska et al. 2015). Lastly, it is also possible that negative

feedback loops required to limit miRNA expression may be compromised in inflamed neurons. For example, miR-223-3p is part of an autoregulatory negative feedback loop with transcription factor E2F1, and disruption of this loop may contribute to the progression of acute myeloid leukemia (Pulikkan, Dengler et al. 2010). Dysregulation of such feedback loops may thus be affected in the neurons of EAE mice.

Next, our comparison of miRNA expression across cell types in EAE and/or MS revealed that miRNA expression is dependent on the cell type even when compared within the same disease model or group of patients (Table 1). Of the differentially expressed miRNAs in motor neurons, half were regulated in the same direction in the RGC layer. This identifies some similarities in neuronal responses to inflammation irrespective of neuronal function. Differences in miRNA regulation in the two neuronal populations could represent physiologic diversity in responses. Alternatively, these divergences could reflect differences in the time course of inflammation in the motor and visual system. Motor neuron loss begins as soon as 14 dpi in the EAE model, whereas RGC loss becomes significant between 25 and 40 dpi (Vogt, Paul et al. 2009, Quinn, Dutt et al. 2011). Another consideration is that motor neurons and their axons can be exposed to a common inflammatory milieu whereas RGCs are compartmentalized from their axons within the optic nerve. Similar proportions of T cell, B cell, macrophage and microglia populations have been described within the spinal cord and optic nerve (Knier, Rothhammer et al. 2015). However, there is a lack of immune infiltrates within the choroid or retina surrounding the RGCs, with CD3+ infiltrates exclusively occurring in the optic nerve whereas activated microglia and astrocytes are present in the choroid (Horstmann, Schmid et al. 2013, Horstmann, Kuehn et al. 2016). Alternatively, in the spinal cord, CD3+ infiltrates are described in close proximity to motor neurons (Vogt, Paul et al. 2009). We cannot rule out the possibility that some differences result from comparing pure motor neurons to the RGC layer, which contains amacrine cells and retinal astrocytes in addition to approximately 50% RGCs (Schlamp, Montgomery et al. 2013).

When comparing our analysis of neurons to prior studies examining EAE or MS tissue, we find that most of the neuronally-regulated miRNAs were not similarly regulated in other EAE/MS tissue. Several miRNAs including miR-127-3p, miR-223-3p, miR-7a-5p,

miR-203-3p and miR-340-5p are differentially regulated depending on the tissue source (Table 1). For example, miR-340-5p was reportedly upregulated in CD4+ T cells in MS but downregulated in MS lesions (Junker, Krumbholz et al. 2009, Guerau-de-Arellano, Smith et al. 2011). The only prior study to investigate neuronal miRNAs compared miRNA expression by fluorescence intensity between myelinated and demyelinated hippocampal human post-mortem MS tissue (Dutta, Chomyk et al. 2013). They investigated a list of candidate miRNAs based on their specific associations with mRNAs that are changed in demyelinated MS hippocampi. Regulated miRNAs in that study were not differentially regulated in our screen.

Our results highlight the importance of performing cell type specific analyses of miRNAs because target genes can have distinct effects in individual cell types. For example, miR-183-5p is elevated in the neurons of a model of spinal muscular atrophy (SMA) and promotes neurodegeneration (Kye, Niederst et al. 2014). However, miR-183 elevation is also important for blocking the cytotoxic effects of natural killer (NK) cells by targeting required receptors for NK cell activation (Donatelli, Zhou et al. 2014). This could have potential protective roles in the inflammatory context of MS (Gross, Schulte-Mecklenbeck et al. 2016). In both models miR-183-5p is upregulated, yet its elevation produces drastically different biologies in the two cell types.

Finally, the putative pathways targeted by the differentially regulated neuronal miRNAs suggest that these miRNAs contribute to axonal pathology and cell death. Using a bioinformatics approach, we determined putative pathways targeted by upregulated miRNAs during neuroinflammation. Many target pathways such as CD28 co-stimulation are known to affect the biology of non-neuronal cells (Supplementary Tables S3-4). While it is possible that neuronal miRNAs may be released in exosomes to affect the biology of other cells (Ebrahimkhani, Vafaei et al. 2017), we will limit our discussion to potential roles in the neuronal response.

Many of the pathways and cellular components described in Table 2 converge on cell survival and growth, cytoskeleton dynamics, and stress response. The predicted direction of regulation suggest that regulated miRNAs could contribute to neuronal degeneration, cell death and an aberrant stress response.

Many genes of the pathways described in Table 2 converge on the promotion of cell survival and growth via the PI3K/Akt/mTOR cascade (Laplante and Sabatini 2012, King, Yeomanson et al. 2015). Genes *Src*, *Mtor*, *Rictor*, *Rptor*, *Akt1*, *Akt2*, *Akt3*, *Pik3r1*, and *Pik3c2a* are directly involved in positive mTOR signaling (Hirsch, Costa et al. 2007, Laplante and Sabatini 2012), and are predicted to be targeted by several of our upregulated miRNAs (Supplementary Table S4). Such a regulation would result in stunted growth and cell death. HIF signaling, downstream of mTOR, promotes survival during hypoxia (Benizri, Ginouves et al. 2008, Laplante and Sabatini 2012). HIF signaling genes *HIF1a* and *Arnt* are also targeted by our upregulated miRNAs (Benizri, Ginouves et al. 2008). *In vivo* knockdown or inhibition of HIF activity limits axon regeneration in axotomized sensory neurons (Cho, Shin et al. 2015, Alam, Maruyama et al. 2016), and exacerbates cerebral ischemia-induced tissue damage (Baranova, Miranda et al. 2007); whilst the pharmacological upregulation of HIF in animal models of cerebral ischemia (Luo, Ouyang et al. 2017), Parkinson's disease (Guo, Hao et al. 2016), and AD (Guo, Yang et al. 2017) alleviates disease. Targeting of the PI3K/Akt/mTOR cascade and its downstream pathways suggests our upregulated miRNAs promote cell death of EAE neurons. This is emphasized by the significant downregulation of genes *HIF1a*, *Pik3c2a* and *Pik3r1* at peak disease in the RGC layer of EAE mice (Fig. 7a).

Another pattern that emerged was that stress granule (SG) formation may be disrupted in response to miRNA upregulation (Table 2, Supplemental Table S5). Many SG initiating genes, including *Tia1*, *Tial1*, *G3bp1*, *Zfp36*, *Fmr1*, *Pum1*, and *Pum2*, are targeted by the upregulated miRNAs (Kedersha, Gupta et al. 1999, Tourriere, Chebli et al. 2003, Murata, Morita et al. 2005, Kim, Dong et al. 2006, Vessey, Vaccani et al. 2006), along with other essential components of SGs listed in Supplementary Table S5. Some of these genes were downregulated throughout EAE, with *Pum1* significantly downregulated at both peak and chronic EAE in the RGC layer; where *Pum1* was one of the most targeted genes by the upregulated miRNAs (Fig. 7b). SGs are non-membrane bound cytoplasmic aggregates of RNA and protein that form in response to environmental stress such as hypoxia, endoplasmic reticulum (ER) stress, reactive oxygen species, and nutrient deprivation (Mahboubi and Stochaj 2017). ER stress is a hallmark of MS and chronic stress in neurons that leads to failed SG assembly (McMahon, McQuaid et al.

2012, Haile, Deng et al. 2017, Shelkownikova, Dimasi et al. 2017). SGs are transient and can act to protect untranslated mRNA from stress-dependent damage (Kedersha, Cho et al. 2000). Use of the SG-stabilizing drug guanabenz in EAE alleviates clinical symptoms (Tsaytler, Harding et al. 2011, Way, Podojil et al. 2015). The implication from our study is that upregulated miRNAs may block adaptive SG formation, limiting the ability of neurons to recover from chronic inflammatory stress associated with EAE.

Interestingly, we also identified genes ascribed to axon guidance pathways as targets of upregulated miRNAs. *Mena*, *Rac1*, *Cdc42*, *DCC*, *Smad4*, and *Bmpr1a* are some predicted gene targets of the upregulated miRNAs (Supplementary Tables S3-4). Several of these targets can positively influence cytoskeleton rearrangement, such as *Bmpr1a* and *Cdc42*, which we identified as significantly downregulated at peak disease in the RGC layer (Fig. 7c). This raises the possibility that miRNA-dependent downregulation contributes to the formation of retraction bulbs in MS lesions and failure to reform a new growth cone and mount a regenerative response (Trapp, Peterson et al. 1998, Forcet, Stein et al. 2002, Chen, Wirth et al. 2012, Zhong and Zou 2014, Vidaki, Drees et al. 2017).

The current understanding of how neurons are affected during EAE and MS has been unclear. Our assessment of the affected miRNAs and their targeted pathways over the course of EAE suggests that the upregulated miRNAs themselves target pathways related to cell survival and growth, cytoskeletal rearrangement, and stress response. We also identified the downregulation of representative targets in the same tissue, validating our *in silico* approach and emphasizing the contribution of these pathways to EAE. This novel information concerning the neuronal response lends information on what we may be able to target therapeutically to promote neuroprotection or repair for a disease largely discussed in an inflammatory context alone.

3.5 Acknowledgments

A.E.F. is supported by grants from the Canadian Institutes of Health Research (CIHR) and the Multiple Sclerosis Society of Canada. C.A.J. was supported by a fellowship from the Montreal Neurological Institute and a Vanier Canada Graduate Scholarship. We thank Isabel Rambaldi, Margarita Souleimanova, Dr. Hong Zhao, Mardja Bueno and Dr. Luke Healy for their expert technical advice; McGill University Life Sciences Complex Advanced Biomedical Imaging Facility (ABIF), and Dr. Ian Bates for aid with the PALM MicroBeam; Drs. Samuel David, Samuel Ludwin, and Timothy Kennedy for their valuable discussions.

3.6 Competing Financial Interests

Dr. Bar-Or has participated as a speaker in meetings sponsored by and received consulting fees and/or grant support from: Atara Biotherapeutics, Biogen Idec, Celgene/Receptos, Genentech/Roche, GlaxoSmithKline, MAPI, Medimmune, Merck/EMD Serono, Novartis, Sanofi-Genzyme.

3.7 Material and Methods

3.7.1 Active EAE Disease Induction and Scoring - EAE was induced in 6-9 week old female C57BL/6 mice as previously published (Lecuyer, Saint-Laurent et al. 2017). Animals were immunized subcutaneously with 200 µg of myelin oligodendrocyte glycoprotein 35–55 (MOG_{35–55}) (MEVGWYRSPFSRVVHLYRNGK; Alpha Diagnostic International) in a 100 µl emulsion of Complete Freund's Adjuvant (4 mg/ml *Mycobacterium tuberculosis*; Fisher Scientific). On day 0 and day 2, Pertussis toxin (500 ng PTX, Sigma-Aldrich) was injected intra-peritoneally (i.p.). Animals were scored as follows: 0 = normal; 1 = limp tail; 2 = slow righting-reflex; 2.5 = difficulty walking/ataxia; 3 = paralysis of one hindlimb (monoparalysis); 3.5 = hindlimb monoparalysis and severe weakness in the other hindlimb; 4 = paralysis of both hindlimbs (paraparalysis); 4.5 = hindlimbs paraparalysis and forelimbs weakness; 5 = moribund (requires sacrifice). All animal procedures were approved by the Centre de Recherche du Centre Hospitalier de l'Université de Montréal Animal Care Committee (N11023APs) and followed guidelines of the Canadian Council on Animal Care.

3.7.2 CNS tissue isolation - Animals were injected with a lethal dose of Euthanyl® (Pentobarbital Sodium). Animals showing no sign of pedal and palpebral reflex were perfused intracardially using cold saline. The spinal cord and retina were isolated and frozen at -80°C in Tissue-Tek® O.C.T. compound. Spinal cords were collected at naïve (score 0), onset (score 0.5-1), and peak (score 3-3.5) clinical points; and retinæ were collected at presymptomatic (score 0, 8 dpi), peak (score 3.5-4), and chronic endpoints (score 2, endpoint at 35 dpi). Frozen sections were obtained using a Leica® cryostat CM3050S. Sections were mounted onto RNase-free MembraneSlide 1.0 polyethylene-naphthalate (PEN) (Zeiss), at a thickness of 10 µm. Slides were stored at -80°C until further processing by LCM.

3.7.3 Laser capture microdissection - Individual MembraneSlide 1.0 PEN were fixed, stained, washed and dried using the Arcturus® HistoGene® LCM Frozen Section Staining Kit (ThermoFisher) following manufacturer's recommendations. Individual slides

were thawed and dried for 20 sec on an RNAase-free glass surface; fixed in 70% ethanol for 30 sec; washed in water for 30 sec; stained with HistoGene for 30 sec; washed in 70% ethanol for 30 sec; washed in 95% ethanol for 30 sec; washed in 100% ethanol for 30 sec; dehydrated in xylene for 5 min; and dried to remove excess xylene for 1 min. All solutions and materials used were RNase-free. HistoGene-stained large motor neuron cell bodies from the ventral horn, and RGC layers from the retina, were laser dissected by PALM MicroBeam (Zeiss) and collected in 15 µl Qizol (QIAGEN) into the cap of an RNase-free 200 µl centrifuge tube. Collected material was vortexed and left at room temperature (RT) for 1 min before being stored at -80°C until further RNA extraction. Overall, approximately 3000 motor neurons and 700 RGC layers were captured per animal by combining multiple serial sections.

3.7.4 RNA extraction from LCM tissue- Material from each frozen 200 µl centrifuge tube were pooled together for each individual mouse for RNA extraction. Collected material was topped off to 700 µl QIAzol, and 140 µl of chloroform. Samples were shaken, incubated at RT for 5 min and centrifuged (12,000 g at 4°C for 15 min). The upper phase was mixed with 2 times volume of 100% ethanol and 1.5 µl GlycoBlue™ Coprecipitant (ThermoFisher), and left at -80°C overnight to precipitate all nucleic acids. Precipitant was centrifuged at 16,000 g at 4°C for 30 min. Liquid was removed and the pellet containing the nucleic acid was washed two times with 400 µl ice cold 75% EtOH. The pellet was air dried for 10 min, resuspended in 10 µl water, and suspended in 700 µl QIAzol. RNA was extracted from the resuspended pellet using the miRNeasy kit (QIAGEN) as per manufacturer's instructions.

3.7.5 Cell cultures- All studies were approved by the McGill University Animal Care and Use Committee. To obtain astrocyte and microglial cultures, cortices were dissected from P2-P4 CD1 mouse pups in cold Lebovitz L15 medium (ThermoFisher), and seeded onto dishes coated with 100 µg/mL poly-L-lysine (PLL). At approximately 11 days in vitro (DIV), T75 flasks containing a mixed cortical culture were shook for 30 min at 180 rpm on an orbital shaker to remove microglia. Supernatant containing microglia was spun down at 1

rpm for 5 min to pellet cells, pelleted cells were suspended in QIAzol. Simultaneously fresh DMEM 10% fetal bovine serum (FBS) containing 1% penicillin-streptomycin and 2 mM glutamine were added to the cultures. The flasks were left at 37°C and 5% CO₂ for 1h and later shook at 240 rpm for 2h in order to remove oligodendrocyte precursor cells. Astrocytes were lysed with QIAzol. To obtain cortical neurons, cortices were dissected from embryonic day 16-17 (E16-17) C57/Bl6 mice and dissociated with 0.25% EDTA-trypsin for 20 min at 37°C, 5% CO₂, followed by mechanical titration 10 times with a sterile 1000 uL pipette tip in DMEM 10% FBS containing 1% penicillin-streptomycin and 2 mM glutamine, and seeded onto PLL-coated dishes. Media was changed to Neurobasal medium supplemented with 2% B27, 1% N2, 1% penicillin-streptomycin and 2 mM glutamine 1h after seeding. At 5 DIV, medium was removed and neurons lysed with QIAzol. To obtain PBMCs, whole blood was collected by cardiac puncture from adult C57Bl/6 mice. Mouse PBMCs were separated by Ficoll-Plaque density centrifugation, and suspended in QIAzol. RNA was extracted from QIAzol lysed cells using the miRNeasy kit (QIAGEN) as per manufacturer's instructions.

3.7.6 Next-Generation Sequencing (NGS) - Total extracted RNA from the lumbar motor neurons was sent to Arraystar, Inc for NGS. Total RNA was isolated from each sample and used to prepare the miRNA sequencing library with the following steps: 1) 3'-adapter ligation; 2) 5'-adapter ligation; 3) cDNA synthesis; 4) PCR amplification; 5) size selection of approximately 130-150 bp PCR amplified fragments (corresponding to approximately 15-35 nt small RNAs). The libraries were denatured as single-stranded DNA molecules, captured on Illumina flow cells, amplified *in situ* as clusters and finally sequenced for 51 cycles on Illumina HiSeq 2000 according to manufacturer's instructions. The sequencing reads were quality controlled by CHASTITY onboard the sequencing system with Q-scores. The FASTQ files were processed by a combination of FastQC v.0.11.2, SolexaQA v.2.0, fastq_screen_v0.4.4 (--subset 1500000), and Perl 10 script to remove the reads that contained ambiguous bases "N", poly(A/T); and the read lengths < 14. Q-score folds were 25 for the 3'-end, 10 for < 4 bases or 13 for < 6 bases in the first 30 bases, and 20 for > 75% of all bases. The adaptor sequences were trimmed with cutadapt called from

Python environment with --overlap set to 2. Trimmed reads were aligned to a combined mouse pre-miRNA in miRBase 21 and the predicted novel pre-miRNAs with Novoalign v2.07.11, allowing no more than 1 mismatch. miRDeep2 was used to predict novel miRNAs with the trimmed reads. miRNA read counts were processed and normalized with the DeSeq2 (version 3.5) Bioconductor package and used to detect differentially expressed miRNAs in lumbar motor neurons (Love, Huber et al. 2014). Significantly differentially expressed miRNAs (adjusted $p < 0.05$) were visualized as heatmaps created with the Morpheus tool (<http://software.broadinstitute.org/morpheus/>).

3.7.7 Quantitative RT-PCR (qRT-PCR) - For qRT-PCR validation of miRNA expression in lumbar motor neurons, samples from deep sequencing and additional naïve and peak time points samples were analyzed (n=3-6). The expression of 41 differentially regulated miRNAs was analyzed using multiplex qRT-PCR. Forty-one miRNAs were profiled using a Taqman MicroRNA Assay, of which 5 were novel miRNAs that required custom designs (Supplementary Table S2). Multiplexed RT reactions were performed using a mix of miRNA-specific RT primers and a TaqMan miRNA RT kit, with 10 specific primers per RT reaction and 10 ng of RNA per RT reaction. A pre-amplification reaction was run with 5 μ l of the RT-generated cDNA using again a pooled set of TaqMan miRNA-specific probes to increase the number of target copies, as previously described (Moore, Rao et al. 2013). Individual miRNA expression assays were performed using specific miRNA TaqMan probes on the pre-amplified cDNA material. Small nuclear RNA (snRNA) snoRNA202 was used as an endogenous control. Fold change calculations for miRNA expression were performed using the $2^{-\Delta\Delta Ct}$ method (Livak and Schmittgen 2001), with normalized miRNA expression compared to the naïve mouse controls (score 0). miRNAs identified as significantly regulated in the lumbar motor neurons were assessed in the RGC layer of EAE mice using the multiplex qRT-PCR system with miRNA expression compared to presymptomatic mouse controls (score 0). For the RGC layer, 3-8 animals were assessed per condition. Statistical analysis was done using one-way ANOVA, and a Dunnett's multiple comparisons test (GraphPad Prism 6). For qRT-PCR of mRNA, total RNA from cell culture or LCM tissue was transcribed using Superscript Vilo or IV Vilo

cDNA Synthesis Kit (ThermoFisher), respectively, using manufacturer's instructions. Individual gene expression was determined using FAM-labeled Taqman probes, and as endogenous controls FAM-labeled GapDH probe for cell culture tissue and VIC-labeled GapDH probe for LCM tissue. For determination of neuronal purity in LCM tissue, RNA markers for other cell types were relative to neuronal Tubb3 expression (n=3) after GapDH normalization. For assessment of *in silico* identified genes in LCM RGC layer tissue, mRNA expression was compared to presymptomatic levels. Statistical analysis was done using one-way ANOVA, and a Tukey's multiple comparisons test with n=3-6 per disease stage (GraphPad Prism 6).

3.7.8 *in silico* assessment of predicated targets - For significantly regulated miRNAs, a bioinformatics assessment of putative target genes was performed based on a comparative analysis by seven prediction programs. These include: Diana-microT (Reczko, Maragkakis et al. 2012, Paraskevopoulou, Georgakilas et al. 2013), microRNA.org (Betel, Wilson et al. 2008), miRDP (Wong and Wang 2015), miRTarBase (Chou, Chang et al. 2016), RNA22 (Miranda, Huynh et al. 2006), TargetScan (Agarwal, Bell et al. 2015), and TarBase (Vlachos, Paraskevopoulou et al. 2015). Only mRNAs that were identified as putative targets across 3 of the 7 prediction programs were analyzed further. These were termed as "filtered targets". To determine conserved pathways between the neuronal subtypes in EAE, we overlapped the filtered targets of the upregulated miRNAs in lumbar motor neurons and the RGC layer (3969 genes). The functional classification of the overlapping filtered targets was performed using an overrepresentation test by PANTHER classification system (<http://www.pantherdb.org/>) (Mi, Muruganujan et al. 2013, Mi, Huang et al. 2017). The p-values were determined by PANTHER using the binomial statistic with a Bonferroni correction for multiple testing. From the overrepresentation assessment, we focused on PANTHER Pathways, Reactome Pathways and GO cellular components with a Fold Enrichment above 3. An overrepresentation assessment was repeated for the filtered targets of miRNAs downregulated in both neuronal subtypes (143 genes); however, this list was not comprehensive enough to determine any overrepresentation. An overrepresentation test

of the filtered targets of the upregulated miRNAs in the motor neurons alone (4346 genes); upregulated miRNAs in the RGC layer alone (4226 genes); downregulated miRNAs in the motor neurons alone (1422 genes) were also performed. Again, the list of filtered targets of downregulated miRNAs in the RGC layer alone (143 genes) was not comprehensive enough to determine any overrepresentation.

3.8 Supplementary Tables

Table 1 Supplemental

miRNA sequence information for custom design Taqman MicroRNA Assays

miRNA	pre-miRNA arm	MATURE-SEED	MATURE-LENGTH	MATURE-SEQ
mmu-miR-92b-3p	3p	AUUGCA	22	UAUUGCACUCGUCCCGGCCUCC
mmu-miR-novel-chr2_10423	5p	GGGCGU	17	CGGGCGUGGGGGUGGGG
mmu-miR-novel-chr2_7634	5p	GGGCUG	19	AGGGCUGGAGAGAUGGCUC
mmu-miR-novel-chr7_31864	5p	CCGAUC	22	ACCGAUCCCGGGUUAGUCUCCU
mmu-miR-novel-chr7_35252	3p	GAUUAU	22	UGAUUAAGCCAAGCCCCGACUGU
mmu-miR-novel-chr12_57357	5p	UGGGGG	19	GUGGGGGGCGGGGCGGACA
mmu-miR-novel-chr16_70802	5p	GAGGUA	18	GGAGGUAGUAGGUUGUGU

Table 2 Supplemental

Predicted gene targets in affected PANTHER Pathways of upregulated neuronal miRNAs

PANTHER Pathways	Filtered targets	Targeting miRNAs
Hypoxia response via HIF activation	Mtor	miR-101a-3p
	Hif1a	miR-340-5p, miR-203-3p, miR-101a-3p
	Pten	miR-142a-5p, miR-205-5p, miR-381-3p, miR-374b-5p
	Akt3	miR-101a-3p
	Pik3r1	miR-203-3p, miR-381-3p
	Pik3c2a	miR-101a-3p, miR-381-3p
	Egln1	miR-203-3p
	Egln3	miR-142a-5p
	Akt1	miR-374b-5p
	Pik3cd	miR-7a-5p
	Akt2	miR-203-3p
	Arnt	miR-340-5p
	Pik3r3	miR-7a-5p
	Pik3c2b	miR-101a-3p
	Ngly1	miR-381-3p
Axon guidance mediated by Slit/Robo	Pik3cb	miR-7a-5p
	Pik3ca	miR-340-5p
	Srgap1	miR-142a-5p, miR-205-5p
	Enah	miR-340-5p, miR-7a-5p
	Slit2	miR-381-3p
	Ntn1	miR-199b-5p, miR-205-5p
	Robo1	miR-340-5p, miR-142a-5p
	Cxcr4	miR-381-3p
	Abl1	miR-203-3p
	Rac1	miR-101a-3p
	Slit3	miR-340-5p, miR-374b-5p
	Cdc42	miR-340-5p, miR-381-3p
	Dcc	miR-381-3p
	Ntn1	miR-340-5p, miR-381-3p, miR-374b-5p
Rhoc	miR-142a-5p	
Robo2	miR-101a-3p	

Table 3 Supplemental

*Predicted gene targets in affected Reactome Pathways of
upregulated neuronal miRNAs*

Reactome Pathways	Filtered targets	Targeting miRNAs	
Regulation of KIT signaling	Socs6	miR-340-5p, miR-203-3p, miR-381-3p	
	Socs1	miR-142a-5p	
	Src	miR-203-3p	
	Kitl	miR-142a-5p, miR-101a-3p	
	Kit	miR-142a-5p	
	Fyn	miR-203-3p	
	Sh2b3	miR-101a-3p	
	Sos1	miR-374b-5p	
	Yes1	miR-340-5p, miR-205-5p, miR-7a-5p, miR-381-3p	
	Cbl	miR-101a-3p	
	Lyn	miR-203-3p	
	Prkca	miR-340-5p, miR-203-3p	
	Signaling by BMP	Acvr2a	miR-203-3p, miR-101a-3p, miR-381-3p
		Bmpr1a	miR-203-3p, miR-381-3p
Nog		miR-340-5p	
Bmpr2		miR-7a-5p	
Zfyve16		miR-203-3p, miR-205-5p, miR-381-3p	
Smad1		miR-203-3p	
Bmpr1b		miR-101a-3p	
Grem2		miR-340-5p	
Smurf1		miR-203-3p	
Ube2d1		miR-340-5p, miR-142a-5p, miR-101a-3p	
Smad6		miR-374b-5p	
Ube2d3		miR-101a-3p, miR-381-3p	
Bmp2		miR-381-3p, miR-374b-5p	
Ski		miR-340-5p	
Smad4		miR-340-5p, miR-381-3p	
Netrin-1 signaling	Ezr	miR-205-5p	
	Neo1	miR-1969, miR-374b-5p	
	Src	miR-203-3p	
	Trio	miR-205-5p, miR-101-3p	
	Nck1	miR-340-5p	
	Myh10	miR-423-5p, miR-381-3p	
	Rac1	miR-101a-3p	
	Fyn	miR-203-3p	
	Unc5c	miR-340-5p, miR-205-5p	
	Cdc42	miR-340-5p, miR-381-3p	
	Pitpna	miR-7a-5p	
	Ptk2	miR-340-5p, miR-7a-5p, miR-381-3p	
	Dcc	miR-381-3p	
	Ntn1	miR-340-5p, miR-381-3p, miR-374b-5p	
	Siah1a	miR-205-5p, miR-381-3p	
CD28 co-stimulation	Mtor	miR-101a-3p	
	Src	miR-203-3p	
	Pik3r1	miR-203-3p, miR-381-3p	
	Pdpk1	miR-1969, miR-7a-5p, miR-374b-5p	
	Akt1	miR-374b-5p	
	Map3k14	miR-205-5p	
	Rac1	miR-101a-3p	
	Fyn	miR-203-3p	
	Pak2	miR-340-5p	
	Cdc42	miR-340-5p, miR-381-3p	
	Mapkap1	miR-7a-5p	
	Yes1	miR-340-5p, miR-205-5p, miR-7a-5p, miR-381-3p	
	Stk4	miR-381-3p, miR-374b-5p	
	Map3k8	miR-101a-3p	

	Rictor	miR-340-5p, miR-203-3p, miR-381-3p
	Cd28	miR-142a-5p, miR-203-3p
	Lyn	miR-203-3p
	Pik3ca	miR-340-5p
PKMTs methylate histone lysines	Setd1a	miR-142a-5p
	Rbbp5	miR-1969
	Setd7	miR-101a-3p
	Aebp2	miR-205-5p
	Mecom	miR-7a-5p
	Ezh2	miR-101a-3p
	Dpy30	miR-101a-3p
	Suz12	miR-340-5p
	Kmt2a	miR-205-5p
	Dot1l	miR-101a-3p
	Whsc1l1	miR-340-5p
	Rbbp7	miR-101a-3p
	Kmt2d	miR-1969
	Whsc1	miR-101a-3p
	Setd8	miR-7a-5p
	Setd2	miR-142a-5p
	Setd3	miR-340-5p
	Ehmt1	miR-101a-3p
	Eed	miR-101a-3p
	Atf7ip	miR-340-5p, miR-203-3p, miR-205-5p, miR-101a-3p, miR-7a-5p
Synthesis of PIPs at the plasma membrane	Mttr3	miR-7a-5p
	Pip4k2a	miR-205-5p
	Pten	miR-142a-5p, miR-205-5p, miR-381-3p, miR-374b-5p
	Synj1	miR-340-5p, miR-142a-5p, miR-203-3p
	Pik3r1	miR-203-3p, miR-381-3p
	Pip5k1c	miR-101a-3p
	Pip4k2c	miR-1969
	Pik3c2a	miR-101a-3p, miR-381-3p
	Inpp1	miR-101a-3p, miR-7a-5p
	Ocr1	miR-374b-5p
	Pik3cd	miR-7a-5p
	Pip5k1b	miR-142a-5p, miR-101a-3p, miR-381-3p
	Pik3r3	miR-7a-5p
	Synj2	miR-205-5p
	Pik3c2b	miR-101a-3p
	Pi4k2a	miR-203-3p
	Pik3cb	miR-7a-5p
	Pik3ca	miR-340-5p

Table 4 Supplemental

Predicted gene targets in affected GO cellular components of upregulated neuronal miRNAs

Cellular components	Filtered targets	Targeting miRNAs
CCR4-NOT complex	Cnot2	miR-381-3p, miR-374b-5p
	Pat1	miR-1969, miR-7a-5p, miR-381-3p
	Rqcd1	miR-1969
	Cnot6l	miR-374b-5p
	Zfp36	miR-142a-5p
	Tnks1bp1	miR-1969
	Cnot4	miR-381-3p
	Cnot6	miR-381-3p
	Cpeb3	miR-340-5p, miR-142a-5p, miR-101a-3p
	Cnot7	miR-381-3p
	Cnot8	miR-7a-5p
	Cnot10	miR-203-3p
	Tob1	miR-1969, miR-7a-5p, miR-381-3p
	cytoplasmic stress granule	Larp4b
Fmr1		miR-101a-3p, miR-7a-5p, miR-374b-5p
Stau2		miR-101a-3p
Larp1		miR-205-5p, miR-381-3p, miR-374b-5p
Habp4		miR-205-5p
Pum1		miR-340-5p, miR-142a-5p, miR-203-3p, miR-205-5p, miR-381-3p
Ogfod1		miR-7a-5p
Rc3h1		miR-381-3p, miR-374b-5p
Lsm14a		miR-101a-3p, miR-381-3p
Eif4e		miR-203-3p, miR-205-5p, miR-1969, miR-7a-5p
Stau1		miR-142a-5p, miR-203-3p
Zfp36		miR-142a-5p
Pum2		miR-340-5p, miR-142a-5p, miR-101a-3p, miR-1969, miR-381-3p
Caprin1		miR-203-3p
Lin28a		miR-381-3p
Rptor		miR-1969
Ddx3x		miR-340-5p, miR-101a-3p
Nufip2		miR-203-3p, miR-205-5p
Ddx6		miR-203-3p, miR-381-3p
Larp4		miR-203-3p
Tia1		miR-101a-3p
G3bp1		miR-381-3p
Mbnl1		miR-203-3p, miR-101a-3p, miR-381-3p
Tial1		miR-203-3p, miR-205-5p

Table 5 Supplemental

Predicted gene targets in affected PANTHER Pathways of downregulated miRNAs in lumbar motor neurons

PANTHER Pathways	Filtered targets	Targeting miRNAs
Histamine H₁ receptor mediated signaling pathway	Gng7	miR-92b-5p
	Prkch	miR-183-3p
	Gng5	miR-183-3p
	Gna11	miR-335-5p
	Gnb1	miR-183-3p
	Prkcz	miR-148a-3p
	Prkci	miR-183-3p
	Prkce	miR-129-1-3p
	Gng4	miR-183-3p
	Plcb1	miR-148a-3p
	Prkca	miR-183-3p
	Oxytocin receptor mediated signaling pathway	Gng7
Prkch		miR-183-3p
Gng5		miR-183-3p
Cacna1d		miR-129-1-3p
Gna11		miR-335-5p
Gnb1		miR-183-3p
Prkcz		miR-148a-3p
Prkci		miR-183-3p
Cacnb4		miR-129-1-3p
Prkce		miR-129-1-3p
Gng4		miR-183-3p
Plcb1		miR-148a-3p
Prkca		miR-183-3p
Vamp2		miR-127-3p
PI3 kinase pathway	Pten	miR-148a-3p
	Irs1	miR-183-3p
	Ccnd2	miR-183-3p
	Gna11	miR-335-5p
	Gnb1	miR-183-3p
	Rps6kb1	miR-148a-3p, miR-335-5p
	Sos2	miR-148a-3p
	Pik3r3	miR-148a-3p
	Sos1	miR-148a-3p
	Gadd45a	miR-148a-3p
	Nras	miR-148a-3p
	Foxo1	miR-183-3p
	Thyrotropin-releasing hormone receptor signaling pathway	Gng7
Prkch		miR-183-3p
Gng5		miR-183-3p
Gna11		miR-335-5p
Gnb1		miR-183-3p
Prkcz		miR-148a-3p
Prkci		miR-183-3p
Trh		miR-335-5p
Cacnb4		miR-129-1-3p
Prkce		miR-129-1-3p
Gng4		miR-183-3p
Plcb1		miR-148a-3p
Prkca		miR-183-3p
Vamp2		miR-127-3p
AD-amyloid secretase pathway	Bace2	miR-335-5p
	Mapk4	miR-183-3p
	Chrm2	miR-129-1-3p
	Prkch	miR-183-3p
	Adam10	miR-148a-3p

	Mapk11	miR-335-5p
	Cacna1d	miR-129-1-3p
	Psen2	miR-183-3p
	Prkcz	miR-148a-3p
	Prkci	miR-183-3p
	Mapk1	miR-335-5p
	Prkce	miR-129-1-3p
	Furin	miR-129-1-3p
	Prkca	miR-183-3p
EGF receptor signaling pathway	Ppp6c	miR-335-5p
	Map3k1	miR-129-1-3p, miR-183-3p
	Ppp2ca	miR-183-3p
	Prkch	miR-183-3p
	Mapk11	miR-335-5p
	Map3k2	miR-335-5p
	Ar	miR-335-5p
	Ppp2r5e	miR-125b-1-3p
	Phldb2	miR-183-3p
	Ywhab	miR-148a-3p
	Mras	miR-148a-3p
	Hbegf	miR-183-3p
	Prkcz	miR-148a-3p
	Prkci	miR-183-3p
	Map3k4	miR-183-3p
	Sfn	miR-127-3p
	Mapk1	miR-335-5p
	Sos2	miR-148a-3p
	Sos1	miR-148a-3p
	Ppp2r5c	miR-183-3p
	Cblb	miR-148a-3p
	ErbB3	miR-148a-3p
	Rasal2	miR-129-1-3p
	Prkce	miR-129-1-3p
	Rasa1	miR-335-5p
	Spry2	miR-183-3p
	Ppp2cb	miR-183-3p
	Nras	miR-148a-3p
	Prkca	miR-183-3p
5-HT₂ type receptor mediated signaling pathway	Gng7	miR-92b-5p
	Prkch	miR-183-3p
	Gng5	miR-183-3p
	Cacna1d	miR-129-1-3p
	Gna11	miR-335-5p
	Gnb1	miR-183-3p
	Prkcz	miR-148a-3p
	Prkci	miR-183-3p
	Cacnb4	miR-129-1-3p
	Prkce	miR-129-1-3p
	Gng4	miR-183-3p
	Plcb1	miR-148a-3p
	Prkca	miR-183-3p
	Vamp2	miR-127-3p
FGF signaling pathway	Ppp6c	miR-335-5p
	Map3k1	miR-129-1-3p, miR-183-3p
	Ppp2ca	miR-183-3p
	Prkch	miR-183-3p
	Mapk11	miR-335-5p
	Map3k2	miR-335-5p
	Ppp2r5e	miR-125b-1-3p
	Ywhab	miR-148a-3p
	Fgf9	miR-183-3p
	Prkcz	miR-148a-3p
	Prkci	miR-183-3p
	Map3k4	miR-183-3p
	Sfn	miR-127-3p
	Mapk1	miR-335-5p

	Ppp2r2a	miR-183-3p
	Sos2	miR-148a-3p
	Sos1	miR-148a-3p
	Ppp2r5c	miR-183-3p
	Prkce	miR-129-1-3p
	Rasa1	miR-335-5p
	Spry2	miR-183-3p
	Ppp2cb	miR-183-3p
	Nras	miR-148a-3p
	Prkca	miR-183-3p

Table 6 Supplemental

Predicted gene targets in affected Reactome Pathways of downregulated miRNAs in lumbar motor neurons

Reactome Pathways	Filtered targets	Targeting miRNAs	
Post-transcriptional silencing by small RNAs	Ago1	miR-148a-3p	
	Tnrc6b	miR-125b-1-3p, miR-129-1-3p, miR-148a-3p	
	Ago4	miR-148a-3p	
	Ago2	miR-92b-5p, miR-148a-3p, miR-183-3p	
	Tnrc6c	miR-148a-3p	
	Tnrc6a	miR-148a-3p	
Signaling by TGF-beta Receptor Complex	Tgfb1	miR-148a-3p	
	Smad2	miR-148a-3p	
	Phip	miR-148a-3p	
	Arhgef18	miR-183-3p	
	Cdk8	miR-148a-3p	
	Usp9x	miR-125b-1-3p, miR-148a-3p	
	Ube2d1	miR-148a-3p	
	Sp1	miR-335-5p	
	Prkcz	miR-148a-3p	
	Skil	miR-183-3p	
	Ube2d3	miR-148a-3p	
	Ccnt2	miR-335-5p	
	Parp1	miR-129-1-3p	
	Furin	miR-129-1-3p	
	Smurf2	miR-148a-3p	
	Tgif2	miR-148a-3p	
GAB1 Signosome	Pip4k2a	miR-125b-1-3p	
	Mtor	miR-92b-5p	
	Pten	miR-148a-3p	
	Ppp2ca	miR-183-3p	
	Irs1	miR-183-3p	
	Pag1	miR-148a-3p	
	Lck	miR-183-3p	
	Ppp2r5e	miR-125b-1-3p	
	Fgf9	miR-183-3p	
	Hbegf	miR-183-3p	
	Kitl	miR-125b-1-3p	
	Mlst8	miR-148a-3p	
	Mapk1	miR-335-5p	
	Creb1	miR-125b-1-3p, miR-129-1-3p	
	Cdkn1b	miR-148a-3p	
	Ppp2r5c	miR-183-3p	
	ErbB3	miR-148a-3p	
	Rictor	miR-148a-3p	
	Chuk	miR-148a-3p	
	Ppp2cb	miR-183-3p	
	Foxo1	miR-183-3p	
	PI3K cascade: FGFR4,	Pip4k2a	miR-125b-1-3p

PI3K cascade: FGFR3, PI3K events in ERBB4 signaling, PI3K cascade: FGFR2, PI3K cascade: FGFR1, PIP3 activates AKT signaling, PI3K/AKT activation	Mtor	miR-92b-5p
	Pten	miR-148a-3p
	PPP2CA	miR-183-3p
	Irs1	miR-183-3p
	Lck	miR-183-3p
	PPP2R5E	miR-125b-1-3p
	Fgf9	miR-183-3p
	Hbegf	miR-183-3p
	Kitl	miR-125b-1-3p
	Mlst8	miR-148a-3p
	Mapk1	miR-335-5p
	Creb1	miR-125b-1-3p, miR-129-1-3p
	Cdkn1b	miR-148a-3p
	PPP2R5C	miR-183-3p
	ErbB3	miR-148a-3p
	Rictor	miR-148a-3p
	Chuk	miR-148a-3p
	PPP2CB	miR-183-3p
	Foxo1	miR-183-3p

Table 7 Supplemental

Predicted gene targets in affected GO cellular components of downregulated miRNAs in lumbar motor neurons

Cellular components	Filtered targets	Targeting miRNAs
PP2A complex	PPP2CA	miR-183-3p
	PPP2R5E	miR-125b-1-3p
	PPP2R3A	miR-92b-5p
	PPP2R2A	miR-183-3p
	PPP2R5C	miR-183-3p
	PPP2R4	miR-335-5p
	PPP2CB	miR-183-3p
endocytic vesicle	Rab8b	miR-183-3p
	Dpp4	miR-148a-3p
	Syt11	miR-335-5p
	Uvrag	miR-183-3p
	Rab14	miR-148a-3p
	Rapgef6	miR-125b-1-3p, miR-335-5p
	Unc13b	miR-183-3p
	Ehd1	miR-335-5p
	Rabep1	miR-127-3p
	Lrp2	miR-148a-3p, miR-183-3p
	Sh3kbp1	miR-335-5p
	Amot	miR-148a-3p
	Lck	miR-183-3p
	Epn2	miR-148a-3p
	Lamp2	miR-148a-3p
	Rab9b	miR-183-3p
	Rab34	miR-148a-3p
	Abca1	miR-148a-3p, miR-183-3p
	Rab11b	miR-335-5p
	Snap91	miR-148a-3p
	Eps15	miR-148a-3p
	Nrxn1	miR-335-5p
	Cln3	miR-183-3p
	Rab11fip4	miR-183-3p
	Ocln	miR-183-3p
	Rala	miR-183-3p
	Lamp1	miR-125b-1-3p
	Atg14	miR-148a-3p
	Picalm	miR-148a-3p, miR-183-3p

Preface

As a follow up to the analysis of neuronal miRNA expression in EAE (Chapter 2), we assessed the functional role of candidate miRNAs in EAE. We identified two miRNAs, miR-27a-3p and miR-223-3p, that are upregulated in both EAE neurons and in MS leukocortical lesions. We show that these miRNAs are neuroprotective by targeting glutamate receptor signaling, as determined by functional assays, genetic manipulations, and pharmacological approaches. Our results suggest a neuronal response to inflammation, which we can modulate to promote repair and regeneration in EAE. Chapter 2 and 3 thus successfully profile miRNA regulation across EAE and determine their functional relevance to neuroinflammation. These results emphasize the dichotomy of neuroinflammation, where these miRNAs that are upregulated in response to inflammation prove to mediate a neuroprotective response.

4 Chapter 3. MicroRNA-223 protects neurons from degeneration in Experimental Autoimmune Encephalomyelitis

Barbara Morquette*¹, Camille A. Juźwik*¹, Sienna S. Drake¹, Marc Charabati², Yang Zhang¹, Marc-André Lécuyer³, Dylan A. Galloway⁵, Aline Dumas⁶, Omar de Faria Junior⁴, Nicolas Paradis-Isler¹, Mardja Bueno¹, Isabel Rambaldi¹, Stephanie Zandee², Craig Moore⁵, Amit Bar-Or^{1,6}, Luc Vallières⁷, Alexandre Prat², and Alyson E. Fournier¹

*co-contributing author

¹ McGill University, Montréal Neurological Institute, Montréal, QC H3A 2B4, Canada

² Centre de Recherche du Centre Hospitalier de l'Université de Montréal, Université de Montréal, Montréal, QC H2X 0A9, Canada

³ Institute for Multiple Sclerosis Research, Gottingen, Germany

⁴ Stem Cell Institute, University of Cambridge, UK

⁵ Division of BioMedical Sciences, Faculty of Medicine, Memorial University of Newfoundland

⁶ Perelman School of Medicine, University of Pennsylvania, Philadelphia, PA 19104 USA

⁷ Neuroscience Unit, University Hospital Centre of Québec - Laval University, Québec City, QC, Canada

Originally Published in *BioRxiv* on September 30 2018: <https://doi.org/10.1101/430777>

Submitted to *Brain* November 2018 (revisions submitted March 26 2019).

4.1 Abstract

Multiple sclerosis (MS) is a chronic inflammatory, demyelinating, and neurodegenerative disease affecting the brain, spinal cord and optic nerves. Neuronal damage is triggered by various harmful factors that engage diverse signalling cascades in neurons; thus, therapeutic approaches to protect neurons will need to focus on agents that can target multiple biological processes. To do so, we have focused on non-coding small microRNAs (miRNAs). miRNAs are epigenetic regulators of protein expression that target messenger RNAs (mRNAs) and inhibit their translation. A single miRNA can target many functionally related mRNAs making them powerful post-transcriptional regulators. Dysregulation of miRNAs has been described in many neurodegenerative diseases including MS. Here, we report that two miRNAs, miR-223-3p and miR-27a-3p, are upregulated in neurons in the experimental autoimmune encephalomyelitis (EAE) mouse model of CNS inflammation and confirmed to be upregulated in leukocortical MS lesions. Prior work has shown peripheral blood mononuclear cell conditioned media (PBMC-CM) causes sub-lethal degeneration of neurons in culture. Overexpression of miR-27a-3p or miR-223-3p protects dissociated cortical neurons from PBMC-CM mediated degeneration. Introduction of miR-223-3p *in vivo* in mouse retinal ganglion cells (RGCs) protects RGC axons from degeneration in the EAE model. *In silico* analysis revealed that mRNAs in the glutamate receptor (GluR) pathway are enriched in miR-27a-3p and miR-223-3p targets. Antagonism of the GluR pathway protects neurons from PBMC-CM-dependent degeneration. Our results suggest that miR-223-3p and miR-27a-3p are upregulated in response to inflammation to mediate a compensatory neuroprotective gene expression program that desensitizes neurons to glutamate by downregulating mRNAs involved in GluR signalling.

4.2 Introduction

Multiple Sclerosis (MS) is a complex disease manifesting at the neuro-immune interface. Peripheral immune cells invade the central nervous system (CNS), leading to inflammation and focal demyelinating lesions (Compston and Coles 2008). Most cases manifest as a relapsing-remitting (RRMS) clinical disease course, with about half of the cases developing progressive clinical deterioration. Approximately 15% of MS cases manifest as a progressive disease at onset without remission, termed primary progressive MS (PPMS) (Antel, Antel et al. 2012). While focal demyelination correlates with RRMS, axonal degeneration and neuronal death correlate better with progressive forms of the disease (Bjartmar, Kidd et al. 2000, Wujek, Bjartmar et al. 2002). The presence of diffuse axonal damage throughout the CNS in MS implies that degeneration occurs even in the absence of acute inflammation (Nikic, Merkler et al. 2011, Criste, Trapp et al. 2014). Currently available MS therapies are immunomodulatory, thus developing therapies targeting the neurodegeneration underlying progressive and irreversible disability of patients remains an area of unmet clinical need (Kasarello, Cudnoch-Jedrzejewska et al. 2017).

Multiple factors including cytokines, complement, free radicals, nitric oxide, proteases, excess glutamate and calcium are thought to contribute to a harmful environment for vulnerable demyelinated axons in MS (Trapp, Peterson et al. 1998, Yong, Giuliani et al. 2007, Gonsette 2008). Similarly, neuronal damage in MS is likely triggered by multiple intracellular molecular cascades (Yang, Hao et al. 2015). Interventions aimed at individual molecular targets may offer only partial neuroprotection while targeting programs of functionally related gene expression represents a viable strategy for the development of more effective neuroprotective agents (Yong, Giuliani et al. 2007, Gonsette 2008). MicroRNAs (miRNAs) are evolutionarily conserved short non-coding RNAs that regulate gene expression in healthy and pathological conditions (Bartel 2004). Mature miRNAs regulate programs of gene expression by binding to the 3' untranslated regions (3'UTR) of target messenger RNAs (mRNAs) and inhibiting protein translation or initiating mRNA degradation of multiple mRNA transcripts simultaneously (Grimson, Farh et al. 2007, Friedman, Farh et al. 2009, Quinlan, Kenny et al. 2017). A major advantage

of targeting miRNAs is that one can modulate a pool of functionally related genes rather than a single gene.

In MS, miRNA profiles are altered in immune cells, cerebrospinal fluid (CSF) and within CNS lesions including white matter lesions as well as demyelinated hippocampal neurons (Junker, Krumbholz et al. 2009, de Faria Jr, Moore et al. 2012, Dutta, Chomyk et al. 2013, Miyazaki, Li et al. 2014, Regev, Healy et al. 2017). miRNAs are also dysregulated in experimental autoimmune encephalomyelitis (EAE), an animal model of CNS inflammation that typically results in ascending paralysis and exhibits CNS pathology including neuron damage and death (Bannerman, Hahn et al. 2005, Vogt, Paul et al. 2009, de Faria Jr, Moore et al. 2012, Lewkowicz, Cwiklinska et al. 2015, Hoflich, Beyer et al. 2016, Juzwik, Drake et al. 2018). The visual system is also affected in both MS and EAE with loss of retinal ganglion cells (RGCs) and an associated optic nerve pathology that includes immune cell infiltration, demyelination and glial activation (Shindler, Ventura et al. 2008, Quinn, Dutt et al. 2011, Horstmann, Schmid et al. 2013).

Using the EAE model, miRNAs have been profiled in purified cell types including immune cell subsets, oligodendrocytes, and neurons; together providing valuable information about molecular substrates that may be targeted to manipulate cell specific responses (de Faria Jr, Moore et al. 2012, Lewkowicz, Cwiklinska et al. 2015, Juzwik, Drake et al. 2018). We previously profiled miRNA expression in lumbar motor neurons and retinal neurons in EAE to identify molecular substrates that may be targeted to promote neuroprotection (Juzwik, Drake et al. 2018). Here we study two miRNAs, miR-223-3p and miR-27a-3p, that are upregulated in motor neurons in mice subjected to EAE. We report that these miRNAs are regulated in leukocortical lesions from post-mortem MS patient tissue and that overexpression of these miRNAs mediates neuronal protection in part through regulation of glutamate receptor signalling.

4.3 Results

4.3.1 miR-23a-3p, miR-27a-3p, miR-146a-5p and miR-223-3p are upregulated in EAE and MS

miRNA expression has been profiled previously in tissue from MS lesions, providing a rich resource of disease-relevant miRNAs (Junker *et al.*, 2009). Using the EAE model, we sought to determine if candidate miRNA from that study were regulated within neurons in the inflamed setting where they could contribute to neuronal pathology. Neurons were captured from mice subjected to EAE at peak disease by laser capture micro-dissection (LCM) and miRNA expression was analyzed by qPCR. Four miRNAs were significantly upregulated in lumbar motor neurons from EAE animals when compared to naïve control animals: miR-146a-5p (~2 fold), miR-27a-3p (~5 fold), miR-23a-3p (~7 fold), and miR-223-3p (~40 fold) (Fig. 1a). We then profiled these regulated miRNAs in the RGC layer isolated from EAE mice to see if their regulation was conserved in multiple neuronal cell types. In retinal neurons miR-146a-5p (~2 fold), miR-27a-3p (~7 fold) and miR-23a-3p (~30 fold) were significantly upregulated when compared to pre-symptomatic control animals whereas expression of miR-223-3p was unaffected (Fig. 1b). To examine whether these miRNAs are regulated in MS we assessed their regulation in post mortem human brain samples from the control and SPMS patients. Tissue was analyzed from normal appearing white matter (NAWM), active lesions with mild to severe inflammation and demyelination, and from leukocortical and subpial lesions with neuronal involvement (Supp Fig. 1) (Reynolds *et al.*, 2011; Whittaker Hawkins *et al.*, 2017). Active lesions are those with early inflammatory events and initial axonal damage involving activated macrophages/microglia (Ferguson *et al.*, 1997; Reynolds *et al.*, 2011). By qPCR, miR-146a-5p, miR-27a-3p, and miR-223-3p were significantly upregulated in active lesions compared to NAWM from non-MS tissue (Fig. 1c, d, f). In our patient cohort we did not detect the previously reported up-regulation of miR-23a-3p in active lesions (Fig. 1e) (Junker *et al.*, 2009). miR-27a-3p, miR-23a-3p, and miR-223-3p were significantly upregulated 10- to 70-fold in leukocortical lesions (including one subpial lesion, marked in purple), whereas miR-146-5p was significantly downregulated. A defining feature of leukocortical lesions is the presence of neuronal cell bodies,

suggesting that miR-27a-3p, miR-23a-3p, and miR-223-3p are upregulated in neurons in MS tissue lesions.

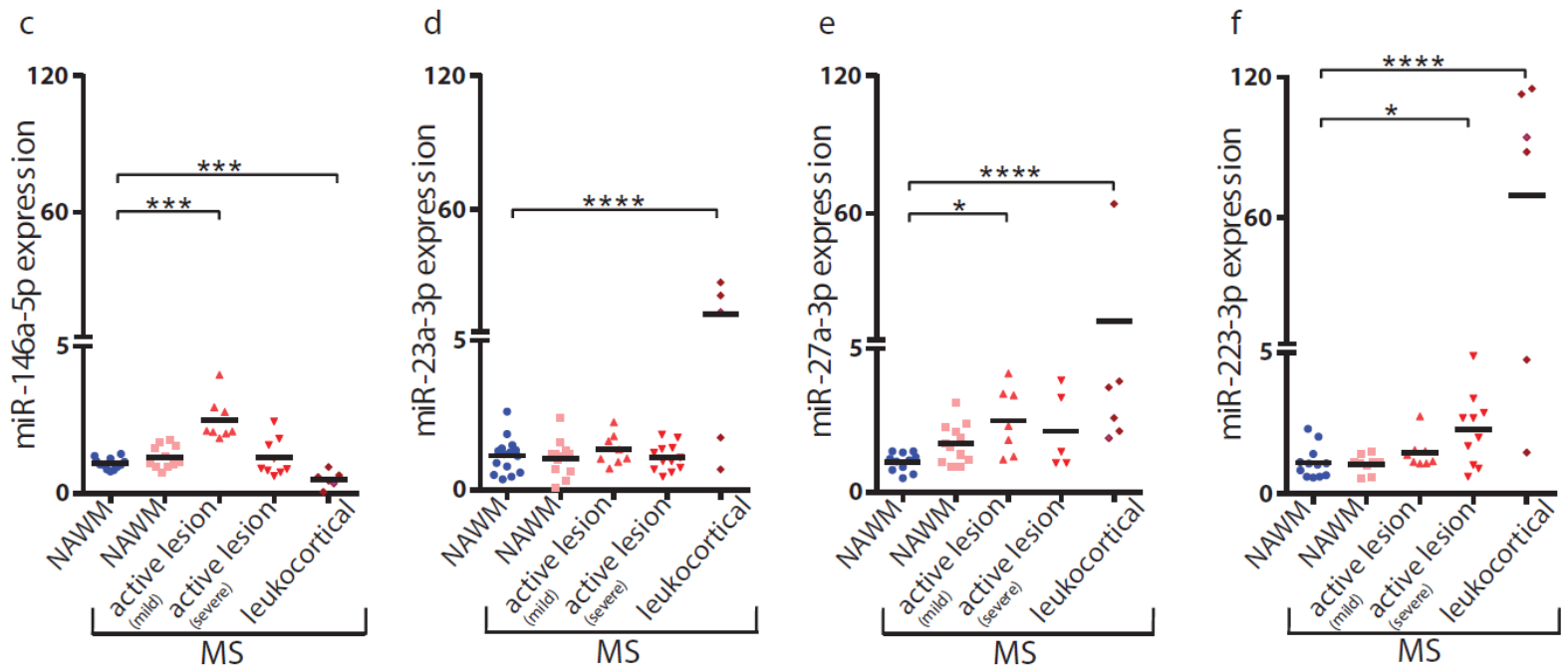
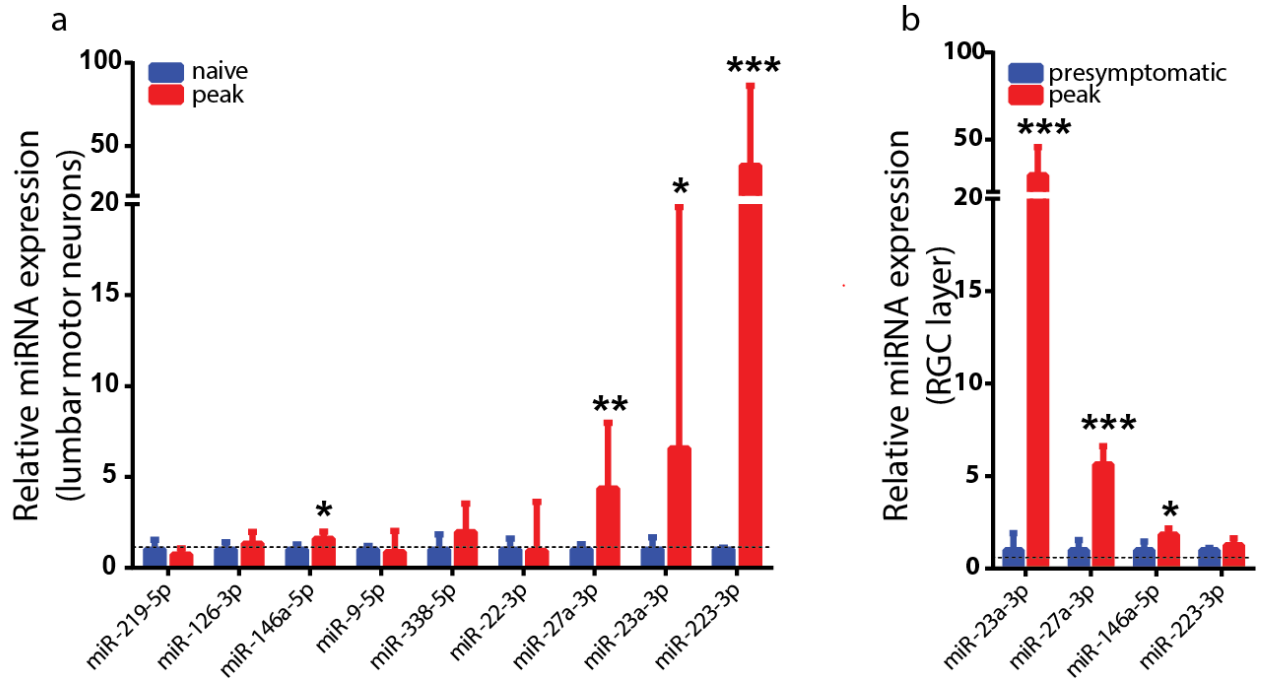


Figure 1. Candidate miRNA expression in EAE and MS. (a-b) qPCR expression data for miRNA collected from lumbar motor neurons **(a)** and retinal neurons **(b)** from EAE mice. miR-23a-3p, miR-27a-3p, miR-146a-5p, and miR-223-3p are upregulated in EAE lumbar motor neurons compared to naïve mice (n=3-6, two-tailed student's t-test). miR-23a-3p, miR-27a-3p, and miR-146-5p are upregulated in the EAE RGC layer compared to presymptomatic mice (n=3-8, two-tailed student's t-test). **(c-f)** qPCR expression data of miR-146a-5p **(c)**, miR-23a-3p **(d)**, miR-27a-3p **(e)** and miR-223-3p **(f)** in control NAWM, NAWM from MS patients, active white-matter lesions with mild to severe inflammation and demyelination, and leukocortical lesions compared to the NAWM of post-mortem-MS. One subpial lesion was included with the leukocortical lesion group, it is marked in purple (n=5-15, one-way ANOVA, p<0.05, Dunnett's post-hoc). qPCR data is represented as fold change control.

4.3.2 miR-27a-3p and miR-223-3p are neuroprotective - Previous studies have described neuroprotective roles for miR-223-3p and miR-27a-3p in models of stroke and traumatic brain injury (Harraz *et al.*, 2012; Cai *et al.*, 2016; Sun *et al.*, 2017). We focused on miR-27a-3p and miR-223-3p as they were upregulated in both active and leukocortical lesions of post-mortem MS tissue (Fig. 1d,f). To determine whether these miRNAs contribute to axon degeneration or compensatory neuroprotection in neurons, we performed overexpression and loss-of-function experiments in dissociated mouse cortical neurons. miRNA mimics for miR-27a-3p and miR-223-3p (M27a, M223) and a negative control mimic (NC) were transfected into dissociated cortical neurons at 2 DIV. Successful transfection of miRNA mimics was validated by qPCR (Supp. Fig 2). Neurons transfected with mimics for miR-223-3p and miR-27a-3p grew normally and did not exhibit any axonal swellings, breaks or other signs that one might associate with degeneration (Fig. 2a).

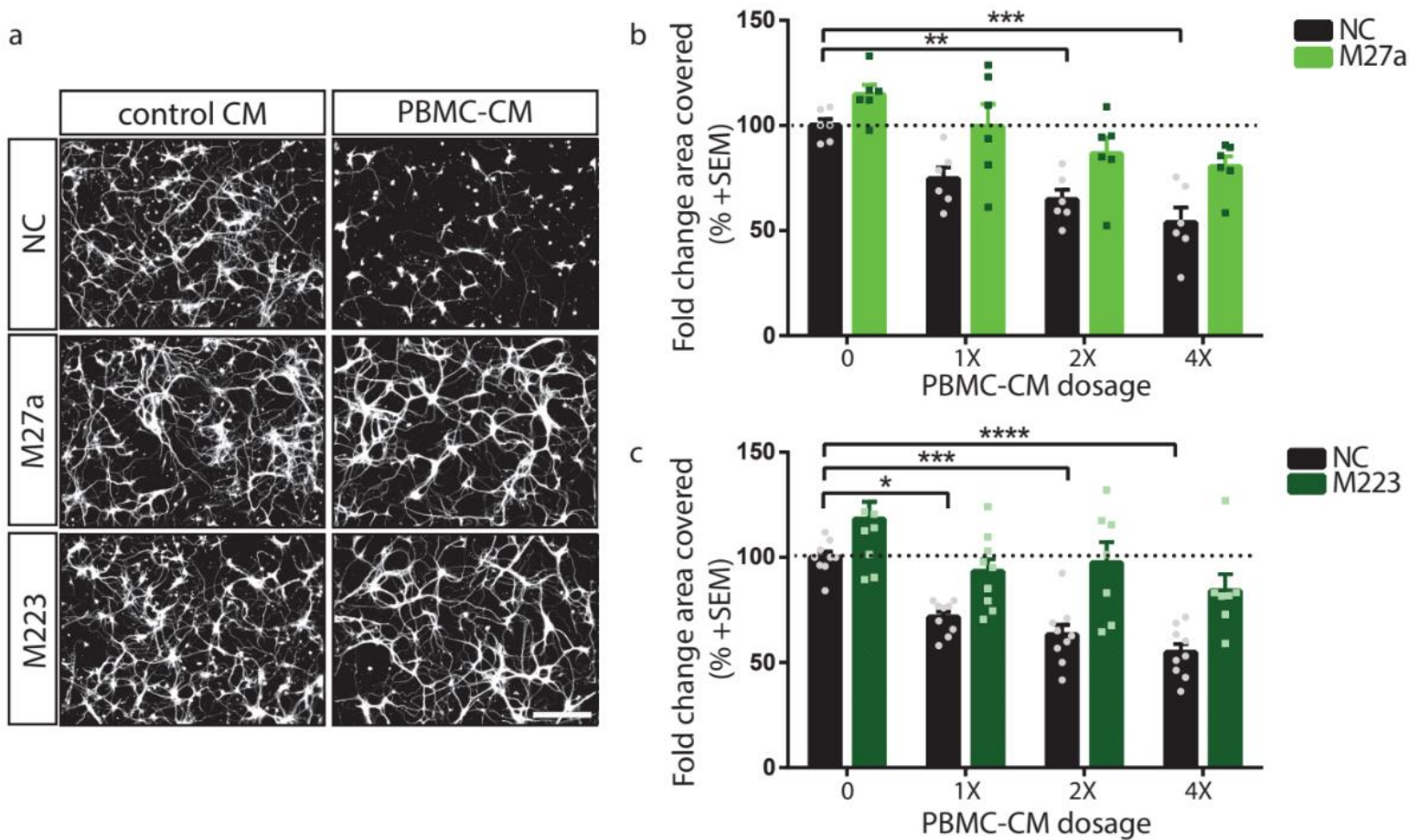


Figure 2. miR-27a-3p and miR-223-3p overexpression prevents PBMC-CM-dependent neurodegeneration. (a) β III-tubulin-stained mouse cortical neurons transfected with miR-27a-3p, miR-223-3p, or a negative control mimic (M27a, M223, and NC, respectively) at 2 DIV and then treated for 24h with increasing dosages of PBMC-CM at 4 DIV. (b, c) Quantification of the percent area covered by β III-tubulin positive signal from thresholded images (n=6-9, two-way ANOVA, $p < 0.05$, Tukey's post-hoc). Scale bar; 100 μ m.

We next asked if miR-223-3p and miR-27a-3p would regulate the neuronal response to MS-relevant pathological stimuli. We have previously reported that

conditioned media from resting or PMA/Ionomycin (P/I)- activated PBMCs inhibits the outgrowth of dissociated neurons in culture and that this effect is mediated by secreted factors from myeloid-lineage cells (Pool *et al.*, 2011; Pool *et al.*, 2012). We found that dissociated cortical neurons that had been cultured at high density for 4 DIV to permit neurite outgrowth exhibited significant loss of neurite processes when treated for 12-24 hours with PBMC-CM (Fig. 2; Supp. Fig. 3). As such, PBMC-CM-dependent neurite loss represents a type of sub-lethal neurite degeneration. We then treated cortical neurons transfected with miRNA mimics with PBMC-CM or control-CM. Introduction of M27a or M223 protected cortical neurons from PBMC-CM-dependent neurite degeneration (Fig. 2a-c).

We hypothesized that inhibition of miR-223-3p or miR-27a-3p would sensitize neurons to the harmful effects of PBMC-CM. To test this, we transfected small, chemically modified single-stranded miRNA inhibitors that bind and inhibit endogenous miRNA molecules. Inhibition of miR-27a-3p resulted in compensatory upregulation of miR-23a-3p, a miRNA that is a member of the same miRNA cluster, thus we co-transfected neurons with miR-23a-3p and miR-27a-3p inhibitors. Inhibition of miR-23a-3p/miR-27a-3p (I23a/27a) modestly but significantly suppressed neurite growth without affecting cell death consistent with the idea that this miRNA cluster may protect neurons from degeneration (Fig. 3a-c). To assess the role of miR-223, we evaluated growth of dissociated cortical neurons from miR-223^{-/-} mice (Johnnidis *et al.*, 2008). We found that loss of miR-223 also resulted in a significant reduction in neurite growth from dissociated cortical neurons independent of cell death (Fig. 3d-f). To determine if miR-23a/27a and miR-223 loss-of-function further sensitized neurons to PBMC-CM, we treated I23a/27a-transfected neurons and miR-223^{-/-} neurons with PBMC-CM. I23a/27a-transfected neurons were not more sensitive to PBMC-CM than NC-transfected neurons when normalized to their own basal growth (Fig. 3g). Similarly, the sensitivity of neurons from miR-223^{-/-} mice to PBMC-CM was unchanged (Fig. 3h). These results demonstrate that overexpression of either miR-27a-3p or miR-223-3p can prevent neuronal process loss, but loss-of-function of the individual miRNAs is insufficient to further sensitize neurons to PBMC-dependent neurite loss.

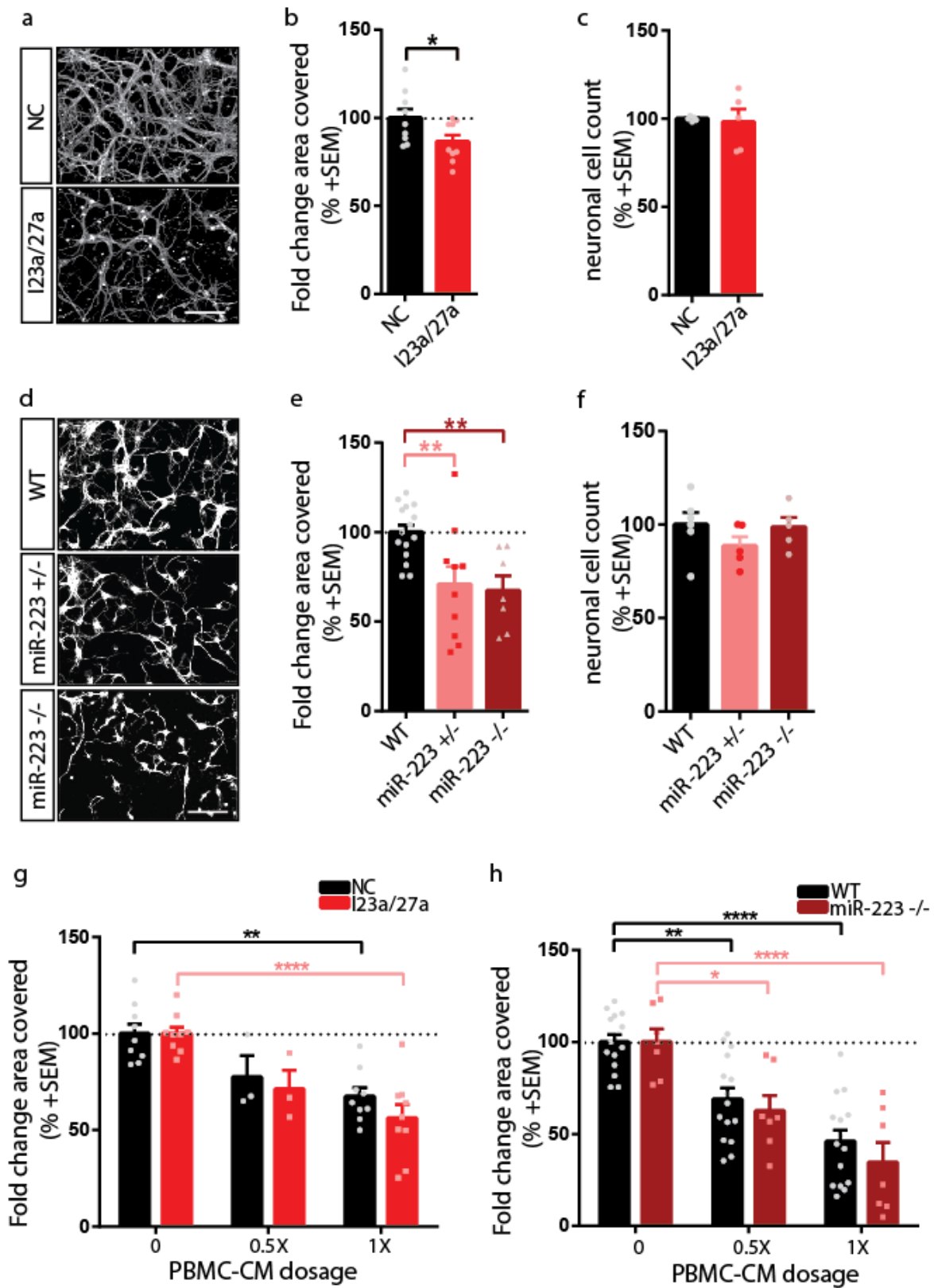


Figure 3. miR-27a-3p and miR-223 loss-of-function reduces basal neurite growth without further sensitization to PBMC-CM. (a) β III-tubulin stained mouse cortical neurons co-transfected with miR-23a-3p and miR-27a-3p inhibitors (I23a/27a) or a negative control (NC) inhibitor at 2 DIV. (b, c) Quantification of neurite growth expressed as the percent of β III-tubulin positive area in the thresholded image (b) or neuronal cell numbers (c) from I23a/27a- or NC-transfected cells (d) β III-tubulin stained mouse cortical neurons from WT, miR-223^{+/-} and miR-223^{-/-} mice. (e, f) Quantification of β III-tubulin-positive area coverage (e) and neuronal cell numbers (f) from miR-223^{+/-} and miR-223^{-/-} neurons. (g, h) Quantification of β III-tubulin-positive area coverage from I23a/27a- and NC-transfected neurons (g) or miR-223^{-/-} neurons (h) treated with PBMC-CM. Percent area covered is normalized to the respective transfection condition to determine if there is greater sensitization to PBMC-CM (n=3-9, two-way ANOVA, p<0.05, Tukey's post-hoc). Scale bar; 100 μ m.

4.3.3 miR-223 overexpression rescues axonal degeneration in EAE optic nerve –

To determine if overexpression of miRNA could also have neuroprotective activity in an *in vivo* model of CNS inflammation we chose to analyze RGCs and their axon projections in the EAE model. The optic nerve forms part of the CNS and contains the axons of RGCs, which relay visual information to the brain (London *et al.*, 2013). Because of its accessibility, the visual system represents an excellent system to investigate the effect of molecules of interest on CNS neurodegeneration and protection. The RGCs are also readily accessible to molecular manipulation by transduction with adeno-associated virus 2 (AAV2), which preferentially infects RGCs and produces sustained transgene expression following intravitreal injection (Cheng *et al.*, 2002). Profiling of motor neurons and retinal neurons from EAE mice revealed that both miR-223-3p and miR-27a-3p were upregulated in motor neurons, whereas only miR-27a-3p was upregulated in retinal neurons (Fig. 1). We took advantage of this finding to ask if overexpression of miR-223-3p in RGCs would mediate neuroprotection *in vivo*. First, we optimized an iDISCO protocol to visualize axonal morphology during the progression of EAE. Optic nerves were immuno-stained with anti-neurofilament-H antibody and optically cleared to enable the visualization of axonal structure in 3D (Renier *et al.*, 2014). Axonal swellings, ovoids and fragmentation were visible in the optic nerve throughout the progression of EAE (Fig. 4a-j). Axonal swellings were present at disease onset before significant RGC death, reached maximal density at the peak of disease and largely resolved at the chronic stage (Fig. 4a-j, m). RGC density significantly decreases at peak disease and continues to

decrease at the chronic stage (Fig. 4n). The approximate 30% loss of RGC density at the chronic stage may account for the decreased axonal swellings at the chronic stage. Alternatively, axonal swellings may be resolving.(Nikic *et al.*, 2011). AAV2-miR-223 and an AAV control with a non-targeting (NT) miRNA (AAV2-NT) were injected intravitreally into the left eyes of mice four weeks prior to EAE. AAV2 was used to allow for miR-223 overexpression uniquely in neuronal cells of the retina (Davidson *et al.*, 2000). Overexpression of miR-223-3p in the RGCs and optic nerve was validated by qPCR (Fig. 4o). In the contralateral optic nerve containing axons projecting from a non-injected eye, EAE induction resulted in visible focal degeneration, as evidenced by the presence of characteristic axonal swellings, ovoids, and fragmentation at peak disease (Fig. 4k). In the ipsilateral optic nerve containing axons projecting from the retina injected with control AAV2-NT, a similar degree of axon degeneration was apparent (Fig. 4k,p). In contrast, optic nerves projecting from AAV2-miR-223-injected eyes exhibited significantly fewer axonal swellings when compared to the non-injected contralateral eye (Fig. 4l,p). These results demonstrate that axonal swellings accumulate throughout the time course of EAE and that this injury can be prevented through neuron-specific miR-223 overexpression.

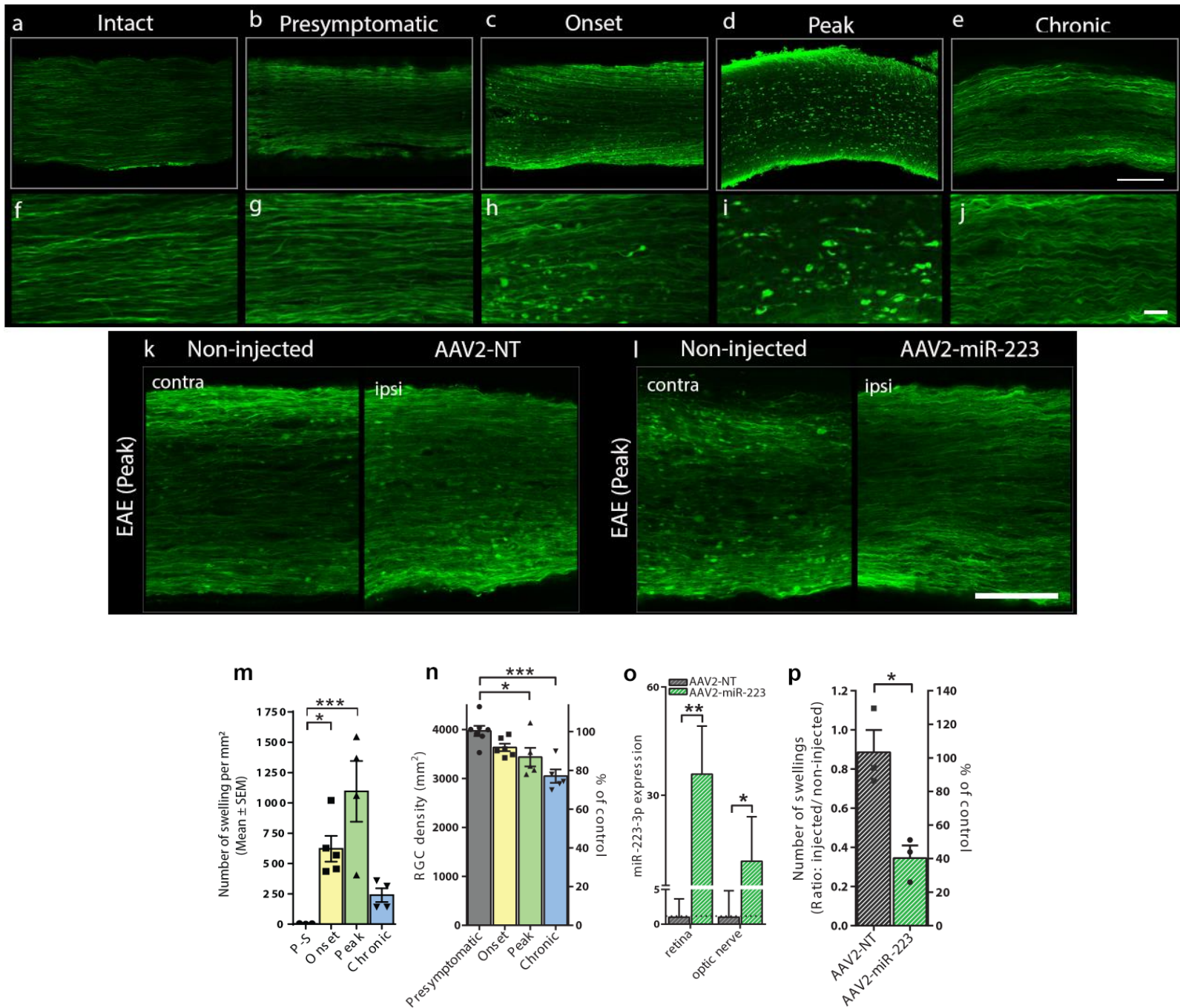


Figure 4. Axonal degeneration is rescued by neuronal overexpression of miR-223 *in vivo* in the EAE model. (a-l), Confocal images of iDisco processed whole mount EAE optic nerves stained with non-phosphorylated neurofilament-H antibody showing axonal swellings occurring throughout the course of the disease in control EAE animals (a-j), from optic nerves projecting from AAV2-NT-injected eyes or contralateral non-injected eyes (k) and from optic nerves projecting from AAV-miR-223-injected eyes or contralateral non-injected eyes (l). Each optical section (f-j) are magnifications of the boxed areas in panels (a-e). (m) Quantification of the density of axonal swellings in control EAE mice (n=3-5, one-way ANOVA, $p < 0.05$, Dunnett's post-hoc). (n) Quantification of RGC survival in non-injected control EAE mice (n=5-7, $p < 0.05$, Dunnett's post-hoc). (o) Quantification of miR-223-3p expression in retina and optic nerve of AAV2-NT and AAV2-miR-223 injected mice. (p) Quantification of the number of axonal swellings in AAV2-NT and AAV2-miR-223 injected mice relative to non-injected control mice.

one-way ANOVA, $p < 0.05$, Dunnett's post-hoc. **(o)** qPCR analysis of miR-223-3p expression in retina and optic nerve collected following intravitreal injection of AAV2-miR-223 and non-targeting AAV2 (AAV2-miR-NT) ($n=3-4$, two-tailed student's t-test). **(p)** Quantification of the number of axonal swellings in optic nerves following injection of AAV2-miR-223 or AAV-miR-NT expressed as a ratio of ipsi/contra; ($n = 3$, two-tailed student's t-test). Ipsi represents the ipsilateral optic nerve that received AAV-miR treatment and contra the contralateral optic nerve that did not receive treatment and was thus used as an internal control. Scale bar; 100 μ m **(a-e)** and **(k-l)**; 15 μ m **(f-j)**.

4.3.4 miR-27a-3p and miR-223-3p mediate neuroprotection through glutamate receptor (GluR) signaling - We were interested in identifying common mRNAs regulated by miR-223-3p and miR-27a-3p that may be implicated in conferring neuroprotection. To identify putative mRNA targets, we used an *in silico* approach to mine predicted targets from seven databases: Diana-microT (Reczko *et al.*, 2012; Paraskevopoulou *et al.*, 2013), microRNA.org (Betel *et al.*, 2008), miRDP (Wong and Wang, 2015), miRTarBase (Chou *et al.*, 2016), RNA22 (Miranda *et al.*, 2006), TargetScan (Agarwal *et al.*, 2015), and TarBase (Vlachos *et al.*, 2015). We filtered our data for predicted targets that occurred in at least four of seven databases (Supp. Table 1). Targets were assessed for overrepresentation of cellular pathways using PANTHER Pathway Analysis (Mi *et al.*, 2013; Mi *et al.*, 2017). PANTHER identified eight significantly overrepresented pathways formed by the putative targets of miR-27a-3p and miR-223-3p (Fig. 5a). We reasoned that miR-223-3p and miR-27a-3p may mediate neuroprotection by downregulating these signalling pathways and that inhibitors of these candidate pathways may therefore also protect neurons from PBMC-CM. We first investigated the gonadotropin hormone receptor (GnRH) pathway as it contained the most targets out of the pathways with 29 putative targets (Supp. Table 2). GnRH receptor signaling is best described in the hypothalamic-pituitary-gonadal axis, regulating the reproductive system; however GnRH and its receptor can also be found in other tissue such as the cortex and spinal cord (Albertson *et al.*, 2008; Quintanar and Salinas, 2008). We treated neurons with the GnRH antagonist cetrorelix or the agonist leuprolide and assessed their effects in a PBMC-CM assay. Neither agent significantly affected PBMC-CM induced neurite loss compared to their respective controls (Fig. 5b,c).

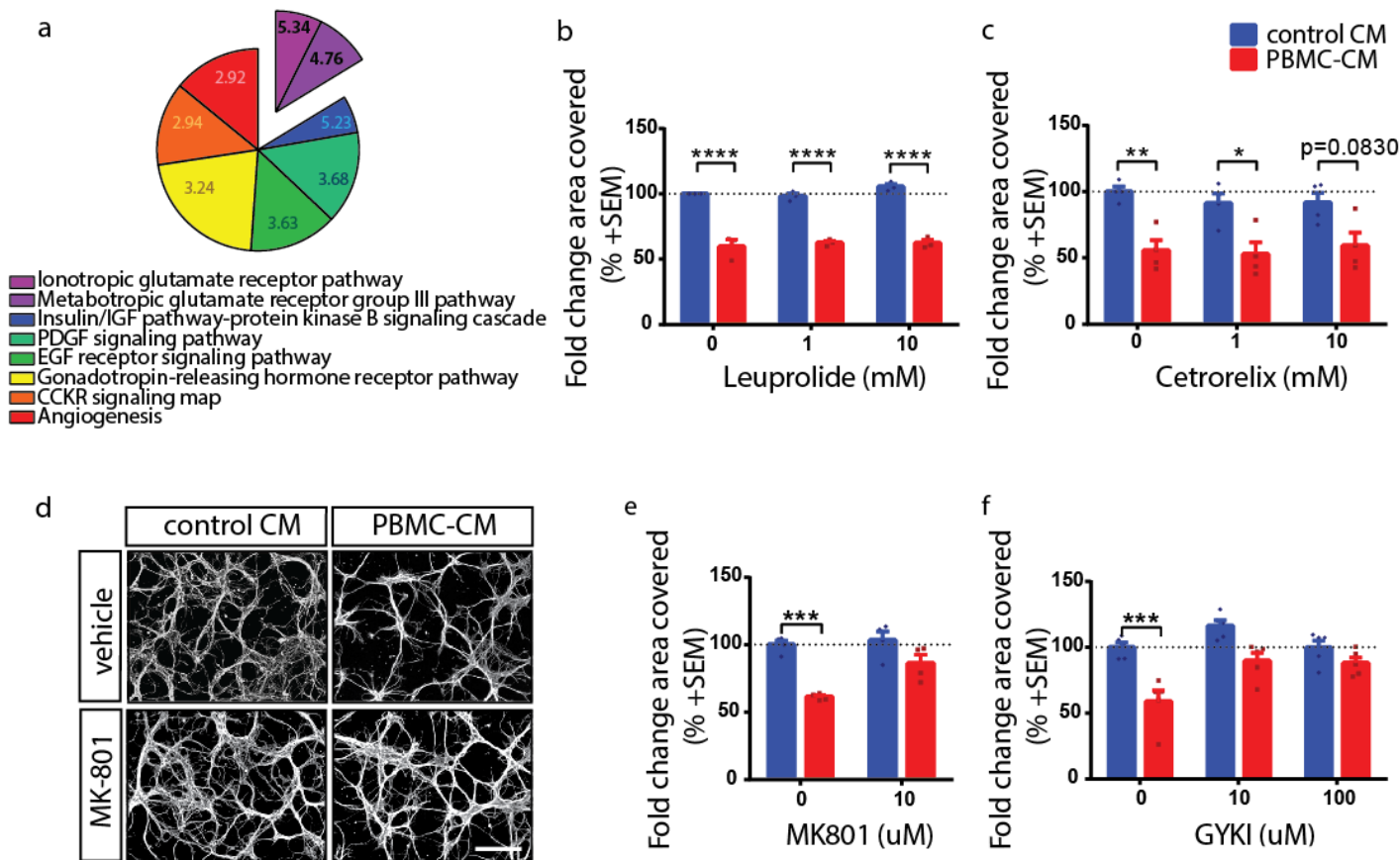


Figure 5. Inhibition of GluR signaling protects against neurodegeneration *in vitro*. (a) *In silico* identified targets of miR-27a-3p and miR-223-3p identified by a PANTHER overrepresentation test. Ionotropic GluR pathway was the most enriched pathway for miR-27a-3p and miR-223-3p targets at 5.34 fold enrichment ($p=0.004$), and metabotropic glutamate receptor pathway was the third most enriched pathway at 4.76 fold enrichment ($p=0.002$). All other significantly overrepresented pathways are depicted within the pie ($p<0.05$, Binomial Bonferroni correction for multiple testing). (b, c) Fold change in the percent area covered by β III-tubulin positive neuronal cell bodies and their neurites, grown for 4 DIV and treated for 24h with PBMC-CM or control CM in the presence of GnRH agonist leuprolide (b) or antagonist Cetrorelix (c) ($n=3-6$, two-way ANOVA, $p<0.05$, Tukey's multiple comparisons test). (d) β III-tubulin stained mouse cortical neurons in the presence or absence of MK-801 and treated with control- or PBMC-CM. (e, f) Quantification of fold change in percent area covered by β III-tubulin following treatment with PBMC-CM in the presence of the NMDAR antagonist MK-801 (e) or the AMPAR antagonist GYKI (f) ($n=4-5$; two-way ANOVA, $p<0.05$, Tukey's multiple comparisons test).

We then investigated the ionotropic glutamate receptor (GluR) pathway, as it showed the highest fold enrichment at 5.34 fold (Fig 5a). There are three main families of ionotropic glutamate receptors: AMPA receptors (AMPA), kainate receptors, and NMDA

receptors (NMDAR) (Stojanovic *et al.*, 2014). MiR-223-3p has been previously found to target the transcripts of ionotropic glutamate receptor subunits, AMPA type subunit 2 (GluA2; *GRIA2*) and NMDA-receptor subtype 2B (NR2B; *GRIN2B*) (Haraz, et al. 2012). In a stroke mouse model, an overexpression of miR-223 and subsequent downregulation of both glutamate receptor targets presented neuroprotection against excitotoxic injury. To interrogate whether PBMC-CM-dependent degeneration could be blocked with ionotropic GluR antagonists, we treated cortical neurons with the NMDAR antagonist, MK-801. Notably, MK-801 prevented PBMC-CM mediated process degeneration relative to vehicle control (Fig. 5d,e). As NMDAR activation depends upon membrane depolarization, which is typically enacted through AMPAR activation we next sought to determine if this effect was also mediated through upstream AMPAR activation (Lau Anthony and Tymianski, 2010). Application of a small molecule inhibitor of AMPARs and kainate receptors (GYKI53655, herein GYKI) also inhibited neurite loss from treatment with PBMC-CM (Fig. 5f). GYKI is predicted to inhibit greater than 90% of AMPARs at 10 μ M but less than 5% of kainate receptors (Wilding, 1995). Its neuroprotective effect was therefore likely mediated through the inhibition of AMPARs as 10 μ M was sufficient to prevent PBMC-CM induced degeneration (Fig. 5f).

We observed reduced neurite growth in miR-223 and miR-27a loss-of-function experiments (Fig. 3) and hypothesized that this might be a result of increased GluRs on the neuronal cell surface that would sensitive neurons to the low concentration of glutamate in the media. We found that MK-801 and GYKI were both able to rescue LNA-mediated miR-223-3p loss-of-function, restoring growth to that of control neurons (Fig. 6 a-c). Similarly, MK-801 and GYKI were also able to rescue miR-23a-3p/27a-3p loss-of-function (Fig. 6 d-f). To further test the role of glutamate in miR-223-3p- and miR-27a-3p-dependent neuroprotection we cultured neurons 10DIV and treated with glutamate to induce excitotoxicity. As expected, treatment with 10 or 20 μ M glutamate in NC transfected neurons resulted in a significant decrease in neurons (quantified as Hoescht/ β III-tubulin positive cell bodies) (Fig. 6g). However, transfection of M27a prevented significant neuronal cell loss at 10 μ M glutamate, and M223 protected neurons from up to 20 μ M glutamate (Fig. 6h,i). This further supports the hypothesis that both miRNAs have neuroprotective effects within the glutamate signalling pathway.

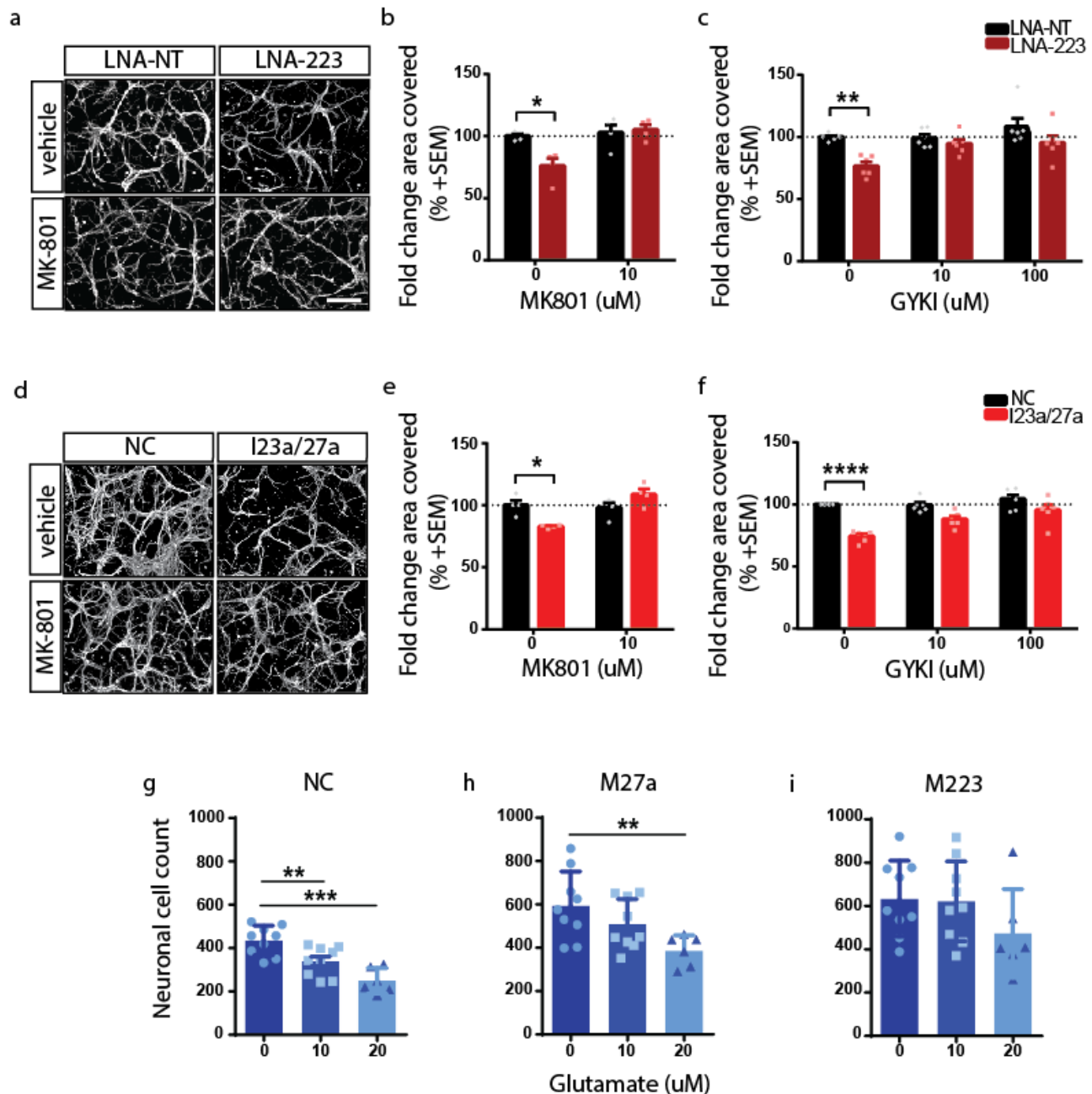


Figure 6. miR-27a-3p and miR-223-3p loss-of-function growth deficits can be restored through ionotropic GluR inhibition. (a,d) β III-tubulin-positive cortical neurons transfected with miR-223-3p LNA inhibitor or LNA non-targeting control (a, LNA-223, LNA-NT) or miR-23a-3p and miR-27a-3p inhibitors or negative control inhibitor (d, I23a/27a, NC) in the presence of MK-801. (b, c, e, f) Quantification of the fold change area covered by β III-tubulin in miR-223 (b, c) and I23a/27a (e, f) knockdown conditions in the presence of MK801 (b, e) or GYKI (c, f). (g-i) Quantification of the number of neurons per well for NC (h), M27a (i), and M223 (j) transfected neurons treated with 0, 10, or 20 μ M glutamate. For (a-f), Neurons were transfected with miRNA inhibitors at 2 DIV and treated at 4 DIV for 24h with MK-801 or GYKI (n=4-6, two-way ANOVA, Tukey's multiple comparisons test). For (g-i), neurons were transfected with miRNA mimics at 2 DIV and treated at 8 DIV for 24h with L-glutamate (n=5-9, one-way ANOVA, Dunnett's multiple comparisons test). Scale bar; 100 μ m.

Next, we investigated the targeting of GluA2 and NR2B 3'UTR by both miR-223-3p and miR-27a-3p. Target 3'UTRs were cloned into a pEZX-MT06 dual-luciferase construct immediately downstream of firefly luciferase and reporter activity was measured through relative luminescence signals. Consistent with previous literature, we found that expression of the miR-223-3p mimic suppressed luciferase activity for both the GluA2 and NR2B constructs (Fig. 7a,b; Haraz, et al. 2012). Further, the miR-27a-3p mimic also suppressed luciferase activity regulated by both GluA2 and NR2B 3'UTRs (Fig. 7a,b). We also analyzed retinal sections from eyes that were transduced with AAV2-miR-223 or AAV2-NT constructs to assess the effects of glutamate receptor expression. We found that RGCs transduced with AAV2-miR-223 exhibited reduced expression of NR2B *in vivo* (Fig. 7c). Visual inspection of transduced RGCs showed a decreased intensity of NR2B staining compared to their non-transduced neighbours in AAV2-miR-223 injected retinas, whereas in the AAV2-NT condition both transduced and non-transduced RGCs showed similar intensity staining (Fig. 7c). In sum, this supports a model whereby miR-223-3p and miR-27a-3p suppress the expression of GluA2 and NR2B, which may be contributing to their neuroprotective effects.

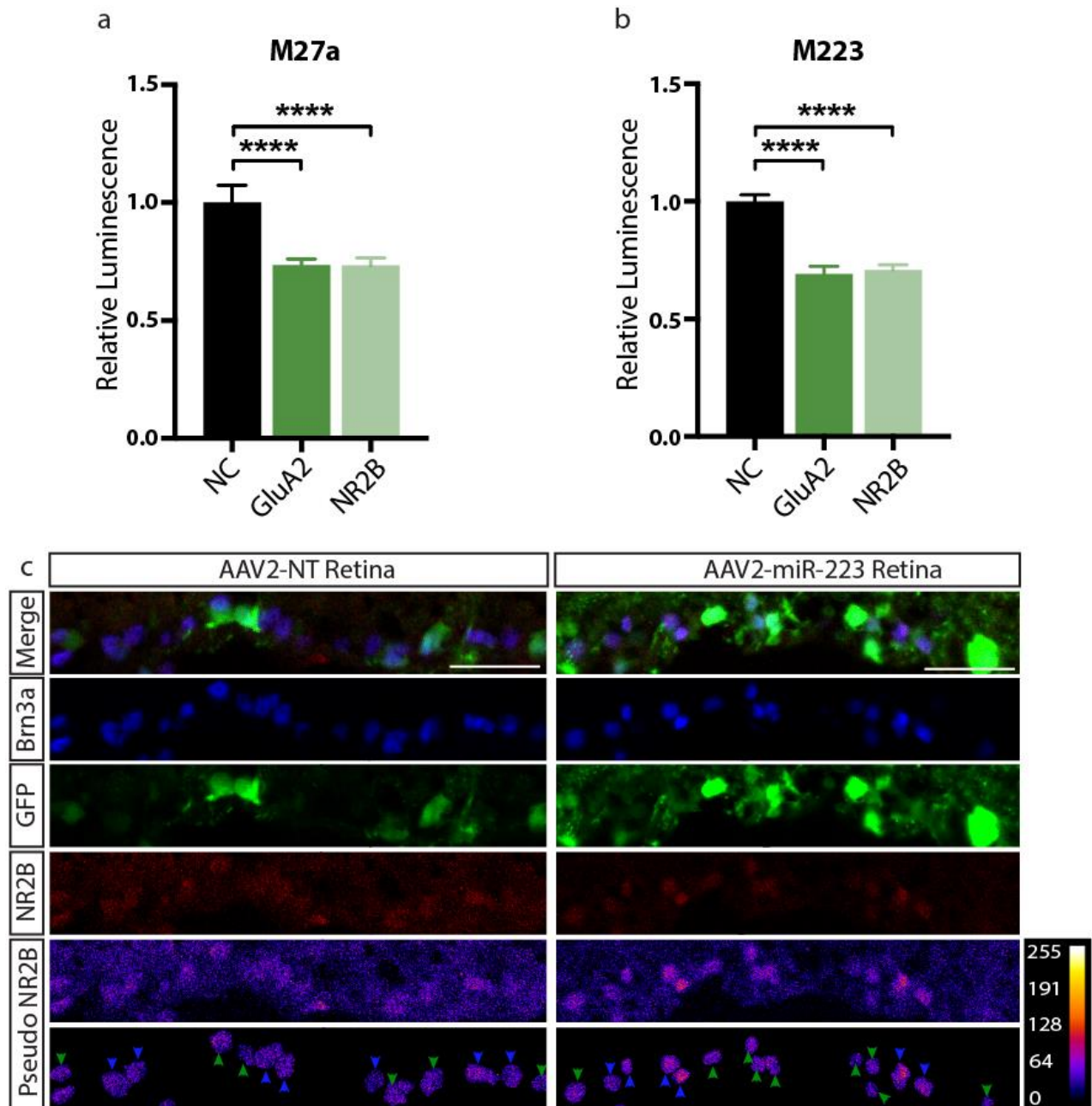


Figure. 7. miR-27a-3p and miR-223-3p target ionotropic glutamate receptor subunits. (a,b) Luciferase reporter assays illustrate that introduction of mimics for miR-27a-3p (**a**) and miR-223-3p (**b**) suppress the expression of luciferase regulated by the 3'UTR of GluA2 or NR2B. (**c**) Immunofluorescent staining of RGCs transduced with control AAV-NT virus or AAV-miR-223 with antibodies recognizing NR2B. A mask of the Brn3a channel was used to identify RGCs in the NR2B pseudo-colour image. Green arrowheads indicate transduced RGCs positive for both Brn3a and GFP, whereas blue arrowheads indicate non-transduced RGCs. Blue channel is Brn3a; green channel is GFP; red channel and pseudo-colour images are NR2B. Scale bar; 40µm.

4.4 Discussion

It is generally thought that neuronal/axonal pathology is an important factor in progressive forms of MS and the accrual of irreversible neurological disability (Chiaravalloti and DeLuca, 2008). MRI and histological studies demonstrate the occurrence of axonal injury and transection early in the disease process, and have revealed that the level of axonal loss positively correlates with poor clinical status (De Stefano *et al.*, 1998; Trapp *et al.*, 1998a; Wujek *et al.*, 2002). Brain atrophy, reflective of cell death, is also a significant feature of progressive MS (Bermel and Bakshi, 2006). Our results describe characteristic neurodegeneration in the optic nerve in EAE, which can be ameliorated through overexpression of miR-223-3p. We propose this effect is mediated in part through the suppression of glutamate excitotoxicity.

A multitude of signals including cytokines, complement, free radicals, nitric oxide, proteases, excess glutamate and calcium contribute to a deleterious environment for neurons in MS (Trapp *et al.*, 1998b; Yong *et al.*, 2007; Gonsette, 2008). To recapitulate this complex environment *in vitro* we used PBMC-CM treatment, having previously shown that neurons grown in the presence of PBMC-CM undergo loss of neurites, a process independent of cell death (Pool *et al.*, 2011; Pool *et al.*, 2012). PBMC-CM has been shown to contain glutamate in the 100 μ M range (O'Driscoll *et al.*, 2013). Glutamate is an excitatory neurotransmitter and amino acid, which also plays a role in metabolism (Stojanovic *et al.*, 2014). Elevated glutamate levels have been shown in the plasma and CSF of MS patients (Levite, 2017). In adult neurons, high levels of glutamate can potentiate excitotoxicity, a neurotoxic mechanism primarily mediated by the influx of excess Ca^{2+} through NMDARs leading to activation of intracellular Ca^{2+} -dependent caspases, breakdown of cytoskeletal components, accumulation of reactive oxygen species, and energetic failure resulting in death of mature neurons (Lau Anthony and Tymianski, 2010). Immature neurons however are relatively resistant to this canonical glutamate toxicity. Rather, treatment of immature neurons with 100 μ M glutamate results in a significant loss of dendritic arbors *in vitro* without cell death or a decrease in viability whereas in aged cortical cultures much lower concentrations of glutamate causes significant cell death (Monnerie *et al.*, 2003; Hao *et al.*, 2014). Much higher concentrations

can induce cell death in immature neurons through inhibition of cystine uptake (Murphy *et al.*, 1990). Our results show that neurons treated with PBMC-CM experience a reduction in neurite coverage that can be reversed by overexpression of miR-27a-3p or miR-223-3p, or by treatment with MK801 or GYKI. Further, mature neurons overexpressing miR-27a-3p or miR-223-3p are protected from glutamate toxicity. Conversely, inhibition of either miRNA resulted in basal growth deficits, and these basal growth deficits could similarly be rescued by application of the glutamate receptor antagonists MK801 and GYKI. Based on this evidence, we propose that both miRNAs are involved in regulating components of the ionotropic GluR pathway. This is consistent with luciferase reporter assays demonstrating that GluA2 and NR2B 3'UTRs are targeted by M27 and M223 and with analysis of NR2B expression in RGCs transduced with AAV-223 (Harras *et al.*, 2012).

Both the miR-23a~27a~24-2 cluster (which produces miR-27a) and miR-223 represent miRNAs with previously characterized roles in regulating the immune system in MS and EAE. miR-27a-3p drives a pro-inflammatory phenotype in macrophages and promotes the expression of pathogenic Th17 cells in MS (Xie *et al.*, 2014; Ahmadian-Elmi *et al.*, 2016). Similarly, miR-223-3p promotes pro-inflammatory macrophages and Th1/Th17 differentiation. This is emphasized in miR-223 KO mice, which have reduced EAE disease severity linked to decreased inflammation and dysregulated macrophage M2 polarization (Ifergan *et al.*, 2016; Satoorian *et al.*, 2016; Cantoni *et al.*, 2017; Galloway *et al.*, 2019). However, very little was previously known about their roles exclusively in the neuronal compartment. The retina and optic nerve in EAE represented an attractive model of CNS degeneration to study because of their accessibility and relevance to MS (Green *et al.*, 2010; London *et al.*, 2013). We described the accumulation of axonal swellings in the optic nerve over the time course of EAE using an optimized protocol combining 3DISCO and iDISCO. Using AAV2-mediated overexpression of miR-223, we successfully manipulated miR-223 expression *in vivo*, allowing us to study its role specifically within neurons during disease. We chose to overexpress miR-223 as opposed to miR-27a-3p in the RGCs as miR-223-3p was not intrinsically upregulated in RGCs in EAE. Here we saw a robust neuroprotective effect of miR-223 where its overexpression led to a considerable reduction of axonal damage in the optic nerve in EAE. This suggests

that miR-223 can have a significant protective role within neurons in addition to its well-characterized immunomodulatory roles.

Our *in silico* analysis identified *Gria2* and *Grin2b* as putative targets of miR-27a-3p and miR-223-3p (Suppl. Table 2). Harraz and colleagues previously validated *Gria2* and *Grin2b* as bona fide targets of miR-223-3p in rat hippocampal neurons through luciferase assay and western blot (Harraz *et al.*, 2012). Overexpression of miR-223 also directly inhibited NMDA-induced Ca²⁺ influx *in vitro* and *in vivo* enhancing neuroprotection in a model of stroke (Harraz *et al.*, 2012). We suspect that AAV2-mediated overexpression of miR-223 may be likewise potentiating neuroprotection through the inhibition of NMDAR mediated Ca²⁺ influx, resulting in reduced glutamate excitotoxicity during EAE. *Gria2*, an AMPAR subunit, is another validated target of miR-223-3p. Downregulation of *Gria2* has been shown to lead to less efficient AMPAR assembly, contributing to an overall reduction of AMPARs at the synapse (Sans *et al.*, 2003). *Gria2* targeting by miR-223-3p may therefore contribute to a decrease in AMPAR expression. As glutamate is produced and released in large quantities by activated immune cells which are known to congregate at active demyelinating lesions in MS (Kostic *et al.*, 2013), a global decrease in AMPARs and a concomitant reduction of NMDAR-mediated Ca²⁺ influx by miR-223-3p-mediated gene silencing may effectively diminish the toxicity of increased glutamate present in the extracellular milieu in EAE.

In sum, we describe upregulation of miR-27a-3p and miR-223-3p in human MS lesions and characterized their expression in neurons from EAE. Previous studies have used GluR antagonists to treat EAE: treatment with either the AMPAR/kainate receptor antagonist NBQX or NMDAR antagonist, memantine, resulted in a decreased clinical score and reduced axonal damage (Wallstrom *et al.*, 1996; Pitt, 2000; Kostic *et al.*, 2013). Likewise, we demonstrated that overexpression of miR-223 is neuroprotective in EAE which we propose to be in part mediated through its previously described function in targeting components of the ionotropic GluR pathway thereby reducing glutamate excitotoxicity in the disease. By luciferase assay, we saw that both miR-27a-3p and miR-223-3p target components of the GluR pathway. Based on this and our *in vitro*

experiments, we propose that both miRNAs may modulate the GluR pathway to exert a neuroprotective effect.

4.5 Acknowledgments and Funding

The authors would like to acknowledge Drs. Matthew Parsons, Jack Antel, Samuel Ludwin, Luke Healy, Samuel David, and Timothy Kennedy for their helpful discussions; Marie-Pier Girouard and Reesha Raja for their technical expertise; Dr. Jason Karamchandani for his advice and histological review of post-mortem MS tissue; Dr. Valina Dawson for providing the AAV2-miR-223 plasmid; and McGill University Life Sciences Complex Advanced Biomedical Imaging Facility (ABIF) for their expert technical advice. AEF is funded by the Canadian Institutes for Health Research and the Multiple Sclerosis Society of Canada (MSSOC). BM, CAJ, and SSD were funded by awards from the MSSOC/Fonds de recherche du Quebec, MSSOC/Vanier Canada Graduate Scholarships, and Canada Graduate Scholarship – master’s award allocation, respectively. YZ and DAG were funded by studentships from the MSSOC.

4.6 Competing Financial Interests

Dr. Bar-Or has participated as a speaker in meetings sponsored by and received consulting fees and/or grant support from: Atara Biotherapeutics, Biogen Idec, Celgene/Receptos, Genentech/Roche, GlaxoSmithKline, MAPI, Medimmune, Merck/EMD Serono, Novartis, Sanofi-Genzyme.

4.7 Materials and Methods

4.7.1 Experimental animals – Adult female Sprague-Dawley rats were housed in pairs, at constant temperature ($23\pm 1^\circ\text{C}$) with free access to regular chow and water, and a 12h light-dark cycle. Adult C57/Bl6 mice were housed similarly, but with four mice per cage. All housing and procedures were performed in accordance with animal use protocols approved by the Montreal Neurological Institute Animal Care and Use Committee, following the Canadian Council on Animal Care (CCAC) guidelines. All procedures involving EAE were approved by the Centre de Recherche du Centre Hospitalier de l'Université de Montréal Animal Care Committee following CCAC guidelines. No statistical methods were used to determine sample sizes.

4.7.2 Preparation of peripheral blood mononuclear cell conditioned media (PBMC-CM) - Blood from adult Sprague-Dawley rats was collected by cardiac puncture in accordance with procedures approved by the Montreal neurological Institute Animal Care and Use Committee. Rat PBMCs were separated by Ficoll-Plaque density centrifugation and cultured in Ultraculture serum-free medium (Lonza) containing 1% penicillin-streptomycin for 4 days in vitro (DIV) at 37°C , 5% CO_2 (Pool, Rambaldi et al. 2011, Pool, Rambaldi et al. 2012). Control media was Ultraculture serum-free medium (Lonza) containing 1% penicillin-streptomycin incubated without cells for 4 DIV. Individual batches of PBMC-CM were titered by determining the dose that mediated 50% neurite outgrowth inhibition; this was defined as the 1X treatment concentrations. Dose curves of conditioned media were then applied at 0.5X – 4X doses by diluting PBMC-CM into volumes of control CM such that all neurons were treated with equal volumes.

4.7.3 Degeneration assays - Cortical neurons from wildtype (WT) C57Bl/6 mice were prepared as previously described (Juzwik, Drake et al. 2018, Pare, Mailhot et al. 2018). Neurons were seeded in 48-wells at 80 000 cells/well and aged 4 DIV prior to addition of PBMC-CM. Treated neurons were fixed with 4% paraformaldehyde (PFA)/20% sucrose and stained with anti- β III tubulin antibody (Covance), Hoechst 33342 dye (Sigma-Aldrich)

and fluorescent secondary antibodies. Apoptotic cells were identified by TUNEL staining (In Situ Cell Death Detection Kit, Roche). Automated image acquisition and analysis were performed using ImageXpress and the Multi Wavelength Cell Scoring (MWSC) module of MetaXpress (Molecular Devices) to determine the number of neuronal cell bodies by overlapping β III-tubulin and Hoechst staining. Fixed and imaged neurons were analyzed for loss of neurite processes using ImageJ, where images were thresholded and the percent area covered by β III-tubulin positive neurites recorded. The fold change in percent area covered was calculated for PBMC-CM treated neurons relative to control CM. For overexpression and loss-of-function assays, *miRVana* miRNA mimics of miR-27a-3p, miR-223-3p, or Negative Control #1 (ThermoFisher); *miRVana* miRNA inhibitors miR-23a-3p, miR-27a-3p, or Negative Control #1 (ThermoFisher); and miRCURY LNA miRNA inhibitor miR-223-3p or Negative Control A (Qiagen) were used. Neurons were cultured without antibiotics and transfected at 2 DIV with a 20 nM final concentration of mimic or inhibitor using Lipofectamine RNAiMax (ThermoFisher), according to manufacturer's instructions. miRNA inhibitors miR-23a-3p and miR-27a-3p were transfected together at a final 10 nM concentration for each inhibitor. Animal procedures for miR-223 knockout (KO) mice were approved by the Memorial University Animal Care Committee following CCAC guidelines. miR-223^{-/-} and miR-223^{-y} KO mice (B6.Cg-Ptprc^aMir223^{tm1Fcam}/J) were purchased from Jackson Laboratories and maintained on a CD45.1⁺ Background (B6.SJL-Ptprc^aPepc^b/BoyJ) (Johnnidis, Harris et al. 2008). For miR-223^{-/-} neuronal cultures, female miR-223^{+/-} and male miR-223^{-y} mice were crossed to gain WT, heterozygous and KO embryos such that each embryo was dissected individually before genotypes were confirmed. Genotyping was performed using common 5'-TTCTGCTATTCTGGCTGCAA-3'; WT 5'-CAGTGTCACGCTCCGTGTAT-3'; and KO 5'-CTTCCTCGTGCTTTACGGTATCG-3' primers (Integrated DNA Technologies). Small molecule inhibitors for neurodegeneration assays included Cetrorelix acetate (Sigma-Aldrich), Leuprolide acetate salt (Sigma-Aldrich), GYKI 53655 hydrochloride (abcam), and MK801 hydrogen maleate (Sigma-Aldrich).

4.7.4 Neuronal survival assay - Cortical neurons from WT C57Bl/6 mice were seeded in 96-well plates (Corning; #3904) at 14 000 cells/well. Neurons were cultured without antibiotics and transfected at 2 DIV with *miRVana* miRNA mimics of miR-27a-3p, miR-223-3p, or Negative Control #1 (ThermoFisher) at a final concentration of 30 nM using Lipofectamine RNAiMax (ThermoFisher). At 8 DIV, neurons were treated with 10 or 20 mM glutamate (L-glutamic acid monosodium salt hydrate; Sigma #G5889) for 48 hrs. At 10 DIV, neurons were fixed with 4% paraformaldehyde (PFA)/20% sucrose and stained with anti- β III tubulin antibody (Covance), Hoechst 33342 dye (Sigma-Aldrich) and fluorescent secondary antibodies. Automated image acquisition and analysis were performed using ImageXpress and the Multi Wavelength Cell Scoring (MWSC) module of MetaXpress (Molecular Devices) to determine the number of neuronal cell bodies by overlapping β III-tubulin and Hoechst staining.

4.7.5 Cell viability - Cell viability was assessed with the CellTitre-Glo (CTG) Assay (Promega) according to manufacturer's instructions. Neurons treated with CTG Reagent were transferred to black-walled clear bottom 96-well plates, and luminescence was assessed using Victor3 Plate Reader.

4.7.6 Quantitative RT-PCR (qRT-PCR) - Total RNA extraction was done using miRNeasy Mini Kit, according to manufacturer's instruction. miRNA expression was assessed using multiplex qRT-PCR with Taqman miRNA Assays (ThermoFisher) and snoRNA202 or RNU48 as the endogenous control, as previously described (Moore, Rao et al. 2013, Juzwik, Drake et al. 2018). Fold change calculations for miRNA expression were performed using the $-\Delta\Delta CT$ method (Livak and Schmittgen 2001).

4.7.7 Active EAE Induction - All animal procedures related to EAE induction were approved by the Centre de Recherche du Centre Hospitalier de l'Université de Montréal Animal Care Committee following CCAC guidelines. EAE was induced in 7-11 week old female C57BL/6 mice, and clinical signs of EAE were assessed daily, as described previously (Lecuyer, Saint-Laurent et al. 2017). Animals were immunized with subcutaneous injections of 200 μ g of MOG₃₅₋₅₅ (MEVGWYRSPFSRVVHLYRNGK; Alpha

Diagnostic International) in 100- μ L emulsion of complete Freud's adjuvant (CFA) (4 mg/mL *Mycobacterium tuberculosis*; Fisher Scientific). On day 2, Pertussis toxin (500 ng PTX, Sigma-Aldrich) was injected intraperitoneally. The scoring system used was as follows: 0, normal; 1, limp tail; 2, slow righting reflexes; 2.5, difficulty walking/ataxia; 3, paralysis of one hind limb (monoparalysis); 3.5, hind limb monoparalysis and severe weakness in the other hind limb; 4, paralysis of both hind limbs (paraparalysis); 4.5, hind limb paraparalysis and forelimb weakness; 5, moribund (requires sacrifice). Animals were injected with a lethal dose of Euthanyl® and perfused intracardially using cold saline for laser capture micro-dissection (LCM). For other analysis, animals were perfused with cold phosphate buffer (PBS) [0.1M] followed with 4% PFA (Electron microscopy sciences).

4.7.8 Laser-capture micro-dissection - The spinal cord and retina were isolated and frozen at -80°C in Tissue-Tek® optimal cutting temperature (OCT) compound. Preparation of slides for LCM, LCM procedure, and extraction of RNA from laser-captured material were done as described previously (Juzwik, Drake et al. 2018). For LCM, lumbar motor neurons were isolated from EAE mice at naïve and peak stage; and the retinal ganglion cell (RGC) layer was isolated from EAE mice at pre-symptomatic and peak stages. Only LCM samples with a RIN greater than 4 were used. In an evaluation of RIN and reliable cycle threshold (Ct) values during qPCR, it was demonstrated that samples with a RIN of 4 show reliable Ct values for amplicons up to 200 bp in size (Fleige, Walf et al. 2006). miRNA amplicons are 80-90 bp.

4.7.9 Human brain samples - Snap-frozen post-mortem brain samples from MS and control patients were obtained from the University Hospital Centre of Québec (Whittaker Hawkins, Patenaude et al. 2017). Tissue samples were classified as normal appearing white matter (NAWM) from non-MS or SPMS patients, active lesions (stage 1 and 2, white matter involvement only), or leukocortical lesions from SPMS patients. Active lesions were further broken down into mild or severe, where severe refers to lesions with greater inflammation and demyelination as previously described (Reynolds, Roncaroli et al. 2011). Leukocortical refers to lesions with white and gray matter involvement, where 4 lesions are leukocortical from the cortex, one leukocortical lesion from the cerebellum,

and one subpial cortical lesion (with only gray matter involvement). Frozen sections were cut containing the lesion area exclusively with a cryostat to obtain approximately 20 mg of tissue, which was homogenized with QIAzol Lysis Reagent and total RNA extracted using miRNeasy Mini Kit according to manufacturer's instructions.

4.7.10 Histology - Post-mortem human tissue was stained with luxol fast blue (LFB) and hematoxylin and eosin (H&E) as previously published ((Lecuyer, Saint-Laurent et al. 2017)). BaseScope was done according to manufacturer's instructions for fresh frozen tissue followed by the BaseScope Detection Reagent Kit v2, using the BA-Hs-pre-MIR223-2zz-st probe to detect miR-223-3p (ACDBio).

4.7.11 Whole mount Optic Nerve Staining and Clearing - Optic nerves with eye cups and chiasm attached were collected from EAE mice. The nerves were dissected and post-fixed for an additional 2h. We used an optimized protocol of immunolabeling-enabled three-dimensional imaging of solvent cleared organs (iDISCO) to immuno-stain whole mount optic nerve. In brief, the nerves were dehydrated with increasing concentrations of methanol (MeOH, Fisher Chemical) followed by incubation with hydrogen peroxide (Fisher Chemical) overnight. The optic nerves were rehydrated again with MeOH and washed in PBS before incubation for seven days with non-phosphorylated Alexa 488 conjugated-neurofilament-H antibody (5 μ g/ml per nerve; Millipore). Nerves were then washed three times with PBS, embedded in agar blocks (1%; Fisher scientific) and cleared using increasing concentration of tetrahydrofuran (THF 50%, 80% and 100%; Sigma-Aldrich) followed by immersion in benzyl ether (DBE, Sigma-Aldrich). Transparent nerves were imaged using SP8 Leica confocal microscope at one to three different portions (proximal, central or distal portions). The density of axonal swellings was quantified in 9 to 20 optical sections per portion of nerves. Optic nerves were analyzed at multiple stages throughout EAE progression: presymptomatic (score 0, 8-day post-injection (dpi)), onset (score 1-2.5, 12 dpi), peak (score 3 - 4.5; 14 dpi), and chronic (35 dpi).

4.7.12 Intravitreal injection and AAV2-virus delivery - Intravitreal injections (2 μ l) were made in the vitreous chamber of the left eye using a custom-made glass micro-needle

(Wiretrol II capillary, Drummond Scientific Co). The sclera was exposed under general anaesthesia, and the tip of the needle inserted into the superior ocular quadrant at a 45° angle through the sclera and retina into the vitreous space. AAV2-miR-223 virus (8×10^{12} GC/ml) or AAV2-NT virus (AAV2-NT; 2.1×10^{12} GC/ml; Penn Vector Core) were injected four weeks prior to EAE induction. qPCR analyses of miR-223-3p were assessed in the optic nerve and retina of injected mice for validation.

4.7.13 Immunohistochemistry (IHC) in retinal sections - Eye cups were dissected out from mice and incubated overnight in 30% sucrose before being embedded in OCT. Twelve microns thick retinal sections were incubated with blocking solution (3% BSA, 0.3% Triton in PBS), followed by incubation with primary antibodies overnight at 4 degrees. The following day, the sections were washed with PBS and incubated with secondary antibodies at 1:500. Images were acquired using a Zeiss LSM-710 and Zen. Imaging parameters were kept the same between all retinal sections, and all images were acquired on the same day. Expression of NR2B receptors were assessed in the retinal ganglion layer of AAV2-NT and AAV2-miR-223 injected mice. The primary antibodies used were: anti-NR2B (Cell Signaling) 1:100, and anti-Brn3a+ (C-20, Santa Cruz) 1:300.

4.7.14 Quantification of RGC survival - The retinas were dissected out of the eyes and stained with Brn3a+ antibodies as previously described (Galindo-Romero, Aviles-Trigueros et al. 2011). In brief, free-floating retinas were permeabilized with 0.5% Tx + PBS buffer twice, before being frozen for 15 minutes at -80°C following by sequential washes. The retinas were then incubated overnight at 4°C in anti-Brn3a+ primary antibody (C-20, Santa Cruz), washed and incubated 2h at room temperature in secondary antibody. RGCs were quantified in the 4 retinal quadrants (12 squares total) and total RGC density analyzed as RGC/mm². The number of retinas analyzed per experimental group as been reported in the legend sections.

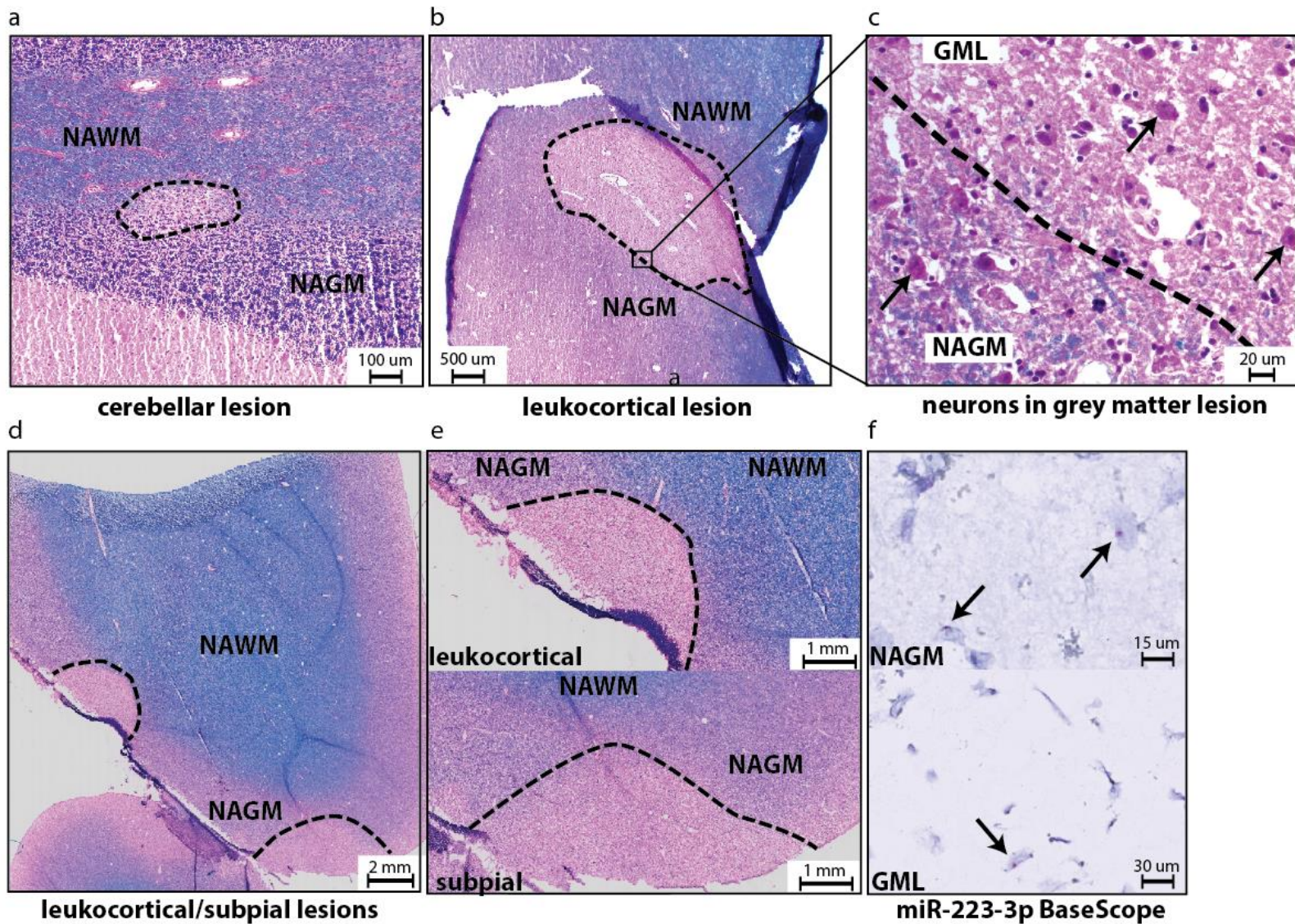
4.7.15 *In silico* assessment of predicated targets - A bioinformatics assessment of putative target genes was performed for miR-27a-3p and miR-223-3p based on a comparative analysis by seven prediction programs for mouse transcripts. These include:

Diana-microT (Reczko, Maragkakis et al. 2012, Paraskevopoulou, Georgakilas et al. 2013), microRNA.org (Betel, Wilson et al. 2008), miRDP (Wong and Wang 2015), miRTarBase (Chou, Chang et al. 2016), RNA22 (Miranda, Huynh et al. 2006), TargetScan (Agarwal, Bell et al. 2015), and TarBase (Vlachos, Paraskevopoulou et al. 2015). Only mRNAs that were identified as putative targets across 4 of the 7 prediction programs were analyzed further, termed 'filtered targets' (Juzwik, Drake et al. 2018). Pathways regulated by overlapping filtered targets were determined using an overrepresentation test by Protein ANALysis THrough Evolutionary Relationships (PANTHER) classification system (<http://www.pantherdb.org/>) (Mi, Muruganujan et al. 2013, Mi, Huang et al. 2017). The p-values for the PANTHER Pathways were determined by PANTHER using the binomial statistic with a Bonferroni correction for multiple testing.

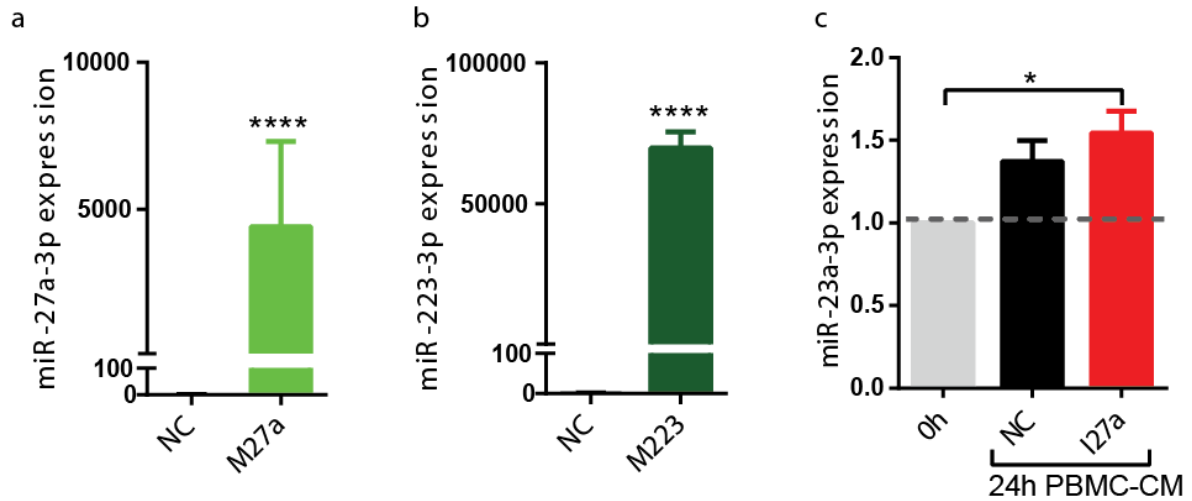
4.7.16 Luciferase assays - HEK 293T cells were seeded in 24-well plates and transfected 24hr later with mmu-miR-223-3p, mmu-miR-27a-3p mimics, or non-specific cel-miR-39-3p control (Dharmacon) and pEZX-MT06 dual-luciferase constructs flanked with target 3'UTR (GeneCopoeia). Transfection was performed with lipofectamine 2000 (Invitrogen) as per manufacturer's instructions. 72h later, cell lysate was collected for analysis using the Luc-Pair Duo-Luciferase HS assay kit (GeneCopoeia) and luminescence was detected using the EnSpire Multimode Plate Reader (PerkinElmer, Inc.). Firefly luciferase activity was normalized to Renilla luciferase and mimic overexpression conditions were then normalized to negative control mimic and empty vector conditions.

4.7.17 Statistical analyses - Statistical analyses were performed using GraphPad Prism 6. As indicated in figure legends, the following statistical tests were used: student's t-test; one-way ANOVA; two-way ANOVA; post-hocs include Dunnett's and Tukey's multiple comparisons tests. Sample sizes are indicated in the figure legends and significance was defined as * $p < 0.05$, with ** $p < 0.01$, *** $p < 0.001$, and **** $p < 0.0001$.

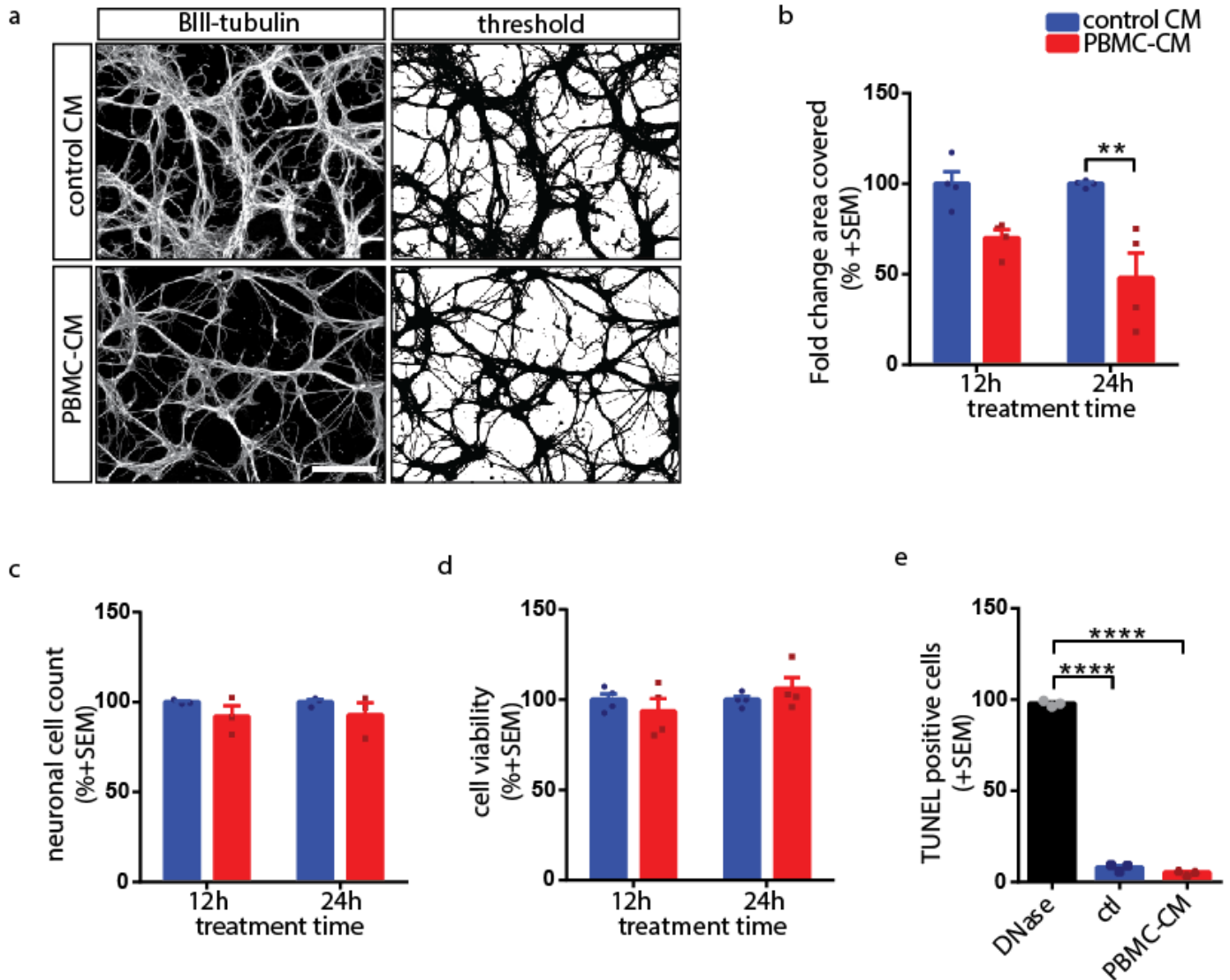
4.8 Supplementary Figures and Tables



Supplementary Figure 1. Characterization of human MS lesion material. (a-e) Luxol fast blue and H&E staining of human MS lesions shows involvement of both white matter and grey matter in the cerebellum (a) and cortex (b,d,e) of three separate MS patients. Higher magnification shows the presence of neurons in both the normal appearing grey matter and within the grey matter lesion (c) as indicated by the arrows, and the lack of white matter involvement in the subpial lesion (e, bottom inset). BaseScope for miR-223-3p demonstrated the presence of miR-223-3p (visualized as the red dots) within neurons (f) in normal appearing grey matter and within the subpial grey matter lesion (top and bottom insets respectively).



Supplementary Figure 2. Transfection validation of miRNA mimics and inhibitors. (a,b) qPCR analysis of miR-27a-3p and miR-223-3p expression following transfection of miRNA mimics (M27a, M223) and mimic negative control (NC) in dissociated cortical neurons (n=3-4, student's t-test). (c) miR-23a-3p expression in the presence of miR-27a-3p inhibitor (I27a) during 24h PBMC-CM challenge relative to baseline levels (n=3, one-way ANOVA, $p < 0.05$, Tukey's multiple comparisons test).



Supplementary Figure 3. PBMC-CM induces significant neurite degeneration independent of cell loss or death. (a) β III-tubulin stained neurons at 4 DIV challenged with PBMC-CM and control CM for 24h. Scale bar; 100 μ m. (b) Quantification of the fold change area covered by neuronal cell bodies and their neurites quantified by thresholding images using ImageJ for 12h and 24h treatment with PBMC-CM and control CM (n=4, two-way ANOVA, $p < 0.05$, Tukey's multiple comparisons test). (c) Quantification of the percent neuronal cells following PBMC-CM and control-CM treatment for 12h and 24h by overlapping β III-tubulin stained neurons with Hoechst (n=3, two-way ANOVA, $p < 0.05$, Tukey's multiple comparisons test). (d) Assessment of cell viability by CTG Luminescent Cell Viability Assay in PBMC-CM and control-CM treated neurons for 12h and 24h (n=4, two-way ANOVA, $p < 0.05$, Tukey's multiple comparisons test). (e) Detection of apoptosis by TUNEL in neurons challenged with PBMC-CM for 24h, with DNase treatment as a positive control (n=3, one-way ANOVA, $p < 0.05$, Tukey's multiple comparisons test).

Table 1 Supplemental

Putative filtered mRNA targets of miR-27a-3p and miR-223-3p

miR-27a-3p targets								miR-223-3p targets		
1200014J11Rik	Cacnb2	E2f7	Gpd1	Man2a1	Nup50	Rffi	Srl	Whsc1	5031414D18Rik	Mt2
1600012H06Rik	Camk2a	Ebf3	Gpd2	Maneal	Nxf1	Rfx3	Ss18l1	Wjpf2	Abca1	Mtpn
1810011O10Rik	Camk2d	Ech1	Gpr126	Map2k4	Nxt2	Rgl2	Ssh1	Wnk1	Abhd13	Mylh10
2410004B18Rik	Camta1	Edar	Gpr174	Map2k7	Nyap2	Rgs1	St14	Wnt3a	Aco1	Ndnf
2510003E04Rik	Capza1	Edem1	Gpt2	Map3k14	Oaf	Rgs8	Stag1	Wsb1	Acsf3	Nefh
4930402H24Rik	Car10	Edem3	Gria3	Map3k2	Onecut2	Rhot1	Stard7	Xirp2	Acvr2a	Nf1
4932438A13Rik	Casc3	Ednra	Grik3	Map4k3	Opa1	Rictor	Stbd1	Xkrx	Alcam	Nfat5
4933426M11Rik	Cbfa2t3	Edrf1	Grin2b	Mapk14	Orc5	Rmnd5a	Stim2	Ypel2	Ankrd17	Nfia
9430016H08Rik	Cbfb	Eepd1	Grm5	March6	Otx2	Rnf111	Stk38	Ypel3	Anks1b	Nfib
A230046K03Rik	Cblb	Efnb2	Gse1	March7	Pak6	Rnf139	Stk39	Ywhab	Apool	Nhh2
Abca1	Ccdc50	Egfr	Gspt1	Marcks	Palms2	Rnf14	Strbp	Zadh1	Arfp1	Otud4
Abhd17c	Ccl22	Ehd3	Gtf2i	Mark1	Pappa	Rnf144a	Stx16	Zbtb20	Arid1a	Pacs2
Abl2	Ccm2	Ehf	Gxylt1	Masp1	Paqr9	Rnf38	Styk1	Zbtb34	Ar15a	Pde4d
Acer2	Ccng1	Eif2s2	H3f3b	Matn3	Pard6b	Rnft1	Suc1g2	Zbtb39	Armc1	Pdia6
Acly	Ccnj	Eif5	Hapln1	Mbnl2	Pax9	Rngtt	Suco	Zbtb42	Armxc1	Pds5b
Acvr1	Ccnk	Elavl2	Hbegf	Mbtd1	Pcnx	Ror1	Suz12	Zc3h12d	Arvcf	Pea15a
Acvr1c	Ccnt2	Efn2	Hcn4	Mdfi	Pde10a	Rora	Syde1	Zcchc24	Atg4d	Pgrmc1
Acvr2a	Ccny	Elf2	Heg1	Mdn1	Pde3a	Rpgrip1l	Syt2	Zdhc17	Atp1b1	Phf201l
Adam19	Cd28	Elmo1	Hic1	Med12l	Pde3b	Rpn1	Szrd1	Zfhx4	Atp2b1	Phip
Adamts10	Cd2ap	Eml1	Hipk2	Med13	Pdgra	Rps6ka5	Tab3	Zfp143	Atrn	Pik3c2a
Adamts6	Cdh11	En2	Hivep2	Med14	Pdhx	Rps6kb1	Tada1	Zfp148	Capn6	Pkn2
Adamts11	Cdh5	Enox2	Hivep3	Meis2	Pdia5	Rreb1	Taf8	Zfp361l	Cbfb	Pknox1
Adcy6	Cdip1	Epb4.1	Hlx	Melk	Pdpk1	Rsbn1l	Tax1bp1	Zfp3612	Cbx5	Plagl2
Add1	Cdk18	Epb4.111	Hmgcr	Mecpe	Pds5b	Runx1	Tbc1d4	Zfp462	Ccnt2	Plg
Adora2b	Cds1	Epb4.114a	Hnrmpf	Met	Pdzk1ip1	Runx1t1	Tet1	Zfp473	Cd2ap	Pnma2
Afap1	Cecr2	Erlcc1	Hoxa10	Mfhas1	Pel12	Ruvbl2	Tet3	Zfp597	Cdk17	Polr3g
Aff4	Cecr6	Ero1l	Hoxa5	Mfsd2a	Pgap1	Satb2	Tfam	Zfp608	Cdkn1b	Prdm1
Aggf1	Celf1	Eya1	Hoxb8	Mier3	Phb	Scaf11	Tgfb1	Zfp652	Zfr	Prkar2b
Agrn	Cemip	Eya4	Hoxc6	Mkl1n1	Phf13	Scd2	Tgfb3	Zfp800	Cep120	Psm6
Ak2	Cep135	Fam102a	Hsd1l	Mknk2	Phlpp2	Scn9a	Tgoln1	Zfp827	Clasp2	Ptpb2
Akirin1	Chd2	Fam120b	Hsp90aa1	Mmd	Pigc	Sdc2	Thrb	Cpne4	Rab8b	
Akirin2	Chd6	Fam126a	Hspd1	Mmp16	Pik3ca	Sdha	Tlk2	Zhx1	Crebzf	Rabgap1
Alg11	Chd7	Fam126b	Hyou1	Mob1b	Pikfyve	Sdpr	Tmbim6	Zkscan4	Csnk1g1	Ralgps2
Alg9	Chka	Fam133b	Icos	Mrv1	Pkia	Sec24a	Tmcc1	Zmat3	Ctsl	Rap2a
Ammecr1l	Chst2	Fam134c	Ifrng	Msn	Pknox2	Seh1l	Tmcc3	Znrf2	Ddn	Rasa1
Ank1b1	Cipc	Fam13a	Iglon5	Mttr4	Pla2g6	Sema6a	Tmed5	Zzz3	Ddx17	Rbpj
Ankrd17	Kcap4	Fam171a1	Ikzf1	Mtss1l	Plagl2	Sema6d	Tmem170b		Dennd5b	Rhob
Anks1	Cln3	Fam184a	Ikzf3	Myef2	Plcx2	Sema7a	Tmem19		Dennd6a	Rnf34
Ap1s2	Cln5	Fam193b	Ikzf5	Myt1	Plek	Sept8	Tmem194		Der1l	Rps6kb1
Apaf1	Clic5	Fam222a	Il7r	Naa15	Plekha6	Serp1	Tmem194b		Dnajc6	Rras2
Appbp2	Clock	Fam49b	Ing5	Naa50	Plekhh1	Serpini1	Tmem206		Dock1	Rsrc2
Aqp11	Cnot1	Fam69a	Ino80d	Nabp1	Plk2	Setd5	Tmem9b		Eaf1	Scn1a
Arfge1	Cnot7	Fam73b	Inpp5j	Nap112	Plxn1	Sfrp1	Tmprss11f		Em16	Scn2a1
Arhgap1	Cnrip1	Fam78a	Lpo5	Nav2	Plxnd1	Sfxn1	Tmtc2		Eva1a	Scn3a
Arhgap12	Cntnap2	Fam84b	Lrf4	Ncapd3	Pnk1	Sgcb	Tnik		F11r	Sept6
Arhgap32	Cog6	Fasn	Irs1	Nck1	Poglut1	Sgk3	Tnpo1		F3	Sept8
Arid1b	Cop21	Fbxl14	Isl1	Ncoa7	Poldip2	Sgms1	Tnrc6a		Fam120c	Sgms1
Arid2	Cpeb3	Fbxl20	Itga5	Ndufs4	Pom121	Sgpp1	Tor1b		Fam13a	Siah1a
Arl6ip1	Creb1	Fbxo32	Itsn2	Nebi	Pou2f3	Sh3bgrl2	Tox		Fam199x	Slc23a2
Arl8b	Crebrf	Fbxo33	Jmjd1c	Nedd4	Ppap2b	Sh3rf1	Tppp		Fam89a	Slc39a1
Arrdc4	Creml	Fbxw7	Jph1	Nek6	Ppara	Shc4	Trappc8		Fat1	Slc44a
Arx	Csd2	Fgd6	Kat2b	Neo1	Pparg	Shisa6	Tril		Fbxo8	Smarcd1
Atg2a	Csf1	Flrt3	Kbtbd8	Neto1	Ppif	Shprh	Trim23		Fbxw7	Sox6
Atp11c	Csnk1g1	Fosb	Kcmf1	Neto2	Ppig	Sik1	Trim44		Foxo3	Sp3
Atp2b1	Csrnp1	Foxo1	Kcnk2	Neurl1b	Ppm1e	Sim1	Trove2		Foxp1	Spag9
Atrn1l	Csrp2	Foxp2	Kdm3a	Neurl4	Ppm1g	Six1	Tsc1		Frm4a	Spata13
Atrx	Ctcf	Foxp4	Khsrp	Neurod6	Ppm1k	Slc1a2	Ttyh1		Golga1	Srek1
Atxn10	Cth	Frk	Kif5c	Nf1	Ppp1cc	Slc22a23	Ube2f		Golgb1	Srgap3
AU040320	Cts8	Frs3	Klh29	Nfat5	Ppp1r3f	Slc27a4	Ube2n		Gpr155	Stk39
B3gnt7	Cyp39a1	Fryl	Klh31	Nfe2l2	Ppp1r9a	Slc35f1	Ube2v1		Gpr22	Syn1
B4galt3	D15Ert621e	Fubp1	Kmt2c	Nfkbid	Prkar2a	Slc35f3	Ube2w		Gria2	Syncrip
Bag2	D3Ert6751e	Fzd3	Kpna3	Nfx1	Prrg3	Slc36a4	Ube4a		Gria3	Tgfb3
Baz2a	Dcaf12	Fzd7	Kpnb1	Ngfr	Psm1a	Slc38a4	Ubp1		Grm7	Tnfrsf19
Baz2b	Dcaf7	Gab1	Kras	Ngfrap1	Ptbp2	Slc39a11	Ubr1		Gtpbp8	Trp53bp1
Bbc3	Dcbl1	Gabbr3	Ksr1	Nipal4	Ptgd1	Slc6a1	Ubr5		Hlf	Tshz3
BC030336	Dcp2	Galnt3	Larp4	Nln	Ptger4	Slc6a6	Ugcg		Hmgcs1	Tspan7
Bcor1l	Dcun1d4	Galnt7	Lats1	Nmur2	Ptprk	Slc7a11	Unc13c		Hsp90b1	Ttc4
Bdp1	Dcx	Gata2	Lbh	Nol4	Pura	Slco5a1	Unc80		Igf1r	Ttc9
Blm	Dffa	Gata3	Ldlr	Notch2	Pxx	Siltrk1	Unkl		Itgb1	Ube2a
Bmi1	Dhrs9	Gatc	Lifr	Nova1	Pxmp2	Smad9	Usp21		Jmjd1c	Ube2q2
Bmp2k	Dicer1	Gcc2	Limk1	Npepps	Qk	Smoc2	Usp24		Kat6a	Ulk2
Bmpr1a	Diras1	Gfpt1	Limk2	Nptn	Rab11fip1	Snap25	Usp25		Kif1b	Usp40
Bod1l	Dkk2	Gfpt2	Liph	Nr1d2	Rap1b	Snn	Usp42		Kif21b	Usp6nl
Brd8	Dll4	Glipr2	Lonrf1	Nr2f2	Rap2b	Snx18	Usp45		Kpna3	Vopp1
Brpf3	Dnajc13	Gira2	Lox	Nr2f6	Rapgef2	Snx30	Usp46		Ktn1	Vti1a

Table 2 Supplemental

Putative mRNA targets of miR-27a and miR-223 in investigated pathways as identified by PANTHER

Investigated Pathway	Target mRNA Mapped ID
Ionotropic glutamate receptor (iGluR) pathway	Cacna1a
	Camk2d
	Slc1a2
	Camk2a
	Grik3
	Grin2b
	Camk2d
	Gria2
	Snap25
	Gria3
Metabotropic glutamate receptor (mGluR) group III pathway	Cacna1a
	Vti1a
	Grm5
	Slc1a2
	Grik3
	Prkar2a
	Grin2b
	Prkar2b
	Grm7
	Gria2
Snap25	
Gria3	
Gonadotropin-releasing hormone receptor (GnRH) pathway	Sos1
	Fosb
	Camk2d
	Isl1
	Map2k7
	Tgfbr3
	Pknox1
	Egfr
	Map4k3
	Creb1
	Smad9
	Map2k4
	Ptger4
	Pparg
	Arhgap32
	Bmpr1a
	Kat2b
	Mapk14
	Pla2g6
	Ksr1
	Igf1r
	Map3k2
	Irs1
	Itgb1
	Map3k14
	Gata2
	Acvr2a
	Ppara
	Rap1b

Preface

In this chapter we study a model of positive inflammation that promotes neuronal survival and regrowth. Intraocular inflammation has been demonstrated to promote neuronal protection and regrowth following acute nerve damage. We screened a list of candidate miRNAs involved in neuronal survival and regeneration and identified miR-383-5p as a miRNA that is downregulated in neurons in response to intraocular inflammation. We demonstrated that miR-383-5p downregulation promotes neurite outgrowth *in vitro* and promotes axon regeneration following optic nerve crush *in vivo*. We found that growth factors released by intraocular inflammation suppress expression of miR-383-5p and that this relieves miR-383-5p-dependent suppression of the cytoskeletal regulator Collapsin Response Mediator Protein 2 and the antioxidant protein peroxiredoxin 3. This work thus describes miRNA profiling in a model of positive inflammation that revealed vital information about the global neuronal response to inflammation and suggested novel molecular avenues to promote neuronal repair following damage.

5 Chapter 4. Inhibition of miR-383 promotes axon regeneration following injury by a distributed relief of targets

Camille A. Juźwik*¹, Barbara Morquette*¹, Yang Zhang¹, Isabel Rambaldi¹, Elizabeth Gowing¹, Camille Boudreau-Pinsonneault¹, Ziyu Liu¹, Vamshi Vangoor², Jeroen Pasterkamp², Craig Moore³, Amit Bar-Or^{1,4}, Alyson E. Fournier¹

***co-contributing author**

¹ McGill University, Montréal Neurological Institute, Montréal, QC H3A 2B4, Canada

² UMC Utrecht, Universiteitsweg 100, STR. 4.229, 3584 CG Utrecht, The Netherlands

³ Division of BioMedical Sciences, Faculty of Medicine, Memorial University of Newfoundland

⁴ Perelman School of Medicine, University of Pennsylvania, Philadelphia, PA 19104 USA

Manuscript in preparation

5.1 Abstract

Neuroinflammation can positively influence axon regeneration following injury in the central nervous system (CNS) but the molecular mechanisms underlying this effect are not fully understood. We have evaluated how microRNAs may be regulated in the context of inflammation because they target multiple mRNAs simultaneously and may help to identify signaling hubs that can be targeted to promote regeneration. We identified miR-383-5p as a miRNA that is downregulated in retinal ganglion cells in response to intraocular inflammation and in response to treatment with outgrowth-promoting astrocyte conditioned media (ACM). miR-383-5p downregulation is sufficient to promote axon growth *in vitro* and injection of a miR-383-5p inhibitor into the eye promotes axon regeneration following optic nerve crush. Previous studies have demonstrated that astrocyte-derived ciliary neurotrophic factor (CNTF) stimulates axon regeneration in response to intraocular inflammation. We found that CNTF downregulated the expression of neuronal miR-383-5p. Furthermore, we acquired evidence that inhibiting miR-383-5p de-represses the expression of mitochondrial antioxidant genes and microtubule-associated proteins that are important for the pro-regenerative effects of the miR-383-5p inhibitor. We have implicated miR-383-5p as a molecule that suppresses axon regeneration with detailed characterization of both its upstream effectors and its downstream targets. The distributed function of miR-383-5p demonstrates the tight-regulatory networks controlled by miRNAs, and suggests it is an effective target for the design of therapies promoting neuronal repair and regeneration while bypassing inflammatory stimulation.

5.2 Introduction

Following injury to the adult mammalian central nervous system (CNS), axon regeneration is limited (Ramón y Cajal, DeFelipe et al. 1991). The inability to regenerate is through an age-dependent decrease in the intrinsic ability of neurons to grow and the presence of extrinsic growth-inhibitory factors such as myelin debris and elements of the glial scar (Cai, Qiu et al. 2001, Fournier, GrandPre et al. 2001, Bradbury, Moon et al. 2002, Park, Liu et al. 2008, Qin, Zou et al. 2013). Regulating intrinsic signalling mechanisms including phosphatase and tensin homolog (PTEN), suppressor of cytokine 3 (SOCS3), or krüppel-like factor 4 (KLF4) can promote extensive axon regeneration following acute axonal injury (Park, Liu et al. 2008, Smith, Sun et al. 2009, Qin, Zou et al. 2013). Antagonism of Nogo-66 receptor or dissolution of the glial scar by chondroitinase ABC are examples of successful attempts to neutralize the extrinsic factors blocking axon regeneration (Bradbury, Moon et al. 2002, GrandPre, Li et al. 2002). Combinatorial approaches promoting the intrinsic potential and blocking the extrinsic factors simultaneously are successful in promoting regeneration past the lesion site in models of spinal cord injury (Kadoya, Tsukada et al. 2009, Garcia-Alias, Petrosyan et al. 2011, Wang, Hasan et al. 2012, Geoffroy, Lorenzana et al. 2015). A combinatorial approach has been able to promote repair and regeneration when administered a year following spinal cord injury (Kadoya, Tsukada et al. 2009). Thus, multiprong approaches targeting several pathways are the most promising in the treatment of CNS injury.

microRNAs (miRNAs) regulate hubs of gene expression, making them lucrative candidates to investigate in CNS injury as we can investigate multiple affected pathways (Lewis, Shih et al. 2003, Cui, Yu et al. 2006, Shalgi, Lieber et al. 2007, Iorio, Piovani et al. 2010, Moutinho and Esteller 2017). miRNAs are small, non-coding RNA sequences approximately 22 nucleotides in length (Lewis, Shih et al. 2003). Each miRNA contains a short seed region from nucleotide positions 2 to 7 that binds complementary regions within the 3' untranslated region (3'UTR) of target messenger RNA (mRNA), leading to target mRNA degradation or translational repression. Through their promiscuous nature, a single miRNA can target several mRNA species simultaneously to regulate multiple pathways (Grimson, Farh et al. 2007). We are interested in determining miRNA regulation

of neuronal repair and regeneration to uncover multiple affected pathways during CNS axotomy.

We selected candidate miRNAs identified in dorsal root ganglion (DRG) neurons following a sciatic nerve lesion in mice (Strickland, Richards et al. 2011). A sciatic nerve lesion severs the peripheral processes of DRG neurons and generates a robust cell body response that drives regeneration of DRG axons, while injury to the central processes does not prompt a regenerative response. However, the central processes of DRG neurons can be primed for regeneration into and past the site of injury if the peripheral processes are severed one to two weeks prior to injury to the dorsal column, what is referred to as a conditioning lesion (Neumann and Woolf 1999). Candidate miRNAs identified in DRG neurons following a sciatic nerve lesion thus represent those involved in neuronal survival and regeneration (Strickland, Richards et al. 2011). We identified miR-383-5p as downregulated in response to pro-growth stimuli and upregulated in response to outgrowth inhibitory stimuli; as well as downregulated in the retinal neurons of zymosan-injected mice following optic nerve crush (ONC). Intravitreal injection of zymosan, a microbial polysaccharide, or lens injury (LI) concurrently with ONC can overcome the intrinsic and extrinsic barriers to regeneration in the CNS (Leon, Yin et al. 2000). Zymosan and LI promote intraocular inflammation that activates macrophages, neutrophils, retinal astrocytes, and Müller cells (Leon, Yin et al. 2000, Yin, Cui et al. 2003, Muller, Hauk et al. 2007, Leibinger, Muller et al. 2009, Kurimoto, Yin et al. 2013). Activated astrocytes secrete ciliary neurotrophic factor (CNTF), which binds a receptor complex formed by the CNTF receptor α (CNTFR α), Lif receptor (LifR) and glycoprotein 130 (gp130) expressed on RGCs to elicit activation of the JAK/STAT3 pathway, enabling axon regeneration (Muller, Hauk et al. 2007, Leibinger, Muller et al. 2009). Activated neutrophils and macrophages secrete oncomodulin that also signals through an RGC-expressed cell surface receptor to promote a survival and regenerative response, however the exact identity has yet to be identified (Yin, Cui et al. 2009, Kurimoto, Yin et al. 2013). While such efforts appear promising for CNS injury, manipulating inflammation post-injury can be a double-edged sword as uncontrolled processes can lead to increased degeneration. *In vitro* DRG cultures treated with zymosan-activated macrophages (ZAM) conditioned media displayed 60% cell loss as early as 48h (Gensel, Nakamura et al.

2009). Experiments with mouse spinal cord similarly showed that while ZAMs promoted significant outgrowth of DRGs, there was a concurrent neurotoxic effect leading to 33% loss of cells at 72h (Gensel, Nakamura et al. 2009). This demonstrates a narrow window for advantageous stimulation of inflammatory processes, thus rendering potential therapeutic options unsafe. Investigations into mechanisms underlying inflammation-mediated regeneration can reveal therapies that may bypass inflammatory stimulation to directly target the effective regenerative pathways. miR-383-5p loss-of-function was able to promote regeneration following ONC, phenocopying the effects of zymosan and LI without necessitating inflammation. This was mediated through the relief of multiple miR-383-5p targets, and thus multiple pathways. In turn, demonstrating a distributed inhibitory role by miR-383-5p that can be relieved to promote regeneration through miR-383-5p inhibition.

5.3 Results

5.3.1 miR-383-5p is downregulated in growth-permissive conditions and upregulated in growth-inhibitory conditions- To identify miRNA that may affect axon regeneration in the CNS, we profiled the neuronal expression of candidate miRNAs under several conditions that promote or inhibit neurite outgrowth. We first assessed miRNA expression in cortical neurons treated with outgrowth promoting Astrocyte Conditioned Media (ACM) and outgrowth inhibiting Peripheral Blood Mononuclear Cell Conditioned Media (PBMC-CM). Candidate miRNAs were selected based on their differential expression in DRG neurons following a conditioning sciatic nerve lesion (Strickland, Richards et al. 2011). E16 mouse cortical neurons were treated with ACM for 24h. Expression of candidate miRNA in ACM-treated neurons was evaluated by semi-quantitative RT-PCR and validated by qPCR (Supplementary Tables 1,2). miR-383-5p was the only miRNA regulated by treatment ACM exhibiting a 20% decrease in expression levels compared to neurons treated with control media (Supplementary Fig.1, Fig.1c). miR-383-5p was also identified as the most downregulated miRNA in DRG neurons subjected to a conditioning lesion that triggers a pro-regenerative response in neurons (Strickland, Richards et al. 2011). Next, we asked if miR-383-5p expression is inversely regulated in a growth-inhibitory environment. Conditioned media from PBMCs, which consist of lymphocytes and myeloid-lineage cells such as macrophages, inhibit neurite outgrowth (Pool, Rambaldi et al. 2011, Pool, Rambaldi et al. 2012). Mouse cortical neurons treated with PBMC-CM for 48h exhibited a 50% decrease in neurite outgrowth compared to those treated with control media (Fig.1c, d). miR-383-5p was significantly upregulated by 70% in PBMC-CM-treated neurons compared to those treated with control media (Supplementary Fig.1; Fig.1f). These results demonstrate that miR-383-5p expression inversely correlates with cortical neurite outgrowth.

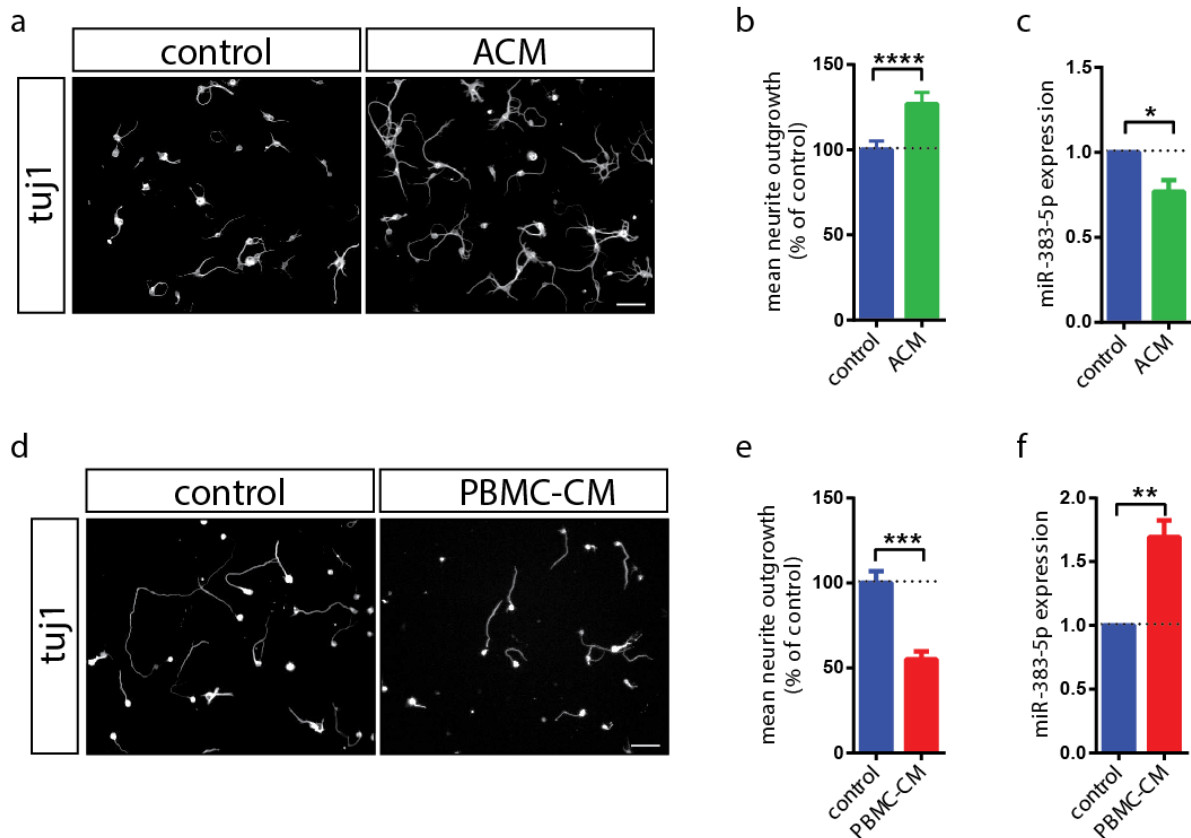


Figure 1. miR-383-5p is inversely regulated to neurite outgrowth. (a) β III-tubulin-stained mouse cortical neurons treated with ACM or control media for 24h, (b) quantified mean neurite outgrowth (n=10). (c) qPCR expression of miR-383-5p in neurons treated with ACM or control media (n=6). (d) β III-tubulin-stained mouse cortical neurons treated with PBMC-CM or control media for 48h, (e) quantified mean neurite outgrowth (n=4-8). (f) qPCR expression of miR-383-5p in neurons treated with PBMC-CM or control media (n=5). qPCR data is represented as fold change. All statistics are two-tailed student's t-tests. Scale bar 100 μ m.

To determine if miR-383-5p expression was also regulated in an outgrowth-dependent manner in other types of neurons, we evaluated its expression in Retinal Ganglion Cells (RGCs) subjected to zymosan-dependent intraocular inflammation. Previous studies have demonstrated that a single injection of zymosan into the eye leads to robust inflammation, and RGC survival and regeneration following ONC (Hauk, Muller et al. 2008). Zymosan or PBS were injected into one eye of C57Bl/6 mice following ONC at 3 dpi (Fig. 2a), animals were sacrificed, and the RGC layer was isolated from retinal sections by laser capture microdissection (Fig. 2b). Consistent with the pro-growth state of zymosan treated RGCs, miR-383-5p was downregulated in the RGC layer of zymosan-injected eyes relative to PBS-injected controls (Fig.2c). Together, this data describes significant downregulation of miR-383-5p in three different neuronal growth-promoting paradigms: DRG neurons following a sciatic nerve lesion, mouse cortical neurons stimulated with ACM (Supplementary Fig.1, Fig.1c), and in the RGC layer of zymosan-injected eyes (Fig.2c) (Strickland, Richards et al. 2011).

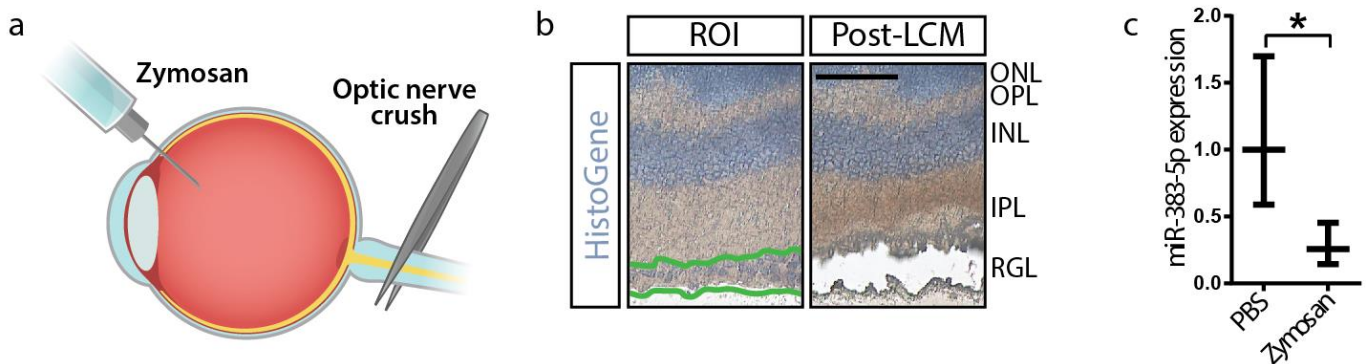


Figure 2. miR-383-5p is downregulated in retinal neurons in a model of CNS regeneration. (a) Schematic of optic nerve crush model depicting intravitreal injection of zymosan or PBS vehicle control at the time of crush injury. (b) Representative retinal sections stained with HistoGene for LCM (ROI = region of interest, RGL= RGC layer, IPL = inner plexiform layer, INL = inner nuclear layer, OPL = outer plexiform layer, ONL = outer nuclear layer), scale bar 50 μ m. (c) qPCR expression of miR-383-5p in the RGC layer at 3 dpi (n=3, two-tailed student's t-test). qPCR data is represented as fold change range.

5.4.2 miR-383-5p downregulation is sufficient to promote axon growth *in vitro*- We next asked if regulating the expression of miR-383-5p would be sufficient to regulate neuronal outgrowth. Mouse cortical neurons were treated with a locked nucleic acid targeting miR-383-5p (LNA-383) to sequester endogenous miR-383-5p or a miR-383-5p mimic (M383). E16 cortical neurons were seeded at a low-density and treated with LNA-383 or non-targeting LNA control (LNA-NT) at 2h post-dissection where the LNA was taken up by gymnosis, independent of Lipofectamine RNAi Max. Neurons were fixed 4 DIV later. Treatment of cortical neurons with LNA-383 resulted in a dose-dependent increase in neurite outgrowth compared to LNA-NT, demonstrating that its loss-of-function is sufficient to promote neurite growth (Fig. 3a, b). For overexpression experiments, neurons were transfected at 1 DIV with miR-383 mimic (M383) or negative control mimic (NC), trypsinized and re-seeded at 4 DIV (72h later) to mediate miR-383-5p overexpression and retraction of neurites, then fixed 24h later to study new neurite growth. Introduction of M383 resulted in robust overexpression of the mimic; however, this was not sufficient to significantly inhibit neurite outgrowth (Supplementary Fig. 2a; Fig. 3). However, neurons overexpressing M383 were resistant to the outgrowth-promoting activity of ACM (Fig. 3c,d), indicating that downregulation of miR-383-5p is required for its outgrowth-promoting effects of ACM.

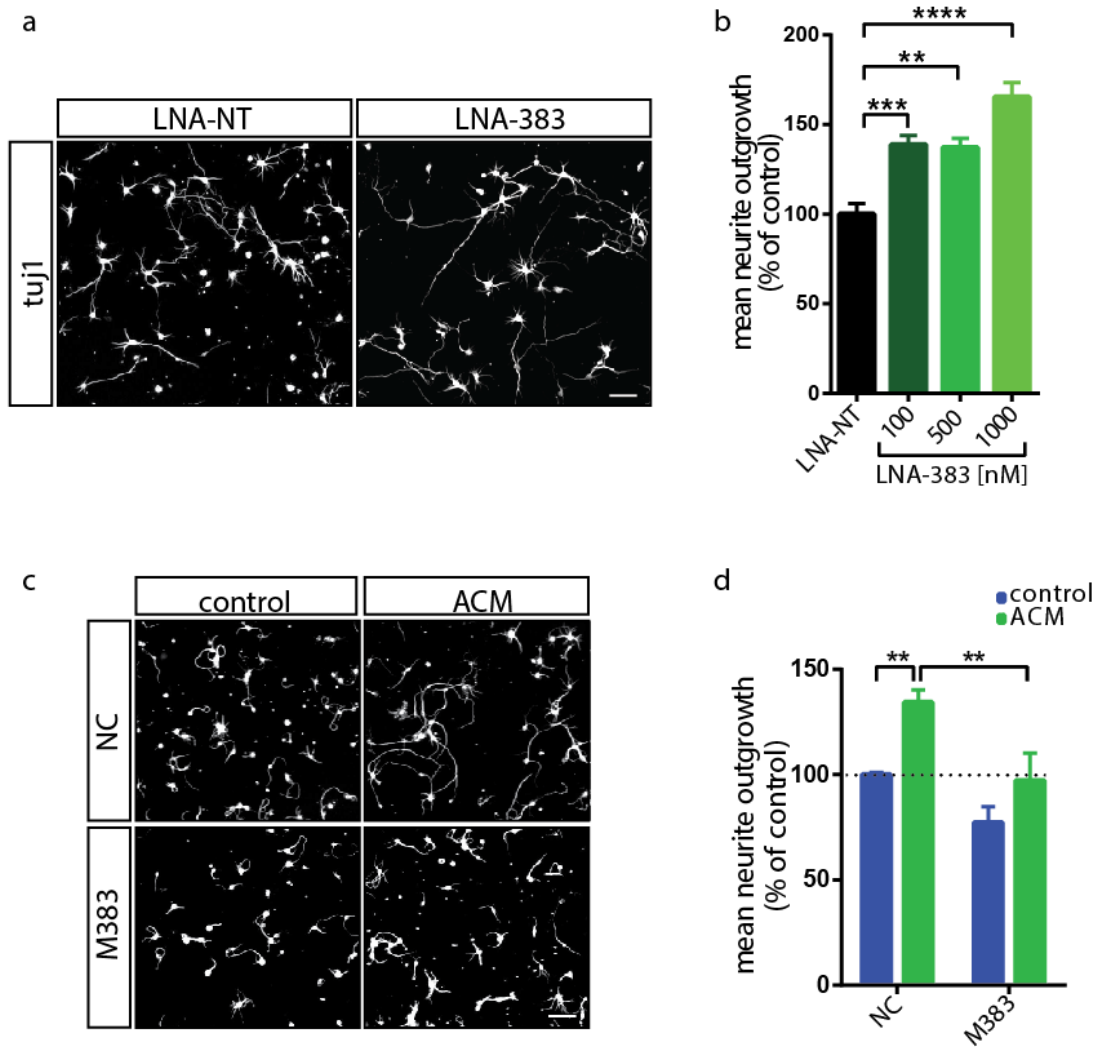


Figure 3. miR-383-5p negatively regulates neurite outgrowth. (a) β III-tubulin-stained mouse cortical neurons treated with LNA-383 or LNA-NT at 1000 nM for 4 DIV, taken up by gymnosy; (b) quantified mean neurite outgrowth for increasing LNA doses ($n=4-5$, one-way ANOVA, $p<0.05$, Dunnett's multiple comparisons test). (c) β III-tubulin-stained mouse cortical neurons transfected with M383 and NC at 1 DIV, reseeded 72h later, and treated with ACM and control media for 24h, (d) quantified mean neurite outgrowth ($n=5-8$, two-way ANOVA, $p<0.05$, Tukey's multiple comparisons test). Scale bar 100 μ m.

5.3.3 Inhibition of miR-383-5p promotes RGC axon regeneration following ONC-

Having demonstrated that miR-383-5p loss-of-function was sufficient to promote outgrowth of cortical neurons, we asked if miR-383-5p loss-of-function would be sufficient to promote regeneration of RGCs following optic nerve crush (ONC). Fluorescently labeled LNA-383 (FAM) was injected intravitreally to uninjured nerves to confirm successful uptake by RGCs (Fig. 4a). We then injected un-labeled LNA-383 or LNA-NT at the time of ONC and 7 days later (Fig. 4b). Cholera toxin Beta (Ctb), an anterograde tracer, was injected 2 days prior to sacrifice to label regenerating axons and optic nerve regeneration was assessed at 14 dpi in optic nerves that were whole mounted, cleared, and imaged using Lavisision light sheet microscope (Fig.4c). 3-dimensional (3D) whole mounts were opened with ImageJ/FIJI to quantify Ctb-positive axons. Quantification of axons projecting past the lesion site revealed that LNA-383 significantly promoted axon regeneration compared to LNA-NT with an average of approximately 20 regenerating axon fibers at 1000 μm past the injury site and with some regenerating fibres as far as 2000 μm (Fig.4c, d). LNA-NT injected eyes also showed some axon fibres at 1000 μm , with a mean of 5 fibers per nerve (Fig.4d). This is likely due to repeated intraocular injections.

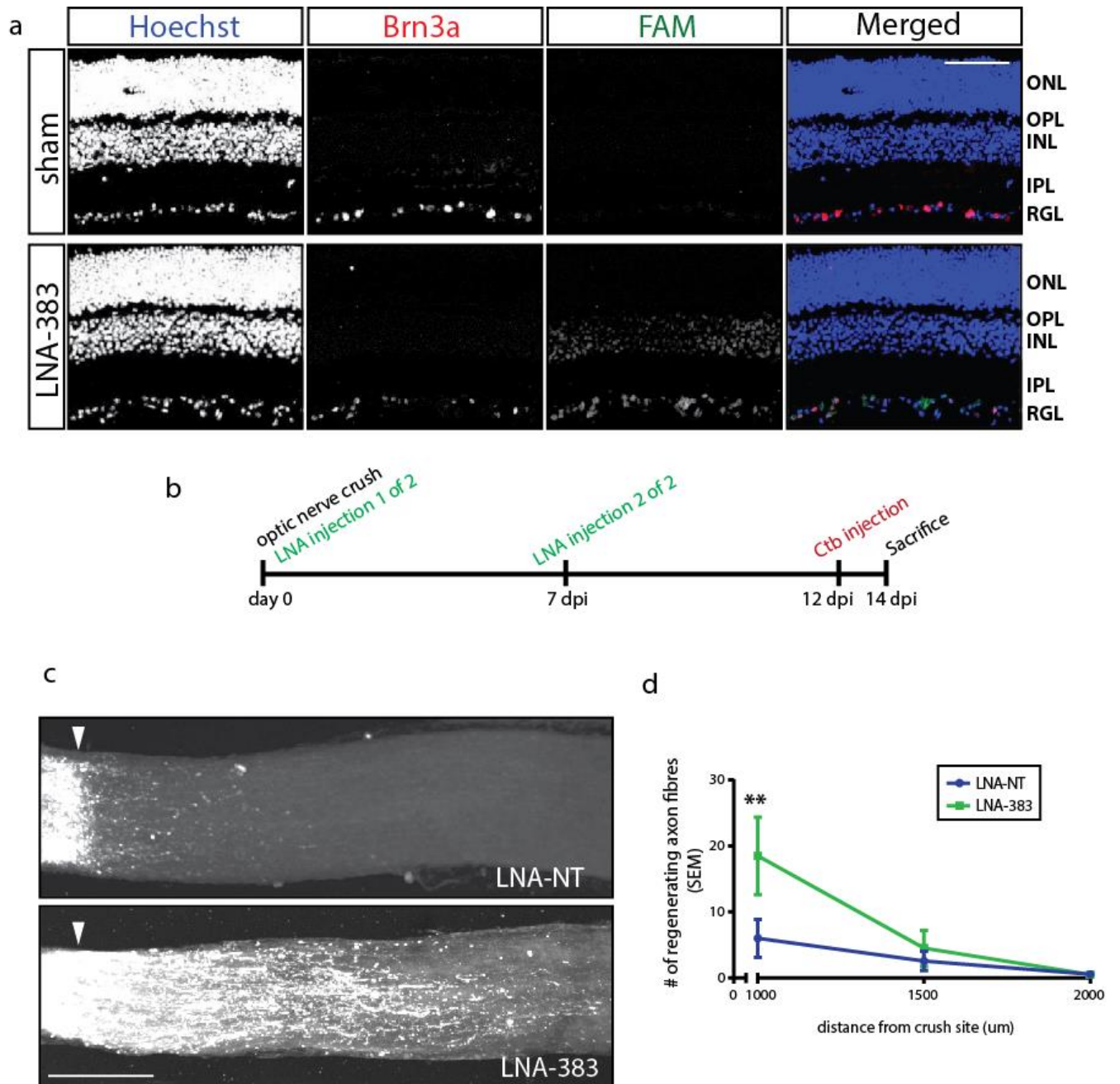


Figure 4. Inhibition of miR-383-5p significantly promotes optic nerve regeneration following ONC.

(a) Retinal sections of sham-injected and fluorescently-labeled LNA-383 (FAM) injected eyes 3 days post-injection in the eyes of uninjured optic nerves. Scale bar 50 μm . (b) Timeline of injections following ONC, where LNA was injected at 0 and 7 dpi at 1.5 nmol/2 μL , and Ctb was injected at 12 dpi. Mice were sacrificed at 14 dpi. (c) Maximal projection of z-stacks for whole mount imaged optic nerves at 14 dpi, cleared and regenerating fibers visualized by Ctb. Arrowheads mark crush site. Scale bar 300 μm (d) Quantified regeneration (n=4-7, two-way ANOVA, $p < 0.05$ Sidak's multiple comparisons test).

5.3.4 miR-383-5p is regulated by CNTF- A previous study has demonstrated that intraocular inflammation stimulates axon regeneration through the release of astrocyte-derived CNTF (Muller, Hauk et al. 2007). To begin to delve into the molecular mechanisms that regulate miR-383-5p expression, we assessed if CNTF could directly regulate miR-383-5p expression. Mouse cortical neurons treated with CNTF for 8 DIV exhibited a significant dose-dependent decrease in expression levels to approximately 50% of baseline expression (Fig.5a). This suggests miR-383-5p downregulation is a novel component of the inflammatory CNTF-dependent regeneration axis.

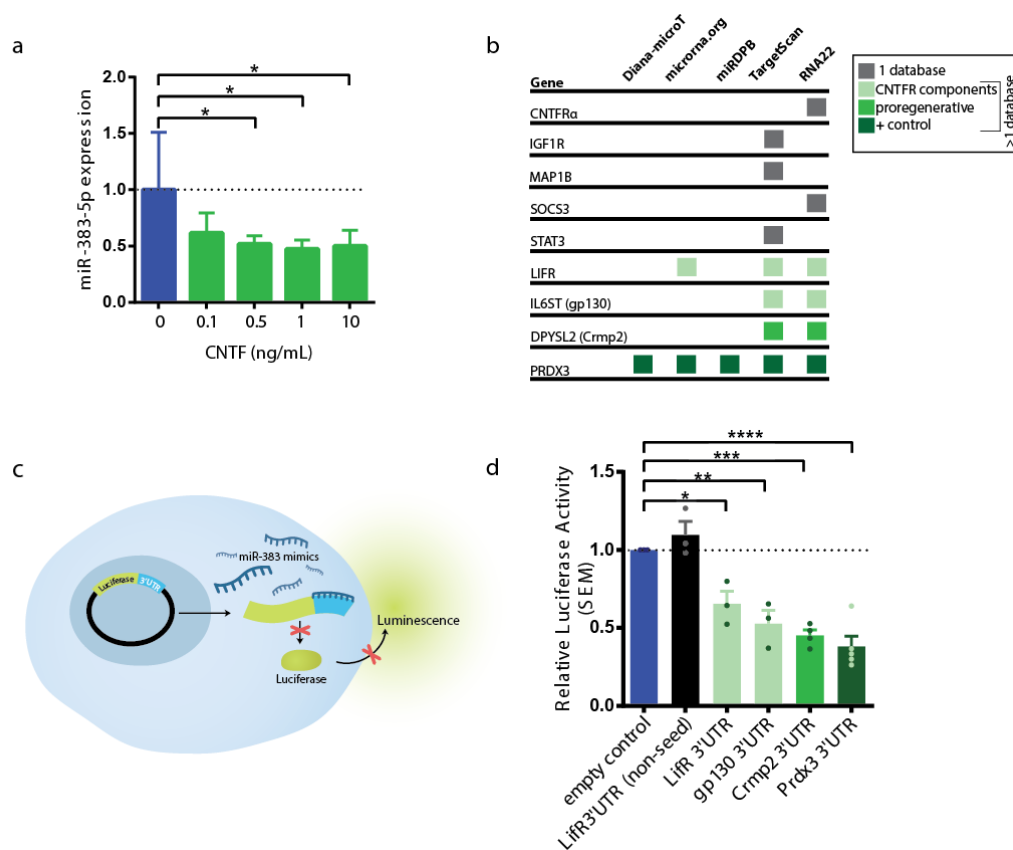


Figure 5. miR-383-5p is regulated by CNTF and regulates multiples cues promoting axon regeneration. (a) miR-383-5p expression in mouse cortical neurons treated with increasing dosages of CNTF for 8 DIV (n=3). (b) Genes promoting axon regeneration following ONC that are targeted by miR-383-5p, and their respective prediction databases. Legend: gray square are genes identified by a single database predicting miR-383-5p targets; all green shaded squares represent targets predicted by two or more databases, where light green is CNTF receptor components, medium green is other pro-regeneration genes, and dark green is a positive control. (c) Schematic depicting a Luciferase Assay where the 3'UTR of predicted gene targets flanks the luciferase gene. Targets regulated by M383 show decreased luminescence owing to decreased translation of the luciferase mRNA. (d) Luciferase Assay of HEK293 cells co-transfected with M383 and luciferase vectors with 3'UTR predicted targets (n=3-5, one-way ANOVA, $p < 0.05$ Dunnett's multiple comparisons test).

5.3.5 miR-383-5p targets multiple genes contributing to axon regeneration-

To further elucidate how miR-383-5p downregulation may act to promote axon regeneration, we performed an *in silico* analysis to predict mRNA targets of miR-383-5p using the following databases: Diana-microT (Reczko, Maragkakis et al. 2012, Paraskevopoulou, Georgakilas et al. 2013), microRNA.org (Betel, Wilson et al. 2008), miRDP (Wong and Wang 2015), miRTarBase (Chou, Chang et al. 2016), RNA22 (Miranda, Huynh et al. 2006), TargetScan (Agarwal, Bell et al. 2015), and TarBase (Vlachos, Paraskevopoulou et al. 2015). We cross-referenced predicted targets to a list of candidate genes previously identified to play a role in optic nerve regeneration (Fig. 5b) Intriguingly, CNTF receptor components LifR and gp130 were identified as putative miR-383-5p targets in at least 2 databases (Fig. 5b). This raised the interesting possibility that CNTF-dependent downregulation of miR-383-5p may enhance expression of CNTF receptor components to further sensitize cells to the pro-regenerative activity of CNTF. We tested if LifR and gp130 are bona fide targets of miR-383-5p using Luciferase reporter assays. HEK293 cells were co-transfected with M383 and a vector containing the luciferase gene flanked by the target 3'UTR or empty flanking control for 24h (Fig. 5c). M383 significantly suppressed luciferase gene expression when regulated by the 3'UTR of LifR or gp130 (Fig.5d). As a negative control, we demonstrated that a region of the LifR 3'UTR lacking the complementary miR-383-5p seed sequence was insensitive to the effect of M383 (Fig. 5d). *In silico* analysis of predicted miR-383-5p targets also identified microtubule associated protein CRMP2 and the anti-oxidant protein Prdx3 as putative targets of miR-383-5p in at least 2 databases (Fig. 5b). Crmp2, or collapsin response mediator protein 2, is an actin and microtubule-associated protein that promotes axon development and elongation (Fukata, Itoh et al. 2002, Tan, Cha et al. 2015). Following ONC, Crmp2 overexpression attenuates axonal degeneration; and phosphorylation or cleavage of Crmp2, blocking Crmp2 microtubule-affinity, limits neurite growth (Wilson, Moutal et al. 2014, Zhang, Michel et al. 2016, Leibinger, Andreadaki et al. 2017). Luminescence was reduced by 50% for the 3'UTR of Crmp2 in M383-transfected HEK293 cells relative to empty control vector (Fig.5d). Prdx3 is an anti-oxidant protein expressed exclusively in the mitochondrial matrix (Chidlow, Wood et al. 2016). Prdx3 has been previously validated as a miR-383-5p target by both Luciferase reporter assay and Western blot (Li,

Pang et al. 2013). As a positive control we assessed the ability of miR-383-5p to suppress Prdx3 expression. Prdx3 3'UTR luminescence was the most strongly decreased by 60% relative to empty control vector (Fig.5d). Together, these results suggest that miR-383-5p functions in a CNTF-dependent positive feedback loop to enhance neuronal sensitivity to CNTF by regulating expression of CNTF receptors, while also affecting expression of antioxidant and cytoskeletal regulatory proteins that may impact axon regeneration.

5.3.6 Crmp2 and Prdx3 regulates neurite outgrowth *in vitro*- As miR-383-5p overexpression blocked ACM-growth promotion *in vitro*, we sought to determine if miR-383-5p overexpression downregulated Crmp2 and Prdx3 expression. Mouse cortical neurons at 1 DIV were transfected with M383 or NC for 72h. M383-transfected neurons significantly decreased both Crmp2 and Prdx3 expression by approximately 50% relative to NC-transfected neurons (Fig. 6).

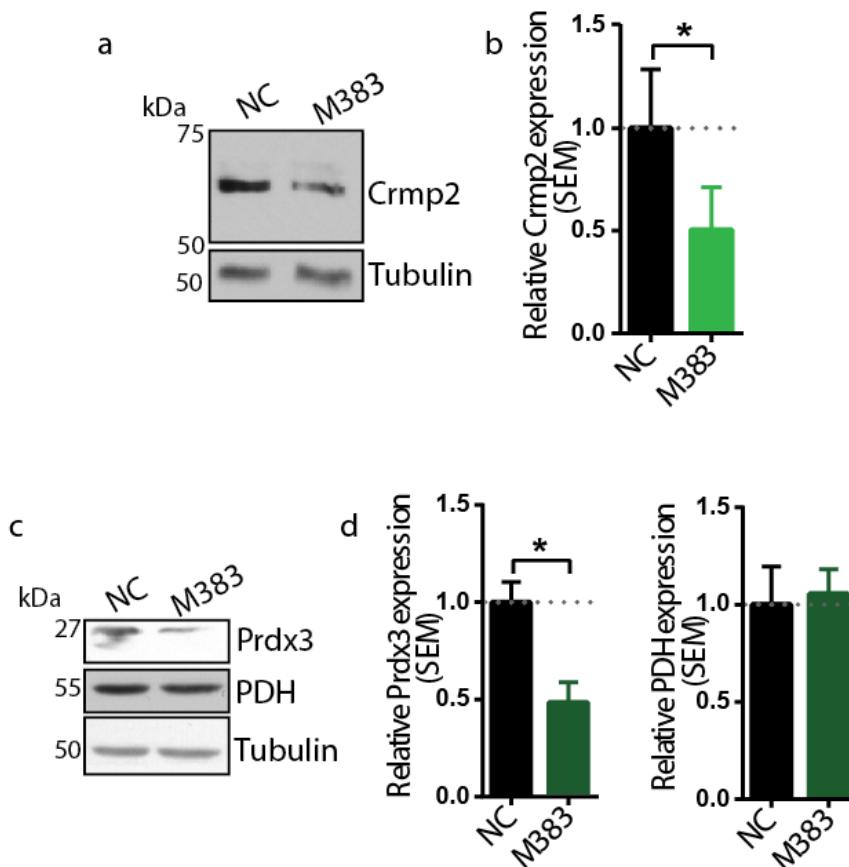


Figure 6. miR-383-5p overexpression downregulates targets Crmp2 and Prdx3 in mouse cortical neurons. Mouse cortical neurons transfected with 20 nM negative control mimic (NC) or miR-383-5p mimic (M383) at 1 DIV for 72h. (a,b,) Western blot for Crmp2 expression (n=6), and (c,d) Prdx3 expression, with mitochondrial marker PDH (n=4-5). Two-tailed student's t-test.

Next, we asked if miR-383-5p loss-of-function growth-promotion was dependent on Crmp2 and Prdx3. Mouse cortical neurons were transfected with siRNA targeting either Crmp2, Prdx3, or negative control siRNA (siCrmp2, siPrdx3, siNC), as validated by Western blot (Fig. 7a). 72h-post siRNA transfection, neurons were reseeded to retract all neuronal processes, transfected with LNA-383 or LNA-NT, and neurite outgrowth assessed 48h later. LNA-383 with siNC-primed neurons significantly promoted neurite outgrowth by approximately 30% compared to LNA-NT transfected neurons (Fig. 7b, c). Both siCrmp2- and siPrdx3-primed neurons were insensitive to LNA-383 and did not show neurite outgrowth promotion. These results demonstrate that LNA-383 outgrowth promotion is mediated through Crmp2 and Prdx3 expression.

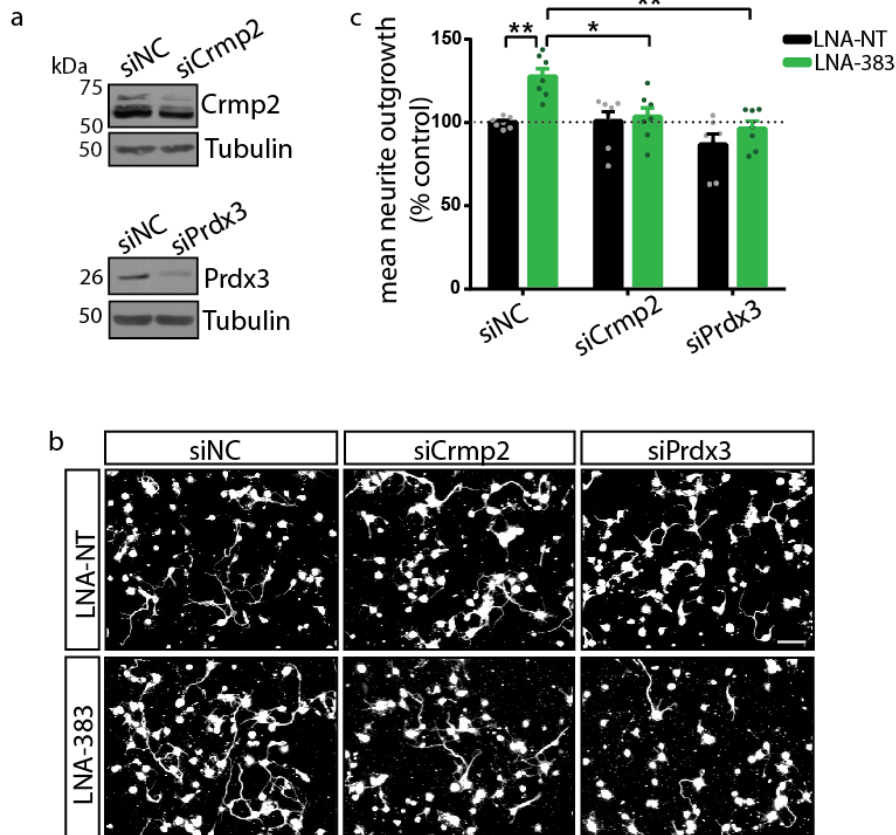


Figure 7. Crmp2 or Prdx3 knockdown prevents LNA-383 induced neurite outgrowth promotion. (a) Western blot of mouse cortical neurons transfected with 15 nM of siRNA targeting Crmp2 (siCrmp2), Prdx3 (siPrdx3), or negative control (siNC) at 1 DIV for 72h. (b) siRNA transfected with siRNA at 1 DIV, reseeded 72h later to retract all neuronal processes, and transfected with 15 nM LNA-NT or LNA-383 for 48h. Scale bar 100 μ m. (c) Quantified neurite outgrowth relative siNC reseeded neurons transfected with LNA-NT (n=7, two-way ANOVA, p<0.05, Sidak's multiple comparisons test).

5.3.8 Crmp2 and Prdx3 are upregulated in retinal neurons following zymosan-primed ONC- As astrocytic CNTF signaling through the CNTF receptor complex promotes axon regeneration in zymosan-injected eyes following ONC, we asked if Crmp2 and Prdx3 are also regulated in the same model (Muller, Hauk et al. 2007, Leibinger, Muller et al. 2009). We looked at Crmp2 and Prdx3 expression by immunohistochemistry in retinal sections from mice at 3 dpi following ONC with intravitreal injection of zymosan or PBS. Retinal sections were stained with RGC marker Brn3a, Crmp2 or Prdx3, and cell nuclei marker Hoechst (Fig.8). Fluorescence intensity was assessed for all Brn3a-positive cells. Mean Crmp2 fluorescence intensity increased by approximately 90% in zymosan-injected eyes relative to PBS-injected eyes, and Prdx3 fluorescence intensity increased by approximately 40%. Thus, Crmp2 and Prdx3 were inversely regulated with miR-383-5p, suggesting they play a role during zymosan-driven axon regeneration.

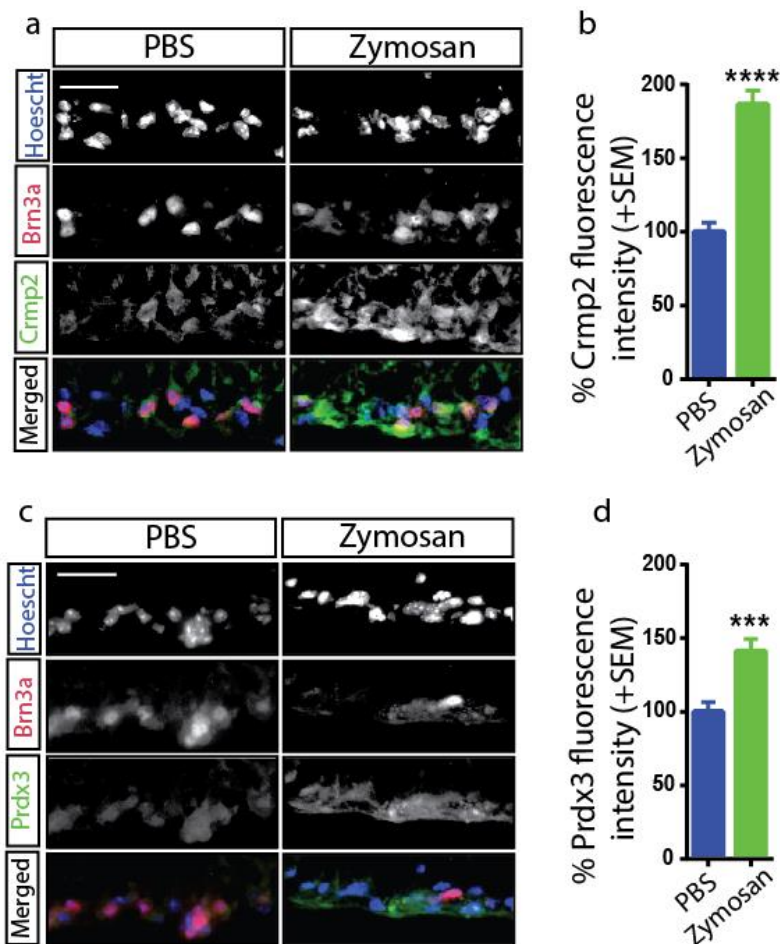


Figure 8. Crmp2 and Prdx3 are upregulated in retinal neurons of zymosan-injected eyes post-ONC. RGC layer of mice intravitreally injected with zymosan or PBS following ONC at 3 dpi, with inner plexiform layer (IPL) oriented above the RGC layer. (a) Crmp2 staining (green) with retinal neuron marker Brn3a (red) and nuclei marker Hoescht (blue), with (b) quantified fluorescence intensity of Crmp2 in Brn3a-positive cells (n=200-206 for Brn3a-positive cells per condition, from 3 independent mice). (c) Prdx3 staining (green) with retinal neuron marker Brn3a and nuclei marker Hoescht, with (d) quantified fluorescence intensity of Prdx3 in Brn3a-positive cells (n=186 for Brn3a-positive cells per condition, from 3-4 independent mice). Two-tailed student's t-test. Scale bar is 25 μ m.

5.4 Discussion

There is limited neuronal survival and axon regeneration in the adult mammalian CNS following injury due to decreased neuro-intrinsic repair abilities, and increased sensitivity to extrinsic inhibitory cues (Cai, Qiu et al. 2001, Fournier, GrandPre et al. 2001, Bradbury, Moon et al. 2002, Park, Liu et al. 2008, Qin, Zou et al. 2013). Intravitreal injection of zymosan or LI can overcome these intrinsic and extrinsic barriers to regeneration in the CNS (Leon, Yin et al. 2000). Zymosan alone is not ideal for therapy as it also mediates a cytotoxic response. Microinjections of zymosan into intact corpus callosum or spinal cord promote lesion formation, characterized by phagocytosing macrophages, demyelination, and axonal loss (Fitch, Doller et al. 1999, Popovich, Guan et al. 2002). Investigations into mechanisms underlying these inflammation-mediated regeneration models could reveal therapies that may bypass inflammatory stimulation and directly target the effective regenerative pathways. Using the zymosan model to study mechanisms of regeneration, we identified that miR-383-5p loss-of-function phenocopies the regenerative effects of zymosan by a distributed effect without promoting inflammation. As summarized in Figure 9, during regeneration in the optic nerve, retinal CNTF expression limits miR-383-5p expression, releasing its hold on multiple regeneration-promoting targets that are CNTF receptor components LifR and gp130; microtubule-stabilizing Crmp2; and mitochondrial antioxidant Prdx3. We propose that these targets are part of three unique pathways through which miR-383-5p loss-of-function promotes regeneration following axotomy.

The first pathway is a feedforward loop with retinal CNTF and the CNTF receptor complex expressed on RGCs. miRNA-mediated feedback or feedforward loops are common network motifs in mammals (Tsang, Zhu et al. 2007). In this feedforward loop, CNTF-mediated repression of miR-383-5p further enhances signaling through LifR/gp130 by preventing miR-383-5p mediated inhibition of LifR/gp130, in turn promoting activation of JAK/STAT3 regenerative signaling (Muller, Hauk et al. 2007, Leibinger, Muller et al. 2009). For CNTF to elicit a cellular response, it first binds to its high affinity receptor CNTFR α and then recruits LifR and gp130 (Heinrich, Behrmann et al. 2003, Leibinger, Andreadaki et al. 2016). During axotomy, miR-383-5p is likely disrupting assembly of the

CNTF receptor complex formed by CNTFR α and a LifR/gp130 heterodimer. In addition to CNTF, inflammation-activated astrocytes also secrete LIF and interleukin-6 (IL-6) (Muller, Hauk et al. 2007, Leibinger, Muller et al. 2009, Leibinger, Andreadaki et al. 2016). LIF signals through a LifR/gp130 heterodimer, and IL-6 through the IL-6 receptor partnered with a gp130 homodimer, both of which contribute to inflammation-mediated regeneration (Leibinger, Muller et al. 2009, Leibinger, Andreadaki et al. 2016). miR-383-5p is likely also disrupting LIF and IL-6 mediated signaling by targeting LifR and gp130. Thus miR-383-5p loss-of-function promotes JAK/STAT3 regenerative signaling via enhanced expression LifR and gp130.

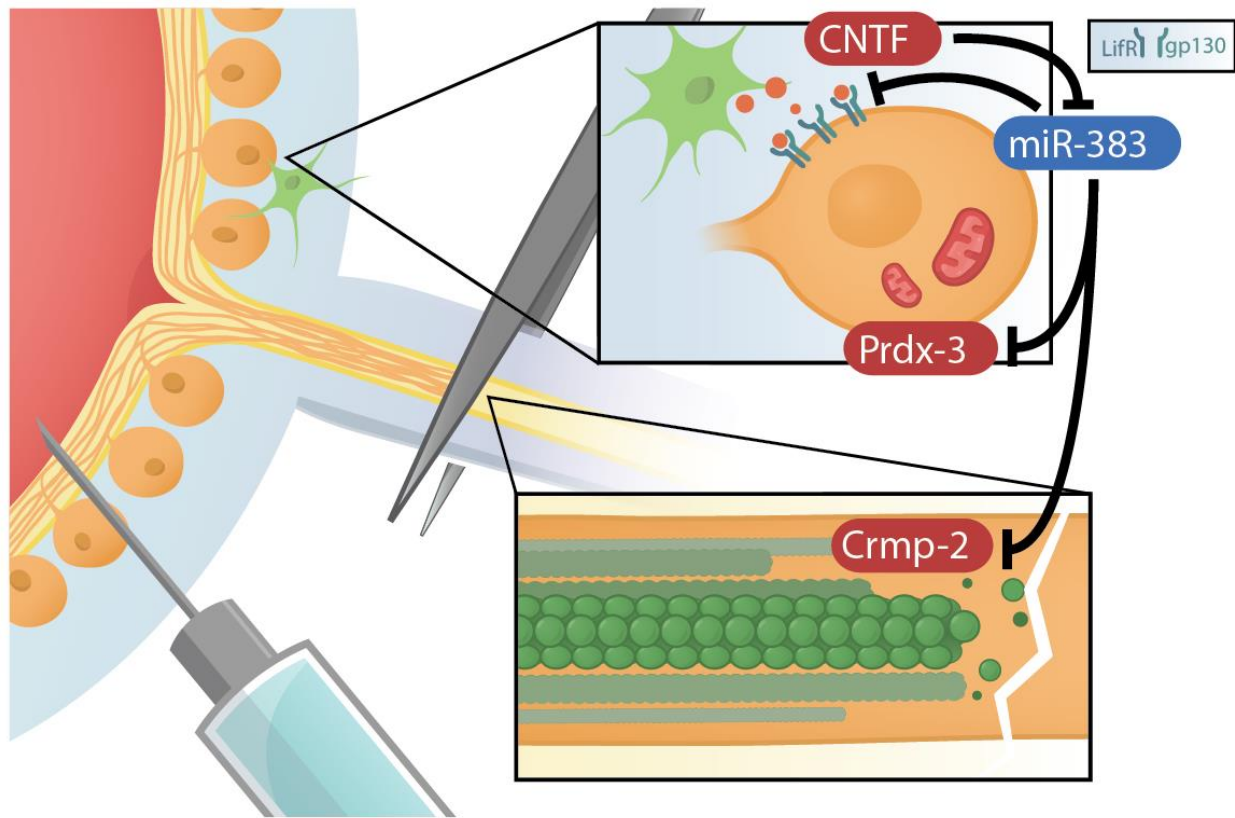


Figure 9. Inhibition of miR-383-5p promotes axon regeneration following injury through a distributed relief of regenerative and growth associated mRNA targets. Injection of zymosan following ONC stimulates astrocytic release of CNTF. CNTF in turn downregulates miR-383-5p, releasing its break on CNTF receptor components LifR and gp130, microtubule-stabilizing Crmp2, and mitochondrial-antioxidant Prdx3. Inhibition of miR-383-5p relieves multiple pro-regenerative and pro-survival pathway components to elicit a distributed axon regenerative response following injury.

Next, miR-383-5p loss-of-function contributes to microtubule-stabilization via Crmp2, where disrupted microtubules are a hallmark of CNS axotomy (Erturk, Hellal et al. 2007). We demonstrated *in vitro* that Crmp2 mediated neurite outgrowth downstream of miR-383-5p antagonism through the abolishment of LNA-383-growth-promotion by siCrmp2 (Fig.8). We also demonstrated an upregulation of retinal Crmp2 in both zymosan-injected eyes following axotomy (Fig.6), suggesting Crmp2 contributes to axon regeneration by promoting microtubule polymerization and thus axonal extension. Limiting phosphorylation of Crmp2, where phosphorylated Crmp2 loses its affinity for cytoskeleton proteins, promotes enhanced growth of motor neurons following spinal cord injury through microtubule stabilization (Nagai, Owada et al. 2016). Crmp2 also contributes to the transport of essential retrograde cargo along stabilized microtubules, as Crmp2 interacts with motor proteins kinesin-1 and dynein (Kimura, Watanabe et al. 2005, Arimura, Hattori et al. 2009). In support of this, Crmp2 overexpression attenuates axonal degeneration by maintaining axonal mitochondrial transport in a model of ONC (Zhang, Michel et al. 2016). High axonal transport of mitochondria is characteristic of regenerating axons (Cartoni, Pekkurnaz et al. 2017). Thus, miR-383-5p loss-of-function permits Crmp2-mediated microtubule stabilization to aid in regeneration.

Lastly, miR-383-5p loss-of-function limits oxidative stress through increased Prdx3 expression. Peroxiredoxins (Prdx) are a family of antioxidant enzymes with a major cellular peroxide-removal mechanism that is crucial to limiting oxidative stress (Chidlow, Wood et al. 2016). Prdx3 of the Prdx family is specifically localized to the mitochondrial matrix where it is regarded as the most important enzyme in eliminating mitochondrial H₂O₂; in turn, Prdx3 is expressed most highly in mitochondria rich-areas, such as the retina and optic nerve head (De Simoni, Goemaere et al. 2008, Kil, Lee et al. 2012, Chidlow, Wood et al. 2016). Thus, Prdx3 is also crucial for proper mitochondrial homeostasis (Wonsey, Zeller et al. 2002, Liu, Hu et al. 2016, Wu, Menon et al. 2016). In rodent models of hippocampal excitotoxicity, traumatic brain injury (TBI), and cerebral ischemia, Prdx3 overexpression protected against neuronal damage by limiting both oxidative stress and preserving mitochondrial function (Hattori, Murayama et al. 2003, Hwang, Yoo et al. 2010, Hu, Dang et al. 2018). As discussed earlier, high axonal transport of mitochondria is necessary for regenerating axons (Cartoni, Pekkurnaz et al. 2017).

Maintenance of mitochondrial integrity and limiting oxidative stress by promoting Prdx3 expression is thus the third potential pathway through which miR-383-5p loss-of-function promotes regeneration and survival.

For our future directions, we hope to further enhance regeneration during miR-383-5p loss-of-function by administering an adeno-associated virus 2 (AAV2) containing a sponge sequence that sequesters miR-383-5p. AAV2-mediated infection will also overcome repeated injections and target neuronal cells exclusively, as AAV2 preferentially infects RGCs and produces long-term transgene expression following intravitreal injection (Cheng, Sapieha et al. 2002). The miR-383-sponge contains four tandem repeat sequences complementary to mmu-miR-383-5p (Supplementary Fig.3), and has been validated by Luciferase assay (Supplementary Fig.2b). Briefly, HEK293 cells were co-transfected with M383, miR-383-sponge or control sponge, and luciferase reporters containing Prdx3 3'UTR or control 3'UTR. miR-383-sponge completely relieved M383-induced repression of Prdx3 3'UTR (Supplementary Fig.2b). The validated miR-383-sponge was cloned into an AAV2 vector, and AAV2-miR-383-sponge was injected 4 weeks prior to ONC to allow for miR-383-sponge expression (Cheng, Sapieha et al. 2002). We will perform ONC next and assess expression of validated miR-383-5p targets Lifr, gp130, Crmp2, and Prdx3 in the retinal neurons of AAV2-injected eyes 2 weeks post-injury. We anticipate robust axon regeneration from AAV2-miR-383-sponge injected eyes based on our *in vivo* results with LNA-383, with increased expression of the aforementioned targets.

Thus, through miR-383-5p loss-of-function, we can promote axon regeneration by releasing the brake on multiple regenerative signaling pathways by increased expression of the targets LifR, gp130, Crmp2, and Prdx3. As miRNAs are promiscuous, this does not rule out additional targets which show relieved expression following miR-383-5p loss-of-function during axon regeneration. miR-383-5p is a worthwhile target for future disease-modifying therapies and demonstrates the relevance of miRNA signaling on multiple signaling pathways during CNS disease and injury.

5.5 Acknowledgments

A.E.F. is funded by the Canadian Institutes for Health Research and the Multiple Sclerosis Society of Canada (MSSOC). C.A.J. supported by a fellowship from the Montreal Neurological Institute, MSSOC, and a Vanier Canada Graduate Scholarship. B.M. is funded by MSSOC and Fonds de recherche du Québec. Y.Z. is funded by a MSSOC Master's studentship. We thank Dylan Galloway for providing us with additional ACM; and Drs. Samuel David, Timothy Kennedy, Larry Benowitz, and Heidi McBride for their valuable discussions. We would also like to emphasize our gratitude to Dr. Heidi McBride for providing us with an excellent Prdx3 antibody.

5.6 Competing Financial Interests

Dr. Bar-Or has participated as a speaker in meetings sponsored by and received consulting fees and/or grant support from: Atara Biotherapeutics, Biogen Idec, Celgene/Receptos, Genentech/Roche, GlaxoSmithKline, MAPI, Medimmune, Merck/EMD Serono, Novartis, Sanofi-Genzyme.

5.7 Materials and Methods

5.7.1 Preparation of conditioned media- Human primary astrocytes were derived from human fetal cortex material, gestational age 10–20 weeks, as previously described (Galloway, Williams et al. 2017). Cells were plated in tissue culture flasks in DMEM (Gibco) containing 5% fetal bovine serum (FBS), 1% penicillin/streptomycin and 1% L-glutamine at 37°C, 5% CO₂, and passaged every 7–14 days or until confluent. At passage 4 or 5, astrocytes were culture in Ultraculture serum-free medium (Lonza) containing 1% penicillin-streptomycin, and astrocyte conditioned media (ACM) was collected 24h later. Control media was medium alone.

Blood from adult Sprague-Dawley rats was collected by cardiac puncture. Rat PBMCs were separated by Ficoll-Paque density centrifugation and cultured in Ultraculture serum-free medium containing 1% penicillin-streptomycin for 4 days in vitro (DIV) at 37°C, 5% CO₂ (Pool, Rambaldi et al. 2011, Pool, Rambaldi et al. 2012). Control media was medium alone. All animals were approved by the Montreal Neurological Institute Animal Care and Use Committee, following the Canadian Council on Animal Care (CCAC) guidelines.

5.7.2 Neuronal cultures- Cortical neurons from WT C57Bl/6 mice were prepared as previously described (Juzwik, Drake et al. 2018, Pare, Mailhot et al. 2018). Cortical neurons were seeded in 96-wells at 10 000 cells/well and cultured in ACM, PBMC-CM, or control media supplemented with 2% B27, 1% N2, and 1% L-glutamine for 24h at 37°C, 5% CO₂. Neurons were fixed with 4% paraformaldehyde (PFA)/20% sucrose and stained with anti-tubulin- β 3 (801202, BioLegend), Hoechst 33342 dye (Sigma-Aldrich) nuclear counter stain, and Alexa Fluor 488-conjugated antibody (Thermo Fisher). Automated image acquisition and analysis were performed using ImageXpress and the Neurite Outgrowth module of MetaXpress (Molecular Devices) to determine the mean neurite outgrowth of Hoechst/tubulin- β 3 double positive cells.

For overexpression and loss-of-function assays, *miRVana* miRNA mimics miR-383-5p, and Negative Control #1 (ThermoFisher); miRCURY LNA miRNA inhibitor miR-

383-5p and Negative Control A (Qiagen); and ON-TARGET plus SMART pool mouse Prdx3, ON-TARGET plus SMART pool mouse Dpysl2, and ON-TARGET plus Non-targeting siRNA #1 (Dharmacon) were used. Mimics were transfected at 20 nM final concentration, and LNA and siRNA at 15 nM, unless otherwise specified. Neurons were cultured without antibiotics and transfected at 1 DIV using Lipofectamine RNAiMax (ThermoFisher), according to manufacturer's instructions, unless taken up by gymnosis. For mimic experiments, media was removed at 3 DIV, and cells were treated with trypsin for 7 min at 37°C, 5% CO₂ to retract all neuronal processes. Trypsin was quenched with DMEM and 10% FBS, then cells were spun at 1 rpm for 3 min. Pelleted cells were resuspended in DMEM and 10% FBS, and seeded in 96-well plates at 10 000 cells/well. Reseeded neurons were swapped to supplemented ACM or control media for 24h at 37°C, 5% CO₂. For siRNA experiments, siRNA was transfected at 1 DIV, neurons reseeded at 3 DIV, neurons transfected with LNA inhibitors 2h post-reseeding, and fixed 48h later.

For CNTF treatment (Pepro Tech), neurons were treated with CNTF from 0.1-10 ng/ul for 8 DIV, and 50% media swap with freshly supplemented factors every 3-4 days, as previously done (Ip, Li et al. 1991). For staurosporine treatment (Sigma-Aldrich), neurons were treated at 1 DIV with staurosporine from 250- 1000 nM or DMSO vehicle control for 24h.

5.7.3 Semi-quantitative RT-PCR- Candidate miRNAs were selected by searching for miRNA arrays performed on injured or transected mouse neurons on the open access EMBL-EBI site through the ArrayExpress Archive of Functional Genomics Data (Rustici, Kolesnikov et al. 2013). A study identifying differential miRNA expression between axotomized lumbar four (L4) to L5 mouse dorsal root ganglion (DRG) neurons and control non-injured neurons was selected, as miRNA regulated following a sciatic nerve transection represent those involved in a neuronal growth program (Strickland, Richards et al. 2011). Microarray data was taken from the Array Express database (www.ebi.ac.uk/arrayexpress), accession number E-GEOD-29096. These results were

used to create a list of 22 candidate miRNAs, listed in Supplementary Table 1 along with their reverse transcription polymerase chain reaction (RT-PCR) primer designs.

Cortical neurons were treated with ACM, PBMC-CM or control media for 24h. Neurons were lysed with QIAzol Lysis Reagent (QIAGEN), and total RNA extracted using miRNeasy Mini Kit (QIAGEN), according to manufacturer's instructions. miRNA-specific stem-loop primers were designed as previously described for semi-quantitative profiling of candidate miRNA (Chen, Ridzon et al. 2005, Tang, Hajkova et al. 2006, Schmittgen, Lee et al. 2008). Multiplex RT reactions were performed on 100-200 ng RNA combined with 5 nM miR-specific stem loop primers, 1x First Strand buffer, 1 mM dNTP, 0.26 U/ μ l RNaseOUT and 3.3 U/ μ L Superscript reverse transcriptase (ThermoFisher) in a 15 μ L total volume reaction, as described (de Faria, Cui et al. 2012). RT was performed in a pulsed reaction with the following parameters: 16°C for 30 min, followed by 60 cycles of 20°C for 30 s, 42°C for 30 s, and 50°C for 1 s. The reaction was inactivated at 85°C for 5 min. A multiplex pre-amplification reaction was performed. miRNA-specific sense primers and a Universal anti-sense primer pairing were designed to the cDNA stem-loop region with sequence 5'GTGTCGTGGAGTCGGCAATTCAGTTGAG 3', as described (Chen, Ridzon et al. 2005, Tang, Hajkova et al. 2006, Schmittgen, Lee et al. 2008). From the RT reaction, 5 μ l was combined with 50 nM sense primer mix, 2 μ M Universal anti-sense primer, 1x Crimson PCR buffer, 0.5 mM dNTP, and 0.25 U/ μ l Crimson Taq polymerase (New England Biolabs) in a 25 μ l total volume reaction. Cycling parameters were set at 95°C for 10 min, 55°C for 2 min followed by 18 cycles of 95°C for 1 s, and 65°C for 1 min. Pre-PCR products were mixed with 1 μ M of the respective sense primer, 1 μ M Universal anti-sense primer, 1X Crimson PCR buffer, 0.5 mM dNTP, and 0.05 U/ μ l Crimson Taq polymerase in a 15 μ l total volume reaction. Cycling parameters were set at 95°C for 3 min followed by 30-40 cycles of 94°C for 30 s, 55-60°C for 30 s, and 72°C for 1 min. Final extension was carried out at 72°C for 10 min. 12 μ l of the PCR samples were loaded onto a 15% polyacrylamide gel made with 1X Tris/Borate/EDTA (TBE), run at a constant 56V in 1x TBE. Gels were stained with ethidium bromide for 30 min and visualized with Bio Rad Gel Doc EZ system. Densitometry analysis was performed using ImageJ to measure the density in pixels of each band minus the background pixels for each

respective lane. Individual miRNA expression is presented as fold change expression of PBMC-CM or ACM treated neurons versus control media treated.

Separate RT-PCR was performed to synthesize housekeeping gene 18S (de Faria, Cui et al. 2012). An equal amount of RNA (100-200 ng) was combined with 300 nM of random hexamer primers for a total volume of 13 μ l and heated to 65°C, 10 min. Samples were allowed to stand on ice for 2 min, and a mixture containing 1x RT buffer, 1 mM dNTP, 2 U/ μ l RNaseOUT and 10 U/ μ L ThermoScript reverse transcriptase (ThermoFisher) were added to the sample for a total reaction volume of 20 μ L. The RT reaction was performed at 25°C, 5 min; 50°C, 30 min; 55°C, 30 min; and inactivated at 70°C, 15 min. 1 μ L RNase H (ThermoFisher) was added to each reaction and run for 20 min at 37°C. PCR products were analyzed on 3% agarose gels in 1x Tris/acetate/EDTA to ensure equal amounts of cDNA across samples.

5.7.4 Quantitative RT-PCR (qRT-PCR) - Total RNA extraction was done using miRNeasy Mini Kit, according to manufacturer's instruction. miRNA expression was assessed using multiplex qRT-PCR with Taqman miRNA Assays (ThermoFisher) and snoRNA202 as the endogenous control, as previously described (Moore, Rao et al. 2013, Juzwik, Drake et al. 2018). Fold change calculations for miRNA expression were performed using the $-\Delta\Delta CT$ method (Livak and Schmittgen 2001).

5.7.5 Luciferase assays - HEK293 cells were seeded in 24-well plates and transfected with mmu-miR-383-5p mimic (ThermoFisher) and 3'UTR dual luciferase constructs (GeneCopoeia) 24h later. Transfection was performed with Lipofectamine 2000 (Invitrogen) as per manufacturer's instructions. Cell lysate was collected 24h later for analysis using the Luc-Pair Duo-Luciferase HS assay kit (GeneCopoeia), and luminescence was detected using the Infinite 100 microplate reader (Tecan). Measures of Firefly luciferase activity was normalized to Renilla luciferase. See Supplementary Table 2 for the 3'UTR sequences of putative mRNA targets of miR-383-5p.

5.7.6 miR-383-5p sponge generation- miR-383-sponge and control sponge were designed as previously described (Ebert, Neilson et al. 2007). Briefly, sponge sequences were composed of four tandem repeat miRNA-binding sites that are reverse complimentary to mmu-miR-383-5p or cel-miR-39-3p (negative control), with an omitted nucleotide opposite site 9 of the miRNA and mismatched nucleotides at sites 10-12 to create a bulge (Supplementary Fig.3). The bulge prevents degradation by miRNA processing proteins and increases inhibitory efficiency by increasing binding stabilization (Ebert and Sharp 2010, McSweeney, Gussow et al. 2016). The tandem repeats were kept to a minimum of four as increased length does not improve effectiveness and can increase the chance of degradation (Ebert and Sharp 2010). The purified miR-383-sponge and control sponge sequences (Integrated DNA Technology) were cloned into AAV2-CAG-GFP viral vector and the AAV2 particle was produced by Vector Labs.

miR-383-sponge and control sponge were validated using Luciferase Assay. Purified miR-383-sponge and control sponge were cloned into a pRRLsinPPT-EmGFP lentivirus vector. HEK293 cells were transfected with 100 ng of vectors plus 0-10 nM M383 and 50 ng pEZX-MT06 vector containing Prdx3 3'UTR or an empty control using Lipofectamine 2000 (Invitrogen) as per manufacturer's protocols. Luciferase Assay was performed 24 h post-transfection.

5.7.7 *In vivo* axonal injury- Adult C57Bl/6 mice 2–3 months old were anaesthetized with isoflurane/oxygen. The left optic nerve was exposed and crushed 0.5-1 mm from the optic disc with fine forceps (Dumont #5) for 10s. Care was taken to avoid damaging of the ophthalmic artery. An examination of the fundus was made after each surgery to verify the vascular integrity of the retina. The right eye and optic nerve were left intact.

To assess miRNA expression in regenerating RGCs, Zymosan A (12.5 $\mu\text{g}/\mu\text{l}$; Sigma) or PBS control were intravitreally injected in the vitreous chamber of the left eye using a custom-made glass micro-needle (Wiretrol II capillary, Drummond Scientific Co) as previously reported (Agostinone et al. 2018) at the time of the optic nerve crush injury. Under general anesthesia, the sclera was exposed, and the tip of the needle inserted into the superior ocular quadrant at a 45° angle through the sclera and retina into the vitreous

space. At 3 days post-injury (dpi), mice were perfused transcardially with cold PBS [0.1M] and the eyes dissected and embedded in Tissue-Tek® optimal cutting temperature (OCT) compound. Preparation of slides for laser capture microdissection (LCM), LCM procedure, and extraction of RNA from LCM-isolated retinal ganglion (RGC) layer were done as described previously (Juzwik, Drake et al. 2018).

For drug delivery, 2 µl of miRCURY LNA miRNA inhibitor miR-383-5p and Negative Control A were intravitreally injected at 1.5 ng/ul at the time of the crush injury (day 0) and again at 7 dpi. To label regenerating axons in LNA-injected animals, cholera toxin beta (Ctb) at 5 ug/ul (Invitrogen) was intravitreally injected 2 to 3 days prior to euthanasia. At 14 dpi, animals were perfused transcardially with cold PBS [0.1M] followed by 4% PFA in PBS. The optic nerves were dissected for further processing by whole mount clearing.

5.7.8 Whole mount optic nerve clearing and axonal quantification- We used an optimized protocol of iDISCO to immuno-stain whole mount optic nerve. Optic nerves were dissected, embedded in agar blocks (1%; Fisher scientific), and cleared using increasing concentration of Tetrahydrofuran (THF 50%, 80% and 100%; Sigma-Aldrich), followed by immersion in Benzyl Ether (DBE, Sigma-Aldrich). Transparent blocks were imaged with Lavisision light sheet microscope (4X zoom) and further processed with InSpectorPro software. 3D whole mounts were opened and analyzed with ImageJ/FIJI software. Whole optic nerve images were straightened prior to the assessment of axonal regeneration. Ctb-positive regenerating axons were quantified at 1000 µm, 1500 µm, and 2000 µm from the lesion, throughout the thickness of the optic nerve using ImageJ/FIJI. Specifically, every 500 µm stacked optic nerve images were visualized in two separate windows with one person counting Ctb-positive axons in the longitudinal plane and a second person counting Ctb-positive axons in the transverse plane to correctly confirm that each longitudinal axon occurs in the transverse plane, and vice versa. Both persons were blinded to the experimental condition during axon counts.

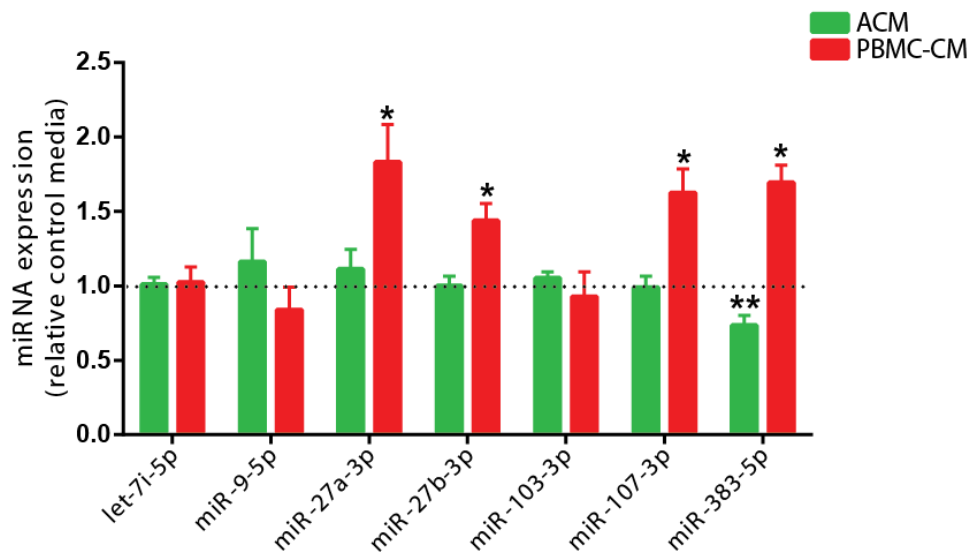
5.7.9 *In silico* assessment of predicated targets - Putative target genes for miR-383-5p was performed by searching through the seven following databases for mice: Diana-microT (Reczko, Maragkakis et al. 2012, Paraskevopoulou, Georgakilas et al. 2013), microRNA.org (Betel, Wilson et al. 2008), miRDP (Wong and Wang 2015), miRTarBase (Chou, Chang et al. 2016), RNA22 (Miranda, Huynh et al. 2006), TargetScan (Agarwal, Bell et al. 2015), and TarBase (Vlachos, Paraskevopoulou et al. 2015).

5.7.10 Immunohistochemistry- For retinal cross-sections, eye cups were dissected and cryoprotected in 30% sucrose at 4°C overnight. Eye cups were further embedded in Tissue-Tek® OCT compound and retinal cross sections of 14 µm thickness were cut using Leica® cryostat CM3050S. Retinal cross-sections were blocked with 3% BSA in 0.3% Tween/PBS for 30 min, probed with primary antibody at 2h, and probed with the appropriate fluorescent secondary antibody for 1h. The following antibodies were used: anti-Crmp2 (ab36201, Abcam), anti-Prdx3 (kindly provided by Dr. McBride (Jeyaraju, Xu et al. 2006)), anti-Brn3a (sc-31984, Santa Cruz), and anti-tubulin-β3 (801202, BioLegend). Alexa Fluor 488 or 568-conjugated antibodies (Thermo Fisher) were used as secondary antibodies and Hoechst 33342 dye as a nuclear counterstain. Images were acquired using a Carl Zeiss Axio Imager M1 with Eclipse (Empix Imaging).

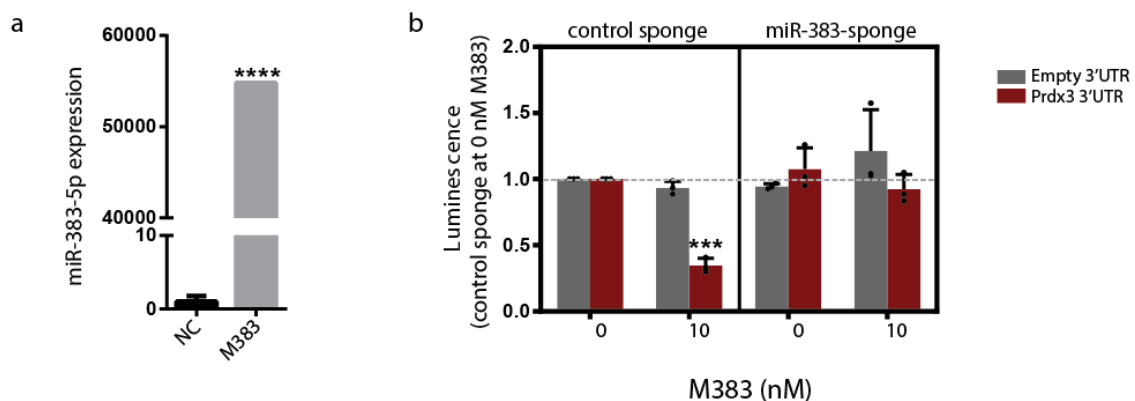
5.7.11 Western blot- miRNA mimics or siRNA were transfected at 1 DIV, and neurons were lysed 72h later with HEPES-based RIPA buffer supplemented with protease inhibitors (Complete protease inhibitor cocktail, Roche) and phosphatase inhibitors (10 mM sodium fluoride and 1 mM sodium orthovanadate). Protein lysates were quantified by DC protein assay (Bio-Rad), boiled in sample buffer, separated by SDS-PAGE, and transferred to PVDF membranes. Membranes were blocked with 5% milk in TBS-T for 1h, probed with primary antibody at 4°C overnight, and probed with the appropriate HRP-conjugated secondary antibody for 1h. The following antibodies were used: anti-Crmp2 (ab36201, Abcam), anti-Prdx3 (kindly provided by Dr. McBride (Jeyaraju, Xu et al. 2006)), anti-PDH E2/E3bp (ab110333, Abcam), and anti-α-tubulin (T9026, Sigma-Aldrich). HRP-conjugated secondary antibodies were from Jackson ImmunoResearch.

5.7.12 Statistical analyses - Statistical analyses were performed using GraphPad Prism 6. As indicated in figure legends, the following statistical tests were used: two-tailed student's t-test; one-way ANOVA; two-way ANOVA; three-way ANOVA. Post-hocs include Dunnett's, Sidak's, and Tukey's multiple comparisons tests. Sample sizes are indicated in the figure legends and significance was defined as * $p < 0.05$, ** $p < 0.01$, *** $p < 0.001$, and **** $p < 0.0001$.

5.8 Supplementary Figures and Tables



Supplementary Figure 1. Candidate miRNA expression in cortical neurons stimulated with CNS injury-relevant conditioned media. qPCR expression data for miRNA collected from mouse cortical neurons treated with ACM for 48h or PBMC-CM for 24h, relative to respective control media (n=3-5, two-tailed student's t-test). qPCR data is represented as fold change control media expression.



Supplementary Figure 2. Validation of miR-383-5p expression for gain-of-function and loss-of-function experiments. (a) Mouse cortical neurons transfected with 20 nM negative control mimic (NC) or miR-383-5p mimic (M383) at 1 DIV for 24h (n=3, two-tailed student's t-test). (b) Luminescence fold change of HEK293 cells transfected with M383, empty 3'UTR luciferase vector or Prdx3 3'UTR luciferase vector, and control sponge or miR-383-sponge at 10 nM (n=3, three-way ANOVA, p<0.05 Tukey's multiple comparisons test).

a **Mature mmu-miR-383-5p:** 5' **AGAUCAGAGGUG**ACUGUGGCU 3'

Sponge:

Sense (reverse complementary to miR-383-5p) 5' AGCCACAGT**ACCTTCTGATCT** 3'
Antisense 5' **AGATCAGAGGT**GACTGTGGCT 3'

With bulge at 9-12 position:

Sense 5' AGCCACAGT**CAA-TCTGATCT** 3'
Antisense 5' **AGATCAGATTG**GACTGTGGCT 3'

Full sponge sequence (130 bp):

5' tagcc**GAATTC**AGCCACAGT**CAA-TCTGATCT**gggaaaAGCCACAGT**CAA-TCTGATCT**gggaaa
AGCCACAGT**CAA-TCTGATCT**gggaaaAGCCACAGT**CAA-TCTGATCT**gggaaa**GATATC**tagcc 3'

LEGEND
seed sequence
miRNA sponge loop
extra nucleotide sequence for enzyme
restriction enzyme sites (5'EcoRI and 3'EcoRV)
gap sequence

b **Mature cel-miR-39-3p:** 5' **UCACCGGUGU**AAUCAGCUUG 3'

Sponge:

Sense (reverse complementary to miR-39-3p) 5' CAAGCTGATT**TACACCCGGTGA** 3'
Antisense 5' **TACCCGGTGT**AATCAGCTTG 3'

With bulge at 9-12 position:

Sense 5' CAAGCTGATT**GCA-CCCGTGA** 3'
Antisense 5' **TACCCGGT**TGCAATCAGCTTG 3'

Full sponge sequence (130 bp):

5' tagcc**GAATTC**CAAGCTGATT**GCA-CCCGTGA**gggaaaCAAGCTGATT**GCA-CCCGTGA**gggaaa
CAAGCTGATT**GCA-CCCGTGA**gggaaaCAAGCTGATT**GCA-CCCGTGA**gggaaa**GATATC**tagcc 3'

Supplementary Figure 3. miR-383-sponge and control sponge design. Sponge design for sequestering (a) miR-383-5p and (b) negative control cel-miR-39-3p. Red letters represent the seed sequence; blue the miRNA sponge loop, with the nucleotide deletion at site 9 and base pair mismatching sites 10-12; grey the extra nucleotide sequence for enzyme; green the restriction enzyme sites of 5'EcoRI and 3'EcoRV; and yellow the gap sequence.

Table 1 Supplemental

Primers of candidate miRNA used for semi-quantitative RT-PCR analysis

miRNA	RT stem-loop reverse primer	PCR forward primer
mmu-let-7i-5p	CTCAACTGGTGTCGTGGAGTCGGCAATTCAGTTGAGAACAGCAC	ACACTCCAGCTGGGTGAGGTAGTAGTTTGT
mmu-miR-9-5p	CTCAACTGGTGTCGTGGAGTCGGCAATTCAGTTGAGTCATACAG	ACACTCCAGCTGGGTCTTTGGTTATCTAGC
mmu-miR-15-5p	CTCAACTGGTGTCGTGGAGTCGGCAATTCAGTTGAGTGAAACC	ACACTCCAGCTGGGTAGCAGCACATCATGG
mmu-miR-16-5p	CTCAACTGGTGTCGTGGAGTCGGCAATTCAGTTGAGCGCCAATA	ACACTCCAGCTGGGTAGCAGCACGTAATA
mmu-miR-21-5p	CTCAACTGGTGTCGTGGAGTCGGCAATTCAGTTGAGTCAACATC	ACACTCCAGCTGGGTAGCTTATCAGACTGA
mmu-miR-22-3p	CTCAACTGGTGTCGTGGAGTCGGCAATTCAGTTGAGACAGTTCT	ACACTCCAGCTGGGAAGCTGCCAGTTGAAG
mmu-miR-24-3p	CTCAACTGGTGTCGTGGAGTCGGCAATTCAGTTGAGCTGTTCT	ACACTCCAGCTGGGTGGCTCAGTTCAGCAG
mmu-miR-27a-3p	CTCAACTGGTGTCGTGGAGTCGGCAATTCAGTTGAGGCGGAAT	ACACTCCAGCTGGGTTACAGTGGCTAAGT
mmu-miR-27b-3p	CTCAACTGGTGTCGTGGAGTCGGCAATTCAGTTGAGGCAGAAT	ACACTCCAGCTGGGTTACAGTGGCTAAGT
mmu-miR-30a-3p	CTCAACTGGTGTCGTGGAGTCGGCAATTCAGTTGAGCTTCCAGT	ACACTCCAGCTGGGTGTAACATCCTCGAC
mmu-miR-92a-3p	CTCAACTGGTGTCGTGGAGTCGGCAATTCAGTTGAGCAGGCCGG	ACACTCCAGCTGGGTATTGCACTTGTCCCG
mmu-miR-99a-5p	CTCAACTGGTGTCGTGGAGTCGGCAATTCAGTTGAGCACAAGAT	ACACTCCAGCTGGGAACCCGTAGATCCGAT
mmu-miR-103-3p	CTCAACTGGTGTCGTGGAGTCGGCAATTCAGTTGAGTCATAGCC	ACACTCCAGCTGGGAGCAGCATTGTACAGG
mmu-miR-107-3p	CTCAACTGGTGTCGTGGAGTCGGCAATTCAGTTGAGTGATAGCC	ACACTCCAGCTGGGAGCAGCATTGTACAGG
mmu-miR-126-3p	CTCAACTGGTGTCGTGGAGTCGGCAATTCAGTTGAGCGCATTAT	ACACTCCAGCTGGGTCGTACCGTGAGTAAT
mmu-miR-134-5p	CTCAACTGGTGTCGTGGAGTCGGCAATTCAGTTGAGCACAAGAT	ACACTCCAGCTGGGAACCCGTAGTACCGAT
mmu-miR-137-5p	CTCAACTGGTGTCGTGGAGTCGGCAATTCAGTTGAGATTATCCA	ACACTCCAGCTGGGACGGGTATTCTTGGGT
mmu-miR-182-5p	CTCAACTGGTGTCGTGGAGTCGGCAATTCAGTTGAGCGGTGTGA	ACACTCCAGCTGGGTTTGGCAATGGTAGAA
mmu-miR-195-5p	CTCAACTGGTGTCGTGGAGTCGGCAATTCAGTTGAGGCCAATAT	ACACTCCAGCTGGGTAGCAGCACAGAAATA
mmu-miR-199a-3p	CTCAACTGGTGTCGTGGAGTCGGCAATTCAGTTGAGTAACCAAT	ACACTCCAGCTGGGACAGTAGTCTGCACAT
mmu-miR-204-5p	CTCAACTGGTGTCGTGGAGTCGGCAATTCAGTTGAGAGGCATAG	ACACTCCAGCTGGGTTCCCTTTGTCATCCT
mmu-miR-206-3p	CTCAACTGGTGTCGTGGAGTCGGCAATTCAGTTGAGCCACACAC	ACACTCCAGCTGGGTGGAATGTAAGGAAGT
mmu-miR-383-5p	CTCAACTGGTGTCGTGGAGTCGGCAATTCAGTTGAGCTGTGGCT	ACACTCCAGCTGGGAGATCAGAAGGTGACT

For all miRNA, a Universal reverse primer was used with the sequence 5'GTGTCGTGGAGTCGGCAATTCAGTTGAG 3'.

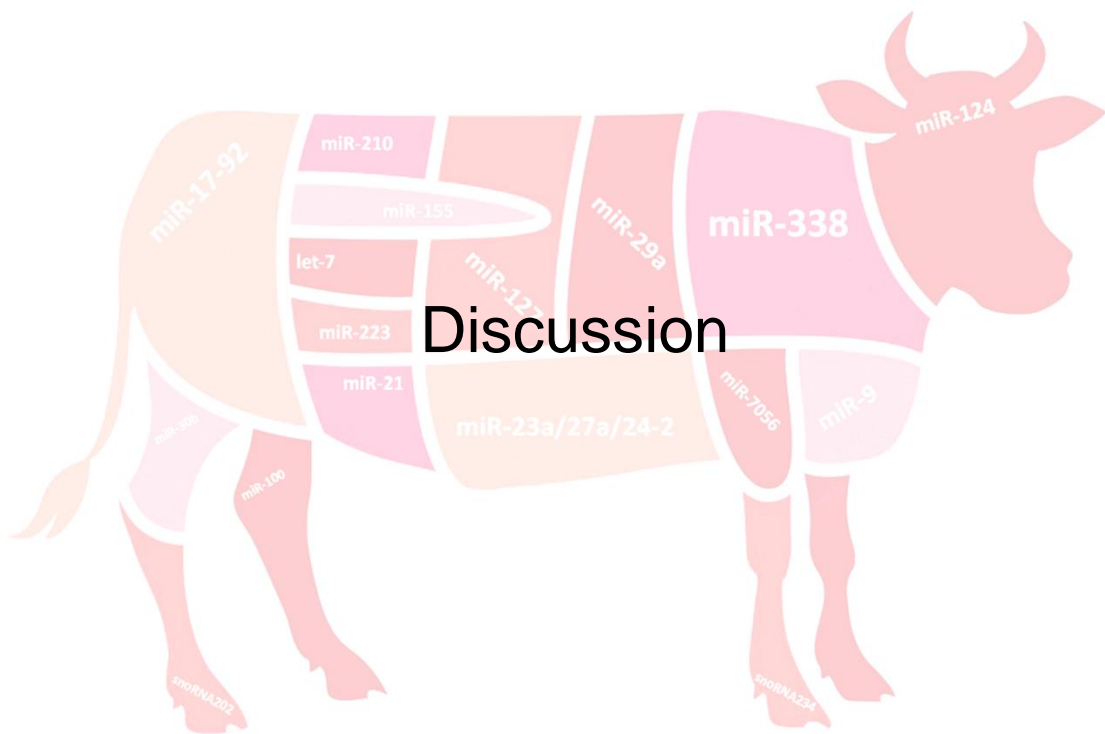
Table 2 Supplemental
*Expression of candidate miRNA in cortical neurons as assessed by
semi-quantitative RT-PCR*

miRNA	miRNA expression		
	DRGs post-axotomy (log 2) <small>(Strickland, Richards et al. 2011)</small>	cortical neurons (\pm SEM)	
		ACM treated	PBMC-CM treated
mmu-let-7i-5p	0.21	1.06 \pm 0.25	1.08 \pm 0.04
mmu-miR-15b-5p	0.52	0.99 \pm 0.22	1.02 \pm 0.03
mmu-miR-16-5p	0.13	0.94 \pm 0.22	1.02 \pm 0.07
mmu-miR-21-5p	2.34	1.47 \pm 0.55	1.08 \pm 0.07
mmu-miR-22-3p	-0.12	0.68 \pm 0.32	0.72 \pm 0.17
mmu-miR-24-3p	0.09	0.99 \pm 0.20	2.28 \pm 1.13
mmu-miR-27a-3p	0.14	0.97 \pm 0.30	1.20 \pm 0.06
mmu-miR-27b-3p	0.02	1.08 \pm 0.29	1.07 \pm 0.01
mmu-miR-30a-3p	-0.34	0.98 \pm 0.13	1.07 \pm 0.16
mmu-miR-92a-3p	0.19	0.97 \pm 0.18	1.01 \pm 0.03
mmu-miR-99a-5p	-0.26	0.90 \pm 0.14	1.02 \pm 0.01
mmu-miR-103-3p	-0.31	1.29 \pm 0.03	1.38 \pm 0.17
mmu-miR-107-3p	-0.36	0.95 \pm 0.01	0.77 \pm 0.06
mmu-miR-126-3p	0.05	0.77 \pm 0.12	0.63 \pm 0.24
mmu-miR-134-5p	0.67	0.95 \pm 0.08	1.06 \pm 0.00
mmu-miR-137-5p	-0.68	0.94 \pm 0.18	1.03 \pm 0.21
mmu-miR-182-5p	-0.35	0.83 \pm 0.34	0.97 \pm 0.14
mmu-miR-195-5p	0.06	0.89 \pm 0.14	1.00 \pm 0.14
mmu-miR-199a-3p	0.51	0.98 \pm 0.22	1.15 \pm 0.28
mmu-miR-204-5p	0.16	0.89 \pm 0.15	1.00 \pm 0.01
mmu-miR-206-3p	-0.16	0.72 \pm 0.33	1.12 \pm 0.03
mmu-miR-383-5p	-0.99	0.84 \pm 0.33	1.20 \pm 0.11

gtatfttgcaattcaagtagcccttcatatgtcaatgacagaaagtattatctcaaagctcttactgcttaggcacttactcagatagaattgtgtgttgcaactaaggaatttctactgtt
cctgtttgaaactgggttgaatgagcaaaatggcctttaaaggatcccgaagtagcaataacttggcatctcaagtgaaagtgtgggggaaaggccatcagctgtaatgccaggc
acacagtgagagttctgtctgtatgtatgggtcccttctagagtgtagcagattccgtggaactgtctgaaggatgggagagattaagatgtgactgcagatagataaaaaagaa
ttgactgaaagattggatacatgtggaaacagccccacagtgtaggggaaactgtgaagactcataggccttccactagatgcgccctgcagaccctatcactgcagagttg
ttgctttgtgtcatgagctattagcttgagagcccatctgtaccaatctggcttgcgttatgtcaagcagcatgcatgagcgagcttagctgatcactagaagaactcattgtctgttaa
gatataccaaggcatttctgaattg

LifR Negative Control 3'UTR

Ccaggtcacccttgtcacttcagctgccaatctcagtaagtccctgccgctgctggcagcagctggggcatttctggaggaccctgcaaatgtgatagccaggacctca
ctctgggcaagtgacactagaagtgttaatgtgctttaaagtatcctaaaagccagagtgtagtgcactagccctcagccggaactcaagagttgaagctgttttgattgagcc
aaagaaccctcccaaggacctaagactaaccaactctgtgtagtagacatagctaaaccagatctcacaaccgtttctgttgaatggcttctcagcgtgtgatggattg
ctagtggattacagggcaaggagaaaaccttccaagtagcaaacagcgttaattgctgacatttactgctgtagaggagaaccaagcagacagatcttaagccgtggtgatgc
tctgtccacagcatttacaagaacaaactgttttcatgtagcagcagctatctggcgttctgttgataaaagcgtgctgatttctgtcctactgataatggtatcaaacagttgtca
ggggtacaacttggaagcaagtgcgagctgaccagtccgaaatggcatcacaccgtcctgtttctcgggtgtgaaaaccttcccctatcatgagctgcagcagcagct
tccattagtagttgactgcccataatgttgaatctctgaactatgccaaatcttctatttctgttctgttatagggctcgttcgtaagagcgaattatcattattacaggtag
ataattgtaatgagttactacgtaagtagactaagaatagctagtggtgtgtgctgactgcagatgctgattagactcagctcctcctgagaggtataggccattaagcctaacc
aatagctggctgatgactgaggttctcaggagcttccctgctgctcatgagctcggcttctccccctcagggcagttgggggtccagagctcagaccttgccttcaaatccata
aacttaacataaaggagataaactccttggagcagttagtggttaactgtaatagaggtcagaaaaactacggaagtggtaggctgtggcctgtatggttccgtcagcagtg
aagtgccagatcctgagcacagcaccctcaatacaccctggtctctatcagcaacgtgtacagggaaatggattctagaaaagctgtaaaacctaataatgtatgcatgtgttg
ctctgccttgggtgcatgacagttgaaacaccccaggagtagacgaccttatttgtgcatctgaagctccccaaatcttacagataatggctgttcttttagttcagatttatttttt
ttattttttttttttttttttcttctgacaggggtctcactatgcagccctggccttctggaactcactatgtagataaaggccagcctcagactcagagatccacctgttctgtctcccaagttggtgtgcgtgtcaccatgcctggccttattttatcttcaagaatcatgtg
agaaaaaaatacaggatgacaagggacaagtagcatcctgttttaaccctaggattcaactacattttggagctccatgatagtttagtagctctagaaaatttctagactgaa
aaataattcaagccagagccaacaccaaagagtttctgtcttctgtgccctctgctcctcctcctaccagcactaagccctgtgctcctccccacaccacgccctcc
ccttccccccccctccccctccccactcctgaaacatcttactactgctatgcctgttggcctctgcttgtccccagtgagcttctcagtttctattccccatctaattgggatc
agagtttgcgaaggttacagc



Discussion

6 Chapter 5. Discussion and conclusion

6.1 Summary of results

Neuroinflammation is divided into positive and negative roles during neurodegenerative disease. In this thesis we investigated how neurons respond to neuroinflammation such that we can protect them from the negative aspects and harness the positive aspects to promote repair and regeneration in neurodegenerative disease, with emphasis on MS. Specifically, we focused on miRNAs to determine programs of gene expression such that we could mediate neuroprotection and repair. As was demonstrated in Chapters 2-4, miRNAs can modulate a pool of genes, in turn targeting multiple pathways that determine the neuron's capacity for repair or regeneration. In Chapter 2 we characterized neuronal miRNA expression throughout the disease course of EAE and determined through *in silico* analysis potential pathways which these miRNAs may target cooperatively. Targeted pathways converged on cell survival, cytoskeleton rearrangement, and stress response, suggesting that the upregulated miRNAs promote neuronal axotomy and cell death. Key genes of the *in silico* identified pathways were shown to be downregulated in EAE neurons. In Chapter 3 we pursued the functional roles of miR-27a-3p and miR-223-3p, which we identified as upregulated in EAE neurons and MS leukocortical lesions. We demonstrated that in fact they are neuroprotective by blocking inflammation-mediated neurodegeneration through glutamate receptor signaling *in vitro*; and validated *in vivo* that miR-223-3p retinal-specific overexpression prevented EAE-mediated axonopathy. The dichotomy of neuroinflammation is emphasized by these results, as miR-27a-3p and miR-223-3p were upregulated by inflammation, and yet simultaneously promote neuroprotection. Finally, in Chapter 4 we used a model of regeneration to determine miRNA regulators of neuronal survival and regeneration, as this knowledge can be applied to multiple neurodegenerative diseases. We identified that miR-383-5p loss-of-function promoted neurite outgrowth *in vitro*, and regeneration *in vivo*. We demonstrated that this is through the previously implicated JAK/STAT3 pathway in optic nerve regeneration, along with additional genes that are major components of cytoskeleton rearrangement and proper oxidative stress maintenance. Thus, we have identified multiple miRNAs whose functions converge on neuronal repair and regeneration. Here we will discuss what implications these results have on the current

field of EAE and MS, as well as other neurodegenerative diseases; what experimental approaches we can take to develop these findings even further; and how this information contributes to the field of miRNA research.

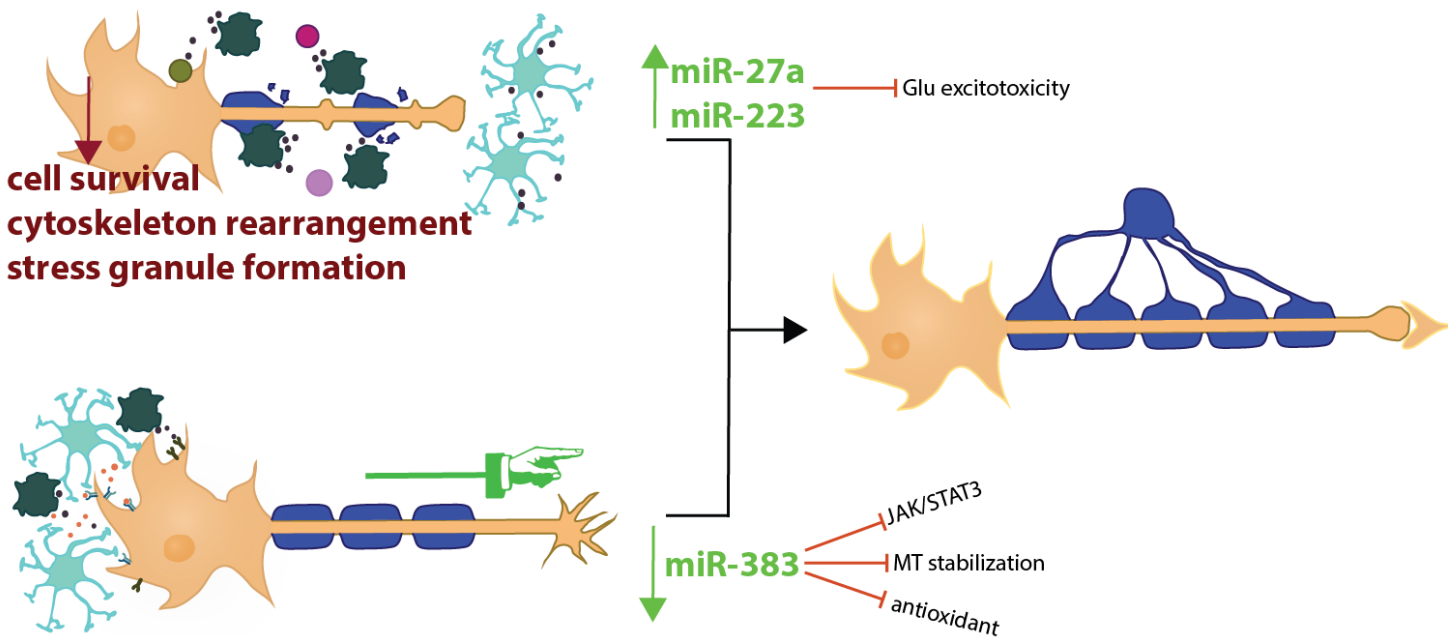


Figure 1. We can harness the positive aspects of neuroinflammation to promote repair and regeneration. Using EAE as a model of neuroinflammation, we profiled differentially regulated miRNAs in the affected neuronal populations and identified that they negatively regulated cytoskeleton rearrangement, cell survival, and stress granule formation; in turn, limiting repair and regeneration (chapter 2). In parallel, we identified that miR-27a-3p and miR-223-3p were upregulated in EAE neurons and in human MS leukocortical lesions. These miRNAs proved to be a neuroprotective response as we demonstrated their ability to limit inflammation-mediated neurodegeneration *in vitro* and *in vivo*. We identified that miR-27a-3p and miR-223-3p were able to protect neurons from inflammation by limiting glutamate receptor signaling, limiting pathological excitotoxicity (chapter 3). Using an artificial model of intraocular inflammation, which drives regeneration, we identified that miR-383-5p was downregulated. We then demonstrated that knocking down miR-383-5p expression both *in vitro* and *in vivo* recapitulated the positive regenerative effects of intraocular inflammation. We demonstrate that miR-383-5p limits JAK/STAT3 signaling, microtubule stabilization (MT), and a healthy antioxidant status, suggesting that knocking down miR-383-5p relieves its inhibitory role on these repair and regeneration pathways (chapter 4). Gathering the cellular signaling from chapters 2-4, we can improve our understanding on how to promote repair and regeneration in neurodegenerative disease and CNS injury.

6.2 How to share your miRNAs with others

For this thesis we focused on neuronal miRNAs as miRNAs can have vastly different functions between cell types based on their mRNA targets, as discussed in chapter 2. For example, miR-183-5p mediates neurodegeneration when elevated in neurons; yet in natural killer cells miR-183-5p blocks limits its cytotoxic effects (Donatelli, Zhou et al. 2014, Kye, Niederst et al. 2014). miR-183-5p elevation promotes drastically different biologies between the two cell types. However, miRNAs can travel between cells via exosomes (Zhang, Li et al. 2015). Exosomes are small lipid vesicles released by multiple cell types and taken up by neighbouring or distant cells, donating their contents of small RNAs, RNA, and protein. Exchange of exosomal miRNA has been described between immune cells, as well as between neurons and glia, as reviewed (Fruhbeis, Frohlich et al. 2012, Selmaj, Mycko et al. 2017). Exosomes can also cross the BBB, which is likely enhanced during neurodegenerative disease and CNS injury where the blood-CNS barriers are compromised (Alvarez-Erviti, Seow et al. 2011, Sweeney, Sagare et al. 2018). In turn, it is difficult to determine from where a miRNA originated, creating a chicken-and-egg situation. Infiltrating immune cells in EAE may be contributing to the upregulation of the miRNAs we identified in EAE neurons from chapters 2 and 3. At peak disease we saw the strongest rise in miRNA expression, which correlates with the increased peripheral immune cell infiltration. By *in silico* analysis and qPCR validation of key genes from predicted pathways, we determined that the miRNAs upregulated in both motor and retinal neurons promote cell death and axonopathy. If these miRNAs are upregulated at peak due to infiltrating immune cells exosome exchange, it would be ideal if we could disrupt the internalization of the exosomes by the recipient neurons to limit cell death and axonopathy. This is possible by disrupting exosomal lipid rafts, as demonstrated in a carcinoma cell line (Koumangoye, Sakwe et al. 2011). FANTOM5 is an online tool that details cell-specific basal miRNA expression based on deep sequencing data from multiple cells types in humans and mice (Halushka, Fromm et al. 2018). Using FANTOM5 we can determine if our EAE dysregulated miRNAs are endogenously more highly expressed in immune cells or neurons. miR-374b-5p, miR-205-5p, and miR-223-3p are up 50 times higher in lymphocytes relative to brain tissue; miR-142a-5p about 20x higher; and miR-23a-3p, miR-27a-3p, and miR-423-5p about 5x

higher. Of course, these are basal levels and do not account for an individual cell's transcriptomic profile during EAE-mediated inflammation, but it does suggest that these seven miRNAs may originate from infiltrating lymphocytes or that their upregulation was additionally attributed by infiltrating lymphocytes. Exosomes do contain selectively packaged miRNAs, and miR-223-3p is described as such (Shurtleff, Temoche-Diaz et al. 2016).

What is more, recently a functional meningeal lymphatic system was described that drains cerebrospinal fluid (CSF) to deep cervical lymph nodes, providing the periphery with access to CNS macromolecules including antigens and potential antigen-presenting cells (Aspelund, Antila et al. 2015, Louveau, Smirnov et al. 2015). This suggests an internal event that triggers an inflammatory response directing peripheral immune cells to the CNS. Blocking CSF draining by the meningeal lymphatic system ameliorates EAE pathology, as well as that of Alzheimer's disease animal models, suggesting this may be a common drainage system that promotes neurodegenerative disease development (Da Mesquita, Louveau et al. 2018, Louveau, Herz et al. 2018). It is conceivable that miRNAs identified as upregulated in the neurons of EAE mice can be trafficked to the CSF, and then to the periphery by exosomes through the meningeal lymphatic drainage route. It is conceivable that one or more of our neuronally upregulated miRNAs are trafficked by exosomes from neurons to the CSF, and from the CSF into the periphery by the meningeal lymphatic system. In fact, miR-223-3p is upregulated in exosomes isolated from the sera of both progressive MS and RRMS individuals compared to healthy controls (Ebrahimkhani, Vafaei et al. 2017). Upregulated neuronal miRNAs also demonstrate immune functions based on our *in silico* results. They may be regulating the immune response through exosomal exchange, either by the meningeal lymphatic system or with infiltrating-immune cells. If so they would be promoting enhanced CNS inflammation by blocking potential CD-28 co-stimulation, yet also reduced cell viability through PI3K/Akt/mTOR signaling (chapter 2, Fig. 6).

Determining the origins of a miRNA and its ability to travel across cell types is thus an important next question for future miRNA research. Animals with transgenic miRNA sequences where they are transcribed with a fluorescent tag may help answer this

question, though the addition of a fluorescent tag could limit the normal migration patterns and functions of the miRNA.

6.3 miR-27a-3p and miR-223-3p

6.3.1 GluR signaling in MS

We identified that miR-27a-3p and miR-223-3p are neuroprotective by targeting neuronal GluR signaling during inflammatory-stimulation *in vitro* and confirmed *in vivo* that miR-223-3p overexpression prevents in EAE-induced axonopathy. Glutamate accumulation in the extracellular space of the CNS results in overactivation of GluRs, including both ionotropic and metabotropic GluRs (iGluR, mGluR, respectively), promoting an influx of excess Ca^{2+} that prompts a cascade of events which invoke neuronal dysfunction and degeneration (Lau Anthony and Tymianski 2010). Glutamate accumulation also potentiates enhanced inflammation. Infiltrating T-cells and macrophages/microglia secrete glutamate, contributing glutamate to the extracellular space (Levite 2017). The pro-inflammatory cytokines secreted by these immune cells impair glutamate handling by astrocytes, where astrocytes are responsible for 90% of extracellular glutamate uptake by glutamate transporters (Ponath, Park et al. 2018). This in turn contributes to even more glutamate in the extracellular space, which can enhance T-cell activity as the AMPAR subunit GluR3 is highly expressed on T cells (Levite 2017). Oligodendrocytes and their myelin are also affected by the excess glutamate, as they express AMPAR, NMDAR and kainate receptors (Tsutsui and Stys 2013). AMPAR subunit GluR1 is also upregulated in oligodendrocytes within active MS lesions (Newcombe, Uddin et al. 2008). At the European Committee for Treatment and Research in MS (ECTRIMS) Congress this October 2018, the group of Dr. Tara DeSilva presented their work investigating the selective depletion of AMPAR subunits on oligodendrocytes in EAE (Evonuk 2018). Using a PLP-Cre-ER^{T2}/GluR4^{fx/fx} double transgenic mice, they selectively removed the AMPAR subunit GluR4. These mice displayed reduced demyelination and axonal degeneration, as demonstrated by decreased APP accumulation. Having discussed the promiscuity of miRNA through exosomal sharing and that miR-223-3p is known as a selectively packaged miRNA (Shurtleff, Temoche-Diaz et al. 2016), it is possible that within our own experiments where we over-expressed miR-

223 in retinal neurons and the optic nerve, miR-223-3p may be shuttled to the ensheathing myelin via exosomes. It would be interesting to characterize the myelin and oligodendrocyte response in future experiments with AAV2 directed overexpression of miR-223 in EAE retina and optic nerve. Thus, these results with our own demonstrate that targeting GluR signaling in MS would promote both neuronal and myelin protection.

New insight into the mechanisms of Ca²⁺-mediated focal axonal degeneration from the group of Kerschensteiner however, challenges the concept of glutamate-induced axonopathy (Witte, Schumacher et al. 2019). Kerchensteiner and colleagues induced EAE in Thy1-CerTN-L15 transgenic mice where neurons contain the genetically encoded calcium sensor CerTn in their cytoplasm. Changes in cytoplasmic Ca²⁺ levels were detected by *in vivo* multi-photon imaging of axonal fibers. Kerchensteiner and colleagues demonstrated that Ca²⁺ enters through axonal nanoruptures during EAE, as demonstrated with the seamless influx of nano-sized dyes. They rule out the contribution of GluR signaling to Ca²⁺ influx, yet they only apply GluR agonists during EAE to demonstrate that intracellular Ca²⁺ levels did not change. It was not demonstrated if GluR antagonists could block Ca²⁺ influx. Regardless, these results suggest that during neuroinflammation there is mechanical disruption of axonal membrane integrity, which could be triggered by ROS, lipid peroxidation, and changes in membrane permeability (Witte, Schumacher et al. 2019). We injected AAV-miR-223 4 weeks prior to EAE induction and saw decreased focal axonal degeneration. This suggests that miR-223-3p can limit or even prevent the disruption of axonal membrane integrity. What stands to be answered is if this is an additional pathway targeted by miR-223-3p, and if this is promoted by exosomal sharing.

6.3.2 miR-27a and miR-223 as general mediators of neuroprotection

Neurodegeneration is the progressive deterioration of neuronal structure and function, with eventual neuronal loss (Bredesen, Rao et al. 2006). In addition to neuronal loss, neurodegenerative diseases share many other commonalities such as deficits in axonal transport, oxidative stress, mitochondrial dysfunction, and inflammation regardless of disease etiology (Glass, Saijo et al. 2010, Burte, Carelli et al. 2015, Kim, Kim et al. 2015). Shared pathophysiological processes across neurodegenerative

diseases raises the possibility that identifying common molecular regulation across various diseases may lead to approaches for therapeutic, which would be effective for multiple indications. Glutamate-mediated excitotoxicity is a common pathway between many neurodegenerative diseases and CNS injury (Lau Anthony and Tymianski 2010). Thus, our work investigating miR-27a-3p and miR-223-3p in limiting GluR-mediated axonopathy in EAE is transferable to other models of neurodegeneration and CNS injury. In fact, miR-27a-3p and miR-223-3p are dysregulated across multiple neurodegenerative diseases and their models, including models of CNS injury. We performed a systematic review of the literature for miRNA dysregulation in neurodegenerative disease, neuroinflammation, and CNS damage. miR-27a-3p was dysregulated in AD, amyotrophic lateral sclerosis (ALS), AMD, myotonic dystrophy (DM), epilepsy, multiple system atrophy (MSA), MS, Parkinson's disease (PD), and SCI. miR-223-3p was dysregulated in AD, ALS, AMD, dementia, Huntington's disease (HD), MS, retinal degeneration, SCI, stroke, and TBI. Table 1 details the material investigated from the specific disease states in humans and/or their relevant animal models. This suggests that overexpressing miR-27a-3p and/or miR-223-3p in these animal models can help alleviate disease pathology by limiting GluR-mediated excitotoxicity. Biohaven Pharmaceutical is fact has two pipeline products that help balance glutamate homeostasis by increasing glutamate transporter modulation and NMDAR antagonism as DMTs for neurodegenerative diseases that include ALS, AD, and spinocerebellar ataxia, and complex regional pain syndrome.

Table 1

*Differential expression of miR-27a-3p and miR-223-3p across CNS disease and injury**

mature miRNA	material	Direction (count)*	Disease state in humans	Animal models**
miR-27a	CNS	Up (11)	AD (Cogswell, Ward et al. 2008, Absalon, Kochanek et al. 2013, Llorens, Thune et al. 2017) Epilepsy (Miller-Delaney, Bryan et al. 2015) MSA (Ubhi, Rockenstein et al. 2014) MS (Junker, Krumbholz et al. 2009) PD (Briggs, Wang et al. 2015)	AD (Barak, Shvarts-Serebro et al. 2013) AMD (Romano, Platania et al. 2017) EAE (Lewkowicz, Cwiklinska et al. 2015) SCI (Tang, Ling et al. 2014)
		Down (5)	AD (Sala Frigerio, Lau et al. 2013, Wang, Visavadiya et al. 2015) ALS (Campos-Melo, Droppelmann et al. 2013)	AD (Kempf, Metaxas et al. 2016) MSA (Schafferer, Khurana et al. 2016)
	blood & related material	Up (7)	ALS (Butovsky, Siddiqui et al. 2012) AMD (Ren, Liu et al. 2017, Romano, Platania et al. 2017) MS (Ahmadian-Elmi, Bidmeshki Pour et al. 2016, Regev, Paul et al. 2016)	EAE (Lewkowicz, Cwiklinska et al. 2015, Singh, Deshpande et al. 2016)
		Down (1)	AMD (Szemraj, Bielecka-Kowalska et al. 2015)	
	muscle	Up (1)	ALS (Pegoraro, Merico et al. 2017)	
		Down (1)	DM (Kalsotra, Singh et al. 2014)	DM (Kalsotra, Singh et al. 2014)
	urine	Down (1)		EAE (Singh, Deshpande et al. 2016)
miR-223	CNS	Up (13)	MS (Junker, Krumbholz et al. 2009, Gueraude-Arellano, Liu et al. 2015)	AD (Barak, Shvarts-Serebro et al. 2013) SOD1(G93A) (Butovsky, Siddiqui et al. 2012, Koval, Shaner et al. 2013) EAE (Satoorian, Li et al. 2016, Cantoni, Cignarella et al. 2017) retinal degeneration (Chung, Gillies et al. 2015, Chung, Gillies et al. 2016) stroke (Harraz, Eacker et al. 2012) SCI (Izumi, Nakasa et al. 2011, Tang, Ling et al. 2014) TBI (Wang, Visavadiya et al. 2015, Harrison, Emanuel et al. 2017)
		Down (3)	AD (Wang, Huang et al. 2011, Lusardi, Phillips et al. 2017) ALS (Campos-Melo, Droppelmann et al. 2013)	
	blood & related material	Up (13)	ALS (Butovsky, Siddiqui et al. 2012) AMD (Ertekin, Yildirim et al. 2014, Szemraj, Bielecka-Kowalska et al. 2015) HD (Diez-Planelles, Sanchez-Lozano et al. 2016) MS (Keller, Leidinger et al. 2009, De Santis, Ferracin et al. 2010, Ridolfi, Fenoglio et al. 2013, Hosseini, Ghaedi et al. 2016, Cantoni, Cignarella et al. 2017, Ebrahimkhani, Vafaee et al. 2017)	EAE (Bergman, James et al. 2013, Ifergan, Chen et al. 2016, Satoorian, Li et al. 2016)
		Down (3)	AD (Jia and Liu 2016) dementia (Ragusa, Bosco et al. 2016) MS (Fenoglio, Ridolfi et al. 2013)	

Colour representations: up in neurodegenerative disease, up in CNS injury models, down in neurodegenerative disease.

*Count is based on unique studies listed per row. If a study is repeated between human disease state and animal models it is counted only once. Studies were taken as part of a systematic review investigating miRNA expression across all neurodegenerative diseases with the most recent literature search conducted on November 7th, 2017.

**AD models included APP/PS1 mice and 3xTg-AD transgenic mice. AMD model was induced by A β -oligomer injection into the eye of rats. DM1 model included tamoxifen-inducible and heart-specific EpA960; MCM DM1 mice. EAE was induced in mice and/or rats as an animal model of MS. Stroke mouse model was induced by a transient global ischemia by temporary bilateral common carotid artery occlusion (BCCAO) for 20 min followed by reperfusion. MSA model included homozygous transgenic PLP- α -synuclein mice. SOD1^(G93A) transgenic mice was used as an ALS model. Retinal degeneration was induced by Müller cell ablation in mice. TBI was done by controlled cortical impact (CCI) in rat. SCI was done by a laminectomy at T11-12 level in mouse, or a brachial roots avulsion in rat.

Increasing evidence in the literature suggests that miR-223-3p may play multiple protective roles during neurodegenerative disease. In MS and EAE, miR-223-3p upregulation is associated with pathogenic polarization of immune cells and increased inflammation. *miR-223*^{-/-} EAE animals possess diminished populations of pathogenic T_h1 and T_h17 cells, either due to a larger population of myeloid-derived regulatory cells or reduced dendritic cell activation (Ifergan, Chen et al. 2016, Satoorian, Li et al. 2016, Cantoni, Cignarella et al. 2017). Yet the group of Dr. Craig Moore recently demonstrated a delay in EAE induction in *miR-223*^{-/-} mice versus WT-littermate controls (Galloway, Blandford et al. 2018). Using the model of lysolecithin-induced demyelination in the corpus callosum, they identified that miR-223 deletion impaired debris clearance and remyelination. This demonstrates that miR-223 promotes a repair macrophage/microglia phenotype. In addition, miR-223 has been demonstrated to play a role in dampening pro-inflammatory signaling via NF- κ B in microglia. NF- κ B signalling can be activated by A β , myelin peptides, and tau to mediate neuroinflammation and neurodegeneration (Srinivasan and Lahiri 2015). miR-223-3p targets several components of the NF- κ B pathway, including TRAF6, Tab1, Cub1ab, and IKK α (Li, Morgan et al. 2010, Zhou, Pal et al. 2018). Similarly, miR-27a-3p negatively regulates lipopolysaccharide-induced activation of microglia by targeting TLR4 and IRAK4 (Lv, Ou-Yang et al. 2017). By promoting the repair-driven phenotype of macrophages/microglia, miR-27a-3p and miR-223-3p prove to be applicable across all neurodegenerative diseases, as debris clearance is necessary for both axonal regeneration and remyelination.

An exciting next step would be to determine the direct mRNA targets of our miRNAs of interest. Currently we used *in silico* approaches and geared our results to what is relevant in neurons. With increasing knowledge about non-canonical mRNA targeting by miRNAs, to accurately determine the functional relevance of our miRNAs, we need to take additional non-biased target searches (Loeb, Khan et al. 2012, Helwak, Kudla et al. 2013, Flamand, Gan et al. 2017). The most direct approach to determine targets is to transfect cells of interest with a biotinylated miRNA-mimic and to pull it down by streptavidin-biotin immunoprecipitation. In complex with the miRNA-mimic we should find RISC, and relevant mRNA targets which can be identified by RNA-Seq. Determining if our EAE-identified miRNA can also travel between cells via exosomes is crucial as miRNAs target vastly different functions between cell types. Comparing biotinylated miRNA-mimic profiles between cell types would also paint us a bigger picture of what role our miRNAs of interest play. We discussed miR-27a-3p and miR-223-3p as mediating repair and regeneration in neurons and microglia. Perhaps they also promote phenotypes that limit and regeneration in astrocytes, or endothelial cells. These are important next questions when determining the efficacy of a miRNA as a druggable target, especially when said miRNA is promiscuously available via exosomal signaling.

6.4 miR-383-5p

We first identified miR-383-5p as the most downregulated miRNA in DRG neurons following a sciatic nerve lesion in mice, a model of neuronal survival and regeneration (Strickland, Richards et al. 2011). This is also true in rat DRG neurons following a sciatic nerve lesion (Zhou, Shen et al. 2012, Lu, Huang et al. 2014). We went on to confirm in Chapter 4 that in a CNS model of inflammation-mediated regeneration, neuronal miR-383-5p is also downregulated. We went on to demonstrate that miR-383-5p negatively regulates neurite outgrowth *in vitro*, and miR-383-5p antagonism promotes optic nerve regeneration *in vivo* through multiple relieved targets that mediate CNTF-driven JAK/STAT3 signaling, cytoskeleton rearrangement, and oxidative stress maintenance. It is worth considering if miR-383-5p can promote repair and regeneration in neurodegenerative disease, and if it contributes to any additional roles.

6.4.1 miR-383-5p in neurodegenerative disease

As emphasized earlier, deficits in axonal transport, oxidative stress, mitochondrial dysfunction, and inflammation are common themes across neurodegenerative diseases (Glass, Saijo et al. 2010, Burte, Carelli et al. 2015, Kim, Kim et al. 2015). Targeting each of these deficits individually is often not enough to promote repair and regeneration. For example, we know that CNTF mediates CNS regeneration through the Jak/STAT3 pathway (Muller, Hauk et al. 2007). Similarly, SOCS deletion promotes optic nerve regeneration, as SOCS3 inhibits Jak/STAT3 signaling (Smith, Sun et al. 2009). Yet, SOCS deletion alone does not promote functional improvement following CNS injury, and requires PTEN co-deletion, promoting activation of an additional pathway (Sun, Park et al. 2011, Jin, Liu et al. 2015). Antagonism of miR-383-5p targets many of the themes of neurodegenerative disease simultaneously, suggesting it is an effective means to promote repair and regeneration in neurodegenerative disease.

The targets of miR-383-5p have also been implicated in neurodegenerative disease. We described CNTF signaling through the CNTF receptor complex, targeted by miR-383-5p, as a means of optic nerve regeneration (Muller, Hauk et al. 2007). CNTF also promotes survival of sensory, sympathetic, and motor neurons, which has led to clinical studies in neurodegenerative diseases such as ALS and HD, though largely unsuccessful (Bloch, Bachoud-Levi et al. 2004, Bongioanni, Reali et al. 2004). Efforts have shifted to an implantable polymeric device containing a cell line that secretes CNTF (“NT-501”), developed by Neurotech Pharmaceuticals, for the treatment of an array of retinal or macular degeneration-related disorders such as achromatopsia, glaucoma, ischemic optic neuropathy, retinitis pigmentosa, macular telangiectasia, and AMD, as listed on clinicaltrials.gov (Emerich and Thanos 2008). The other targets of miR-383-5p, Crmp2 and Prdx3, have also been implicated in neurodegenerative disease. The active form of Crmp2 that promotes microtubule stabilization and neurite extension is unphosphorylated (Fukata, Itoh et al. 2002, Kimura, Watanabe et al. 2005, Tan, Cha et al. 2015). Hyperphosphorylated, thus inactive Crmp2, has been identified in the CNS of AD and MS (Williamson, van Aalten et al. 2011, Petratos, Ozturk et al. 2012). Likewise, non-functional, phosphorylated Prdx3 has been identified in PD, and associated with disrupted mitochondrial function and neuronal death in culture (Angeles, Gan et al. 2011).

Through miR-383-5p antagonism we can thus engage multiple pathways, rather than a single signaling cascade.

6.4.2 Determining additional roles of miR-383-5p

Our reports are the first implicating miR-383-5p in any neuronal functions. miR-383-5p is more largely known for its role in male infertility and cancer (Lian, Tian et al. 2010, Li, Pang et al. 2013, Tian, Cao et al. 2013). miR-383-5p forms a feedback loop with its target Fragile X Mental Retardation Protein (FMRP) during spermatogenesis, this loop is compromised during male infertility (Tian, Cao et al. 2013). FMRP is highly expressed in the testis as well as brain (Bassell and Warren 2008, Tian, Cao et al. 2013). FMRP is a selective-RNA binding protein that regulates many mRNAs in postsynaptic neurons, selectively binding about 4% of the total mammalian brain mRNAs (Bassell and Warren 2008). Loss of FMRP in humans causes fragile X syndrome, an inheritable form of autism spectrum disorder characterized by abnormal dendritic spines at the cellular level (Hagerman, Berry-Kravis et al. 2017). Altered dendritic spines implies altered synaptic function and neural circuits (Bassell and Warren 2008). As miR-383-5p targets FMRP, it implies that an increase in miR-383-5p can also affect dendritic spine formation, synaptic function, and neural circuit formation. Future experimental approaches with miR-383-5p would be to investigate the neuronal architecture following miR-383-5p functional assays to determine if it also impact dendritic spine morphology, and the formation of synaptic connections.

6.5 Making miR-iffic strides

We know that miRNAs regulate hubs of gene expression, and to understand how they modulate a system, we need to determine what hubs they are targeting. Can we target miRNAs for therapy, and are we already being targeted by miRNAs?

6.5.1 miRNAs as druggable targets

miRNAs are exciting drug targets as they regulate gene networks, lending us the ability to target multiple gene networks that are affected during disease (Friedman, Farh

et al. 2009). This is parallel to combinatorial drug approaches in the treatment and repair of CNS damage. Combinatorial approaches promoting the intrinsic potential and blocking the extrinsic factors simultaneously are successful in promoting regeneration past the lesion site in models of CNS injury (Kadoya, Tsukada et al. 2009, Garcia-Alias, Petrosyan et al. 2011, Wang, Hasan et al. 2012, Geoffroy, Lorenzana et al. 2015). A combinatorial approach has even been able to promote repair and regeneration when administered a year following SCI (Kadoya, Tsukada et al. 2009). Thus, multiprong approaches targeting several pathways are the most promising in the treatment of CNS injury. We demonstrated using AAV2-miR-223 overexpression in retinal neurons in EAE, as well as with an antagomiR targeting miR-383-5p during optic nerve injury, that these miRNA-targeted approaches are successful as they allow us to target major and/or multiple signaling hubs.

An emerging method of gene delivery in neurodegenerative DMTs is that of AAV2-packaging, demonstrating that miRNAs can also be delivered by AAV2-packaging for real-life applications in human CNS disease and injury. The AAV2 vector does not induce an adverse inflammatory reaction and is being safely using in clinical trials with long-lasting transgene expression (Daya and Berns 2008). Specifically, AAV2-mediated delivery of RPE65 by subretinal injection in individuals with inherited retinal dystrophy has shown success in a randomised, controlled, open-label, phase III trial (Russell, Bennett et al. 2017). Treated individuals showed significant vision improvement compared to control treated, this was a previously untreatable disease that lead to blindness. This is one example of a successful phase III trial. Many Phase I/II trials are currently underway using AAV-mediated gene delivery for various neurodegenerative diseases such as AD, ALS, HD, PD, and spinal muscular atrophy (SMA), as reviewed (Hocquemiller, Giersch et al. 2016). Thus, the use of AAV-directed miRNA delivery is an exciting tool for future neurodegenerative disease therapies. It is important to note though that exosomal sharing would be an important consideration when designing such tools. As we discussed, some miRNAs, such as miR-223-3p, are more prone for exosomal packaging (Shurtleff, Temoche-Diaz et al. 2016).

6.5.2 miRNAs are on the menu

You are what you eat, or at least 5% of you. Zhang *et al.* identified in a first publication of its kind, that about 5% of all miRNAs in human serum are plant-derived (Zhang, Hou et al. 2012). In the same report, plant-derived miR-168a-5p, abundant in rice, was found to target the human low-density lipoprotein receptor adapter protein 1 (LDLRAP1), demonstrating that plant miRNAs carry the capacity to regulate animal protein expression. Plant miRNAs have a naturally occurring methyl group on the ribose of their last nucleotides, making them resistant to oxidation (Yu, Yang et al. 2005). Thus, plant miRNAs are more stable than animal miRNAs, suggesting they can live in harsher environments such as the gut. In fact, dietary maize miRNAs have been shown to cross the gastrointestinal tract and enter the blood stream of pigs (Luo, Wang et al. 2017). Could plant miRNAs modify our gut microbiota? The gut microbiota refers to the plethora of bacteria colonizing the small and large intestines (Freedman, Shahi et al. 2018). The gut microbiota-brain axis, or gut-brain axis, is the bidirectional communication between the gut and CNS and is an emerging area of interest in neurodegenerative disease research, including AD, MS, and PD, as reviewed (Ghaisas, Maher et al. 2016, Freedman, Shahi et al. 2018). A very convincing experiment was the use of monozygotic twin pairs discordant for MS, where their microbiota were transferred to a transgenic mouse model of spontaneous brain autoimmunity (Berer, Gerdes et al. 2017). MS-derived microbiota induced a significantly higher incidence of autoimmunity than healthy twin-derived microbiota. Can plant miRNAs be participating in the composition of the gut microbiota, and if so, is this contributing to a neurodegenerative disease-related gut-brain axis?

6.4 Conclusion

CNS damage is marked by neuroinflammation. In this thesis we sought to identify and harness the positive aspects of neuroinflammation to promote repair and regeneration following CNS damage, either via neurodegenerative disease or acute injury. We defined a molecular approach to regulate programs of gene expression in neurons in response to injury to mediate neuroprotection or repair. We focused on miRNAs as a single miRNA can target multiple mRNA transcripts from either a shared pathway, or from functionally unrelated pathways (Friedman, Farh et al. 2009). Using models of neuroinflammation, we determined the global neuronal response to inflammation and developed molecular strategies that promote neuroprotection and repair. Ultimately our findings can improve our approach in the development of therapies that promote repair and regeneration following CNS damage.

References

- Abbott, N. J., A. A. K. Patabendige, D. E. M. Dolman, S. R. Yusof and D. J. Begley (2010). "Structure and function of the blood-brain barrier." *Neurobiology of Disease* **37**(1): 13-25.
- Absalon, S., D. M. Kochanek, V. Raghavan and A. M. Krichevsky (2013). "MiR-26b, upregulated in Alzheimer's disease, activates cell cycle entry, tau-phosphorylation, and apoptosis in postmitotic neurons." *Journal of Neuroscience* **33**(37): 14645-14659.
- Agarwal, V., G. W. Bell, J. W. Nam and D. P. Bartel (2015). "Predicting effective microRNA target sites in mammalian mRNAs." *Elife* **4**.
- Ahmadian-Elmi, M., A. Bidmeshki Pour, R. Naghavian, K. Ghaedi, S. Tanhaei, T. Izadi and M. H. Nasr-Esfahani (2016). "miR-27a and miR-214 exert opposite regulatory roles in Th17 differentiation via mediating different signaling pathways in peripheral blood CD4+ T lymphocytes of patients with relapsing-remitting multiple sclerosis." *Immunogenetics* **68**(1): 43-54.
- Akhtar, S., S. R. Patnaik, R. Kotapati Raghupathy, T. M. Al-Mubrad, J. A. Craft and X. Shu (2015). "Histological Characterization of the Dicer1 Mutant Zebrafish Retina." *J Ophthalmol* **2015**: 309510.
- Alam, T., H. Maruyama, C. Li, S. I. Pastuhov, P. Nix, M. Bastiani, N. Hisamoto and K. Matsumoto (2016). "Axotomy-induced HIF-serotonin signalling axis promotes axon regeneration in *C. elegans*." *Nat Commun* **7**: 10388.
- Albertson, A. J., H. Talbott, Q. Wang, D. Jensen and D. C. Skinner (2008). "The gonadotropin-releasing hormone type I receptor is expressed in the mouse cerebellum." *Cerebellum* **7**(3): 379-384.
- Alvarez-Erviti, L., Y. Seow, H. Yin, C. Betts, S. Lakhali and M. J. Wood (2011). "Delivery of siRNA to the mouse brain by systemic injection of targeted exosomes." *Nat Biotechnol* **29**(4): 341-345.
- Ambros, V., B. Bartel, D. P. Bartel, C. B. Burge, J. C. Carrington, X. Chen, G. Dreyfuss, S. R. Eddy, S. Griffiths-Jones, M. Marshall, M. Matzke, G. Ruvkun and T. Tuschl (2003). "A uniform system for microRNA annotation." *RNA* **9**(3): 277-279.
- Anderson, M. A., J. E. Burda, Y. Ren, Y. Ao, T. M. O'Shea, R. Kawaguchi, G. Coppola, B. S. Khakh, T. J. Deming and M. V. Sofroniew (2016). "Astrocyte scar formation aids central nervous system axon regeneration." *Nature* **532**(7598): 195-200.
- Angeles, D. C., B. H. Gan, L. Onstead, Y. Zhao, K. L. Lim, J. Dachsel, H. Melrose, M. Farrer, Z. K. Wszolek, D. W. Dickson and E. K. Tan (2011). "Mutations in LRRK2 increase phosphorylation of peroxiredoxin 3 exacerbating oxidative stress-induced neuronal death." *Hum Mutat* **32**(12): 1390-1397.
- Antel, J., S. Antel, Z. Caramanos, D. L. Arnold and T. Kuhlmann (2012). "Primary progressive multiple sclerosis: part of the MS disease spectrum or separate disease entity?" *Acta Neuropathol* **123**(5): 627-638.
- Arimura, N., A. Hattori, T. Kimura, S. Nakamuta, Y. Funahashi, S. Hirotsune, K. Furuta, T. Urano, Y. Y. Toyoshima and K. Kaibuchi (2009). "CRMP-2 directly binds to cytoplasmic dynein and interferes with its activity." *J Neurochem* **111**(2): 380-390.
- Aspelund, A., S. Antila, S. T. Proulx, T. V. Karlsen, S. Karaman, M. Detmar, H. Wiig and K. Alitalo (2015). "A dural lymphatic vascular system that drains brain interstitial fluid and macromolecules." *Journal of Experimental Medicine* **212**(7): 991-999.
- Aung, L. L. and K. E. Balashov (2015). "Decreased Dicer expression is linked to increased expression of co-stimulatory molecule CD80 on B cells in multiple sclerosis." *Multiple Sclerosis* **21**(9): 1131-1138.
- Balk, L. J., A. Cruz-Herranz, P. Albrecht, S. Arnow, J. M. Gelfand, P. Tewarie, J. Killestein, B. M. Uitdehaag, A. Petzold and A. J. Green (2016). "Timing of retinal neuronal and axonal loss in MS: a longitudinal OCT study." *J Neurol* **263**(7): 1323-1331.

Bannerman, P. G., A. Hahn, S. Ramirez, M. Morley, C. Bonnemann, S. Yu, G. X. Zhang, A. Rostami and D. Pleasure (2005). "Motor neuron pathology in experimental autoimmune encephalomyelitis: studies in THY1-YFP transgenic mice." *Brain* **128**(Pt 8): 1877-1886.

Barak, B., I. Shvarts-Serebro, S. Modai, A. Gilam, E. Okun, D. M. Michaelson, M. P. Mattson, N. Shomron and U. Ashery (2013). "Opposing actions of environmental enrichment and Alzheimer's disease on the expression of hippocampal microRNAs in mouse models." *Transl Psychiatry* **3**: e304.

Baranova, O., L. F. Miranda, P. Pichiule, I. Dragatsis, R. S. Johnson and J. C. Chavez (2007). "Neuron-specific inactivation of the hypoxia inducible factor 1 alpha increases brain injury in a mouse model of transient focal cerebral ischemia." *J Neurosci* **27**(23): 6320-6332.

Bartel, D. P. (2004). "MicroRNAs: genomics, biogenesis, mechanism, and function." *Cell* **116**(2): 281-297.

Bartel, D. P. (2009). "MicroRNAs: target recognition and regulatory functions." *Cell* **136**(2): 215-233.

Bassell, G. J. and S. T. Warren (2008). "Fragile X syndrome: loss of local mRNA regulation alters synaptic development and function." *Neuron* **60**(2): 201-214.

Baulina, N., O. Kulakova, I. Kiselev, G. Osmak, E. Popova, A. Boyko and O. Favorova (2018). "Immune-related miRNA expression patterns in peripheral blood mononuclear cells differ in multiple sclerosis relapse and remission." *J Neuroimmunol*.

Belin, S., H. Nawabi, C. Wang, S. Tang, A. Latremoliere, P. Warren, H. Schorle, C. Uncu, C. J. Woolf, Z. He and J. A. Steen (2015). "Injury-induced decline of intrinsic regenerative ability revealed by quantitative proteomics." *Neuron* **86**(4): 1000-1014.

Benizri, E., A. Ginouves and E. Berra (2008). "The magic of the hypoxia-signaling cascade." *Cell Mol Life Sci* **65**(7-8): 1133-1149.

Berer, K., L. A. Gerdes, E. Cekanaviciute, X. Jia, L. Xiao, Z. Xia, C. Liu, L. Klotz, U. Stauffer, S. E. Baranzini, T. Kumpfel, R. Hohlfeld, G. Krishnamoorthy and H. Wekerle (2017). "Gut microbiota from multiple sclerosis patients enables spontaneous autoimmune encephalomyelitis in mice." *Proc Natl Acad Sci U S A* **114**(40): 10719-10724.

Bergman, P., T. James, L. Kular, S. Ruhrmann, T. Kramarova, A. Kvist, G. Supic, A. Gillett, A. Pivarcsi and M. Jagodic (2013). "Next-generation sequencing identifies microRNAs that associate with pathogenic autoimmune neuroinflammation in rats." *J Immunol* **190**(8): 4066-4075.

Bergman, P., T. James, L. Kular, S. Ruhrmann, T. Kramarova, A. Kvist, G. Supic, A. Gillett, A. Pivarcsi and M. Jagodic (2013). "Next-generation sequencing identifies microRNAs that associate with pathogenic autoimmune neuroinflammation in rats." *Journal of Immunology* **190**(8): 4066-4075.

Berkelaar, M., D. B. Clarke, Y. C. Wang, G. M. Bray and A. J. Aguayo (1994). "Axotomy Results in Delayed Death and Apoptosis of Retinal Ganglion-Cells in Adult-Rats." *Journal of Neuroscience* **14**(7): 4368-4374.

Bermel, R. A. and R. Bakshi (2006). "The measurement and clinical relevance of brain atrophy in multiple sclerosis." *Lancet Neurol* **5**(2): 158-170.

Betel, D., M. Wilson, A. Gabow, D. S. Marks and C. Sander (2008). "The microRNA.org resource: targets and expression." *Nucleic Acids Res* **36**(Database issue): D149-153.

Bhalala, O. G., M. Srikanth and J. A. Kessler (2013). "The emerging roles of microRNAs in CNS injuries." *Nat Rev Neurol* **9**(6): 328-339.

Bittner, S., A. M. Afzali, H. Wiendl and S. G. Meuth (2014). "Myelin oligodendrocyte glycoprotein (MOG35-55) induced experimental autoimmune encephalomyelitis (EAE) in C57BL/6 mice." *J Vis Exp*(86).

Bjartmar, C., G. Kidd, S. Mork, R. Rudick and B. Trapp (2000). "Neurological disability correlates with spinal cord axonal loss and reduced N-acetyl aspartate in chronic multiple sclerosis patients." *Annals of Neurology* **48**(6): 893-901.

Bloch, J., A. C. Bachoud-Levi, N. Deglon, J. P. Lefaucheur, L. Winkel, S. Palfi, J. P. Nguyen, C. Bourdet, V. Gaura, P. Remy, P. Brugieres, M. F. Boisse, S. Baudic, P. Cesaro, P. Hantraye, P. Aebischer and M. Peschanski (2004). "Neuroprotective gene therapy for Huntington's disease, using polymer-

encapsulated cells engineered to secrete human ciliary neurotrophic factor: results of a phase I study." *Hum Gene Ther* **15**(10): 968-975.

Bongioanni, P., C. Reali and V. Sogos (2004). "Ciliary neurotrophic factor (CNTF) for amyotrophic lateral sclerosis/motor neuron disease." *Cochrane Database Syst Rev*(3): CD004302.

Bradbury, E. J., L. D. Moon, R. J. Popat, V. R. King, G. S. Bennett, P. N. Patel, J. W. Fawcett and S. B. McMahon (2002). "Chondroitinase ABC promotes functional recovery after spinal cord injury." *Nature* **416**(6881): 636-640.

Bredesen, D. E., R. V. Rao and P. Mehlen (2006). "Cell death in the nervous system." *Nature* **443**(7113): 796-802.

Briggs, C. E., Y. Wang, B. Kong, T. U. Woo, L. K. Iyer and K. C. Sonntag (2015). "Midbrain dopamine neurons in Parkinson's disease exhibit a dysregulated miRNA and target-gene network." *Brain Res* **1618**: 111-121.

Burte, F., V. Carelli, P. F. Chinnery and P. Yu-Wai-Man (2015). "Disturbed mitochondrial dynamics and neurodegenerative disorders." *Nat Rev Neurol* **11**(1): 11-24.

Butovsky, O., S. Siddiqui, G. Gabriely, A. J. Lanser, B. Dake, G. Murugaiyan, C. E. Doykan, P. M. Wu, R. R. Gali, L. K. Iyer, R. Lawson, J. Berry, A. M. Krichevsky, M. E. Cudkowicz and H. L. Weiner (2012). "Modulating inflammatory monocytes with a unique microRNA gene signature ameliorates murine ALS." *J Clin Invest* **122**(9): 3063-3087.

Cai, D., J. Qiu, Z. Cao, M. McAtee, B. S. Bregman and M. T. Filbin (2001). "Neuronal cyclic AMP controls the developmental loss in ability of axons to regenerate." *J Neurosci* **21**(13): 4731-4739.

Cai, Q., T. Wang, W. J. Yang and X. Fen (2016). "Protective mechanisms of microRNA-27a against oxygen-glucose deprivation-induced injuries in hippocampal neurons." *Neural Regen Res* **11**(8): 1285-1292.

Calabrese, M., R. Magliozzi, O. Ciccarelli, J. J. Geurts, R. Reynolds and R. Martin (2015). "Exploring the origins of grey matter damage in multiple sclerosis." *Nat Rev Neurosci* **16**(3): 147-158.

Campos-Melo, D., C. A. Droppelmann, Z. He, K. Volkening and M. J. Strong (2013). "Altered microRNA expression profile in Amyotrophic Lateral Sclerosis: a role in the regulation of NFL mRNA levels." *Molecular Brain* **6**: 26.

Canada, M. S. o. (2018). "Disease-modifying therapies." from <https://mssociety.ca/managing-ms/treatments/medications/disease-modifying-therapies-dmts>.

Cantoni, C., F. Cignarella, L. Ghezzi, B. Mikesell, B. Bollman, M. M. Berrien-Elliott, A. R. Ireland, T. A. Fehniger, G. F. Wu and L. Piccio (2017). "Mir-223 regulates the number and function of myeloid-derived suppressor cells in multiple sclerosis and experimental autoimmune encephalomyelitis." *Acta Neuropathol* **133**(1): 61-77.

Carassiti, D., D. R. Altmann, N. Petrova, B. Pakkenberg, F. Scaravilli and K. Schmierer (2018). "Neuronal loss, demyelination and volume change in the multiple sclerosis neocortex." *Neuropathology and Applied Neurobiology* **44**(4): 377-390.

Cartoni, R., G. Pekkurnaz, C. Wang, T. L. Schwarz and Z. He (2017). "A high mitochondrial transport rate characterizes CNS neurons with high axonal regeneration capacity." *PLoS One* **12**(9): e0184672.

Charcot, J. M. (1868). *Histologie de la sclérose en plaques*. Paris.

Charil, A., A. P. Zijdenbos, J. Taylor, C. Boelman, K. J. Worsley, A. C. Evans and A. Dagher (2003). "Statistical mapping analysis of lesion location and neurological disability in multiple sclerosis: application to 452 patient data sets." *Neuroimage* **19**(3): 532-544.

Chen, C., D. A. Ridzon, A. J. Broomer, Z. Zhou, D. H. Lee, J. T. Nguyen, M. Barbisin, N. L. Xu, V. R. Mahuvakar, M. R. Andersen, K. Q. Lao, K. J. Livak and K. J. Guegler (2005). "Real-time quantification of microRNAs by stem-loop RT-PCR." *Nucleic Acids Res* **33**(20): e179.

Chen, C., A. Wirth and E. Ponimaskin (2012). "Cdc42: an important regulator of neuronal morphology." *Int J Biochem Cell Biol* **44**(3): 447-451.

Chen, D. F., S. Jhaveri and G. E. Schneider (1995). "Intrinsic Changes in Developing Retinal Neurons Result in Regenerative Failure of Their Axons." Proceedings of the National Academy of Sciences of the United States of America **92**(16): 7287-7291.

Chen, Y. C., T. Liu, C. H. Yu, T. Y. Chiang and C. C. Hwang (2013). "Effects of GC bias in next-generation-sequencing data on de novo genome assembly." PLoS One **8**(4): e62856.

Cheng, L., P. Sapieha, P. Kittlerova, W. W. Hauswirth and A. Di Polo (2002). "TrkB gene transfer protects retinal ganglion cells from axotomy-induced death in vivo." J Neurosci **22**(10): 3977-3986.

Cheng, S., C. Zhang, C. Xu, L. Wang, X. Zou and G. Chen (2014). "Age-dependent neuron loss is associated with impaired adult neurogenesis in forebrain neuron-specific Dicer conditional knockout mice." Int J Biochem Cell Biol **57**: 186-196.

Chiaravalloti, N. D. and J. DeLuca (2008). "Cognitive impairment in multiple sclerosis." Lancet Neurol **7**(12): 1139-1151.

Chidlow, G., J. P. M. Wood, B. Knoop and R. J. Casson (2016). "Expression and distribution of peroxiredoxins in the retina and optic nerve." Brain Structure & Function **221**(8): 3903-3925.

Chmielarz, P., J. Konovalova, S. S. Najam, H. Alter, T. P. Piepponen, H. Erfle, K. C. Sonntag, G. Schutz, I. A. Vinnikov and A. Domanskyi (2017). "Dicer and microRNAs protect adult dopamine neurons." Cell Death Dis **8**(5): e2813.

Cho, Y., J. E. Shin, E. E. Ewan, Y. M. Oh, W. Pita-Thomas and V. Cavalli (2015). "Activating Injury-Responsive Genes with Hypoxia Enhances Axon Regeneration through Neuronal HIF-1alpha." Neuron **88**(4): 720-734.

Chou, C. H., N. W. Chang, S. Shrestha, S. D. Hsu, Y. L. Lin, W. H. Lee, C. D. Yang, H. C. Hong, T. Y. Wei, S. J. Tu, T. R. Tsai, S. Y. Ho, T. Y. Jian, H. Y. Wu, P. R. Chen, N. C. Lin, H. T. Huang, T. L. Yang, C. Y. Pai, C. S. Tai, W. L. Chen, C. Y. Huang, C. C. Liu, S. L. Weng, K. W. Liao, W. L. Hsu and H. D. Huang (2016). "miRTarBase 2016: updates to the experimentally validated miRNA-target interactions database." Nucleic Acids Res **44**(D1): D239-247.

Chu, F., M. Shi, C. Zheng, D. Shen, J. Zhu, X. Zheng and L. Cui (2018). "The roles of macrophages and microglia in multiple sclerosis and experimental autoimmune encephalomyelitis." J Neuroimmunol **318**: 1-7.

Chung, S. H., M. Gillies, Y. Sugiyama, L. Zhu, S. R. Lee and W. Shen (2015). "Profiling of microRNAs involved in retinal degeneration caused by selective Muller cell ablation." PLoS One **10**(3): e0118949.

Chung, S. H., M. Gillies, M. Yam, Y. Wang and W. Shen (2016). "Differential expression of microRNAs in retinal vasculopathy caused by selective Muller cell disruption." Sci Rep **6**: 28993.

Cogswell, J. P., J. Ward, I. A. Taylor, M. Waters, Y. Shi, B. Cannon, K. Kelnar, J. Kemppainen, D. Brown, C. Chen, R. K. Prinjha, J. C. Richardson, A. M. Saunders, A. D. Roses and C. A. Richards (2008). "Identification of miRNA changes in Alzheimer's disease brain and CSF yields putative biomarkers and insights into disease pathways." Journal of Alzheimer's Disease **14**(1): 27-41.

Compston, A. and A. Coles (2008). "Multiple sclerosis." Lancet **372**: 1502-1517.

Cox, M. B., M. J. Cairns, K. S. Gandhi, A. P. Carroll, S. Moscovis, G. J. Stewart, S. Broadley, R. J. Scott, D. R. Booth, J. Lechner-Scott and A. N. M. S. G. Consortium (2010). "MicroRNAs miR-17 and miR-20a inhibit T cell activation genes and are under-expressed in MS whole blood." PLoS One **5**(8): e12132.

Criste, G., B. Trapp and R. Dutta (2014). "Axonal loss in multiple sclerosis: causes and mechanisms." Handb Clin Neurol **122**: 101-113.

Cuellar, T. L., T. H. Davis, P. T. Nelson, G. B. Loeb, B. D. Harfe, E. Ullian and M. T. McManus (2008). "Dicer loss in striatal neurons produces behavioral and neuroanatomical phenotypes in the absence of neurodegeneration." Proc Natl Acad Sci U S A **105**(14): 5614-5619.

Cui, Q., Z. Yu, E. O. Purisima and E. Wang (2006). "Principles of microRNA regulation of a human cellular signaling network." Mol Syst Biol **2**: 46.

Da Mesquita, S., A. Louveau, A. Vaccari, I. Smirnov, R. C. Cornelison, K. M. Kingsmore, C. Contarino, S. Onengut-Gumuscu, E. Farber, D. Raper, K. E. Viar, R. D. Powell, W. Baker, N. Dabhi, R. Bai, R. Cao, S. Hu, S. S. Rich, J. M. Munson, M. B. Lopes, C. C. Overall, S. T. Acton and J. Kipnis (2018). "Functional aspects of meningeal lymphatics in ageing and Alzheimer's disease." *Nature* **560**(7717): 185-191.

Damiani, D., J. J. Alexander, J. R. O'Rourke, M. McManus, A. P. Jadhav, C. L. Cepko, W. W. Hauswirth, B. D. Harfe and E. Strettoi (2008). "Dicer inactivation leads to progressive functional and structural degeneration of the mouse retina." *J Neurosci* **28**(19): 4878-4887.

Dang, C. V. (2013). "MYC, metabolism, cell growth, and tumorigenesis." *Cold Spring Harb Perspect Med* **3**(8).

David, S. and A. J. Aguayo (1981). "Axonal Elongation into Peripheral Nervous-System Bridges after Central Nervous-System Injury in Adult-Rats." *Science* **214**(4523): 931-933.

David, S., J. G. Zarruk and N. Ghasemlou (2012). "Inflammatory Pathways in Spinal Cord Injury." *Axon Growth and Regeneration, Pt 2* **106**: 127-152.

Davidson, B. L., C. S. Stein, J. A. Heth, I. Martins, R. M. Kotin, T. A. Derksen, J. Zabner, A. Ghodsi and J. A. Chiorini (2000). "Recombinant adeno-associated virus type 2, 4, and 5 vectors: transduction of variant cell types and regions in the mammalian central nervous system." *Proc Natl Acad Sci U S A* **97**(7): 3428-3432.

Daya, S. and K. I. Berns (2008). "Gene therapy using adeno-associated virus vectors." *Clin Microbiol Rev* **21**(4): 583-593.

de Faria Jr, O., C. S. Moore, T. E. Kennedy, J. P. Antel, A. Bar-Or and A. S. Dhaunchak (2012). "MicroRNA dysregulation in multiple sclerosis." *Front Genet* **3**: 311.

de Faria, O., Jr., Q. L. Cui, J. M. Bin, S. J. Bull, T. E. Kennedy, A. Bar-Or, J. P. Antel, D. R. Colman and A. S. Dhaunchak (2012). "Regulation of miRNA 219 and miRNA Clusters 338 and 17-92 in Oligodendrocytes." *Front Genet* **3**: 46.

De Santis, G., M. Ferracin, A. Biondani, L. Caniatti, M. Rosaria Tola, M. Castellazzi, B. Zagatti, L. Battistini, G. Borsellino, E. Fainardi, R. Gavioli, M. Negrini, R. Furlan and E. Granieri (2010). "Altered miRNA expression in T regulatory cells in course of multiple sclerosis." *Journal of Neuroimmunology* **226**(1-2): 165-171.

De Santis, G., M. Ferracin, A. Biondani, L. Caniatti, M. Rosaria Tola, M. Castellazzi, B. Zagatti, L. Battistini, G. Borsellino, E. Fainardi, R. Gavioli, M. Negrini, R. Furlan and E. Granieri (2010). "Altered miRNA expression in T regulatory cells in course of multiple sclerosis." *J Neuroimmunol* **226**(1-2): 165-171.

De Simoni, S., J. Goemaere and B. Knoop (2008). "Silencing of peroxiredoxin 3 and peroxiredoxin 5 reveals the role of mitochondrial peroxiredoxins in the protection of human neuroblastoma SH-SY5Y cells toward MPP+." *Neurosci Lett* **433**(3): 219-224.

De Stefano, N., P. M. Matthews, L. Fu, S. Narayanan, J. Stanley, G. S. Francis, J. P. Antel and D. L. Arnold (1998). "Axonal damage correlates with disability in patients with relapsing-remitting multiple sclerosis. Results of a longitudinal magnetic resonance spectroscopy study." *Brain* **121** (Pt 8): 1469-1477.

Dendrou, C. A., L. Fugger and M. A. Friese (2015). "Immunopathology of multiple sclerosis." *Nat Rev Immunol* **15**(9): 545-558.

Diez-Planelles, C., P. Sanchez-Lozano, M. C. Crespo, J. Gil-Zamorano, R. Ribacoba, N. Gonzalez, E. Suarez, A. Martinez-Descals, P. Martinez-Cambor, V. Alvarez, R. Martin-Hernandez, I. Huerta-Ruiz, I. Gonzalez-Garcia, J. M. Cosgaya, F. Visioli, A. Davalos, E. Iglesias-Gutierrez and C. Tomas-Zapico (2016). "Circulating microRNAs in Huntington's disease: Emerging mediators in metabolic impairment." *Pharmacol Res* **108**: 102-110.

DiSabato, D. J., N. Quan and J. P. Godbout (2016). "Neuroinflammation: the devil is in the details." *J Neurochem* **139** Suppl 2: 136-153.

Donatelli, S. S., J. M. Zhou, D. L. Gilvary, E. A. Eksioğlu, X. Chen, W. D. Cress, E. B. Haura, M. B. Schabath, D. Coppola, S. Wei and J. Y. Djeu (2014). "TGF-beta-inducible microRNA-183 silences tumor-associated natural killer cells." *Proc Natl Acad Sci U S A* **111**(11): 4203-4208.

Donnelly, D. J. and P. G. Popovich (2008). "Inflammation and its role in neuroprotection, axonal regeneration and functional recovery after spinal cord injury." *Exp Neurol* **209**(2): 378-388.

Dutta, R., A. M. Chomyk, A. Chang, M. V. Ribaldo, S. A. Deckard, M. K. Doud, D. D. Edberg, B. Bai, M. Li, S. E. Baranzini, R. J. Fox, S. M. Staugaitis, W. B. Macklin and B. D. Trapp (2013). "Hippocampal demyelination and memory dysfunction are associated with increased levels of the neuronal microRNA miR-124 and reduced AMPA receptors." *Ann Neurol* **73**(5): 637-645.

Dutta, R. and B. D. Trapp (2007). "Pathogenesis of axonal and neuronal damage in multiple sclerosis." *Neurology* **68**(22 Suppl 3): S22-31; discussion S43-54.

Dutta, R. and B. D. Trapp (2011). "Mechanisms of neuronal dysfunction and degeneration in multiple sclerosis." *Prog Neurobiol* **93**(1): 1-12.

Ebert, M. S., J. R. Neilson and P. A. Sharp (2007). "MicroRNA sponges: competitive inhibitors of small RNAs in mammalian cells." *Nat Methods* **4**(9): 721-726.

Ebert, M. S. and P. A. Sharp (2010). "MicroRNA sponges: progress and possibilities." *RNA* **16**(11): 2043-2050.

Ebrahimkhani, S., F. Vafae, P. E. Young, S. S. J. Hur, S. Hawke, E. Devenney, H. Beadnall, M. H. Barnett, C. M. Suter and M. E. Buckland (2017). "Exosomal microRNA signatures in multiple sclerosis reflect disease status." *Sci Rep* **7**(1): 14293.

Edstrom, E., S. Kullberg, Y. Ming, H. Zheng and B. Ulfhake (2004). "MHC class I, beta2 microglobulin, and the INF-gamma receptor are upregulated in aged motoneurons." *J Neurosci Res* **78**(6): 892-900.

Emerich, D. F. and C. G. Thanos (2008). "NT-501: an ophthalmic implant of polymer-encapsulated ciliary neurotrophic factor-producing cells." *Curr Opin Mol Ther* **10**(5): 506-515.

Eminaga, S., D. C. Christodoulou, F. Vigneault, G. M. Church and J. G. Seidman (2013). "Quantification of microRNA expression with next-generation sequencing." *Curr Protoc Mol Biol* **Chapter 4**: Unit 4 17.

Ertekin, S., O. Yildirim, E. Dinc, L. Ayaz, S. B. Fidanci and L. Tamer (2014). "Evaluation of circulating miRNAs in wet age-related macular degeneration." *Mol Vis* **20**: 1057-1066.

Erturk, A., F. Hellal, J. Enes and F. Bradke (2007). "Disorganized microtubules underlie the formation of retraction bulbs and the failure of axonal regeneration." *J Neurosci* **27**(34): 9169-9180.

Evonuk, K., Doyle, R., Moseley, C. Thornell, I., Adler, K., Bingaman, A., Bevensee, M., Weaver, C., Min, B., DeSilva, T. (2018). Selective reduction of AMPA receptors on mature oligodendrocytes prevents demyelination and axonal injury in experimental autoimmune encephalomyelitis. European Committee for Treatment and Research in MS, Berlin, Germany.

Fenoglio, C., E. Ridolfi, C. Cantoni, M. De Riz, R. Bonsi, M. Serpente, C. Villa, A. M. Pietroboni, R. T. Naismith, E. Alvarez, B. J. Parks, N. Bresolin, A. H. Cross, L. M. Piccio, D. Galimberti and E. Scarpini (2013). "Decreased circulating miRNA levels in patients with primary progressive multiple sclerosis." *Mult Scler* **19**(14): 1938-1942.

Ferguson, B., M. K. Matyszak, M. M. Esiri and V. H. Perry (1997). "Axonal damage in acute multiple sclerosis lesions." *Brain* **120 (Pt 3)**: 393-399.

Filipowicz, W., S. N. Bhattacharyya and N. Sonenberg (2008). "Mechanisms of post-transcriptional regulation by microRNAs: are the answers in sight?" *Nat Rev Genet* **9**(2): 102-114.

Filippi, M., A. Bar-Or, F. Piehl, P. Preziosa, A. Solari, S. Vukusic and M. A. Rocca (2018). "Multiple sclerosis." *Nat Rev Dis Primers* **4**(1): 43.

Filippi, M., P. Preziosa, M. Copetti, G. Riccitelli, M. A. Horsfield, V. Martinelli, G. Comi and M. A. Rocca (2013). "Gray matter damage predicts the accumulation of disability 13 years later in MS." *Neurology* **81**(20): 1759-1767.

Fiorenza, A., J. P. Lopez-Atalaya, V. Rovira, M. Scandaglia, E. Geijo-Barrientos and A. Barco (2016). "Blocking miRNA Biogenesis in Adult Forebrain Neurons Enhances Seizure Susceptibility, Fear Memory, and Food Intake by Increasing Neuronal Responsiveness." *Cereb Cortex* **26**(4): 1619-1633.

Fisher, J. B., D. A. Jacobs, C. E. Markowitz, S. L. Galetta, N. J. Volpe, M. L. Nano-Schiavi, M. L. Baier, E. M. Frohman, H. Winslow, T. C. Frohman, P. A. Calabresi, M. G. Maguire, G. R. Cutter and L. J. Balcer (2006). "Relation of visual function to retinal nerve fiber layer thickness in multiple sclerosis." *Ophthalmology* **113**(2): 324-332.

Fitch, M. T., C. Doller, C. K. Combs, G. E. Landreth and J. Silver (1999). "Cellular and molecular mechanisms of glial scarring and progressive cavitation: in vivo and in vitro analysis of inflammation-induced secondary injury after CNS trauma." *J Neurosci* **19**(19): 8182-8198.

Fitch, M. T. and J. Silver (2008). "CNS injury, glial scars, and inflammation: Inhibitory extracellular matrices and regeneration failure." *Exp Neurol* **209**(2): 294-301.

Flamand, M. N., H. H. Gan, V. K. Mayya, K. C. Gunsalus and T. F. Duchaine (2017). "A non-canonical site reveals the cooperative mechanisms of microRNA-mediated silencing." *Nucleic Acids Res* **45**(12): 7212-7225.

Fleige, S., V. Walf, S. Huch, C. Prgomet, J. Sehm and M. W. Pfaffl (2006). "Comparison of relative mRNA quantification models and the impact of RNA integrity in quantitative real-time RT-PCR." *Biotechnol Lett* **28**(19): 1601-1613.

Forcet, C., E. Stein, L. Pays, V. Corset, F. Llambi, M. Tessier-Lavigne and P. Mehlen (2002). "Netrin-1-mediated axon outgrowth requires deleted in colorectal cancer-dependent MAPK activation." *Nature* **417**(6887): 443-447.

Fournier, A. E., T. GrandPre and S. M. Strittmatter (2001). "Identification of a receptor mediating Nogo-66 inhibition of axonal regeneration." *Nature* **409**(6818): 341-346.

Freedman, S. N., S. K. Shahi and A. K. Mangalam (2018). "The "Gut Feeling": Breaking Down the Role of Gut Microbiome in Multiple Sclerosis." *Neurotherapeutics* **15**(1): 109-125.

Friedman, R. C., K. K. Farh, C. B. Burge and D. P. Bartel (2009). "Most mammalian mRNAs are conserved targets of microRNAs." *Genome Res* **19**(1): 92-105.

Frohman, E. M., M. K. Racke and C. S. Raine (2006). "Multiple sclerosis--the plaque and its pathogenesis." *N Engl J Med* **354**(9): 942-955.

Fruhbeis, C., D. Frohlich and E. M. Kramer-Albers (2012). "Emerging roles of exosomes in neuron-glia communication." *Front Physiol* **3**: 119.

Fukata, Y., T. J. Itoh, T. Kimura, C. Menager, T. Nishimura, T. Shiromizu, H. Watanabe, N. Inagaki, A. Iwamatsu, H. Hotani and K. Kaibuchi (2002). "CRMP-2 binds to tubulin heterodimers to promote microtubule assembly." *Nat Cell Biol* **4**(8): 583-591.

Galindo-Romero, C., M. Aviles-Trigueros, M. Jimenez-Lopez, F. J. Valiente-Soriano, M. Salinas-Navarro, F. Nadal-Nicolas, M. P. Villegas-Perez, M. Vidal-Sanz and M. Agudo-Barriuso (2011). "Axotomy-induced retinal ganglion cell death in adult mice: quantitative and topographic time course analyses." *Exp Eye Res* **92**(5): 377-387.

Galloway, D. A., S. N. Blandford, T. Berry, J. B. Williams, M. Stefanelli, M. Ploughman and C. S. Moore (2018). "miR-223 promotes regenerative myeloid cell phenotype and function in the demyelinated central nervous system." *Glia*.

Galloway, D. A., J. B. Williams and C. S. Moore (2017). "Effects of fumarates on inflammatory human astrocyte responses and oligodendrocyte differentiation." *Ann Clin Transl Neurol* **4**(6): 381-391.

Garcia-Alias, G., H. A. Petrosyan, L. Schnell, P. J. Horner, W. J. Bowers, L. M. Mendell, J. W. Fawcett and V. L. Arvanian (2011). "Chondroitinase ABC Combined with Neurotrophin NT-3 Secretion and NR2D Expression Promotes Axonal Plasticity and Functional Recovery in Rats with Lateral Hemisection of the Spinal Cord." *Journal of Neuroscience* **31**(49): 17788-17799.

Gass, A. and F. E. Costello (2018). "Optic neuritis in the diagnosis of MS More than meets the eye." Neurology **91**(12): 545-546.

Geddes, J. F., G. H. Vowles, T. W. Beer and D. W. Ellison (1997). "The diagnosis of diffuse axonal injury: implications for forensic practice." Neuropathol Appl Neurobiol **23**(4): 339-347.

Gensel, J. C., S. Nakamura, Z. Guan, N. van Rooijen, D. P. Ankeny and P. G. Popovich (2009). "Macrophages promote axon regeneration with concurrent neurotoxicity." J Neurosci **29**(12): 3956-3968.

Gentleman, S. M., M. J. Nash, C. J. Sweeting, D. I. Graham and G. W. Roberts (1993). "Beta-Amyloid Precursor Protein (Beta-APP) as a Marker for Axonal Injury after Head-Injury." Neuroscience Letters **160**(2): 139-144.

Geoffroy, C. G., A. O. Lorenzana, J. P. Kwan, K. Lin, O. Ghassemi, A. Ma, N. Xu, D. Creger, K. Liu, Z. G. He and B. H. Zheng (2015). "Effects of PTEN and Nogo Codeletion on Corticospinal Axon Sprouting and Regeneration in Mice." Journal of Neuroscience **35**(16): 6413-6428.

Ghaisas, S., J. Maher and A. Kanthasamy (2016). "Gut microbiome in health and disease: Linking the microbiome-gut-brain axis and environmental factors in the pathogenesis of systemic and neurodegenerative diseases." Pharmacol Ther **158**: 52-62.

Gilmour, H., P. L. Ramage-Morin and S. L. Wong (2018). "Multiple sclerosis: Prevalence and impact." Health Rep **29**(1): 3-8.

Glass, C. K., K. Saijo, B. Winner, M. C. Marchetto and F. H. Gage (2010). "Mechanisms underlying inflammation in neurodegeneration." Cell **140**(6): 918-934.

Gold, R., C. Linington and H. Lassmann (2006). "Understanding pathogenesis and therapy of multiple sclerosis via animal models: 70 years of merits and culprits in experimental autoimmune encephalomyelitis research." Brain **129**(Pt 8): 1953-1971.

Goldberg, J. L., J. S. Espinosa, Y. Xu, N. Davidson, G. T. Kovacs and B. A. Barres (2002). "Retinal ganglion cells do not extend axons by default: promotion by neurotrophic signaling and electrical activity." Neuron **33**(5): 689-702.

Gonsette, R. E. (2008). "Neurodegeneration in multiple sclerosis: the role of oxidative stress and excitotoxicity." J Neurol Sci **274**(1-2): 48-53.

GrandPre, T., S. Li and S. M. Strittmatter (2002). "Nogo-66 receptor antagonist peptide promotes axonal regeneration." Nature **417**(6888): 547-551.

Green, A. J., S. McQuaid, S. L. Hauser, I. V. Allen and R. Lyness (2010). "Ocular pathology in multiple sclerosis: retinal atrophy and inflammation irrespective of disease duration." Brain **133**(Pt 6): 1591-1601.

Grimson, A., K. K. Farh, W. K. Johnston, P. Garrett-Engele, L. P. Lim and D. P. Bartel (2007). "MicroRNA targeting specificity in mammals: determinants beyond seed pairing." Mol Cell **27**(1): 91-105.

Gross, C. C., A. Schulte-Mecklenbeck, H. Wiendl, E. Marcenaro, N. Kerlero de Rosbo, A. Uccelli and A. Laroni (2016). "Regulatory Functions of Natural Killer Cells in Multiple Sclerosis." Front Immunol **7**: 606.

Guerau-de-Arellano, M., Y. Liu, W. H. Meisen, D. Pitt, M. K. Racke and A. E. Lovett-Racke (2015). "Analysis of miRNA in Normal Appearing White Matter to Identify Altered CNS Pathways in Multiple Sclerosis." J Autoimmune Disord **1**(1).

Guerau-de-Arellano, M., Y. Liu, W. H. Meisen, D. Pitt, M. K. Racke and A. E. Lovett-Racke (2015). "Analysis of miRNA in Normal Appearing White Matter to Identify Altered CNS Pathways in Multiple Sclerosis." Journal of Autoimmune Disorders **1**(1).

Guerau-de-Arellano, M., K. M. Smith, J. Godlewski, Y. Liu, R. Winger, S. E. Lawler, C. C. Whitacre, M. K. Racke and A. E. Lovett-Racke (2011). "Micro-RNA dysregulation in multiple sclerosis favours pro-inflammatory T-cell-mediated autoimmunity." Brain **134**(Pt 12): 3578-3589.

Guo, C., L. J. Hao, Z. H. Yang, R. Chai, S. Zhang, Y. Gu, H. L. Gao, M. L. Zhong, T. Wang, J. Y. Li and Z. Y. Wang (2016). "Deferoxamine-mediated up-regulation of HIF-1alpha prevents dopaminergic neuronal death via the activation of MAPK family proteins in MPTP-treated mice." Exp Neurol **280**: 13-23.

Guo, C., Z. H. Yang, S. Zhang, R. Chai, H. Xue, Y. H. Zhang, J. Y. Li and Z. Y. Wang (2017). "Intranasal Lactoferrin Enhances alpha-Secretase-Dependent Amyloid Precursor Protein Processing via the ERK1/2-CREB and HIF-1alpha Pathways in an Alzheimer's Disease Mouse Model." *Neuropsychopharmacology*.

Guo, H., N. T. Ingolia, J. S. Weissman and D. P. Bartel (2010). "Mammalian microRNAs predominantly act to decrease target mRNA levels." *Nature* **466**(7308): 835-840.

Ha, M. and V. N. Kim (2014). "Regulation of microRNA biogenesis." *Nat Rev Mol Cell Biol* **15**(8): 509-524.

Ha, Y., H. Liu, S. Zhu, P. Yi, W. Liu, J. Nathanson, R. Kaye, B. Loucas, J. Sun, L. J. Frishman, M. Motamedi and W. Zhang (2017). "Critical Role of the CXCL10/C-X-C Chemokine Receptor 3 Axis in Promoting Leukocyte Recruitment and Neuronal Injury during Traumatic Optic Neuropathy Induced by Optic Nerve Crush." *Am J Pathol* **187**(2): 352-365.

Hagerman, R. J., E. Berry-Kravis, H. C. Hazlett, D. B. Bailey, Jr., H. Moine, R. F. Kooy, F. Tassone, I. Gantois, N. Sonenberg, J. L. Mandel and P. J. Hagerman (2017). "Fragile X syndrome." *Nat Rev Dis Primers* **3**: 17065.

Haile, Y., X. Deng, C. Ortiz-Sandoval, N. Tahbaz, A. Janowicz, J. Q. Lu, B. J. Kerr, N. J. Gutowski, J. E. Holley, P. Eggleton, F. Giuliani and T. Simmen (2017). "Rab32 connects ER stress to mitochondrial defects in multiple sclerosis." *J Neuroinflammation* **14**(1): 19.

Halushka, M. K., B. Fromm, K. J. Peterson and M. N. McCall (2018). "Big Strides in Cellular MicroRNA Expression." *Trends Genet* **34**(3): 165-167.

Hao, P., Z. Liang, H. Piao, X. Ji, Y. Wang, Y. Liu, R. Liu and J. Liu (2014). "Conditioned medium of human adipose-derived mesenchymal stem cells mediates protection in neurons following glutamate excitotoxicity by regulating energy metabolism and GAP-43 expression." *Metab Brain Dis* **29**(1): 193-205.

Harras, M. M., S. M. Eacker, X. Wang, T. M. Dawson and V. L. Dawson (2012). "MicroRNA-223 is neuroprotective by targeting glutamate receptors." *Proc Natl Acad Sci U S A* **109**(46): 18962-18967.

Harrison, E. B., K. Emanuel, B. G. Lamberty, B. M. Morse, M. Li, M. L. Kelso, S. V. Yelamanchili and H. S. Fox (2017). "Induction of miR-155 after Brain Injury Promotes Type 1 Interferon and has a Neuroprotective Effect." *Frontiers in Molecular Neuroscience* **10**: 228.

Hassen, G. W., J. Feliberti, L. Kesner, A. Stracher and F. Mokhtarian (2008). "Prevention of axonal injury using calpain inhibitor in chronic progressive experimental autoimmune encephalomyelitis." *Brain Res* **1236**: 206-215.

Hattori, F., N. Murayama, T. Noshita and S. Oikawa (2003). "Mitochondrial peroxiredoxin-3 protects hippocampal neurons from excitotoxic injury in vivo." *J Neurochem* **86**(4): 860-868.

Hauk, T. G., M. Leibinger, A. Muller, A. Andreadaki, U. Knippschild and D. Fischer (2010). "Stimulation of axon regeneration in the mature optic nerve by intravitreal application of the toll-like receptor 2 agonist Pam3Cys." *Invest Ophthalmol Vis Sci* **51**(1): 459-464.

Hauk, T. G., A. Muller, J. Lee, R. Schwendener and D. Fischer (2008). "Neuroprotective and axon growth promoting effects of intraocular inflammation do not depend on oncomodulin or the presence of large numbers of activated macrophages." *Exp Neurol* **209**(2): 469-482.

Hebert, S. S., A. S. Papadopoulou, P. Smith, M. C. Galas, E. Planel, A. N. Silaharoglu, N. Sergeant, L. Buee and B. De Strooper (2010). "Genetic ablation of Dicer in adult forebrain neurons results in abnormal tau hyperphosphorylation and neurodegeneration." *Hum Mol Genet* **19**(20): 3959-3969.

Heinrich, P. C., I. Behrmann, S. Haan, H. M. Hermanns, G. Muller-Newen and F. Schaper (2003). "Principles of interleukin (IL)-6-type cytokine signalling and its regulation." *Biochem J* **374**(Pt 1): 1-20.

Helwak, A., G. Kudla, T. Dudnakova and D. Tollervey (2013). "Mapping the human miRNA interactome by CLASH reveals frequent noncanonical binding." *Cell* **153**(3): 654-665.

Hirsch, E., C. Costa and E. Ciriaolo (2007). "Phosphoinositide 3-kinases as a common platform for multi-hormone signaling." *Journal of Endocrinology* **194**(2): 243-256.

Hocquemiller, M., L. Giersch, M. Audrain, S. Parker and N. Cartier (2016). "Adeno-Associated Virus-Based Gene Therapy for CNS Diseases." *Hum Gene Ther* **27**(7): 478-496.

Hoflich, K. M., C. Beyer, T. Clarner, C. Schmitz, S. Nyamoya, M. Kipp and T. Hochstrasser (2016). "Acute axonal damage in three different murine models of multiple sclerosis: A comparative approach." Brain Res **1650**: 125-133.

Holley, J. E., D. Gveric, J. Newcombe, M. L. Cuzner and N. J. Gutowski (2003). "Astrocyte characterization in the multiple sclerosis glial scar." Neuropathol Appl Neurobiol **29**(5): 434-444.

Horstmann, L., S. Kuehn, X. Pedreiturria, K. Haak, C. Pfarrer, H. B. Dick, I. Kleiter and S. C. Joachim (2016). "Microglia response in retina and optic nerve in chronic experimental autoimmune encephalomyelitis." J Neuroimmunol **298**: 32-41.

Horstmann, L., H. Schmid, A. Heinen, F. Kurschus, H. Burkhard Dick and S. Joachim (2013). "Inflammatory demyelination induces glia alterations and ganglion cell loss in the retina of an experimental autoimmune encephalomyelitis model." J Neuroinflammation **10**(120).

Horstmann, L., H. Schmid, A. P. Heinen, F. C. Kurschus, H. B. Dick and S. C. Joachim (2013). "Inflammatory demyelination induces glia alterations and ganglion cell loss in the retina of an experimental autoimmune encephalomyelitis model." J Neuroinflammation **10**: 120.

Horvitz, H. R. and J. E. Sulston (1980). "Isolation and genetic characterization of cell-lineage mutants of the nematode *Caenorhabditis elegans*." Genetics **96**(2): 435-454.

Hosseini, A., K. Ghaedi, S. Tanhaei, M. Ganjalikhani-Hakemi, S. Teimuri, M. Etemadifar and M. H. Nasr Esfahani (2016). "Upregulation of CD4+ T-Cell Derived MiR-223 in The Relapsing Phase of Multiple Sclerosis Patients." Cell J **18**(3): 371-380.

Hosseini, A., K. Ghaedi, S. Tanhaei, M. Ganjalikhani-Hakemi, S. Teimuri, M. Etemadifar and M. H. Nasr Esfahani (2016). "Upregulation of CD4+T-Cell Derived MiR-223 in The Relapsing Phase of Multiple Sclerosis Patients." Cell J **18**(3): 371-380.

Howell, O. W., C. A. Reeves, R. Nicholas, D. Carassiti, B. Radotra, S. M. Gentleman, B. Serafini, F. Aloisi, F. Roncaroli, R. Magliozzi and R. Reynolds (2011). "Meningeal inflammation is widespread and linked to cortical pathology in multiple sclerosis." Brain **134**(Pt 9): 2755-2771.

Hu, W., X. B. Dang, G. Wang, S. Li and Y. L. Zhang (2018). "Peroxiredoxin-3 attenuates traumatic neuronal injury through preservation of mitochondrial function." Neurochem Int **114**: 120-126.

Hwang, I. K., K. Y. Yoo, D. W. Kim, C. H. Lee, J. H. Choi, Y. G. Kwon, Y. M. Kim, S. Y. Choi and M. H. Won (2010). "Changes in the expression of mitochondrial peroxiredoxin and thioredoxin in neurons and glia and their protective effects in experimental cerebral ischemic damage." Free Radic Biol Med **48**(9): 1242-1251.

Ichiyama, K., A. Gonzalez-Martin, B. S. Kim, H. Y. Jin, W. Jin, W. Xu, M. Sabouri-Ghomi, S. Xu, P. Zheng, C. Xiao and C. Dong (2016). "The MicroRNA-183-96-182 Cluster Promotes T Helper 17 Cell Pathogenicity by Negatively Regulating Transcription Factor Foxo1 Expression." Immunity **44**(6): 1284-1298.

Ifergan, I., S. Chen, B. Zhang and S. D. Miller (2016). "Cutting Edge: MicroRNA-223 Regulates Myeloid Dendritic Cell-Driven Th17 Responses in Experimental Autoimmune Encephalomyelitis." J Immunol **196**(4): 1455-1459.

Iida, A., T. Shinoe, Y. Baba, H. Mano and S. Watanabe (2011). "Dicer plays essential roles for retinal development by regulation of survival and differentiation." Invest Ophthalmol Vis Sci **52**(6): 3008-3017.

Iorio, M. V., C. Piovano and C. M. Croce (2010). "Interplay between microRNAs and the epigenetic machinery: An intricate network." Biochimica Et Biophysica Acta- Gene Regulatory Mechanisms **1799**(10-12): 694-701.

Ip, N. Y., Y. P. Li, I. van de Stadt, N. Panayotatos, R. F. Alderson and R. M. Lindsay (1991). "Ciliary neurotrophic factor enhances neuronal survival in embryonic rat hippocampal cultures." J Neurosci **11**(10): 3124-3134.

Ishii, H., T. Kubo, A. Kumanogoh and T. Yamashita (2010). "Th1 cells promote neurite outgrowth from cortical neurons via a mechanism dependent on semaphorins." Biochem Biophys Res Commun **402**(1): 168-172.

Ivey, K. N. and D. Srivastava (2015). "microRNAs as Developmental Regulators." Cold Spring Harbor Perspectives in Biology **7**(7).

Izumi, B., T. Nakasa, N. Tanaka, K. Nakanishi, N. Kamei, R. Yamamoto, T. Nakamae, R. Ohta, Y. Fujioka, K. Yamasaki and M. Ochi (2011). "MicroRNA-223 expression in neutrophils in the early phase of secondary damage after spinal cord injury." Neurosci Lett **492**(2): 114-118.

Jernas, M., C. Malmstrom, M. Axelsson, I. Nookaew, H. Wadenvik, J. Lycke and B. Olsson (2013). "MicroRNA regulate immune pathways in T-cells in multiple sclerosis (MS)." BMC Immunol **14**: 32.

Jeyaraju, D. V., L. Xu, M. C. Letellier, S. Bandaru, R. Zunino, E. A. Berg, H. M. McBride and L. Pellegrini (2006). "Phosphorylation and cleavage of presenilin-associated rhomboid-like protein (PARL) promotes changes in mitochondrial morphology." Proc Natl Acad Sci U S A **103**(49): 18562-18567.

Jia, L. H. and Y. N. Liu (2016). "Downregulated serum miR-223 serves as biomarker in Alzheimer's disease." Cell Biochemistry & Function **34**(4): 233-237.

Jin, D., Y. Liu, F. Sun, X. Wang, X. Liu and Z. He (2015). "Restoration of skilled locomotion by sprouting corticospinal axons induced by co-deletion of PTEN and SOCS3." Nat Commun **6**: 8074.

Johnnidis, J. B., M. H. Harris, R. T. Wheeler, S. Stehling-Sun, M. H. Lam, O. Kirak, T. R. Brummelkamp, M. D. Fleming and F. D. Camargo (2008). "Regulation of progenitor cell proliferation and granulocyte function by microRNA-223." Nature **451**(7182): 1125-1129.

Jonkman, L. E., D. M. Rosenthal, M. P. Sormani, L. Miles, J. Herbert, R. I. Grossman and M. Ingles (2015). "Gray Matter Correlates of Cognitive Performance Differ between Relapsing-Remitting and Primary-Progressive Multiple Sclerosis." PLoS One **10**(10): e0129380.

Jr Ode, F., C. S. Moore, T. E. Kennedy, J. P. Antel, A. Bar-Or and A. S. Dhaunchak (2012). "MicroRNA dysregulation in multiple sclerosis." Front Genet **3**: 311.

Junker, A., M. Krumbholz, S. Eisele, H. Mohan, F. Augstein, R. Bittner, H. Lassmann, H. Wekerle, R. Hohlfeld and E. Meinl (2009). "MicroRNA profiling of multiple sclerosis lesions identifies modulators of the regulatory protein CD47." Brain **132**(Pt 12): 3342-3352.

Juzwik, C. A., S. Drake, M. A. Lecuyer, R. M. Johnson, B. Morquette, Y. Zhang, M. Charabati, S. M. Sagan, A. Bar-Or, A. Prat and A. E. Fournier (2018). "Neuronal microRNA regulation in Experimental Autoimmune Encephalomyelitis." Sci Rep **8**(1): 13437.

Kadoya, K., S. Tsukada, P. Lu, G. Coppola, D. Geschwind, M. T. Filbin, A. Blesch and M. H. Tuszynski (2009). "Combined intrinsic and extrinsic neuronal mechanisms facilitate bridging axonal regeneration one year after spinal cord injury." Neuron **64**(2): 165-172.

Kalsotra, A., R. K. Singh, P. Gurha, A. J. Ward, C. J. Creighton and T. A. Cooper (2014). "The Mef2 transcription network is disrupted in myotonic dystrophy heart tissue, dramatically altering miRNA and mRNA expression." Cell Reports **6**(2): 336-345.

Kaneko, H., S. Dridi, V. Tarallo, B. D. Gelfand, B. J. Fowler, W. G. Cho, M. E. Kleinman, S. L. Ponicsan, W. W. Hauswirth, V. A. Chiodo, K. Kariko, J. W. Yoo, D. K. Lee, M. Hadziahmetovic, Y. Song, S. Misra, G. Chaudhuri, F. W. Buaas, R. E. Braun, D. R. Hinton, Q. Zhang, H. E. Grossniklaus, J. M. Provis, M. C. Madigan, A. H. Milam, N. L. Justice, R. J. Albuquerque, A. D. Blandford, S. Bogdanovich, Y. Hirano, J. Witta, E. Fuchs, D. R. Littman, B. K. Ambati, C. M. Rudin, M. M. Chong, P. Provost, J. F. Kugel, J. A. Goodrich, J. L. Dunaief, J. Z. Baffi and J. Ambati (2011). "DICER1 deficit induces Alu RNA toxicity in age-related macular degeneration." Nature **471**(7338): 325-330.

Kasarello, K., A. Cudnoch-Jedrzejewska, A. Czlonkowski and D. Mirowska-Guzel (2017). "Mechanism of action of three newly registered drugs for multiple sclerosis treatment." Pharmacol Rep **69**(4): 702-708.

Kedersha, N., M. R. Cho, W. Li, P. W. Yacono, S. Chen, N. Gilks, D. E. Golan and P. Anderson (2000). "Dynamic shuttling of TIA-1 accompanies the recruitment of mRNA to mammalian stress granules." J Cell Biol **151**(6): 1257-1268.

Kedersha, N. L., M. Gupta, W. Li, I. Miller and P. Anderson (1999). "RNA-binding proteins TIA-1 and TIAR link the phosphorylation of eIF-2 alpha to the assembly of mammalian stress granules." *J Cell Biol* **147**(7): 1431-1442.

Keller, A., P. Leidinger, J. Lange, A. Borries, H. Schroers, M. Scheffler, H. P. Lenhof, K. Ruprecht and E. Meese (2009). "Multiple sclerosis: microRNA expression profiles accurately differentiate patients with relapsing-remitting disease from healthy controls." *PLoS One* **4**(10): e7440.

Keller, A., P. Leidinger, F. Steinmeyer, C. Stahler, A. Franke, G. Hemmrich-Stanisak, A. Kappel, I. Wright, J. Dorr, F. Paul, R. Diem, B. Tocariu-Krick, B. Meder, C. Backes, E. Meese and K. Ruprecht (2014). "Comprehensive analysis of microRNA profiles in multiple sclerosis including next-generation sequencing." *Mult Scler* **20**(3): 295-303.

Kempf, S. J., A. Metaxas, M. Ibanez-Vea, S. Darvesh, B. Finsen and M. R. Larsen (2016). "An integrated proteomics approach shows synaptic plasticity changes in an APP/PS1 Alzheimer's mouse model." *Oncotarget* **7**(23): 33627-33648.

Kil, I. S., S. K. Lee, K. W. Ryu, H. A. Woo, M. C. Hu, S. H. Bae and S. G. Rhee (2012). "Feedback control of adrenal steroidogenesis via H₂O₂-dependent, reversible inactivation of peroxiredoxin III in mitochondria." *Mol Cell* **46**(5): 584-594.

Kim, G. H., J. E. Kim, S. J. Rhie and S. Yoon (2015). "The Role of Oxidative Stress in Neurodegenerative Diseases." *Exp Neurobiol* **24**(4): 325-340.

Kim, S. H., W. K. Dong, I. J. Weiler and W. T. Greenough (2006). "Fragile X mental retardation protein shifts between polyribosomes and stress granules after neuronal injury by arsenite stress or in vivo hippocampal electrode insertion." *Journal of Neuroscience* **26**(9): 2413-2418.

Kim, Y. K. and V. N. Kim (2007). "Processing of intronic microRNAs." *EMBO J* **26**(3): 775-783.

Kimura, T., H. Watanabe, A. Iwamatsu and K. Kaibuchi (2005). "Tubulin and CRMP-2 complex is transported via Kinesin-1." *J Neurochem* **93**(6): 1371-1382.

King, D., D. Yeomanson and H. E. Bryant (2015). "PI3King the Lock: Targeting the PI3K/Akt/mTOR Pathway as a Novel Therapeutic Strategy in Neuroblastoma." *Journal of Pediatric Hematology Oncology* **37**(4): 245-251.

Knier, B., V. Rothhammer, S. Heink, O. Puk, J. Graw, B. Hemmer and T. Korn (2015). "Neutralizing IL-17 protects the optic nerve from autoimmune pathology and prevents retinal nerve fiber layer atrophy during experimental autoimmune encephalomyelitis." *J Autoimmun* **56**: 34-44.

Kostic, M., N. Zivkovic and I. Stojanovic (2013). "Multiple sclerosis and glutamate excitotoxicity." *Rev Neurosci* **24**(1): 71-88.

Koumangoye, R. B., A. M. Sakwe, J. S. Goodwin, T. Patel and J. Ochieng (2011). "Detachment of Breast Tumor Cells Induces Rapid Secretion of Exosomes Which Subsequently Mediate Cellular Adhesion and Spreading." *Plos One* **6**(9).

Koval, E. D., C. Shaner, P. Zhang, X. du Maine, K. Fischer, J. Tay, B. N. Chau, G. F. Wu and T. M. Miller (2013). "Method for widespread microRNA-155 inhibition prolongs survival in ALS-model mice." *Human Molecular Genetics* **22**(20): 4127-4135.

Kuhlmann, T., S. Ludwin, A. Prat, J. Antel, W. Bruck and H. Lassmann (2017). "An updated histological classification system for multiple sclerosis lesions." *Acta Neuropathol* **133**(1): 13-24.

Kurimoto, T., Y. Yin, G. Habboub, H. Y. Gilbert, Y. Li, S. Nakao, A. Hafezi-Moghadam and L. I. Benowitz (2013). "Neutrophils express oncomodulin and promote optic nerve regeneration." *J Neurosci* **33**(37): 14816-14824.

Kye, M. J., E. D. Niederst, M. H. Wertz, C. Goncalves Ido, B. Akten, K. Z. Dover, M. Peters, M. Riessland, P. Neveu, B. Wirth, K. S. Kosik, S. P. Sardi, U. R. Monani, M. A. Passini and M. Sahin (2014). "SMN regulates axonal local translation via miR-183/mTOR pathway." *Hum Mol Genet* **23**(23): 6318-6331.

La Mantia, L., L. Vacchi, M. Rovaris, C. Di Pietrantonj, G. Ebers, S. Fredrikson and G. Filippini (2013). "Interferon beta for secondary progressive multiple sclerosis: a systematic review." J Neurol Neurosurg Psychiatry **84**(4): 420-426.

Laplante, M. and D. M. Sabatini (2012). "mTOR Signaling in Growth Control and Disease." Cell **149**(2): 274-293.

Lau Anthony, A. and M. Tymianski (2010). "Glutamate receptors, neurotoxicity and neurodegeneration." Pflügers Archiv - European Journal of Physiology **460**(2): 525-542.

Lecuyer, M. A., O. Saint-Laurent, L. Bourbonniere, S. Larouche, C. Larochelle, L. Michel, M. Charabati, M. Abadier, S. Zandee, N. Haghayegh Jahromi, E. Gowing, C. Pittet, R. Lyck, B. Engelhardt and A. Prat (2017). "Dual role of ALCAM in neuroinflammation and blood-brain barrier homeostasis." Proc Natl Acad Sci U S A **114**(4): E524-E533.

Lee, R. C., R. L. Feinbaum and V. Ambros (1993). "The C. elegans heterochronic gene lin-4 encodes small RNAs with antisense complementarity to lin-14." Cell **75**(5): 843-854.

Lee, Y., C. Ahn, J. Han, H. Choi, J. Kim, J. Yim, J. Lee, P. Provost, O. Radmark, S. Kim and V. N. Kim (2003). "The nuclear RNase III Drosha initiates microRNA processing." Nature **425**(6956): 415-419.

Lee, Y., K. Jeon, J. T. Lee, S. Kim and V. N. Kim (2002). "MicroRNA maturation: stepwise processing and subcellular localization." EMBO J **21**(17): 4663-4670.

Lee, Y., M. Kim, J. Han, K. H. Yeom, S. Lee, S. H. Baek and V. N. Kim (2004). "MicroRNA genes are transcribed by RNA polymerase II." EMBO J **23**(20): 4051-4060.

Leibinger, M., A. Andreadaki, P. Gobrecht, E. Levin, H. Diekmann and D. Fischer (2016). "Boosting Central Nervous System Axon Regeneration by Circumventing Limitations of Natural Cytokine Signaling." Mol Ther **24**(10): 1712-1725.

Leibinger, M., A. Andreadaki, R. Golla, E. Levin, A. M. Hilla, H. Diekmann and D. Fischer (2017). "Boosting CNS axon regeneration by harnessing antagonistic effects of GSK3 activity." Proc Natl Acad Sci U S A **114**(27): E5454-E5463.

Leibinger, M., A. Muller, A. Andreadaki, T. G. Hauk, M. Kirsch and D. Fischer (2009). "Neuroprotective and axon growth-promoting effects following inflammatory stimulation on mature retinal ganglion cells in mice depend on ciliary neurotrophic factor and leukemia inhibitory factor." J Neurosci **29**(45): 14334-14341.

Leon, S., Y. Yin, J. Nguyen, N. Irwin and L. I. Benowitz (2000). "Lens injury stimulates axon regeneration in the mature rat optic nerve." J Neurosci **20**(12): 4615-4626.

Levite, M. (2017). "Glutamate, T cells and multiple sclerosis." Journal of Neural Transmission **124**(7): 775-798.

Lewis, B. P., C. B. Burge and D. P. Bartel (2005). "Conserved seed pairing, often flanked by adenosines, indicates that thousands of human genes are microRNA targets." Cell **120**(1): 15-20.

Lewis, B. P., I. H. Shih, M. W. Jones-Rhoades, D. P. Bartel and C. B. Burge (2003). "Prediction of mammalian microRNA targets." Cell **115**(7): 787-798.

Lewkowicz, P., H. Cwiklinska, M. P. Mycko, M. Cichalewska, M. Domowicz, N. Lewkowicz, A. Jurewicz and K. W. Selmaj (2015). "Dysregulated RNA-Induced Silencing Complex (RISC) Assembly within CNS Corresponds with Abnormal miRNA Expression during Autoimmune Demyelination." J Neurosci **35**(19): 7521-7537.

Lewkowicz, P., H. Cwiklinska, M. P. Mycko, M. Cichalewska, M. Domowicz, N. Lewkowicz, A. Jurewicz and K. W. Selmaj (2015). "Dysregulated RNA-Induced Silencing Complex (RISC) Assembly within CNS Corresponds with Abnormal miRNA Expression during Autoimmune Demyelination." Journal of Neuroscience **35**(19): 7521-7537.

Li, K. K. W., J. C. S. Pang, K. M. Lau, L. F. Zhou, Y. Mao, Y. Wang, W. S. Poon and H. K. Ng (2013). "MiR-383 is Downregulated in Medulloblastoma and Targets Peroxiredoxin 3 (PRDX3)." Brain Pathology **23**(4): 413-425.

Li, T., M. J. Morgan, S. Choksi, Y. Zhang, Y. S. Kim and Z. G. Liu (2010). "MicroRNAs modulate the noncanonical transcription factor NF-kappaB pathway by regulating expression of the kinase IKKalpha during macrophage differentiation." *Nat Immunol* **11**(9): 799-805.

Lian, J., H. Tian, L. Liu, X. S. Zhang, W. Q. Li, Y. M. Deng, G. D. Yao, M. M. Yin and F. Sun (2010). "Downregulation of microRNA-383 is associated with male infertility and promotes testicular embryonal carcinoma cell proliferation by targeting IRF1." *Cell Death & Disease* **1**.

Liang, H. and W. H. Li (2007). "MicroRNA regulation of human protein protein interaction network." *RNA* **13**(9): 1402-1408.

Liddelow, S. A. and B. A. Barres (2017). "Reactive Astrocytes: Production, Function, and Therapeutic Potential." *Immunity* **46**(6): 957-967.

Liddelow, S. A., K. A. Guttenplan, L. E. Clarke, F. C. Bennett, C. J. Bohlen, L. Schirmer, M. L. Bennett, A. E. Munch, W. S. Chung, T. C. Peterson, D. K. Wilton, A. Frouin, B. A. Napier, N. Panicker, M. Kumar, M. S. Buckwalter, D. H. Rowitch, V. L. Dawson, T. M. Dawson, B. Stevens and B. A. Barres (2017). "Neurotoxic reactive astrocytes are induced by activated microglia." *Nature* **541**(7638): 481-487.

Lim, L. P., N. C. Lau, P. Garrett-Engele, A. Grimson, J. M. Schelter, J. Castle, D. P. Bartel, P. S. Linsley and J. M. Johnson (2005). "Microarray analysis shows that some microRNAs downregulate large numbers of target mRNAs." *Nature* **433**(7027): 769-773.

Lindberg, R. L., F. Hoffmann, M. Mehling, J. Kuhle and L. Kappos (2010). "Altered expression of miR-17-5p in CD4+ lymphocytes of relapsing-remitting multiple sclerosis patients." *Eur J Immunol* **40**(3): 888-898.

Liu, S., H. Jia, S. Hou, T. Xin, X. Guo, G. Zhang, X. Gao, M. Li, W. Zhu and H. Zhu (2018). "Recombinant Mtb9.8 of Mycobacterium bovis stimulates TNF-alpha and IL-1beta secretion by RAW264.7 macrophages through activation of NF-kappaB pathway via TLR2." *Sci Rep* **8**(1): 1928.

Liu, Z., Y. Hu, Y. Gong, W. Zhang, C. Liu, Q. Wang and H. Deng (2016). "Hydrogen peroxide mediated mitochondrial UNG1-PRDX3 interaction and UNG1 degradation." *Free Radic Biol Med* **99**: 54-62.

Livak, K. J. and T. D. Schmittgen (2001). "Analysis of relative gene expression data using real-time quantitative PCR and the 2^{-Delta Delta C(T)} Method." *Methods* **25**(4): 402-408.

Llorens, F., K. Thune, P. Andres-Benito, W. Tahir, B. Ansoleaga, K. Hernandez-Ortega, E. Marti, I. Zerr and I. Ferrer (2017). "MicroRNA Expression in the Locus Coeruleus, Entorhinal Cortex, and Hippocampus at Early and Middle Stages of Braak Neurofibrillary Tangle Pathology." *Journal of Molecular Neuroscience* **05**: 05.

Loeb, G. B., A. A. Khan, D. Canner, J. B. Hiatt, J. Shendure, R. B. Darnell, C. S. Leslie and A. Y. Rudensky (2012). "Transcriptome-wide miR-155 binding map reveals widespread noncanonical microRNA targeting." *Mol Cell* **48**(5): 760-770.

London, A., I. Benhar and M. Schwartz (2013). "The retina as a window to the brain-from eye research to CNS disorders." *Nat Rev Neurol* **9**(1): 44-53.

Louveau, A., J. Herz, M. N. Alme, A. F. Salvador, M. Q. Dong, K. E. Viar, S. G. Herod, J. Knopp, J. C. Setliff, A. L. Lupi, S. Da Mesquita, E. L. Frost, A. Gaultier, T. H. Harris, R. Cao, S. Hu, J. R. Lukens, I. Smirnov, C. C. Overall, G. Oliver and J. Kipnis (2018). "CNS lymphatic drainage and neuroinflammation are regulated by meningeal lymphatic vasculature." *Nat Neurosci* **21**(10): 1380-1391.

Louveau, A., I. Smirnov, T. J. Keyes, J. D. Eccles, S. J. Rouhani, J. D. Peske, N. C. Derecki, D. Castle, J. W. Mandell, K. S. Lee, T. H. Harris and J. Kipnis (2015). "Structural and functional features of central nervous system lymphatic vessels." *Nature* **523**(7560): 337-+.

Love, M. I., W. Huber and S. Anders (2014). "Moderated estimation of fold change and dispersion for RNA-seq data with DESeq2." *Genome Biol* **15**(12): 550.

Lu, A., Z. Huang, C. Zhang, X. Zhang, J. Zhao, H. Zhang, Q. Zhang, S. Wu and X. Yi (2014). "Differential expression of microRNAs in dorsal root ganglia after sciatic nerve injury." *Neural Regen Res* **9**(10): 1031-1040.

Luo, C., M. W. Ouyang, Y. Y. Fang, S. J. Li, Q. Zhou, J. Fan, Z. S. Qin and T. Tao (2017). "Dexmedetomidine Protects Mouse Brain from Ischemia-Reperfusion Injury via Inhibiting Neuronal Autophagy through Up-Regulating HIF-1 α ." *Front Cell Neurosci* **11**: 197.

Luo, Y., P. Wang, X. Wang, Y. Wang, Z. Mu, Q. Li, Y. Fu, J. Xiao, G. Li, Y. Ma, Y. Gu, L. Jin, J. Ma, Q. Tang, A. Jiang, X. Li and M. Li (2017). "Detection of dietetically absorbed maize-derived microRNAs in pigs." *Sci Rep* **7**(1): 645.

Lusardi, T. A., J. I. Phillips, J. T. Wiedrick, C. A. Harrington, B. Lind, J. A. Lapidus, J. F. Quinn and J. A. Saugstad (2017). "MicroRNAs in Human Cerebrospinal Fluid as Biomarkers for Alzheimer's Disease." *J Alzheimers Dis* **55**(3): 1223-1233.

Lv, Y. N., A. J. Ou-Yang and L. S. Fu (2017). "MicroRNA-27a Negatively Modulates the Inflammatory Response in Lipopolysaccharide-Stimulated Microglia by Targeting TLR4 and IRAK4." *Cell Mol Neurobiol* **37**(2): 195-210.

Machado-Santos, J., E. Saji, A. R. Troscher, M. Paunovic, R. Liblau, G. Gabriely, C. G. Bien, J. Bauer and H. Lassmann (2018). "The compartmentalized inflammatory response in the multiple sclerosis brain is composed of tissue-resident CD8+ T lymphocytes and B cells." *Brain* **141**(7): 2066-2082.

Magliozzi, R., O. W. Howell, C. Reeves, F. Roncaroli, R. Nicholas, B. Serafini, F. Aloisi and R. Reynolds (2010). "A Gradient of neuronal loss and meningeal inflammation in multiple sclerosis." *Ann Neurol* **68**(4): 477-493.

Magner, W. J., B. Weinstock-Guttman, M. Rho, D. Hojnacki, R. Ghazi, M. Ramanathan and T. B. Tomasi (2016). "Dicer and microRNA expression in multiple sclerosis and response to interferon therapy." *J Neuroimmunol* **292**: 68-78.

Mahboubi, H. and U. Stochaj (2017). "Cytoplasmic stress granules: Dynamic modulators of cell signaling and disease." *Biochim Biophys Acta* **1863**(4): 884-895.

Mar, F. M., A. Bonni and M. M. Sousa (2014). "Cell intrinsic control of axon regeneration." *EMBO Rep* **15**(3): 254-263.

Marriott, J. J., J. M. Miyasaki, G. Gronseth, P. W. O'Connor, Therapeutics and N. Technology Assessment Subcommittee of the American Academy of (2010). "Evidence Report: The efficacy and safety of mitoxantrone (Novantrone) in the treatment of multiple sclerosis: Report of the Therapeutics and Technology Assessment Subcommittee of the American Academy of Neurology." *Neurology* **74**(18): 1463-1470.

McKiernan, R. C., E. M. Jimenez-Mateos, I. Bray, T. Engel, G. P. Brennan, T. Sano, Z. Michalak, C. Moran, N. Delanty, M. Farrell, D. O'Brien, R. Meller, R. P. Simon, R. L. Stallings and D. C. Henshall (2012). "Reduced mature microRNA levels in association with dicer loss in human temporal lobe epilepsy with hippocampal sclerosis." *PLoS ONE [Electronic Resource]* **7**(5): e35921.

McMahon, J. M., S. McQuaid, R. Reynolds and U. F. FitzGerald (2012). "Increased expression of ER stress- and hypoxia-associated molecules in grey matter lesions in multiple sclerosis." *Mult Scler* **18**(10): 1437-1447.

McSweeney, K. M., A. B. Gussow, S. S. Bradrick, S. A. Dugger, S. Gelfman, Q. Wang, S. Petrovski, W. N. Frankel, M. J. Boland and D. B. Goldstein (2016). "Inhibition of microRNA 128 promotes excitability of cultured cortical neuronal networks." *Genome Res* **26**(10): 1411-1416.

Mi, H., X. Huang, A. Muruganujan, H. Tang, C. Mills, D. Kang and P. D. Thomas (2017). "PANTHER version 11: expanded annotation data from Gene Ontology and Reactome pathways, and data analysis tool enhancements." *Nucleic Acids Res* **45**(D1): D183-D189.

Mi, H., A. Muruganujan, J. T. Casagrande and P. D. Thomas (2013). "Large-scale gene function analysis with the PANTHER classification system." *Nat Protoc* **8**(8): 1551-1566.

Michell-Robinson, M. A., H. Touil, L. M. Healy, D. R. Owen, B. A. Durafourt, A. Bar-Or, J. P. Antel and C. S. Moore (2015). "Roles of microglia in brain development, tissue maintenance and repair." *Brain* **138**(Pt 5): 1138-1159.

Miller-Delaney, S. F., K. Bryan, S. Das, R. C. McKiernan, I. M. Bray, J. P. Reynolds, R. Gwinn, R. L. Stallings and D. C. Henshall (2015). "Differential DNA methylation profiles of coding and non-coding genes define hippocampal sclerosis in human temporal lobe epilepsy." *Brain* **138**(Pt 3): 616-631.

Miller, E. (2012). "Multiple sclerosis." *Adv Exp Med Biol* **724**: 222-238.

Miller, S. D., W. J. Karpus and T. S. Davidson (2010). "Experimental autoimmune encephalomyelitis in the mouse." *Curr Protoc Immunol* **Chapter 15**: Unit 15 11.

Miranda, K. C., T. Huynh, Y. Tay, Y. S. Ang, W. L. Tam, A. M. Thomson, B. Lim and I. Rigoutsos (2006). "A pattern-based method for the identification of MicroRNA binding sites and their corresponding heteroduplexes." *Cell* **126**(6): 1203-1217.

Miron, V. E., A. Boyd, J. W. Zhao, T. J. Yuen, J. M. Ruckh, J. L. Shadrach, P. van Wijngaarden, A. J. Wagers, A. Williams, R. J. M. Franklin and C. Ffrench-Constant (2013). "M2 microglia and macrophages drive oligodendrocyte differentiation during CNS remyelination." *Nat Neurosci* **16**(9): 1211-1218.

Miyazaki, Y., R. Li, A. Rezk, H. Misirliyan, C. Moore, N. Farooqi, M. Solis, L. G. Goiry, O. de Faria Junior, V. D. Dang, D. Colman, A. S. Dhaunchak, J. Antel, J. Gommerman, A. Prat, S. Fillatreau, A. Bar-Or, C. M. N. E. T. G. i. C. Autoimmunity and M. C. B. c. i. M. Team (2014). "A novel microRNA-132-sirtuin-1 axis underlies aberrant B-cell cytokine regulation in patients with relapsing-remitting multiple sclerosis [corrected]." *PLoS One* **9**(8): e105421.

Monnerie, H., S. Shashidhara and P. Le Roux (2003). "Effect of excess extracellular glutamate on dendrite growth from cerebral cortical neurons at 3 days in vitro: Involvement of NMDA receptors." *Journal of Neuroscience Research* **74**(5): 688-700.

Montgomery, D. L. (1994). "Astrocytes: form, functions, and roles in disease." *Vet Pathol* **31**(2): 145-167.

Moore, C. S., V. T. Rao, B. A. Durafourt, B. J. Bedell, S. K. Ludwin, A. Bar-Or and J. P. Antel (2013). "miR-155 as a multiple sclerosis-relevant regulator of myeloid cell polarization." *Ann Neurol*.

Moutinho, C. and M. Esteller (2017). "MicroRNAs and Epigenetics." *Adv Cancer Res* **135**: 189-220.

Muller, A., T. G. Hauk and D. Fischer (2007). "Astrocyte-derived CNTF switches mature RGCs to a regenerative state following inflammatory stimulation." *Brain* **130**(Pt 12): 3308-3320.

Munoz-Culla, M., H. Irizar, M. Saenz-Cuesta, T. Castillo-Trivino, I. Osorio-Querejeta, L. Sepulveda, A. Lopez de Munain, J. Olascoaga and D. Otaegui (2016). "SncRNA (microRNA & snoRNA) opposite expression pattern found in multiple sclerosis relapse and remission is sex dependent." *Sci Rep* **6**: 20126.

Murata, T., N. Morita, K. Hikita, K. Kiuchi, K. Kiuchi and N. Kaneda (2005). "Recruitment of mRNA-destabilizing protein TIS11 to stress granules is mediated by its zinc finger domain." *Experimental Cell Research* **303**(2): 287-299.

Murphy, K., P. Travers, M. Walport and C. Janeway (2012). *Janeway's immunobiology*. New York, Garland Science.

Murphy, T. H., R. L. Schnaar and J. T. Coyle (1990). "Immature cortical neurons are uniquely sensitive to glutamate toxicity by inhibition of cystine uptake." *FASEB journal* **4**(6): 1624-1633.

Nagai, J., K. Owada, Y. Kitamura, Y. Goshima and T. Ohshima (2016). "Inhibition of CRMP2 phosphorylation repairs CNS by regulating neurotrophic and inhibitory responses." *Exp Neurol* **277**: 283-295.

Nakagawa, Y. and K. Chiba (2015). "Diversity and plasticity of microglial cells in psychiatric and neurological disorders." *Pharmacol Ther* **154**: 21-35.

Nelson, P. T., W. X. Wang and B. W. Rajeev (2008). "MicroRNAs (miRNAs) in neurodegenerative diseases." *Brain Pathol* **18**(1): 130-138.

Neumann, H., A. Cavalie, D. E. Jenne and H. Wekerle (1995). "Induction of MHC class I genes in neurons." *Science* **269**(5223): 549-552.

Neumann, S., F. Bradke, M. Tessier-Lavigne and A. I. Basbaum (2002). "Regeneration of sensory axons within the injured spinal cord induced by intraganglionic cAMP elevation." *Neuron* **34**(6): 885-893.

Neumann, S. and C. J. Woolf (1999). "Regeneration of dorsal column fibers into and beyond the lesion site following adult spinal cord injury." *Neuron* **23**(1): 83-91.

Newcombe, J., A. Uddin, R. Dove, B. Patel, L. Turski, Y. Nishizawa and T. Smith (2008). "Glutamate receptor expression in multiple sclerosis lesions." *Brain Pathol* **18**(1): 52-61.

Nikic, I., D. Merkler, C. Sorbara, M. Brinkoetter, M. Kreutzfeldt, F. M. Bareyre, W. Bruck, D. Bishop, T. Misgeld and M. Kerschensteiner (2011). "A reversible form of axon damage in experimental autoimmune encephalomyelitis and multiple sclerosis." *Nat Med* **17**(4): 495-499.

Noorbakhsh, F., K. K. Ellestad, F. Maingat, K. G. Warren, M. H. Han, L. Steinman, G. B. Baker and C. Power (2011). "Impaired neurosteroid synthesis in multiple sclerosis." *Brain* **134**(Pt 9): 2703-2721.

O'Driscoll, C. M., W. E. Kaufmann and J. P. Bressler (2013). "MeCP2 deficiency enhances glutamate release through NF- κ B signaling in myeloid derived cells." *Journal of Neuroimmunology* **265**(1): 61-67.

Ohno, S. (1972). "So much "junk" DNA in our genome." *Brookhaven Symp Biol* **23**: 366-370.

Paraskevopoulou, M. D., G. Georgakilas, N. Kostoulas, I. S. Vlachos, T. Vergoulis, M. Reczko, C. Filippidis, T. Dalamagas and A. G. Hatzigeorgiou (2013). "DIANA-microT web server v5.0: service integration into miRNA functional analysis workflows." *Nucleic Acids Res* **41**(Web Server issue): W169-173.

Pare, A., B. Mailhot, S. A. Levesque, C. Juzwik, P. M. I. A. Doss, M. A. Lecuyer, A. Prat, M. Rangachari, A. Fournier and S. Lacroix (2018). "IL-1 beta enables CNS access to CCR2(hi) monocytes and the generation of pathogenic cells through GM-CSF released by CNS endothelial cells." *Proceedings of the National Academy of Sciences of the United States of America* **115**(6): E1194-E1203.

Park, K. K., K. Liu, Y. Hu, P. D. Smith, C. Wang, B. Cai, B. Xu, L. Connolly, I. Kramvis, M. Sahin and Z. He (2008). "Promoting axon regeneration in the adult CNS by modulation of the PTEN/mTOR pathway." *Science* **322**(5903): 963-966.

Pegoraro, V., A. Merico and C. Angelini (2017). "Micro-RNAs in ALS muscle: Differences in gender, age at onset and disease duration." *Journal of the Neurological Sciences* **380**: 58-63.

Peterson, J. W., L. Bo, S. Mork, A. Chang and B. D. Trapp (2001). "Transected neurites, apoptotic neurons, and reduced inflammation in cortical multiple sclerosis lesions." *Ann Neurol* **50**(3): 389-400.

Peterson, L. K. and R. S. Fujinami (2007). "Inflammation, demyelination, neurodegeneration and neuroprotection in the pathogenesis of multiple sclerosis." *J Neuroimmunol* **184**(1-2): 37-44.

Petratos, S., E. Ozturk, M. F. Azari, R. Kenny, J. Y. Lee, K. A. Magee, A. R. Harvey, C. McDonald, K. Taghian, L. Moussa, P. M. Aui, C. Siatskas, S. Litwak, M. G. Fehlings, S. M. Strittmatter and C. C. A. Bernard (2012). "Limiting multiple sclerosis related axonopathy by blocking Nogo receptor and CRMP-2 phosphorylation." *Brain* **135**: 1794-1818.

Pitt, D. D. (2000). "Glutamate excitotoxicity in a model of multiple sclerosis." *Nature Medicine* **6**(1): 67-70.

Ponath, G., C. Park and D. Pitt (2018). "The Role of Astrocytes in Multiple Sclerosis." *Front Immunol* **9**: 217.

Pool, M., I. Rambaldi, P. J. Darlington, M. C. Wright, A. E. Fournier and A. Bar-Or (2012). "Neurite outgrowth is differentially impacted by distinct immune cell subsets." *Mol Cell Neurosci* **49**(1): 68-76.

Pool, M., I. Rambaldi, B. A. Durafourt, M. C. Wright, J. P. Antel, A. Bar-Or and A. E. Fournier (2011). "Myeloid lineage cells inhibit neurite outgrowth through a myosin II-dependent mechanism." *J Neuroimmunol* **237**(1-2): 101-105.

Popovich, P. G., Z. Guan, V. McGaughy, L. Fisher, W. F. Hickey and D. M. Basso (2002). "The neuropathological and behavioral consequences of intraspinal microglial/macrophage activation." *J Neuropathol Exp Neurol* **61**(7): 623-633.

Popovich, P. G. and T. B. Jones (2003). "Manipulating neuroinflammatory reactions in the injured spinal cord: back to basics." *Trends Pharmacol Sci* **24**(1): 13-17.

Pulikkan, J. A., V. Dengler, P. S. Peramangalam, A. A. Peer Zada, C. Muller-Tidow, S. K. Bohlander, D. G. Tenen and G. Behre (2010). "Cell-cycle regulator E2F1 and microRNA-223 comprise an autoregulatory negative feedback loop in acute myeloid leukemia." *Blood* **115**(9): 1768-1778.

Qin, S., Y. Zou and C. L. Zhang (2013). "Cross-talk between KLF4 and STAT3 regulates axon regeneration." *Nat Commun* **4**: 2633.

Qiu, J., D. Cai, H. Dai, M. McAtee, P. N. Hoffman, B. S. Bregman and M. T. Filbin (2002). "Spinal axon regeneration induced by elevation of cyclic AMP." *Neuron* **34**(6): 895-903.

Qu, J. and T. C. Jakobs (2013). "The Time Course of Gene Expression during Reactive Gliosis in the Optic Nerve." *PLoS One* **8**(6): e67094.

Quinlan, S., A. Kenny, M. Medina, T. Engel and E. M. Jimenez-Mateos (2017). Chapter Seven - MicroRNAs in Neurodegenerative Diseases. *International Review of Cell and Molecular Biology*. L. Galluzzi and I. Vitale, Academic Press. **334**: 309-343.

Quinn, T. A., M. Dutt and K. S. Shindler (2011). "Optic neuritis and retinal ganglion cell loss in a chronic murine model of multiple sclerosis." *Front Neurol* **2**: 50.

Quintanar, J. L. and E. Salinas (2008). "Neurotrophic effects of GnRH on neurite outgrowth and neurofilament protein expression in cultured cerebral cortical neurons of rat embryos." *Neurochem Res* **33**(6): 1051-1056.

Ragusa, M., P. Bosco, L. Tamburello, C. Barbagallo, A. G. Condorelli, M. Tornitore, R. S. Spada, D. Barbagallo, M. Scalia, M. Elia, C. Di Pietro and M. Purrello (2016). "miRNAs Plasma Profiles in Vascular Dementia: Biomolecular Data and Biomedical Implications." *Frontiers in Cellular Neuroscience* **10**: 51.

Ramón y Cajal, S., J. DeFelipe and E. G. Jones (1991). *Cajal's degeneration and regeneration of the nervous system*. New York, Oxford University Press.

Ransohoff, R. M. (2016). "A polarizing question: do M1 and M2 microglia exist?" *Nature Neuroscience* **19**(8): 987-991.

Recks, M. S., E. R. Stormanns, J. Bader, S. Arnhold, K. Addicks and S. Kuerten (2013). "Early axonal damage and progressive myelin pathology define the kinetics of CNS histopathology in a mouse model of multiple sclerosis." *Clin Immunol* **149**(1): 32-45.

Reczko, M., M. Maragkakis, P. Alexiou, I. Grosse and A. G. Hatzigeorgiou (2012). "Functional microRNA targets in protein coding sequences." *Bioinformatics* **28**(6): 771-776.

Regev, K., B. C. Healy, F. Khalid, A. Paul, R. Chu, S. Tauhid, S. Tummala, C. Diaz-Cruz, R. Raheja, M. A. Mazzola, F. von Glehn, P. Kivisakk, S. L. Dupuy, G. Kim, T. Chitnis, H. L. Weiner, R. Gandhi and R. Bakshi (2017). "Association Between Serum MicroRNAs and Magnetic Resonance Imaging Measures of Multiple Sclerosis Severity." *JAMA Neurol* **74**(3): 275-285.

Regev, K., A. Paul, B. Healy, F. von Glenn, C. Diaz-Cruz, T. Gholipour, M. A. Mazzola, R. Raheja, P. Nejad, B. I. Glanz, P. Kivisakk, T. Chitnis, H. L. Weiner and R. Gandhi (2016). "Comprehensive evaluation of serum microRNAs as biomarkers in multiple sclerosis." *Neurol Neuroimmunol Neuroinflamm* **3**(5): e267.

Reinhart, B. J., F. J. Slack, M. Basson, A. E. Pasquinelli, J. C. Bettinger, A. E. Rougvie, H. R. Horvitz and G. Ruvkun (2000). "The 21-nucleotide let-7 RNA regulates developmental timing in *Caenorhabditis elegans*." *Nature* **403**(6772): 901-906.

Ren, C., Q. Liu, Q. Wei, W. Cai, M. He, Y. Du, D. Xu, Y. Wu and J. Yu (2017). "Circulating miRNAs as Potential Biomarkers of Age-Related Macular Degeneration." *Cellular Physiology & Biochemistry* **41**(4): 1413-1423.

Renier, N., Z. Wu, D. J. Simon, J. Yang, P. Ariel and M. Tessier-Lavigne (2014). "iDISCO: a simple, rapid method to immunolabel large tissue samples for volume imaging." *Cell* **159**(4): 896-910.

Reynolds, R., F. Roncaroli, R. Nicholas, B. Radotra, D. Gveric and O. Howell (2011). "The neuropathological basis of clinical progression in multiple sclerosis." *Acta Neuropathol* **122**(2): 155-170.

Ridolfi, E., C. Fenoglio, C. Cantoni, A. Calvi, M. De Riz, A. Pietroboni, C. Villa, M. Serpente, R. Bonsi, M. Vercellino, P. Cavalla, D. Galimberti and E. Scarpini (2013). "Expression and Genetic Analysis of MicroRNAs Involved in Multiple Sclerosis." *Int J Mol Sci* **14**(3): 4375-4384.

Rocca, M. A., M. P. Amato, N. De Stefano, C. Enzinger, J. J. Geurts, I. K. Penner, A. Rovira, J. F. Sumowski, P. Valsasina, M. Filippi and M. S. Grp (2015). "Clinical and imaging assessment of cognitive dysfunction in multiple sclerosis." *Lancet Neurology* **14**(3): 302-317.

Rocca, M. A., M. P. Sormani, M. Rovaris, D. Caputo, A. Ghezzi, E. Montanari, A. Bertolotto, A. Laroni, R. Bergamaschi, V. Martinelli, G. Comi and M. Filippi (2017). "Long-term disability progression in primary progressive multiple sclerosis: a 15-year study." *Brain* **140**(11): 2814-2819.

Romano, G. L., C. B. M. Platania, F. Drago, S. Salomone, M. Ragusa, C. Barbagallo, C. Di Pietro, M. Purrello, M. Reibaldi, T. Avitabile, A. Longo and C. Bucolo (2017). "Retinal and Circulating miRNAs in Age-Related Macular Degeneration: An In vivo Animal and Human Study." *Frontiers in Pharmacology* **8**: 168.

Rostami, A. and B. Ciric (2013). "Role of Th17 cells in the pathogenesis of CNS inflammatory demyelination." *J Neurol Sci* **333**(1-2): 76-87.

Russell, S., J. Bennett, J. A. Wellman, D. C. Chung, Z. F. Yu, A. Tillman, J. Wittes, J. Pappas, O. Elci, S. McCague, D. Cross, K. A. Marshall, J. Walshire, T. L. Kehoe, H. Reichert, M. Davis, L. Raffini, L. A. George, F. P. Hudson, L. Dingfield, X. Zhu, J. A. Haller, E. H. Sohn, V. B. Mahajan, W. Pfeifer, M. Weckmann, C. Johnson, D. Gewaily, A. Drack, E. Stone, K. Wachtel, F. Simonelli, B. P. Leroy, J. F. Wright, K. A. High and A. M. Maguire (2017). "Efficacy and safety of voretigene neparvovec (AAV2-hRPE65v2) in patients with RPE65-mediated inherited retinal dystrophy: a randomised, controlled, open-label, phase 3 trial." *Lancet* **390**(10097): 849-860.

Rustici, G., N. Kolesnikov, M. Brandizi, T. Burdett, M. Dylag, I. Emam, A. Farne, E. Hastings, J. Ison, M. Keays, N. Kurbatova, J. Malone, R. Mani, A. Mupo, R. Pedro Pereira, E. Pilicheva, J. Rung, A. Sharma, Y. A. Tang, T. Ternent, A. Tikhonov, D. Welter, E. Williams, A. Brazma, H. Parkinson and U. Sarkans (2013). "ArrayExpress update--trends in database growth and links to data analysis tools." *Nucleic Acids Res* **41**(Database issue): D987-990.

Sailer, M., B. Fischl, D. Salat, C. Tempelmann, M. A. Schonfeld, E. Busa, N. Bodammer, H. J. Heinze and A. Dale (2003). "Focal thinning of the cerebral cortex in multiple sclerosis." *Brain* **126**(Pt 8): 1734-1744.

Sala Frigerio, C., P. Lau, E. Salta, J. Tournoy, K. Bossers, R. Vandenberghe, A. Wallin, M. Bjerke, H. Zetterberg, K. Blennow and B. De Strooper (2013). "Reduced expression of hsa-miR-27a-3p in CSF of patients with Alzheimer disease." *Neurology* **81**(24): 2103-2106.

Salou, M., B. Nicol, A. Garcia and D. A. Laplaud (2015). "Involvement of CD8(+) T Cells in Multiple Sclerosis." *Front Immunol* **6**: 604.

Sans, N., B. Vissel, R. Petralia, Y. Wang, K. Chang, G. Royle, C. Wang, S. O'Gorman, S. Heinemann and R. Wenthold (2003). "Aberrant formation of glutamate receptor complexes in hippocampal neurons of mice lacking the GluR2 AMPA receptor subunit." *J Neuro* **23**(28): 9367-9373.

Satoorian, T., B. Li, X. Tang, J. Xiao, W. Xing, W. Shi, K. H. Lau, D. J. Baylink and X. Qin (2016). "MicroRNA223 promotes pathogenic T-cell development and autoimmune inflammation in central nervous system in mice." *Immunology* **148**(4): 326-338.

Schafferer, S., R. Khurana, V. Refolo, S. Venezia, E. Sturm, P. Piatti, C. Hechenberger, H. Hackl, R. Kessler, M. Willi, R. Gstir, A. Krogdham, A. Lusser, W. Poewe, G. K. Wenning, A. Huttenhofer and N. Stefanova (2016). "Changes in the miRNA-mRNA Regulatory Network Precede Motor Symptoms in a Mouse Model of Multiple System Atrophy: Clinical Implications." *PLoS One* **11**(3): e0150705.

Schlamp, C. L., A. D. Montgomery, C. E. Mac Nair, C. Schuart, D. J. Willmer and R. W. Nickells (2013). "Evaluation of the percentage of ganglion cells in the ganglion cell layer of the rodent retina." *Mol Vis* **19**: 1387-1396.

Schmittgen, T. D., E. J. Lee, J. Jiang, A. Sarkar, L. Yang, T. S. Elton and C. Chen (2008). "Real-time PCR quantification of precursor and mature microRNA." *Methods* **44**(1): 31-38.

Schroeter, M. and S. Jander (2005). "T-cell cytokines in injury-induced neural damage and repair." *Neuromolecular Med* **7**(3): 183-195.

Selmaj, I., M. P. Mycko, C. S. Raine and K. W. Selmaj (2017). "The role of exosomes in CNS inflammation and their involvement in multiple sclerosis." *J Neuroimmunol* **306**: 1-10.

Shalgi, R., D. Lieber, M. Oren and Y. Pilpel (2007). "Global and local architecture of the mammalian microRNA-transcription factor regulatory network." *PLoS Comput Biol* **3**(7): e131.

Shelkownikova, T. A., P. Dimasi, M. S. Kukharsky, H. An, A. Quintiero, C. Schirmer, L. Buee, M. C. Galas and V. L. Buchman (2017). "Chronically stressed or stress-preconditioned neurons fail to maintain stress granule assembly." *Cell Death Dis* **8**(5): e2788.

Sherriff, F. E., L. R. Bridges and S. Sivaloganathan (1994). "Early detection of axonal injury after human head trauma using immunocytochemistry for beta-amyloid precursor protein." *Acta Neuropathol* **87**(1): 55-62.

Shin, D., J. Y. Shin, M. T. McManus, L. J. Ptacek and Y. H. Fu (2009). "Dicer ablation in oligodendrocytes provokes neuronal impairment in mice." *Ann Neurol* **66**(6): 843-857.

Shindler, K. S., E. Ventura, M. Dutt and A. Rostami (2008). "Inflammatory demyelination induces axonal injury and retinal ganglion cell apoptosis in experimental optic neuritis." *Exp Eye Res* **87**(3): 208-213.

Shurtleff, M. J., M. M. Temoche-Diaz, K. V. Karfilis, S. Ri and R. Schekman (2016). "Y-box protein 1 is required to sort microRNAs into exosomes in cells and in a cell-free reaction." *Elife* **5**.

Siegel, S. R., J. Mackenzie, G. Chaplin, N. G. Jablonski and L. Griffiths (2012). "Circulating microRNAs involved in multiple sclerosis." *Mol Biol Rep* **39**(5): 6219-6225.

Sievers, C., M. Meira, F. Hoffmann, P. Fontoura, L. Kappos and R. L. Lindberg (2012). "Altered microRNA expression in B lymphocytes in multiple sclerosis: towards a better understanding of treatment effects." *Clin Immunol* **144**(1): 70-79.

Singh, J., M. Deshpande, H. Suhail, R. Rattan and S. Giri (2016). "Targeted Stage-Specific Inflammatory microRNA Profiling in Urine During Disease Progression in Experimental Autoimmune Encephalomyelitis: Markers of Disease Progression and Drug Response." *J Neuroimmune Pharmacol* **11**(1): 84-97.

Skripuletz, T., D. Hackstette, K. Bauer, V. Gudi, R. Pul, E. Voss, K. Berger, M. Kipp, W. Baumgartner and M. Stangel (2013). "Astrocytes regulate myelin clearance through recruitment of microglia during cuprizone-induced demyelination." *Brain* **136**: 147-167.

Smith, P. D., F. Sun, K. K. Park, B. Cai, C. Wang, K. Kuwako, I. Martinez-Carrasco, L. Connolly and Z. He (2009). "SOCS3 deletion promotes optic nerve regeneration in vivo." *Neuron* **64**(5): 617-623.

Society, N. M. (2018). "Disease-Modifying Therapies for MS." [nationalMSsociety.org](https://www.nationalsmsociety.org/For-Professionals/Clinical-Care/Managing-MS/Disease-Modification), from <https://www.nationalsmsociety.org/For-Professionals/Clinical-Care/Managing-MS/Disease-Modification>.

Sorbara, C. D., N. E. Wagner, A. Ladwig, I. Nikic, D. Merkler, T. Kleele, P. Marinkovic, R. Naumann, L. Godinho, F. M. Bareyre, D. Bishop, T. Misgeld and M. Kerschensteiner (2014). "Pervasive axonal transport deficits in multiple sclerosis models." *Neuron* **84**(6): 1183-1190.

Srinivasan, M. and D. K. Lahiri (2015). "Significance of NF-kappa B as a pivotal therapeutic target in the neurodegenerative pathologies of Alzheimer's disease and multiple sclerosis." *Expert Opinion on Therapeutic Targets* **19**(4): 471-487.

Stojanovic, I. R., M. Kostic and S. Ljubisavljevic (2014). "The role of glutamate and its receptors in multiple sclerosis." *J Neural Transm (Vienna)* **121**(8): 945-955.

Stout, R. D., C. Jiang, B. Matta, I. Tietzel, S. K. Watkins and J. Suttles (2005). "Macrophages sequentially change their functional phenotype in response to changes in microenvironmental influences." *J Immunol* **175**(1): 342-349.

Strickland, I. T., L. Richards, F. E. Holmes, D. Wynick, J. B. Uney and L. F. Wong (2011). "Axotomy-induced miR-21 promotes axon growth in adult dorsal root ganglion neurons." *PLoS One* **6**(8): e23423.

Sun, F., K. K. Park, S. Belin, D. Wang, T. Lu, G. Chen, K. Zhang, C. Yeung, G. Feng, B. A. Yankner and Z. He (2011). "Sustained axon regeneration induced by co-deletion of PTEN and SOCS3." Nature **480**(7377): 372-375.

Sun, L., M. Zhao, Y. Wang, A. Liu, M. Lv, Y. Li, X. Yang and Z. Wu (2017). "Neuroprotective effects of miR-27a against traumatic brain injury via suppressing FoxO3a-mediated neuronal autophagy." Biochemical and Biophysical Research Communications **482**(4): 1141-1147.

Sundermeier, T. R., S. Sakami, B. Sahu, S. J. Howell, S. Gao, Z. Dong, M. Golczak, A. Maeda and K. Palczewski (2017). "MicroRNA-processing Enzymes Are Essential for Survival and Function of Mature Retinal Pigmented Epithelial Cells in Mice." J Biol Chem **292**(8): 3366-3378.

Sundermeier, T. R., N. Zhang, F. Vinberg, D. Mustafi, H. Kohno, M. Golczak, X. Bai, A. Maeda, V. J. Kefalov and K. Palczewski (2014). "DICER1 is essential for survival of postmitotic rod photoreceptor cells in mice." FASEB J **28**(8): 3780-3791.

Sweeney, M. D., A. P. Sagare and B. V. Zlokovic (2018). "Blood-brain barrier breakdown in Alzheimer disease and other neurodegenerative disorders." Nat Rev Neurol **14**(3): 133-150.

Szemraj, M., A. Bielecka-Kowalska, K. Oszejca, M. Krajewska, R. Gos, P. Jurowski, M. Kowalski and J. Szemraj (2015). "Serum micrornas as potential biomarkers of AMD." Medical Science Monitor **21**: 2734-2742.

Talebi, F., S. Ghorbani, W. F. Chan, R. Boghuzian, F. Masoumi, S. Ghasemi, M. Vojgani, C. Power and F. Noorbakhsh (2017). "MicroRNA-142 regulates inflammation and T cell differentiation in an animal model of multiple sclerosis." J Neuroinflammation **14**(1): 55.

Tan, M., C. Cha, Y. Ye, J. Zhang, S. Li, F. Wu, S. Gong and G. Guo (2015). "CRMP4 and CRMP2 Interact to Coordinate Cytoskeleton Dynamics, Regulating Growth Cone Development and Axon Elongation." Neural Plast **2015**: 947423.

Tang, F., P. Hajkova, S. C. Barton, K. Lao and M. A. Surani (2006). "MicroRNA expression profiling of single whole embryonic stem cells." Nucleic Acids Res **34**(2): e9.

Tang, Y., Z. M. Ling, R. Fu, Y. Q. Li, X. Cheng, F. H. Song, H. X. Luo and L. H. Zhou (2014). "Time-specific microRNA changes during spinal motoneuron degeneration in adult rats following unilateral brachial plexus root avulsion: ipsilateral vs. contralateral changes." BMC Neurosci **15**: 92.

Tao, J., H. Wu, Q. Lin, W. Wei, X. H. Lu, J. P. Cattle, Y. Ao, R. W. Olsen, X. W. Yang, I. Mody, M. V. Sofroniew and Y. E. Sun (2011). "Deletion of astroglial Dicer causes non-cell-autonomous neuronal dysfunction and degeneration." J Neurosci **31**(22): 8306-8319.

Tezel, G., X. Yang, J. Yang and M. B. Wax (2004). "Role of tumor necrosis factor receptor-1 in the death of retinal ganglion cells following optic nerve crush injury in mice." Brain Res **996**(2): 202-212.

Thomas, K. T., C. Gross and G. J. Bassell (2018). "microRNAs Sculpt Neuronal Communication in a Tight Balance That Is Lost in Neurological Disease." Front Mol Neurosci **11**: 455.

Thompson, A. J., B. L. Banwell, F. Barkhof, W. M. Carroll, T. Coetzee, G. Comi, J. Correale, F. Fazekas, M. Filippi, M. S. Freedman, K. Fujihara, S. L. Galetta, H. P. Hartung, L. Kappos, F. D. Lublin, R. A. Marrie, A. E. Miller, D. H. Miller, X. Montalban, E. M. Mowry, P. S. Sorensen, M. Tintore, A. L. Traboulsee, M. Trojano, B. M. J. Uitdehaag, S. Vukusic, E. Waubant, B. G. Weinshenker, S. C. Reingold and J. A. Cohen (2018). "Diagnosis of multiple sclerosis: 2017 revisions of the McDonald criteria." Lancet Neurol **17**(2): 162-173.

Tian, H., Y. X. Cao, X. S. Zhang, W. P. Liao, Y. H. Yi, J. Lian, L. Liu, H. L. Huang, W. J. Liu, M. M. Yin, M. Liang, G. Shan and F. Sun (2013). "The targeting and functions of miRNA-383 are mediated by FMRP during spermatogenesis." Cell Death Dis **4**: e617.

Toosy, A., O. Ciccarelli and A. Thompson (2014). "Symptomatic treatment and management of multiple sclerosis." Handb Clin Neurol **122**: 513-562.

Tourriere, H., K. Chebli, L. Zekri, B. Courselaud, J. M. Blanchard, E. Bertrand and J. Tazi (2003). "The RasGAP-associated endoribonuclease G3BP assembles stress granules." J Cell Biol **160**(6): 823-831.

Trapp, B., J. Peterson, R. M. Ransohoff, R. Rudick, S. Mork and L. Bo (1998). "Axonal transection in the lesions of Multiple Sclerosis." *New England Journal of Medicine* **338**(5): 278-285.

Trapp, B. D., J. Peterson, R. M. Ransohoff, R. Rudick, S. Mork and L. Bo (1998). "Axonal transection in the lesions of multiple sclerosis." *N Engl J Med* **338**(5): 278-285.

Tsang, J., J. Zhu and A. van Oudenaarden (2007). "MicroRNA-mediated feedback and feedforward loops are recurrent network motifs in mammals." *Mol Cell* **26**(5): 753-767.

Tsaytler, P., H. P. Harding, D. Ron and A. Bertolotti (2011). "Selective inhibition of a regulatory subunit of protein phosphatase 1 restores proteostasis." *Science* **332**(6025): 91-94.

Tsutsui, S. and P. K. Stys (2013). "Metabolic injury to axons and myelin." *Exp Neurol* **246**: 26-34.

Ubhi, K., E. Rockenstein, C. Kragh, C. Inglis, B. Spencer, S. Michael, M. Mante, A. Adame, D. Galasko and E. Masliah (2014). "Widespread microRNA dysregulation in multiple system atrophy - disease-related alteration in miR-96." *Eur J Neurosci* **39**(6): 1026-1041.

Van Der Voorn, P., J. Tekstra, R. H. Beelen, C. P. Tensen, P. Van Der Valk and C. J. De Groot (1999). "Expression of MCP-1 by reactive astrocytes in demyelinating multiple sclerosis lesions." *Am J Pathol* **154**(1): 45-51.

van Langelaar, J., R. M. van der Vuurst de Vries, M. Janssen, A. F. Wierenga-Wolf, I. M. Spilt, T. A. Siepman, W. Dankers, G. Verjans, H. E. de Vries, E. Lubberts, R. Q. Hintzen and M. M. van Luijn (2018). "T helper 17.1 cells associate with multiple sclerosis disease activity: perspectives for early intervention." *Brain* **141**(5): 1334-1349.

Vessey, J. P., A. Vaccani, Y. Xie, R. Dahm, D. Karra, M. A. Kiebler and P. Macchi (2006). "Dendritic localization of the translational repressor Pumilio 2 and its contribution to dendritic stress granules." *J Neurosci* **26**(24): 6496-6508.

Vidaki, M., F. Drees, T. Saxena, E. Lanslots, M. J. Taliaferro, A. Tatarakis, C. B. Burge, E. T. Wang and F. B. Gertler (2017). "A Requirement for Mena, an Actin Regulator, in Local mRNA Translation in Developing Neurons." *Neuron* **95**(3): 608-622 e605.

Vlachos, I. S., M. D. Paraskevopoulou, D. Karagkouni, G. Georgakilas, T. Vergoulis, I. Kanellos, I. L. Anastasopoulos, S. Maniou, K. Karathanou, D. Kalfakakou, A. Fevgas, T. Dalamagas and A. G. Hatzigeorgiou (2015). "DIANA-TarBase v7.0: indexing more than half a million experimentally supported miRNA:mRNA interactions." *Nucleic Acids Res* **43**(Database issue): D153-159.

Vogt, J., F. Paul, O. Aktas, K. Muller-Wielsch, J. Dorr, S. Dorr, B. S. Bharathi, R. Glumm, C. Schmitz, H. Steinbusch, C. S. Raine, M. Tsokos, R. Nitsch and F. Zipp (2009). "Lower motor neuron loss in multiple sclerosis and experimental autoimmune encephalomyelitis." *Ann Neurol* **66**(3): 310-322.

Vogt, J., F. Paul, O. Aktas, K. Muller-Wielsch, J. Dorr, S. Dorr, S. Bharathi, R. Glumm, C. Schmitz, H. Steinbusch, C. S. Raine, M. Tsokos, R. Nitsch and F. Zipp (2009). "Lower Motor Neuron Loss in Multiple Sclerosis and Experimental Autoimmune Encephalomyelitis." *Annals of Neurology* **66**(3): 310-322.

Wallstrom, E., P. Diener, A. Ljungdahl, M. Khademi, C. Nilsson and t. Olsson (1996). "Memantine abrogates neurological deficits, but not CNS inflammation, in Lewis rat experimental autoimmune encephalomyelitis." *Journal of the Neurological Sciences* **137**: 89-96.

Wang, W. X., Q. Huang, Y. Hu, A. J. Stromberg and P. T. Nelson (2011). "Patterns of microRNA expression in normal and early Alzheimer's disease human temporal cortex: white matter versus gray matter." *Acta Neuropathologica* **121**(2): 193-205.

Wang, W. X., N. P. Visavadiya, J. D. Pandya, P. T. Nelson, P. G. Sullivan and J. E. Springer (2015). "Mitochondria-associated microRNAs in rat hippocampus following traumatic brain injury." *Experimental Neurology* **265**: 84-93.

Wang, X., O. Hasan, A. Arzeno, L. I. Benowitz, W. B. Cafferty and S. M. Strittmatter (2012). "Axonal regeneration induced by blockade of glial inhibitors coupled with activation of intrinsic neuronal growth pathways." *Exp Neurol* **237**(1): 55-69.

Waxman, S. G. (2006). "Axonal conduction and injury in multiple sclerosis: the role of sodium channels." Nat Rev Neurosci **7**(12): 932-941.

Way, S. W., J. R. Podojil, B. L. Clayton, A. Zaremba, T. L. Collins, R. B. Kunjamma, A. P. Robinson, P. Brugarolas, R. H. Miller, S. D. Miller and B. Popko (2015). "Pharmaceutical integrated stress response enhancement protects oligodendrocytes and provides a potential multiple sclerosis therapeutic." Nature Communications **6**.

Wegner, C., M. M. Esiri, S. A. Chance, J. Palace and P. M. Matthews (2006). "Neocortical neuronal, synaptic, and glial loss in multiple sclerosis." Neurology **67**(6): 960-967.

Whittaker Hawkins, R. F., A. Patenaude, A. Dumas, R. Jain, Y. Tesfagiorgis, S. Kerfoot, T. Matsui, M. Gunzer, P. E. Poubelle, C. Larochele, M. Pelletier and L. Vallieres (2017). "ICAM1+ neutrophils promote chronic inflammation via ASPRV1 in B cell-dependent autoimmune encephalomyelitis." JCI Insight **2**(23).

Wightman, B., I. Ha and G. Ruvkun (1993). "Posttranscriptional regulation of the heterochronic gene lin-14 by lin-4 mediates temporal pattern formation in *C. elegans*." Cell **75**(5): 855-862.

Wilding, T. J. T. (1995). "Differential antagonism of alpha-amino-3-hydroxy-5-methyl-4-isoxazolepropionic acid-preferring and kainate-preferring receptors by 2,3-benzodiazepines." Molecular Pharmacology **47**(3): 582-587.

Williams, A., G. Piaton and C. Lubetzki (2007). "Astrocytes--friends or foes in multiple sclerosis?" Glia **55**(13): 1300-1312.

Williamson, R., L. van Aalten, D. M. A. Mann, B. Platt, F. Plattner, L. Bedford, J. Mayer, D. Howlett, A. Usardi, C. Sutherland and A. R. Cole (2011). "CRMP2 Hyperphosphorylation is Characteristic of Alzheimer's Disease and not a Feature Common to Other Neurodegenerative Diseases." Journal of Alzheimers Disease **27**(3): 615-625.

Wilson, S. M., A. Moutal, O. K. Melemedjian, Y. Wang, W. Ju, L. Francois-Moutal, M. Khanna and R. Khanna (2014). "The functionalized amino acid (S)-Lacosamide subverts CRMP2-mediated tubulin polymerization to prevent constitutive and activity-dependent increase in neurite outgrowth." Front Cell Neurosci **8**: 196.

Witte, M. E., A. M. Schumacher, C. F. Mahler, J. P. Bewersdorf, J. Lehmitz, A. Scheiter, P. Sanchez, P. R. Williams, O. Griesbeck, R. Naumann, T. Misgeld and M. Kerschensteiner (2019). "Calcium Influx through Plasma-Membrane Nanoruptures Drives Axon Degeneration in a Model of Multiple Sclerosis." Neuron **101**(4): 615-624 e615.

Wolinsky, J. S., X. Montalban, S. L. Hauser, G. Giovannoni, P. Vermersch, C. Bernasconi, G. Deol-Bhullar, H. Garren, P. Chin, S. Belachew and L. Kappos (2018). "Evaluation of no evidence of progression or active disease (NEPAD) in patients with primary progressive multiple sclerosis in the ORATORIO trial." Annals of Neurology **84**(4): 527-536.

Wong, N. and X. Wang (2015). "miRDB: an online resource for microRNA target prediction and functional annotations." Nucleic Acids Res **43**(Database issue): D146-152.

Wonsey, D. R., K. I. Zeller and C. V. Dang (2002). "The c-Myc target gene PRDX3 is required mitochondrial homeostasis and neoplastic transformation." Proceedings of the National Academy of Sciences of the United States of America **99**(10): 6649-6654.

Wu, W. B., R. Menon, Y. Y. Xu, J. R. Zhao, Y. L. Wang, Y. Liu and H. J. Zhang (2016). "Downregulation of peroxiredoxin-3 by hydrophobic bile acid induces mitochondrial dysfunction and cellular senescence in human trophoblasts." Sci Rep **6**: 38946.

Wujek, J. R., C. Bjartmar, E. Richer, R. M. Ransohoff, M. Yu, V. K. Tuohy and B. Trapp (2002). "Axon loss in the spinal cord determines permanent neurological disability in an animal model of multiple sclerosis." Journal of neuropathology and experimental neurology **61**(1): 23-32.

Xie, J. L. and C. G. Proud (2013). "Crosstalk between mTOR complexes." Nature Cell Biology **15**(11): 1263-1265.

Xie, N., H. Cui, S. Banerjee, Z. Tan, R. Salomao, M. Fu, E. Abraham, V. J. Thannickal and G. Liu (2014). "miR-27a regulates inflammatory response of macrophages by targeting IL-10." *J Immunol* **193**(1): 327-334.

Xue, J., S. V. Schmidt, J. Sander, A. Draffehn, W. Krebs, I. Quester, D. De Nardo, T. D. Gohel, M. Emde, L. Schmidleithner, H. Ganesan, A. Nino-Castro, M. R. Mallmann, L. Labzin, H. Theis, M. Kraut, M. Beyer, E. Latz, T. C. Freeman, T. Ulas and J. L. Schultze (2014). "Transcriptome-based network analysis reveals a spectrum model of human macrophage activation." *Immunity* **40**(2): 274-288.

Yang, C., Z. Hao, L. Zhang, L. Zeng and J. Wen (2015). "Sodium channel blockers for neuroprotection in multiple sclerosis." *Cochrane Database Syst Rev*(10): CD010422.

Yi, R., Y. Qin, I. G. Macara and B. R. Cullen (2003). "Exportin-5 mediates the nuclear export of pre-microRNAs and short hairpin RNAs." *Genes Dev* **17**(24): 3011-3016.

Yin, Y., Q. Cui, H. Y. Gilbert, Y. Yang, Z. Yang, C. Berlinicke, Z. Li, C. Zaverucha-do-Valle, H. He, V. Petkova, D. J. Zack and L. I. Benowitz (2009). "Oncomodulin links inflammation to optic nerve regeneration." *Proc Natl Acad Sci U S A* **106**(46): 19587-19592.

Yin, Y., Q. Cui, Y. Li, N. Irwin, D. Fischer, A. R. Harvey and L. I. Benowitz (2003). "Macrophage-derived factors stimulate optic nerve regeneration." *J Neurosci* **23**(6): 2284-2293.

Yiu, G. and Z. He (2006). "Glial inhibition of CNS axon regeneration." *Nat Rev Neurosci* **7**(8): 617-627.

Yong, H., G. Chartier and J. Quandt (2018). "Modulating inflammation and neuroprotection in multiple sclerosis." *J Neurosci Res* **96**(6): 927-950.

Yong, V. W., F. Giuliani, M. Xue, A. Bar-Or and L. M. Metz (2007). "Experimental models of neuroprotection relevant to multiple sclerosis." *Neurology* **68**(22 Suppl 3): S32-37; discussion S43-54.

Young, S. H., J. Ye, D. G. Frazer, X. Shi and V. Castranova (2001). "Molecular mechanism of tumor necrosis factor-alpha production in 1->3-beta-glucan (zymosan)-activated macrophages." *J Biol Chem* **276**(23): 20781-20787.

Yu, B., Z. Y. Yang, J. J. Li, S. Minakhina, M. C. Yang, R. W. Padgett, R. Steward and X. M. Chen (2005). "Methylation as a crucial step in plant microRNA biogenesis." *Science* **307**(5711): 932-935.

Zhang, J., S. Li, L. Li, M. Li, C. Guo, J. Yao and S. Mi (2015). "Exosome and exosomal microRNA: trafficking, sorting, and function." *Genomics Proteomics Bioinformatics* **13**(1): 17-24.

Zhang, J. N., U. Michel, C. Lenz, C. C. Friedel, S. Koster, Z. d'Hedouville, L. Tonges, H. Urlaub, M. Bahr, P. Lingor and J. C. Koch (2016). "Calpain-mediated cleavage of collapsin response mediator protein-2 drives acute axonal degeneration." *Sci Rep* **6**: 37050.

Zhang, L., D. Hou, X. Chen, D. Li, L. Zhu, Y. Zhang, J. Li, Z. Bian, X. Liang, X. Cai, Y. Yin, C. Wang, T. Zhang, D. Zhu, D. Zhang, J. Xu, Q. Chen, Y. Ba, J. Liu, Q. Wang, J. Chen, J. Wang, M. Wang, Q. Zhang, J. Zhang, K. Zen and C. Y. Zhang (2012). "Exogenous plant MIR168a specifically targets mammalian LDLRAP1: evidence of cross-kingdom regulation by microRNA." *Cell Res* **22**(1): 107-126.

Zhong, J. and H. Zou (2014). "BMP signaling in axon regeneration." *Curr Opin Neurobiol* **27**: 127-134.

Zhou, S., D. Shen, Y. Wang, L. Gong, X. Tang, B. Yu, X. Gu and F. Ding (2012). "microRNA-222 targeting PTEN promotes neurite outgrowth from adult dorsal root ganglion neurons following sciatic nerve transection." *PLoS One* **7**(9): e44768.

Zhou, W., A. S. Pal, A. Y. Hsu, T. Gurol, X. Zhu, S. E. Wirbisky-Hershberger, J. L. Freeman, A. L. Kasinski and Q. Deng (2018). "MicroRNA-223 Suppresses the Canonical NF-kappaB Pathway in Basal Keratinocytes to Dampen Neutrophilic Inflammation." *Cell Rep* **22**(7): 1810-1823.